DEPARTAMENTO DE BIOLOGÍA CELULAR, FISIOLOGÍA E INMUNOLOGÍA

Identification of novel endocrine-metabolic and splicing machinery factors with diagnostic, prognostic and/or therapeutic potential in prostate cancer

Identificación de nuevos factores endocrinos-metabólicos y de la maquinaria de splicing con potencial diagnóstico, pronóstico y/o terapéutico en cáncer de próstata

Juan Manuel Jiménez Vacas

Córdoba, Julio 2020

TITULO: *Identification of novel endocrine-metabolic and splicing machinery factors with diagnostic, prognostic and/or therapeutic potential in prostate cancer*

AUTOR: *Juan Manuel Jiménez Vacas*

Campus de Rabanales
Ctra. Nacional IV, Km. 396 A
14071 Córdoba

https://www.uco.es/ucopress/index.php/es/
ucopress@uco.es

DEPARTAMENTO DE BIOLOGÍA CELULAR, FISIOLOGÍA E INMUNOLOGÍA

Identification of novel endocrine-metabolic and splicing machinery factors with diagnostic, prognostic and/or therapeutic potential in prostate cancer

Memoria de Tesis Doctoral presentada por **Juan Manuel Jiménez Vacas**, Graduado en Biología, para optar al grado de **Doctor en Biomedicina**

Los Directores

Dr. Raúl M. Luque Huertas
Profesor Titular
de Biología Celular
de la Universidad de Córdoba

Dr. Manuel David Gahete Ortiz
Profesor Contratado Doctor
de Biología Celular
de la Universidad de Córdoba

En Córdoba, a 26 de Julio de 2020

DEPARTAMENTO DE BIOLOGÍA CELULAR, FISIOLOGÍA E INMUNOLOGÍA

D. Raúl Miguel Luque Huertas y D. Manuel David Gahete Ortiz, Profesor Titular y Profesor Contratado Doctor, respectivamente, del Departamento de Biología Celular Fisiología e Inmunología de la Universidad de Córdoba,

INFORMAN

Que D. Juan Manuel Jiménez Vacas, Graduado en Biología, ha realizado bajo nuestra dirección el trabajo titulado "**Identification of novel endocrine-metabolic and splicing machinery factors with diagnostic, prognostic and/or therapeutic potential in prostate cancer**" y que, bajo nuestro juicio, reúne los méritos suficientes para optar al Grado de Doctor en Biomedicina.

Y para que conste, firmamos la presente en Córdoba, a 26 de Julio de 2020.

Fdo.: Dr. Raúl Miguel Luque Huertas

Fdo.: Manuel David Gahete Ortiz

TÍTULO DE LA TESIS: Identificación de nuevos factores endocrinos-metabólicos y de la maquinaria de splicing con potencial diagnóstico, pronóstico y/o terapéutico en cáncer de próstata

DOCTORANDO: Juan Manuel Jiménez Vacas

INFORME RAZONADO DE LOS DIRECTORES DE LA TESIS

Durante el desarrollo de la presente Tesis Doctoral, en el periodo comprendido entre diciembre de 2016 y Julio de 2020, el doctorando Juan Manuel Jiménez Vacas no solo ha superado con creces los objetivos planteados al comienzo de la misma, sino que también ha desarrollado y validado técnicas experimentales de una gran utilidad para el grupo de investigación, que le han permitido obtener resultados muy relevantes en el campo clínico y molecular del cáncer de próstata, y que quedan patentes en diferentes publicaciones. Concretamente, como fruto de su trabajo durante este periodo, ha publicado 3 trabajos directamente relacionados con su Tesis Doctoral, en las revistas "Translational Research", "Journal of Clinical Medicine" y "EBioMedicine" revistas de referencia dentro de nuestras áreas de investigación. Además, el trabajo realizado en este periodo ha dado lugar a otros cuatro artículos de investigación que está actualmente en fase de redacción o ya sometidos a revistas de las áreas de "Oncología" o "Endocrinología y Metabolismo".

Por último, el doctorando ha presentado sus resultados en diferentes congresos de ámbito nacional e internacional, de los que han derivado varios capítulos de libro, así como ha participado en el desarrollo de varias patentes.

Por todo ello, se autoriza la presentación de la tesis doctoral.

Córdoba, 26 de Julio de 2020

Firma de los directores

Fdo.: Dr. Raúl Miguel Luque Huertas

Fdo.: Manuel David Gahete Ortiz

Esta Tesis Doctoral ha sido realizada en el Departamento de Biología Celular, Fisiología e Inmunología de la Universidad de Córdoba y en el Instituto Maimónides de Investigación Biomédica de Córdoba (IMIBIC), bajo la dirección de los Dres. Raúl M. Luque Huertas y Manuel David Gahete Ortiz. Dicho trabajo fue subvencionado mediante proyectos del Instituto de Salud Carlos III FIS (PI16/00264, PI17/02287, DTS18/00131), Junta de Andalucía (CTS-1406, PI-0639-2012, PI-0541-2013, BIO-0139), Fundación La Caixa (CAIXAIMPULSE_003), Fundación para la Innovación y la Prospectiva en Salud en España (FIPSE-3188-2017), y del Centro de Investigación Biomédica en Red de la Fisiopatología de la Obesidad y Nutrición (CIBERobn). Durante el transcurso de la presente Tesis Doctoral se ha realizado una estancia de tres meses en el Departamento de Biomarcadores del Cáncer en el Instituto de Investigación del Cáncer (ICR) bajo la supervisión del Prof. Johann De Bono, financiada por una ayuda de movilidad internacional de la Universidad de Córdoba para la realización de estancias destinadas a la obtención de la Mención Internacional en el Título de Doctor de la Universidad de Córdoba.

List of publications

This Thesis is based on the research articles listed below, which will be referred in the test by their Roman numerals.

Article I: Juan M. Jimenez-Vacas, Vicente Herrero-Aguayo, Antonio J. Montero-Hidalgo, Enrique Gómez-Gómez, Antonio C. Fuentes-Fayos, Antonio J. Leon-Gonzalez, Prudencio Saez-Martínez, Emilia Alors-Perez, Sergio Pedraza-Arevalo, Teresa Gonzalez-Serrano, Oscar Reyes, Ana Martínez-Lopez, Rafael Sánchez-Sánchez, Sebastian Ventura, Elena M. Yubero-Serrano, María J. Requena-Tapia, Justo P. Castaño, Manuel D. Gahete, Raul M. Luque. *Dysregulation of the splicing machinery is directly associated to aggressiveness of prostate cancer*. 2020. EBioMedicine 51:102547. doi:10.1016/j.ebiom.2019.11.008.

[IF: 5.74, 18/138(Q1) Medicine Research & Experimental (WOS)]

Article II: Juan M. Jiménez-Vacas, Antonio J. Montero-Hidalgo, Enrique Gómez-Gómez, Vicente Herrero-Aguayo, Antonio C. Fuentes-Fayos, Prudencio Saéz-Martínez, Antonio J. León-González, Rafael Sánchez-Sánchez, Teresa González-Serrano, María J. Requena-Tapia, Justo P. Castaño, Manuel D. Gahete, Raúl M. Luque. *RBM22 plays an antitumor role in prostate cancer trough splicing dysregulation and MYC inhibition*. Manuscript submitted on 23/07/2020 to "Molecular Cancer".

Article III: Juan M. Jimenez-Vacas, Vicente Herrero-Aguayo, Enrique Gómez-Gómez, Antonio J. León-González, Prudencio Sáez-Martínez, Emilia Alors-Pérez, Antonio C. Fuentes-Fayos, Ana Martínez-López, Rafael Sánchez-Sánchez, Teresa González-Serrano, Daniel J. López-Ruiz, María J. Requena-Tapia, Justo P. Castaño, Manuel D. Gahete, Raúl M. Luque. *Spliceosome Component SF3B1 as Novel Prognostic Biomarker and Therapeutic Target for Prostate Cancer*. 2019. Translational Research 212:89-103. doi: 10.1016/j.trsl.2019.07.001.

[IF: 5.41, 2/29(D1) Medical Laboratory Technology (WOS)]

Article IV: Juan M. Jiménez-Vacas, Antonio Montero-Hidalgo, André Sarmento-Cabral, Enrique Gómez-Gómez, Miguel López, Manuel D. Gahete, Raúl M. Luque. *Alterations in the splicing machinery as a key molecular mechanism underlying the antitumor effects of metformin in prostate cancer.* Manuscript in preparation for "Cancer & Metabolism".

Article V: Juan M. Jiménez-Vacas, Vicente Herrero-Aguayo, Antonio J. Montero-Hidalgo, Prudencio Sáez-Martínez, Enrique Gómez-Gómez, Antonio J. León-González, Antonio C. Fuentes-Fayos, Elena M. Yubero-Serrano, María J. Requena-Tapia, Miguel Lopez, Justo P. Castaño, Manuel D. Gahete, Raúl M. Luque. *Clinical, cellular and molecular evidence of the additive antitumor effects of biguanides and statins in prostate cancer*. Manuscript submitted on 11/07/2020 to "Journal of Clinical Endocrinology & Metabolism".

Article VI: Juan M. Jiménez-Vacas, Enrique Gómez-Gómez, Antonio J. Montero-Hidalgo, Vicente Herrero-Aguayo, Fernando L-López, Rafael Sánchez-Sánchez, Ipek

Guler, Ana Blanca, María José Méndez-Vidal, Julia Carrasco, José Lopez-Miranda, María J. Requena-Tapia, Justo P. Castaño, Manuel D. Gahete, and Raúl M. Luque. *Clinical Utility of Ghrelin-O-Acyltransferase (GOAT) Enzyme as a Diagnostic Tool and Potential Therapeutic Target in Prostate Cancer*. Journal of Clinical Medicine. 8(12):2056. doi: 10.3390/jcm8122056.

[IF: 3.30, 36/165(Q1) Medicine, General & Internal (WOS)]

Article VII: Juan M. Jiménez-Vacas, Enrique Gómez-Gómez, Antonio Montero-Hidalgo, Ipek Guler, Jesús Delgado-Luque, Francisco Ruiz-Pino, María J. Requena-Tapia, Manuel Tena-Sempere, Justo P. Castaño, Manuel D. Gahete, Raúl M. Luque. *Pathophysiological relation between obesity and prostate cancer: role of In1-ghrelin as a novel non-invasive diagnostic and prognostic biomarker*. Manuscript in preparation for "Cancer Letters".

List of abbreviations

ADT: Androgen Deprivation Therapy

AR: Androgen receptor

AR-v7: Androgen receptor variant 7

AUC: Area under the curve

BMI: Body mass index

BP: Branch point

BPH:Benign prostate Hyperplasia

CI: Confidence interval

CKIs: Cyclin-dependent kinase inhibitor

CRPC: Castration-Resistant PCa

DM: Diabetes Mellitus

DRE: Digital rectal exam

EAU: European Association of Urology

EBRT: External Beam Radiation Therapy

ESE: exonic splicing enhancer

ESS: exonic splicing silencer

FDA: Food drug administration

GHRL: Ghrelin

GOAT: Ghrelin-o-acyl Transferase

GS: Gleason Score

HDR: High dose rate

HFD: High-fat diet

IMRT: Intensity modulated radiotherapy

ISE: intronic splicing enhancer

ISS: intronic splicing silencer

ISUP: International Society of Urological Pathology

OR: Odds Ratio

LBD: Ligand binding domain

LDR: Low dose rate

LFD: Low-fat diet

mCRPC: Metastatic CRPC

NEPC: Neuroendocrine Prostate Cancer

NMD: Nonsense mRNA Decay

NonSigPCa: Non-significant Prostate Cancer

PCa: Prostate Cancer

PHI: Prostate Health Index

PIN: Prostatic Intraepithelial Neoplasia

PSA: Prostate specific antigen

RARP: Robot-Assisted Radical Prostatectomy

RBM: RNA Binding Motif

ROS: Reactive oxigen species

RP: Radical prostatectomy

RT: Radiotherapy

SCs: Spliceosome Components

SFs: Splicing Factors

SigPCa: Significant Prostate Cancer

snRNPs: Small nuclear ribonucleoproteins

T2DM: Type 2 diabetes mellitus

TMD: Transmembrane domain

TNM: Tumor, node and metastasis staging

WHO: world health organization

Table of contents

Contenido

Index of tables and figures

Index of figures

Index of tables

Resumen

Resumen

El Cáncer de Próstata (CaP) es la patología tumoral con mayor incidencia en hombres en países desarrollados y representa una de las principales causas de mortalidad relacionadas con cáncer en este colectivo. A pesar de los avances que se han producido durante los últimos años en el campo del diagnóstico y el tratamiento del CaP, la realidad es que tanto las herramientas diagnósticas como las alternativas terapéuticas que existen actualmente no son todo lo eficientes que se desearía. En concreto, el antígeno prostático específico (PSA) representa el actual "*gold standard*" para el cribado del CaP. Lamentablemente, la prueba del PSA presenta una especificidad discutible, ya que ciertas condiciones fisiológicas o patologías no tumorales (p.ej. hiperplasia benigna de próstata, prostatitis) también se asocian a niveles circulantes de PSA elevados. Además, la capacidad diagnóstica y la utilidad clínica de la prueba del PSA es especialmente baja en pacientes con niveles de PSA entre 3-10 ng/mL (la conocida como zona gris del PSA). Por estos motivos, la prueba del PSA está asociada al sobrediagnóstico de CaP, y, en consecuencia, a la realización de biopsias innecesarias. Además, este procedimiento invasivo puede provocar efectos secundarios como dolor, sangrado e infecciones, disminuyendo significativamente la calidad de vida de los pacientes. Por tanto, es necesaria la búsqueda e identificación de nuevas herramientas diagnósticas que complementen o reemplacen al PSA en la práctica clínica. Lo mismo ocurre en el caso de las alternativas terapéuticas ya que son muy limitadas. En concreto, el tratamiento farmacológico usado como primera opción para el tratamiento de CaP en estadio avanzado o recidivas tumorales consiste en la deprivación androgénica (p.ej. antagonistas de GnRH, abiraterona), debido a la marcada dependencia de

la señalización androgénica que presenta el CaP. Sin embargo, alrededor del 80% de los pacientes tratados con deprivación androgénica desarrollan resistencia frente a este tratamiento, generándose lo que se conoce como CaP resistente a la castración (CPRC), el fenotipo más agresivo de esta enfermedad, el cuál sigue siendo letal en la actualidad. Por ello, la búsqueda de dianas terapéuticas alternativas que puedan ser útiles para el desarrollo de nuevos tratamientos más eficientes que los actuales sigue siendo uno de los principales objetivos de la comunidad científica biomédica.

El CaP se desarrolla principalmente en pacientes de elevada edad, que padecen, con una elevada frecuencia, patologías endocrino-metabólicas (p.ej. obesidad, diabetes), las cuales pueden influenciar el desarrollo y/o la progresión del CaP, aumentando la complejidad de esta patología. En concreto, la obesidad se asocia a un mayor riesgo de desarrollar CaP, además de aumentar su agresividad. En este sentido, se ha descrito que la metformina y las estatinas (drogas comúnmente usadas en pacientes con patologías endocrino-metabólicas como obesidad o diabetes) ejercen efectos antitumorales en numerosos tipos tumorales, tanto *in vitro* como *in vivo*. Sin embargo, aunque la combinación de ambas drogas ha demostrado ejercer un papel antitumoral aditivo en algunos tipos de células tumorales, hasta el momento, esta observación no se ha estudiado en profundidad en el caso del CaP.

Una limitación importante en este campo es que la información disponible sobre los posibles mecanismos moleculares concretos que subyacen la interacción fisiopatológica entre la obesidad y el CaP es muy limitada e incompleta. En este sentido, se conoce que numerosos componentes de diferentes sistemas hormonales (ej. andrógenos, ghrelina, etc.) se encuentran claramente desregulados en CaP y obesidad, pudiendo constituir una fuente de biomarcadores en estas patologías. El sistema ghrelina en un ejemplo claro en este contexto, puesto que es un sistema hormonal pleiotrópico formado por varios ligandos

(p.ej. Ghrelina, In1-ghrelina), enzimas (GOAT) y receptores (GHSR1a, GHSR1b). Así, la In1-ghrelina (variante de splicing alternativo que se forma a partir de la retención del intrón-1) se encuentra sobreexpresada y juega un papel oncogénico en el CaP. De la misma forma, los niveles de GOAT son más elevados en tejidos de CaP con respecto a aquellos de próstata no tumoral, aunque se desconoce hasta el momento el posible papel fisiopatológico de esta enzima en CaP. Además, se ha reportado que tanto los niveles circulantes de In1-ghrelina como los de GOAT se encuentran más elevados en pacientes con CaP que en individuos sanos, lo que sugiere que ambos elementos podrían representar biomarcadores de diagnóstico no invasivo del CaP. Sin embargo, hasta el momento, se desconoce si In1-ghrelina o GOAT pueden ser detectadas en orina y si también están desreguladas en este fluido (que constituye una fuente enriquecida de proteínas derivadas de la próstata) en pacientes con CaP respecto a pacientes sin CaP.

Finalmente, es importante mencionar que la alteración del proceso de *splicing*, un mecanismo fisiológico involucrado en la maduración de los pre-ARNm y que puede generar varios ARNm maduros a partir de un solo gen, lo que aumenta la complejidad transcriptómica de las células eucariotas, se ha erigido como una característica común de un gran número de patologías tumorales, incluyendo el CaP. De hecho, se ha demostrado la existencia de variantes de splicing con potencial oncogénico, asociadas al desarrollo, progresión y/o resistencia a tratamientos de múltiples patológicas tumorales, así como el CaP. Estas desregulaciones del proceso de splicing pueden deberse a una alteración de la maquinaria que lleva a cabo este proceso celular (espliceosoma), así como de las proteínas que interactúan con la misma regulando este mecanismo (factores de splicing), por lo que podrían jugar un papel relevante en el desarrollo y/o progresión del CaP. Así, aunque ciertos estudios han mostrado la desregulación concreta de algunos de estos elementos, no se ha

explorado aún de manera sistemática la desregulación de esta maquinaria y su posible implicación en el desarrollo y/o progresión del CaP.

De acuerdo con lo anteriormente expuesto, el objetivo de esta Tesis Doctoral fue determinar el papel que ejercen ciertos elementos reguladores del mecanismo de splicing (componentes del espliceosoma y factores de splicing) y moduladores metabólicos (tanto elementos endógenos como tratamientos exógenos) en el desarrollo, progresión y/o agresividad del CaP, con el fin de descubrir nuevos biomarcadores (diagnósticos y/o pronósticos) y herramientas diagnósticas que pudieran mejorar el diagnóstico, tratamiento y manejo clínico de los pacientes con CaP.

La primera sección de esta Tesis Doctoral se centró en estudiar la posible desregulación de la maquinaria de splicing en CaP, así como sus consecuencias clínicas y funcionales en esta patología tumoral. Los resultados generados indican que la maquinaria de splicing se encuentra profundamente desregulada en CaP, incluyendo elementos clave de esta maquinaria como son SNRNP200, SRRM1, SRSF3, RBM22 o SF3B1. De entre todos los componentes del espliceosoma y factores de splicing desregulados, SNRNP200, SRRM1 y SRSF3 se seleccionaron inicialmente para llevar a cabo análisis más profundos puesto que se encontraban asociados con todos los parámetros clínicos de agresividad disponibles en nuestra cohorte de pacientes. El silenciamiento de SNRNP200, SRRM1 o SRSF3 produjo una inhibición de rutas de señalización oncogénicas y alteró el patrón de splicing de genes relacionados con el aumento de agresividad tumoral del CaP y/o con el desarrollo de CPRC. Además, el silenciamiento de SNRNP200, SRRM1 y de SRSF3 sensibilizó a células de CPRC frente al tratamiento con un inhibidor del receptor de andrógenos (AR; Abiraterona). Por tanto, estos datos demuestran que SNRNP200, SRRM1 y SRSF3 podrían representar nuevos biomarcadores de diagnóstico y pronóstico, así como dianas

terapéuticas en CaP y CPRC.

Esta Tesis Doctoral también se centró en el estudio de la posible desregulación y papel fisiopatológico en CaP de RBM22, un factor de splicing involucrado en la activación del espliceosoma. En concreto, se encontró que los niveles de RBM22 eran más bajos (a nivel del ARNm y proteína) en tejidos de CaP comparados con los tejidos derivados de próstata no tumoral, y que dichos niveles se asociaron inversamente con parámetros clínicos de agresividad tumoral en pacientes y en un modelo preclínico. Asimismo, se observó que la sobreexpresión de RBM22 disminuyó las características de agresividad de células de CaP tanto *in vitro* como *in vivo* (ej. crecimiento tumoral, proliferación, migración, etc.). Desde un punto de vista molecular, la aplicación de técnicas de análisis a gran escala (RNAseq, CLIP-seq y array de señalización) sobre muestras de CaP *in vitro* e *in vivo* mostró la inhibición de MYC, MYCN y proteínas E2F, así como una profunda desregulación del proceso de splicing como los mecanismos moleculares principales asociados a los descubrimientos previos observados en respuesta a la sobreexpresión de RBM22 en CaP. Por tanto, estos resultados sugieren que RBM22 juega un papel antitumoral relevante en CaP mediante la modulación del proceso de splicing y la reducción de los niveles/actividad de MYC, MYCN y E2F.

En el caso del análisis de SF3B1, un elemento clave para el correcto ensamblaje del espliceosoma, se observó que se encontraba sobreexpresado en CaP y que sus niveles estaban directamente asociados con parámetros de agresividad del CaP. Asimismo, tanto el silenciamiento de SF3B1 como el bloqueo de su actividad (mediante el uso del inhibidor selectivo pladienolide-B) resultó en una reducción de numerosos parámetros funcionales de agresividad tumorales y en un aumento de la tasa apoptótica en células de CaP. Desde el punto de vista molecular, la inhibición de SF3B1 alteró rutas de señalización oncogénicas

como PI3K/AKT o JNK, disminuyó los niveles de variantes de splicing oncogénicas (AR-v7 e In1-ghrelina), y desreguló profundamente el patrón de expresión de numerosos elementos involucrados en procesos de metabolismo de ARN [splicing y degradación del ARNm mediada por mutaciones terminadoras (NMD)]. El conjunto de estos resultados indica que SF3B1 podría representar un nuevo biomarcador pronóstico, así como una diana terapéutica de CaP, lo que sugiere una posible utilidad del pladienolide-B para el tratamiento de esta devastadora patología.

Una vez que demostramos el importante papel que ejercen numerosos elementos involucrados en la regulación del proceso de splicing en CaP, y puesto que se ha demostrado previamente que la metformina ejerce efectos antitumorales en diversos tipos de cáncer y que altera la expresión de factores de splicing concretos en células de distinta naturaleza, decidimos explorar la posible implicación que podría tener la desregulación del splicing en los efectos antitumorales mediados por la metformina en CaP. Los datos generados indican que la metformina provoca una profunda desregulación del patrón de expresión de numerosos componentes del espliceosoma, así como factores de splicing en células de CaP, siendo algunos de estos resultados (ej. disminución de la expresión de *SF3B1*, *SRRM1* y *NOVA1*) validados también *in vivo* en un modelo xenógrafo de CaP. Además, el efecto antiproliferativo de la metformina se bloqueó por completo tras el silenciamiento de la expresión de *SF3B1*, *SRRM1* y *NOVA1* en células de CaP. Por tanto, estos resultados sugieren que la desregulación de algunos de los componentes de la maquinaria de splicing, especialmente SF3B1, SRRM1 y de NOVA1, puede representar un mecanismo molecular subyacente a los efectos antitumorales conocidos de la metformina en CaP.

La segunda sección de esta Tesis se centró en el análisis de las acciones antitumorales de

la metformina, estatinas y su combinación en CaP, así como de los mecanismos moleculares asociados. En concreto, se observó que el tratamiento combinado con metformina y estatinas se asoció a efectos más beneficiosos sobre parámetros clínicos de agresividad en pacientes con CaP con respecto a pacientes que recibieron estas terapias farmacológicas de manera individual. De igual manera, aunque el tratamiento con biguanidas y estatinas, por separado, redujo la agresividad de células de CaP *in vitro*, estos efectos antitumorales fueron más pronunciados cuando estos tratamientos se dieron en combinación. Desde un punto de vista molecular, se observó que el tratamiento con metformina y simvastatina en combinación produjo una hiper-inactivación de AR y mTOR, además de aumentar la expresión de inhibidores de quinasas dependientes de ciclinas (CKIs; *CDKN1A*, *CDKN1B*, *CDKN2A* y *CDKN2D*), siendo algunos de estos cambios validados en muestras derivadas de pacientes con CaP (ej. aumento de la expresión de *CDKN1B* y de *CDKN2A*). Los resultados derivados de este estudio demuestran que la metformina y la simvastatina llevan a cabo efectos antitumorales aditivos en CaP, sugiriendo que esta combinación podría representar una nueva y atractiva aproximación terapéutica para combatir el CaP.

Finalmente, en la tercera sección de esta Tesis Doctoral, se analizaron componentes específicos pertenecientes al sistema ghrelina (concretamente la enzima GOAT y la variante In1-ghrelina) parar determinar su posible papel como herramientas diagnósticas, pronósticas y/o terapéuticas en CaP. Estos resultados mostraron que la GOAT podía ser detectada en muestras de orina, en donde sus niveles eran capaces de mejorar la capacidad diagnóstica del PSA plasmático, especialmente para detectar CaP significativo (definido como Gleason score ≥7), en pacientes con PSA en zona gris. Además, niveles elevados de GOAT en orina se asociaron a un aumento de riesgo de desarrollar CaP y CaP significativo,

y se correlacionaron positivamente con parámetros clínicos y moleculares claves de agresividad en pacientes con CaP. Asimismo, también se demostró que la sobreexpresión de GOAT aumentó la agresividad del CaP tanto *in vitro* como *in vivo*, mientras que su silenciamiento o su bloqueo de su actividad (mediante el uso de un inhibidor de GOAT específico) disminuyó significativamente parámetros funcionales de agresividad en células de CaP *in vitro*. Por tanto, estos resultados demuestran que la enzima GOAT puede representar un biomarcador de diagnóstico no invasivo de CaP adicional, así como una posible herramienta pronóstica y terapéutica de CaP. Además, el análisis de In1-ghrelina en orina de pacientes con PSA en la zona gris, indicaron que sus niveles eran capaces de discriminar entre pacientes con y sin CaP, que se asociaron a un mayor riesgo de CaP, obesidad y diabetes, y se correlacionaron con parámetros metabólicos y de agresividad tumoral. De hecho, se observó que la capacidad diagnóstica de los niveles de In1-ghrelina en orina fue especialmente elevada cuando se analizaron pacientes obesos, lo que sugiere que la In1-ghrelina podría representar un nuevo y más personalizado biomarcador de diagnóstico no invasivo en CaP.

Teniendo en cuenta todos los resultados obtenidos en esta Tesis Doctoral, la **conclusión general** es que la alteración del splicing y la desregulación de ciertos elementos endocrino-metabólicos podría contribuir en el desarrollo, progresión y/o agresividad del CaP, representando una fuente de biomarcadores de diagnóstico y pronóstico, así como dianas terapéuticas novedosas, que podrían ser explotadas para mejorar el diagnóstico de pacientes con CaP, así como para desarrollar herramientas pronosticas y terapéuticas efectivas para combatir esta devastadora patología.

Summary

Summary

Prostate cancer (PCa) is the tumor pathology with the highest incidence among men in developed countries and represents one of the main causes of cancer-related death in this group. Despite the advances achieved during the last years in PCa diagnosis and treatment, the diagnostic and therapeutic tools currently available are not sufficiently efficient. Specifically, prostate specific antigen (PSA) is the current "gold standard" used for PCa screening. Unfortunately, the PSA test has controversial specificity, since certain physiological conditions or non-tumor pathologies (e.g. benign prostatic hyperplasia, prostatitis) are also associated with high circulating PSA levels. Furthermore, the diagnostic capacity and clinical utility of the PSA test is especially low in patients with PSA levels between 3-10 ng/mL (the so-called grey zone). For these reasons, PSA test is associated with PCa overdiagnosis and unnecessary biopsies. Moreover, this invasive method required to subsequently confirm or discard the presence of PCa can cause side effects such as pain, bleeding and infections, which significantly impact patient's quality of live. Therefore, there is an urgent need to identify new diagnostic tools that complement or replace PSA in clinical practice. Similarly, the therapeutic armamentarium in PCa is limited and clearly insufficient. Specifically, the pharmacological treatment used as the first option for the treatment of advanced-stage PCa or tumor recurrences consists of androgen deprivation (e.g. LHRH antagonists, abiraterone), due to the marked dependence of androgenic signaling of PCa cells. However, about 80% of patients treated with androgen deprivation therapy will develop resistance to this treatment, generating the so-called Castration Resistant PCa (CRPC), the most aggressive phenotype of this disease, which remains lethal nowadays. Therefore, the search for alternative therapeutic targets useful for the

development of new, more efficient, treatments than those currently available continues to be one of the main objectives of the biomedical scientific community.

PCa develops mainly in older patients, who suffer, with a high frequency, endocrine-metabolic pathologies (i.e. obesity, diabetes), which can influence the development and/or progression of PCa, increasing the complexity of this pathology. Specifically, obesity is associated with an increased risk of developing PCa, and with higher PCa aggressiveness. In this context, it has been described that metformin and statins (drugs commonly used in patients with endocrine-metabolic pathologies such as obesity or diabetes) exert antitumor effects in numerous tumor types, both *in vitro* and *in vivo*. However, although the combination of both drugs has been shown to exert additive antitumor actions in some cancer cell types, this possibility has not been systematically studied in the case of PCa.

An important limitation in this field is that the information available regarding the exact molecular mechanisms underlying the pathophysiological interaction between obesity and PCa is very limited and fragmentary. In this sense, it is well-known that numerous components of different hormonal systems (i.e. androgen, ghrelin, etc.) are clearly dysregulated in PCa and obesity, which may constitute a source of biomarkers in these pathologies. The ghrelin system is a clear example in this context, since it is a pleiotropic hormonal system consisting of various ligands (e.g. Ghrelin, In1-ghrelin), enzymes (GOAT), and receptors (GHSR1a, GHSR1b). Specifically, In1-ghrelin (an alternative splicing variant derived as the result of the intron-1 retention) is overexpressed and plays an oncogenic role in PCa. Likewise, GOAT levels are higher in PCa tissues compared to non-tumor prostate tissue, but the putative pathophysiological role of this enzyme in PCa is still unknown nowadays. Furthermore, it has been reported that circulating levels of both In1-

ghrelin and GOAT are higher in PCa patients compared to healthy patients, suggesting that both elements could represent non-invasive diagnostic biomarkers of PCa. However, to date, it is unknown whether In1-ghrelin or GOAT can be detected and whether they are dysregulated in urine (which constitutes an enriched source of proteins derived from the prostate) in patients with PCa compared with patients without PCa.

Finally, it is important to mention that the alteration of the splicing process has become a common hallmark of a large number of tumor pathologies, including PCa. Splicing is a physiological mechanism involved in the maturation of pre-mRNAs, which can generate different mature mRNAs from a single gene, thereby increasing the transcriptomic complexity of eukaryotic cells. However, increasing evidence demonstrates the existence of different splicing variants with oncogenic potential which are associated to the development, progression and/or resistance of pharmacological treatments of multiples tumor pathologies, including PCa. These dysregulations of the splicing process may be due to an alteration of the machinery that regulate this cellular process (spliceosome) and/or of the proteins that regulate this mechanism (splicing factors), suggesting that they could play a relevant role in the development and/or progression of PCa. Although certain studies have shown the specific dysregulation of some of these elements in PCa, the possible involvement of the alteration of this machinery and the putative implication in the development and/or progression of PCa has not been systematically explored yet.

Based on the all the information mentioned above, the general aim of this Doctoral Thesis was to determine the potential role that certain splicing-related elements (spliceosome components and splicing factors) and metabolic modulators (endogenous elements and exogenous treatments) play and/or exert in the development, progression

and/or aggressiveness of PCa, with the ultimate goal of discovering novel biomarkers (diagnostic and/or prognostic) and therapeutic tools that could improve the diagnosis, treatment and the clinical management of PCa patients.

The first section of this Doctoral Thesis was focused on exploring the putative dysregulation and the clinical and functional implications of the splicing machinery in PCa. Results presented herein indicate that the splicing machinery is drastically dysregulated in PCa, including pivotal elements of this machinery such as SNRNP200, SRRM1, SRSF3, RBM22 or SF3B1. Among all the dysregulated spliceosome components and splicing factors, SNRNP200, SRRM1 and SRSF3 were selected initially to be further explored because they were associated with all the relevant aggressiveness features available in the cohort of patients used in this study. Mechanistically, silencing of SNRNP200, SRRM1 or SRSF3 inhibited oncogenic pathways and altered the splicing process of genes previously reported to be involved in tumor aggressiveness and/or CRPC development. Consistently, SNRNP200-, SRRM1- and SRSF3-silencing sensitized the CRPC cells to an androgen receptor (AR)-inhibitor (enzalutamide). Therefore, these data demonstrate that SNRNP200, SRRM1 and SRSF3 could represent attractive novel diagnostic and prognostic biomarkers as well as therapeutic targets for PCa and CRPC.

This Doctoral Thesis was also focused on exploring the potential dysregulation and role of RBM22 in PCa, a splicing factor tightly involved in the activation of the spliceosome. Specifically, we found that RBM22 levels were lower (at mRNA and protein levels) in PCa tissues compared to non-tumor prostate tissues, and that these levels were inversely associated to key clinical parameters of aggressiveness in patients and in a preclinical mouse model. Moreover, we observed that the aggressiveness features of PCa cells were

reduced in response to *RBM22* overexpression *in vitro* and *in vivo* (i.e. reduced tumor growth, proliferation, migration, etc.) Mechanistically, results from high-throughput techniques (i.e. RNAseq, CLIP-seq and signaling array) performed in samples from *in vitro* and *in vivo* PCa models pointed out that the inhibition of MYC, MYCN and E2F, as well as a profound dysregulation of the splicing process could be the molecular mechanisms associated to the relevant findings previously observed after the *RBM22* overexpression in PCa. Therefore, these results suggest that RBM22 plays a relevant antitumor role in PCa through the regulation of the splicing process and the reduction of MYC, MYCN and E2F levels/activity.

In the case of SF3B1, a key component involved in the spliceosome assembly, we demonstrated that SF3B1 is overexpressed in PCa and that its levels were directly associated with important aggressiveness features of PCa. Moreover, the downregulation of SF3B1 and the inhibition of its activity (using the selective inhibitor pladienolide-B) significantly reduced functional aggressiveness features and increased the apoptotic rate of PCa cells. From a molecular perspective, SF3B1 inhibition altered PI3K/AKT and JNK oncogenic signaling pathways, down-regulated key oncogenic splicing variants (AR-v7 and In1-ghrelin), and dysregulated the expression of several elements involved in mRNA metabolism [splicing and non-sense mediated mRNA decay (NMD)]. Taken together, these results suggest that SF3B1 could represent a new prognostic biomarker and a therapeutic target in PCa, providing convincing evidence for the putative utility of pladienolide-B as novel therapeutic tool for the treatment of this devastating pathology.

Once demonstrated the key role of several splicing-regulating factors in PCa, and since metformin has been found to exert antitumoral effects in various cancer types and that alter the expression of specific splicing factors in certain cell types, we next aimed to explore the

potential involvement of the splicing dysregulation in the antitumor actions of metformin in PCa. Our data indicate that metformin produced a profound downregulation in the expression of different spliceosome components and splicing factors in PCa cells, being some of these changes (i.e. downregulation of *SF3B1*, *SRRM1* and *NOVA1*) further validated *in vivo* using a PCa xenograft model. Moreover, the antiproliferative response of metformin treatment observed in PCa cells was completely blocked when the expression of *SF3B1*, *SRRM1* or *NOVA1* were silenced. Therefore, these results suggest that the dysregulation of some components of the splicing machinery, especially *SF3B1*, *SRRM1* and *NOVA1*, might represent an additional molecular mechanism underlying the well-known antitumor effects of metformin in PCa.

The second section of this Doctoral Thesis was focused on the analysis of the antitumor actions of metformin, statins and their combination, as well as the underlying molecular mechanisms in PCa. Specifically, PCa patients treated with metformin and statins in combination were associated to more beneficial effects in key clinical parameters of aggressiveness compared to those receiving individual treatments. Consistently, although biguanides and statins significantly decreased the aggressiveness of PCa cells *in vitro*, these antitumor effects were more pronounced when combining both treatments. Mechanistically, we found that the treatment with the combination of metformin and simvastatin *in vitro* resulted in a hyper-inactivation of AR and mTOR, as well as in an upregulation of the expression of different cyclin-dependent kinase inhibitors (CKIs; *CDKN1A*, *CDKN1B*, *CDKN2A* and *CDKN2D*), being some of those changes further validated in samples from patients with PCa (i.e. upregulation of *CDKN1B* and *CDKN2A*). Altogether, this study demonstrates that metformin and simvastatin exert additive antitumor effects in PCa, thus suggesting that this combination might be a novel and attractive therapeutic approach to

tackle PCa.

Finally, in the third section of this Doctoral Thesis, we analysed specific components of the ghrelin system (specifically, GOAT enzyme and In1-ghrelin variant) to unveil their potential role as diagnostic, prognostic and/or therapeutic tools in PCa. These results demonstrated that GOAT could be detected in urine samples, wherein its levels outperformed the capacity of plasma PSA levels to diagnose PCa, especially clinically significant PCa (SigPCa; defined as Gleason score ≥7) in patients with PSA in the grey zone. Moreover, high urine GOAT levels were associated to increased risk of developing PCa and SigPCa, and were positively correlated to key clinical and molecular aggressiveness parameters in PCa patients. Furthermore, we demonstrated that GOAT overexpression increased PCa aggressiveness *in vitro* and *in vivo,* while its silencing and the blockade of its activity (using a specific GOAT inhibitor) significantly decreased the aggressiveness features of PCa cells *in vitro*. Therefore, these results demonstrated that GOAT enzyme may represent an additional non-invasive diagnostic biomarker, as well as a potential prognostic and therapeutic tool for PCa. Moreover, the analysis of In1-ghrelin in urine from patients with PSA in the grey zone indicated that its levels were able to distinguish between patients with and without PCa, were associated to higher risk of PCa, obesity and diabetes, and correlated with metabolic and aggressiveness parameters. In fact, we found that the capacity of urine In1-ghrelin levels to diagnose PCa was especially elevated when only obese patients were considered, suggesting its potential utility as a non-invasive diagnostic biomarker from a more personalized perspective.

Altogether, the **general conclusion** derived from this Doctoral Thesis is that the

alteration of the splicing process and the dysregulation of certain endocrine-metabolic systems could contribute to the development, progression and/or aggressiveness of PCa, representing a source of novel diagnostic and prognostic biomarkers, as well as therapeutic targets that could be exploited to improve the diagnosis of PCa patients, and to develop more effective prognostic and therapeutic tools to tackle this devastating pathology.

1. Introduction

1.1. Prostate cancer

Prostate cancer (PCa) is a disease characterized by uncontrolled growth and proliferation of prostate gland cells. The natural history of this tumor pathology implies the progression from benign tissue to prostatic intraepithelial neoplasia [**PIN**; which is considered a precursor of PCa (1)] and finally PCa, by acquiring numerous alterations at genomic, transcriptomic and epigenetic levels, in addition to other key molecular dysregulations (2). The vast majority of PCa cases are adenocarcinomas (90%), mainly characterized by the expression of androgen receptor (**AR**) and the lack of basal-cell markers (e.g. CK5, CK14 and p63) (3). The other PCa types are presented with very low frequency, including ductal carcinoma, mucinous PCa, prostate sarcomas, signet ring cell PCa and neuroendocrine tumors (**NEPC**), being all of them associated with poor prognosis (4, 5). Among the rare PCa types, the most common are the NEPC (<2% of total PCa), which arises from neuroendocrine prostate cells and are mainly characterized by the lack of AR expression (6). In addition to the histopathological classification, PCa is also categorized based on the pharmacological response to androgen deprivation therapy (**ADT**; that will be discussed in next sections of this Doctoral Thesis): i) **Hormone-sensitive PCa** (tumors sensitive to ADT); and ii) **Castration-Resistant PCa (CRPC) or hormone-refractory PCa** [tumors insensitive to castration (7, 8)]. Other factor that increases the complexity of this disease is the intra-tumor heterogeneity of PCa, reflected in its multifocal nature. Indeed, approximately 80% of PCa cases contain more than one focus (9), and each one of them may have different molecular alterations (10).

1.1.1. Epidemiology

Approximately 1.3 million men are diagnosed with PCa every year worldwide (11). Specifically, PCa represents the cancer type with highest incidence among men in the vast majority of countries (Figure 1). Currently, it is the most frequent cancer type among European men, with a higher prevalence in the North and West of Europe, and an increasing trend in East and South Europe (12). The variation in PCa incidence seems to be the result of specific screening and early diagnosis programs (further explained in Diagnosis section).

Fortunately, PCa patient survival has been improved during the last decades. The explanation for this survival rate increase seems to be the earlier diagnosis (due to screening programs) and the development of more effective treatments (13, 14).

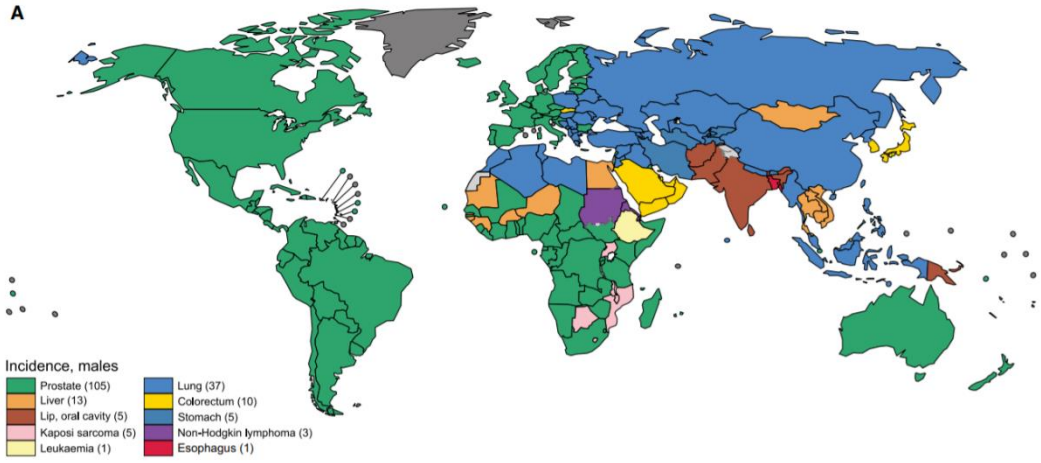

Figure 1: Global map presenting the most common types of cancer incidence in 2018 in each country among men. Source: Bray et al., CA Cancer J Clin 2018.

1.1.2 Risk factors

The development and progression of PCa have been associated with certain known risk factors that increase the probability of developing PCa, including aging, family history and race. Specifically, a systematic review by Bell *et al*. showed that the prevalence of PCa increases from 5% in patients younger than 30 years to 59% in patients older than 79 years [Odds Ratio (OR) = 1.7 by decade of age] (15). It has been hypothesized that the main molecular mechanism underlying the relationship between aging and PCa risk is the increase of reactive oxygen species (ROS) with age, which ultimately drive to DNA damage, thus creating an ideal environment for mutagenesis and tumor initiation (16-18). This hypothesis is reinforced by the fact that several studies have shown the protective effect of antioxidant compounds such as α-tocopherol and lycopene against PCa (19-21).

In addition, familiar cases of PCa and the number of affected relatives have been associated with a higher PCa risk (22-24). In fact, PCa is a tumor pathology with more family cases than breast and colorectal cancers, two malignancies with well recognized familial components (25). According to an epidemiological study by Lichtenstein *et al*., approximately 40% of global PCa risk could be due to hereditary factors (26). Specifically, PCa risk duplicates with one first-degree relative affected, and increases by 5 to 11 times with two or more relatives, being this risk higher when a brother is affected compared to when the father is affected (27). Therefore, hereditary PCa has been defined as “family history of PCa in three generations, and/or three first-degree relatives and/or two first-degree relatives if one was diagnosed below 55 years old” (25). In this scenario, the extraordinary molecular heterogeneity of PCa hampers the finding of hereditary genetic alterations associated with PCa risk (28). However, IMPACT study showed that the

diagnosis of PCa in patients younger than 50 years only occurred in patients with Breast cancer (*BRCA*) genes mutations (29, 30). Likewise, mutations in Homeobox B13 (*HOXB13*) have been also associated with an earlier PCa development (29, 30).

Finally, the influence of race on PCa risk has been broadly documented (31). In particular, African American men have higher PCa risk and more aggressive tumors as compared to Caucasian men (7). In fact, it has been recently reported that, in USA, African Americans are more likely to suffer from PCa than European Americans (2-fold) and Asian Americans (4-fold) (32). Likewise, African American men have a more aggressive disease, with higher probability to develop metastasis at diagnosis, and higher mortality rate, compared to European Americans (32-35). In addition, Cotter *et al*. found that family history of incidence of PCa was more common among African Americans PCa patients (31.2%) than among Caucasian PCa patients (22.2%) (36).

1.1.3. Diagnosis

1.1.3.1. PSA, DRE and biopsy

PCa diagnosis has undergone a remarkable revolution since the establishment of the prostate specific antigen (**PSA**) as a non-invasive biomarker for PCa screening. PSA is a kallikrein-serine protease involved in the liquefaction of seminal coagulum (37, 38), which is mainly secreted by epithelial prostatic cells [although it has also been detected in nipple aspirate fluid, saliva, and amniotic fluid) (39)]. In 1994, PSA was approved by the Food and Drug Administration (FDA) as a PCa diagnostic biomarker for men older than 50 years. The diagnostic value of PSA was supported by the European Randomized Study of

Screening for Prostate Cancer (ERSPC; published in 2014, after 13 years of follow-up), which showed a significant absolute and relative reduction in cancer-specific deaths in the screened cohort (40). In fact, due to the PSA screening, the majority of PCa patients diagnosed nowadays present tumors with a less aggressive nature (e.g. located in the prostate, without metastasis at the time of the diagnosis) (32). However, the main disadvantage associated with PSA screening is the overdiagnosis of PCa patients, with the consequent overtreatment (40). In addition, other problem associated with PSA test is its low specificity, since plasma levels of PSA can also be elevated in response to non-tumor conditions, such as benign prostate hyperplasia (BPH), prostatitis and sexual activity, among others (41, 42). For that reason, nowadays there is not a clear cut-off value of PSA to indicate a prostate biopsy, especially when it is ranged between 3-10 ng/mL (defined as **PSA grey zone**). Therefore, as it has been mentioned above, the low specificity of PSA (especially in the grey zone) for detecting PCa cases makes the finding of additional non-invasive diagnostic biomarkers imperative.

The digital rectal exam (**DRE**) is a clinical procedure by which the urologist is able to detect abnormalities in the prostate gland (43). Specifically, PCa is usually linked to the presence of bumps on the normally smooth surface of the prostate. Previously to the PCa screening using PSA test, PCa was diagnosed after the appearance of symptoms by DRE and biopsy. Nowadays, DRE is considered the main complement for PSA levels to screen PCa. However, it should be noted that DRE diagnostic capability is dramatically reduced when PSA levels are <2 ng/mL (44-46).

Despite the establishment of PSA test for PCa screening and even if its levels are positive, a **prostate biopsy** is always needed to confirm PCa diagnosis. Nowadays, this

technique consists on obtaining a core needle biopsy guided by transrectal ultrasound (TRUS). To interrogate the presence of prostate adenocarcinoma in the biopsy, p63 and cytokeratin 5/14 staining are analysed, which are absent in PCa cells (47). Additionally, the grade of the tumors is evaluated by **Gleason score** (GS) and tumor–node–metastasis (**TNM**) systems (48). Unfortunately, biopsies are associated with adverse effects such as bleeding, pain and infections (49) and, for that reason, the discovery of novel biomarkers with the ability to indicate when a biopsy should be obtained is urgently needed in order to avoid unnecessary biopsies.

1.1.3.2. Gleason score (GS)

GS is a pathological grade reported for the first time by Donald F. Gleason in 1966 (50). Specifically, GS is based on the grade of histological dedifferentiation (glandular pattern) of the PCa tissue. The glandular pattern ranges from 1 (most differentiated) to 5 (least differentiated) (50). GS is the sum of the glandular patterns of the most and second-most dominant (in terms of volume) PCa foci. If only one focus is present, the primary grade is doubled. If a grade comprises <5% of the cancer volume, it is not incorporated in the GS (5% rule).

Importantly, due to the misleading clinical implications of GS2-4, GS starts at 6 in prostate biopsy and radical prostatectomy specimens (51). For that reason, PCa with GS6 is commonly known as non-significant PCa (NonSigPCa) while PCa with GS≥7 as clinically significant PCa (SigPCa).

The last update of GS criteria was accepted in 2016 by the World Health Organization (WHO) (52, 53). Briefly, the new International Society of Urological Pathology (ISUP)

2014 Gleason grading represents a compression of GS<6 to ISUP grade 1, and GS 9-10 to ISUP grade 5, whereas GS 7 is expanded to ISUP grade 2, i.e. 7 (3+4) and ISUP grade 3, i.e. 7 (4+3) showing a better prognosis correlation (52-54) (Figure 2).

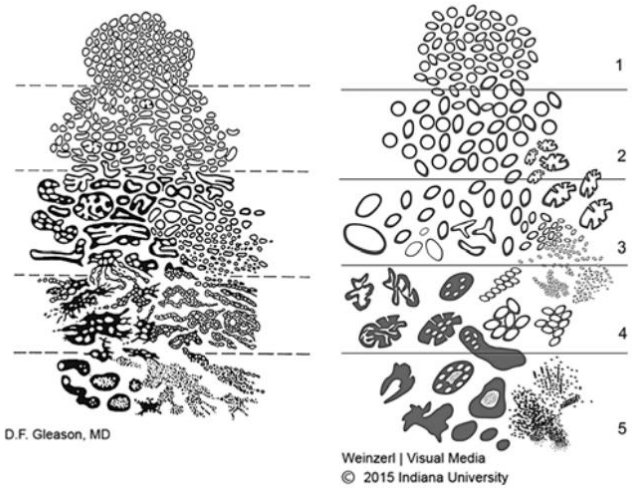

Figure 2: Comparison between the original (left panel) and the 2015 modified ISUP (right panel) Gleason Score schematic diagrams of PCa histologic patterns. Source: Epstein et al., Am J Surg Pathol 2016.

1.1.3.3. Classification

The classification of PCa is based on the TNM staging system, which considers the size of the primary tumor (T), whether it is spread to nearby lymph nodes (N), and the presence of metastasis (M) (48, 55). The clinical staging is based on DRE, PSA test and GS of the biopsy, while the pathologic stage is based on the anatomo-pathologic information obtained from the prostate sample after radical prostatectomy (Table 1).

Table 1. Tumor–node–metastasis (TNM) system classification of prostate cancer (PCa) tumors.

PRIMARY TUMOR (T)	
TX	Primary tumor cannot be assessed
T1	Clinically inapparent tumor that is not palpable
T1a	Tumor incidental histologic finding in 5% or less of tissue resected
T1b	Tumor incidental histologic finding in more than 5% of tissue resected
T1c	Tumor identified by needle biopsy found in one or both sides, but not palpable
T2	Tumor is palpable and confined within prostate
T2a	Tumor involves one-half of 1 lobe or less
T2b	Tumor involves more than one-half of 1 lobe
T2c	Tumor involves both lobes
T3	Extraprostatic tumor that is not fixed or does not invade adjacent structures
T3a	Extraprostatic extension (unilateral or bilateral)
T3b	Tumors invade seminal vesicle(s)
T4	Tumor is fixed or invades adjacent structures other than seminal vesicles
Pathologic (pT)	
pT2	Organ confined
pT3	Extraprostatic extension
pT3a	Extraprostatic extension or microscopic invasion of the bladder neck
pT3b	Tumors invade seminal vesicle(s)
pT4	Tumor is fixed or invades adjacent structures other than seminal vesicles
REGIONAL LYMPH NODES (N)	
NX	Regional lymph nodes were not assessed
N0	No positive regional lymph nodes
N1	Metastases in regional lymph node(s)
DISTANT METASTASIS (M)	
M0	No distant metastasis
M1	Distant metastasis
M1a	Nonregional lymph nodes(s)
M1b	Bone(s)
M1c	Other site(s) with or without bone disease

1.1.3.4. Novel diagnostic biomarkers

The diagnostic ability of PSA is especially questionable in the so-called grey zone (3-10 ng/mL), mainly due to the extremely low specificity of PSA in this range (56). In addition, the prognostic value of PSA test is also very limited (57). These drawbacks of the PSA test are associated with overdiagnosis and overtreatment of PCa patients, which could generate severe side effects in a significant percentage of patients (58, 59). For that reason, the scientific community strive to identify novel PCa biomarkers that: i) could serve as risk indicators for disease with low PSA values (<10 ng/ml); ii) could act as prognostic markers to distinguish indolent from aggressive disease; iii) predict PCa aggressiveness (prognostic biomarkers); and iv) may be useful to diagnose metastatic cancer. In this sense, a broad number of novel biomarker panel tests as well as individual biomarkers have been already approved for the FDA or regulated by Clinical Laboratory Improvement Amendments (CLIA).

Serum based assays targeting kallikreins have been recently developed and proved their efficacy to diagnose PCa, including **Prostate Health Index (PHI) test** and the **four kallikrein (4K) score test**. PHI is based on the levels of total-, free- and pro-PSA, while 4K score is an algorithm including free-, intact- and total PSA and kallikrein-like peptidase 2 (hK2) in addition to clinical data (i.e. Age, DRE and prior biopsy status) (60, 61). Both tests show similar capacity for detecting PCa (PHI-AUC=0.69 vs 4K-AUC=0.70) (62). Unfortunately, their specificity remains low (approximately 30%) (63).

On the other hand, the only FDA-approved urine-based test for reducing unnecessary biopsies is **PCA3 test** [38,39]. Specifically, PCA3 is based on the urine levels, after DRE stimulation, of the prostate cancer specific (PCA3) long non-coding RNA (64), which has

shown high accuracy detecting PCa (sensitivity: 67%; specificity: 83%) (65). Additional available tests based on urine biomarkers, although not yet approved by the FDA, are **SelectMDX** test, **Mi-Prostate Score** and **ExoDx Prostate Intelliscore**. SelectMDx assay is based on the combination of the mRNA levels in urine of *DLX1* and *HOXC6*, resulting in area under the curve (AUC) of 0.73 for detecting PCa (66). In addition, Michigan Prostate (Mi-Prostate) score is based on the detection in urine of a gene fusion that is commonly present in PCa (*TMPRSS2-ERG*) combined with urine levels of PCA3, resulting in a AUC of 0.76 for detecting PCa and 0.78 for detecting high-grade PCa (67). Lastly, ExoDx Prostate Intelliscore assay, based on exosomal mRNA levels of PCA3, ERG and SPDEF has shown an AUC of 0.71 for detecting PCa (68).

Finally, there are also some commercially available biopsy-based tests, including **OncotypeDx**, **Prolaris** and **Decipher**, which are especially useful for predicting PCa outcome. Specifically, OncotypeDx and Prolaris are able to predict biochemical recurrence ($OncotypeDx^{HR}$: 2.9, $Prolaris^{HR}$: 1.22) (69, 70), while Decipher shows the risk for developing metastasis after biochemical recurrence (AUC: 0.82) (71, 72). OncotypeDx is based on 12 cancer-related genes, Prolaris is based on 31 genes involved in cell cycle progression, while 22 coding and non-coding regions are analysed in Decipher test (70).

1.1.4. Treatment

1.1.4.1. Therapeutic options

The therapeutic options used in the current clinical practise to treat PCa are briefly explained below. Firstly, although **active surveillance** is not a treatment by itself, it is a

clinical approach for monitoring slow-growing localised PCa. Indeed, the main purpose of active surveillance is to avoid unnecessary treatments in men with localised PCa but also to assure the appropriate follow-up of the patients that will eventually need a treatment due to cancer progression (73). Patients remain under close surveillance through structured surveillance programmes with regular follow-up, and curative treatment is prompted by predefined thresholds indicative of potentially life-threatening disease.

In the case of surgery, the most common approach used to eradicate PCa is **radical prostatectomy** (RP), which consists on the removal of the entire prostate and seminal vesicles, followed by vesicourethral anastomosis (73). RP can be performed by open-, laparoscopic- or robot-assisted (RARP) approaches. The modern RARP (using the da Vinci Surgical System®) has become the preferred minimally invasive approach for RP (74).

In addition, PCa can be also treated with **radiotherapy** [i.e. External beam radiation therapy (EBRT)], being Intensity-modulated radiotherapy (IMRT) the current gold standard, which is characterized by the fact that the radiation beams are closely directed to the tumoral area in order to avoid any damage of non-tumor cells (75). Moreover, prostate brachytherapy is another form of radiation therapy used to treat prostate cancer, which consists on placing radioactive sources in the prostate gland, where the radiation can kill the cancer cells while causing less damage to healthy tissue nearby. Prostate brachytherapy is divided based on its dose [High dose rate (HDR) or Low dose rate (LDR) brachytherapy] (76).

Due to the crucial role that androgens play on PCa development and aggressiveness (further explained in section “Biology of PCa”), **androgen deprivation** has been stablished

as a key therapeutic option to treat PCa (77), which consists on the blockade or down-regulation of AR signalling by: i) suppression of androgens release (LHRH agonists, antagonists and abiraterone), or ii) inhibition of AR (anti-androgens). These two methods can be combined to achieve what has been known as maximal androgen blockade (77).

Specifically, **LHRH agonists** result in a decrease of LH and FSH secretion due to negative feedback, thus leading to a suppression of testosterone production (optimal levels are usually reached within 2-4 weeks) (78). On the other hand, **LHRH antagonists** immediately bind to LHRH receptors, leading to a rapid decrease in LH, FSH and testosterone levels. Both treatment types have shown similar clinical results (79). Among the old-fashioned non-steroid anti-androgens, the most used is **bicalutamide**, since it is more tolerable than flutamide and nilutamide (80). Novel compounds targeting the AR axis have been developed during the last years, including **abiraterone** (CYP17 inhibitor), **enzalutamide** and **apalutamide** (non-steroid anti-androgens with higher affinity for the AR than bicalutamide) (81-83). Specifically, these novel compounds have been approved for metastatic CRPC (mCRPC), although abiraterone has recently been approved also for hormone sensitive PCa.

Chemotherapy is one of the main therapeutic approaches to treat aggressive PCa. Specifically, different taxanes (e.g. docetaxel, cabazitaxel) are used in clinical practise. **Docetaxel** can be used as a first line treatment for mCRPC. On the other hand, **cabazitaxel** is a second-generation taxane that has been approved as a second- or third-line treatment in mCRPC patients whose disease has progressed following docetaxel or antiandrogens (84).

Finally, **sipuleucel-T** platform remains the only **immunotherapy** approach for CRPC patients (85), while radiotherapy with **radium-223** is only approved for mCRPC patients with symptomatic bone metastasis (86).

It should be mentioned that the type and duration of the specific therapeutic option selected to treat PCa patients strongly depend on several clinical characteristics and on patient preference. The treatments strongly suggested by the European Association of Urology (EAU) Guidelines on Prostate Cancer 2020 according to the stage of the disease are summarized in the Table 2.

Table 2. Therapeutic options for prostate cancer.

Disease stage	Treatment
Low-risk localised disease **PSA<10 ng/mL and** **GS < 7 (ISUP 1) and cT1-2a**	- Active surveillance - LDR brachytherapy - IMRT
Intermediate-risk localised disease **PSA 10-20 ng/mL or** **GS 7 (ISUP 2/3) or cT2b**	- RP - LDR brachytherapy - EBRT plus ADT (4-6 months)
High-risk localised disease **PSA > 20 ng/mL or** **GS > 7 (ISUP 4/5) or cT2c**	- RP - EBRT plus ADT (2-3 years)
Locally advanced disease **Any PSA, any** **GS (any ISUP grade), cT3-4 or N+**	- RP - Adjuvant EBRT after RP - RT in combination with ADT (2-3 years)
Metastatic disease	- ADT plus docetaxel - ADT plus 2nd generation antiandrogens
Biochemical recurrence	- Salvage RT
Castration resistant disease	- Docetaxel - Abiraterone/Enzalutamide/Cabazitaxel - Radium 223 - Sipuleucel-T

LDR: Low dose brachytherapy; IMRT: Intensity-modulated radiotherapy; RP: Radical prostatectomy; EBRT: External beam radiation therapy; ADT: Androgen deprivation therapy.

1.1.4.2. Potential treatments under research

It should be noted that, even today, the treatments used in localized PCa cases are still associated with several side effects, including sexual impotence, urinary incontinence and infections, among others (87). Despite the great advances in the treatment of advanced PCa, this phenotype remains lethal so far. Fortunately, during the last years, a significant improvement in the PCa treatment field has been observed, mainly due to the technological development that has been implemented at the surgical level and to the novel drugs approval (e.g. abiraterone, enzalutamide, olaparib) (88-92). In the case of localized PCa, novel and promising techniques are under research, such as high-intensity focused ultrasound and focal therapy (93). On the other hand, in the case of mCRPC, the results from PROfound phase III clinical trial have resulted in the approval of olaparib (by the FDA), a Poly (ADP-ribose) polymerase (PARP) inhibitor (94), as a novel treatment for CRPC patients with mutations in DNA repair genes, being the first example of personalized medicine in PCa patients (88, 95).

Nevertheless, despite the advances in the last years, it is essential to precisely unveil the molecular, cellular and endocrine-metabolic events underlying the development, progression and aggressiveness of PCa, in order to identify novel diagnostic, prognostic and therapeutic targets in PCa, and especially mCRPC, which represents an urgent and unmet clinical need.

1.1.5. Biology of PCa

As it has been explained in this Doctoral Thesis (above sections), PCa is categorized based on the response to castration (the main pharmacological approach so far, since the growth of these tumors is strongly androgen-dependent) in: i) **Hormone-sensitive PCa**, an early phase of the disease, comprised by tumors sensitive to castration; and ii) **CRPC or hormone-refractory PCa**, a late phase of the disease, comprised by tumors insensitive to castration (7, 8). For that reason, it is important to distinguish between the molecular events involved in the development and progression of the disease (early molecular events), and those involved in the switching from hormone-sensitive to CRPC (late molecular events).

1.1.5.1. Early molecular events

Several genes have been found to be significantly mutated in primary tumors (96-99). Among all mutated genes observed, *SPOP*, *TP53*, *FOXA1*, *PTEN*, *MED12*, *CDKN1B* and *NKX3.1* were the most consistently altered across the different studies published so far (96-99). In addition, fusions of the E-twenty-six (ETS) family genes have also been consistently found in primary tumors (99).

Specifically, the fusion between AR-regulated genes with members of the ETS family is the most common alteration in primary PCa (about 50% of the tumors) (100). The most common ETS family genes-AR rearrangement results in the **TMPRSS2-ERG fusion** oncogene (100). *In vivo* models show that the expression of ERG in mouse prostate epithelial cells causes slow-growing prostate tumors through the activation of Hippo pathway (101).

The Phosphatase and tensin homolog (***PTEN***) gene, which negatively regulates the AKT/PKB signaling pathway (102, 103), is lost (deletion) and/or mutated in 40% of primary PCa (104). *In vivo* studies showed that a uni-allelic loss of *Pten* results in PIN development, while the bi-allelic loss of *Pten* results in invasive PCa (105).

Likewise, genomic alterations of the tumor suppressor protein p53 **(*TP53*)** have been reported in approximately 25–30% of clinically localized PCa (106). Importantly, as occurred when analysing *PTEN* loss, PIN lesions also show *TP53* genomic alterations, indicating the oncogenic role of these dysregulations in PCa (106). A mouse model with *TP53* inactivating mutation has been reported, and this alteration was sufficient to produce PIN lesions and invasive PCa (107).

Moreover, the Speckle Type BTB/POZ Protein **(*SPOP*)** tumor suppressor, which inhibits AR signalling promoting SRC-3 (AR co-activator) degradation, is mutated in 6-15% of localized PCa (96, 99). The role of SPOP in PCa development was confirmed by an *in vivo* study, in which SPOP mutation resulted in PCa trough PI3K/mTOR and AR signaling activation (108).

Less commonly but consistently mutated genes in PCa are *FOXA1*, *CDKN1B* and *MED12*. Specifically, Forkhead Box A1 **(*FOXA1*)**, a regulator of the transcriptional activity of AR (96), has been reported to be mutated in approximately 3-4% of localized PCa (96, 109). It has been recently reported that the mechanism by which *FOXA1* mutations drive PCa might be the dysregulation of the normal luminal epithelial differentiation programs of prostate cells (110). The tumor suppressor Cyclin-dependent kinase inhibitor 1B **(*CDKN1B*)**, which encodes the cell cycle inhibitor P27(KIP1), is

significantly mutated in about the 2% of primary PCa (99). Importantly, although *Cdkn1b*$^{-/-}$ mice did not develop prostate tumors, PCa at complete penetrance was observed in *Pten*$^{+/-}$/*Cdkn1b*$^{-/-}$ mice (111). NK3 Homeobox 1 **(NKX3-1)** is a transcription factor that acts as a negative regulator of epithelial cell growth in prostate tissue (112). Deletion of *NKX3-1* is a common event in early phases of PCa and cooperates with the activation of TMPRSS2:ERG (113). Remarkably, *in vivo* models show that the loss of *Nkx3-1*, in conjunction with the loss of *Pten*, produces a constitutive activation of PI3K/AKT pathway, promoting PCa development (114). Finally, **Mediator Complex Subunit 12 (*MED12*)**, a gene that encodes a modulator of hedgehog signaling pathway (115), has been found mutated in 5% of the primary PCa (116). However, to date, there are no experimental data demonstrating the role of *MED12* as a PCa driver.

1.1.5.2. Late molecular events

ADT produces a significant remission (24-36 months) of the disease, accompanied by a PSA decline, in patients with locally advanced PCa (117). Unfortunately, these tumors eventually became resistant to the treatment and PSA levels increase again (biochemical recurrence) (117). As mentioned before, this type of PCa is then known as CRPC, which remains lethal nowadays, with a mean survival time of 16-18 months (118). The molecular biology of CRPC is even more complex than the biology of primary PCa since it has been shown that the mutational burden is much higher in CRPC compared with localized PCa (119-121). The molecular events related to CRPC could be classified in those affecting: **i)** AR pathway, and **ii)** Non-AR related pathways.

i) *Molecular events affecting AR pathway:* Data from Robinson *et al.*, after the analysis of 150 mCRPC, revealed that the most altered molecular pathway was AR signalling (71.3% of the events), being *AR* the most mutated gene (121). In addition, some key regulators of the AR pathway were also found to be significantly mutated in CRPC, including *FOXA1*, *NCOR1*, *NCOR2* and *ZBTB16* (120, 121). Furthermore, upregulation of AR splicing variants (some of which lacking the AR binding domain and being constitutively active) is another relevant molecular characteristic of a significant percentage of CRPC tumors (122).

ii) *Molecular events non-affecting AR related pathways:* The second most altered pathway in this pathology is PI3K/AKT, with up to 49% of somatic alterations, characteristically biallelic *PTEN* loss, which has been previously suggested to be associated with worse outcome in patients under abiraterone treatment (123). The following most altered pathway is DNA damage repair (DDR), which is present in 23% of patients. As example, Breast cancer 2 (*BRCA2)* is the most frequent altered gene, which has opened a new therapeutic option for these patients as are perfect candidates to be treated with PARP inhibitors (e.g. Olaparib) (88, 95). The fourth most common alteration is Wnt pathway, with frequent mutations in *APC* and *CTNNB1* (121). Finally, *RB1* and *TP53* loss are more prevalent in CRPC than in primary PCa (104, 124).

There are three different hypothesis that combine the molecular events described above to explain the molecular switch from PCa to CRPC: i) ADT produces an expansion of neuroendocrine cell population, which does not express AR, and therefore is not affected by ADT (clonal expansion theory); ii) ADT produces an acute stress in castration-sensitive PCa cells, which results in a deep molecular alteration (neuroendocrine trans-differentiation theory); and, iii) a mix of both theories.

However, it should be emphasized that the molecular events underlying the development and progression of PCa as well as the switching from hormone-sensitive to CRPC disease are still to be fully defined. Remarkably, the vast majority of events described to date relate to genetic alterations (mutations, genomic rearrangements, etc.), while the dysregulation of alternative cellular and molecular processes that could be a source of oncogenic alterations in PCa have been less explored hitherto. In this sense, one of the main cellular processes that has emerged in the last years for its implication in the oncogenic development is the **splicing process** (125, 126), which represents one of the main focuses of this Doctoral Thesis and is further described below.

1.2. Splicing and PCa

Emerging evidence indicate that alterations in the splicing process can result in major transcriptomic changes, which lead to the development or contribute to the progression of several pathologies, including cancer (127-129). Splicing is a co-transcriptional process by which introns are removed from the pre-mRNA and exons are fused, generating mature RNAs. Biochemically, splicing process is mainly divided in two transesterification reactions. First, the nucleophilic attack of the 5' splice site (5'SS) by the branch point (BP) of the intron results in the formation of the intron lariat. Subsequently, another trans-esterification reaction between the 5'SS and the 3' splice site (3'SS) is carried out, which finally leads to the excision of the intron lariat and the junction between the consecutive exons (130).

1.2.1. Constitutive and alternative splicing

Constitutive splicing consists on the excision of all introns and the binding of the exons present on the pre-mRNA to produce a mature mRNA molecule. However, about 95% of the eukaryotic genes undergo alternative splicing, a more complex process by which several mature mRNA molecules (named "splicing variants") are generated from a single pre-mRNA molecule (131). Specifically, five different alternative splicing events have been defined (Figure 3): i) cassette exon skipping, ii) alternative 5´SS, iii) alternative 3'SS, iv) intron retention, and v) mutually exclusive exons (132, 133).

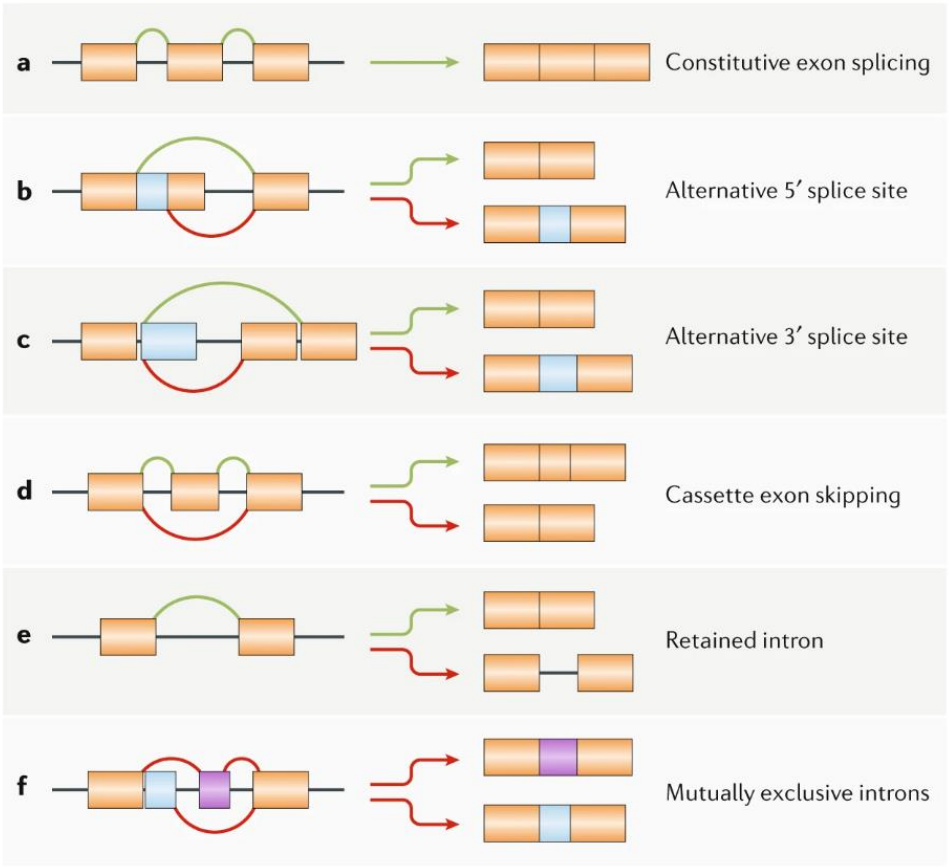

Figure 3: Schematic representation of constitutive splicing events. a) Constitutive exon splicing. **b-f)** Alternative splicing variants are produced following different splicing events [Alternative 5´ splice site **(a)**, alternative 3´ splice site **(b)**, cassette exon skipping **(c)**,

retained intron **(d)** and mutually exclusive exons **(f)**]. Source: *Paschalis et al., Nat Rev Clin Oncol 2018.*

Alternative splicing markedly increases the molecular and functional complexity of eukaryotic cells, inasmuch as it allows the generation of several mature RNAs from a single gene, which may exhibit altered, or even opposite, functions than the canonical one (132, 134).

1.2.2. Splicing regulation

The splicing process is catalysed by the **spliceosome**, a dynamic macromolecular complex composed by small ribonucleoproteins (snRNPs) and associated proteins (131). In mammals, there are two types of spliceosomes, which are involved in the regulation of different types of introns: i) Major spliceosome, which acts on U2-type introns (95% of all introns), and ii) minor spliceosome, which acts on U12-type introns (127, 135). Both major and minor spliceosomes are composed by five snRNPs complexes (major spliceosome: U1, U2, U4, U5 and U6; minor spliceosome: U11, U12, U4atac, U5 and U6atac), which in turn are formed by small nuclear RNAs (snRNAs; major spliceosome: RNU1, RNU2, RNU4, RNU5 and RNU6; minor spliceosome: RNU11, RNU12, RNU4ATAC, RNU5 and RNU6ATAC) and specific proteins (136, 137).

The regulation of the splicing process is carried out by cis- and trans-elements. Specifically, cis-regulatory elements are RNA sequences classified according to their localization and function in the splicing process: ESE (exonic splicing enhancer), ESS (exonic splicing silencer), ISE (intronic splicing enhancer), and ISS (intronic splicing

silencer) (Figure 4) (136, 138). On the other side, the trans-elements are the so-called **splicing factors (SFs)**, proteins with the capacity to interact with RNA sequences (splice sites) and/or elements belonging to the spliceosome. There are two main families of SFs: i) Serine-arginine proteins (SR-proteins), which are usually enhancers of exon splicing, binding to ESE and recruiting the spliceosome components (139, 140), and ii) heterogeneous nuclear ribonucleoproteins (hnRNPs), which repress splicing by directly antagonizing the recognition of splice sites (139, 140). Importantly, SFs are pleiotropic proteins, involved in several processes apart from splicing, including transcription, translation, RNA trafficking and RNA degradation, among others (141-143). Indeed, SFs can also control nonsense-mediated mRNA decay (NMD) (144), an eukaryotic molecular mechanism tightly linked to splicing process, which allows the degradation of aberrant mRNA transcripts (143, 145), thus increasing the complexity and government of RNA metabolism.

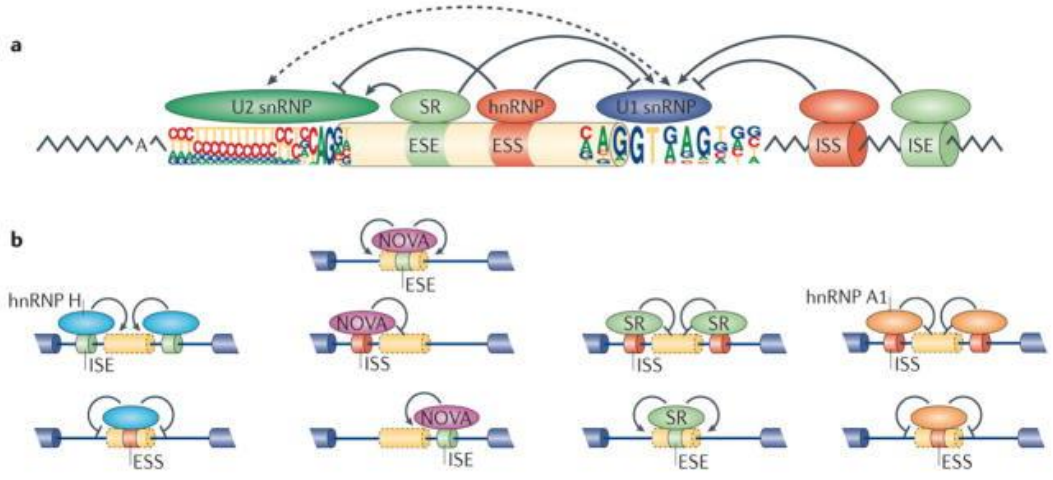

Figure 4: Schematic view of splicing process regulation. a) Splicing process is controlled by the selection of splice sites, according to cis-regulatory splicing elements (i.e. ISE, ISS, ESE, ESS) and trans-regulatory elements (i.e. SFs)**. b)** The action of the SFs depends on the context of the cis elements they bind to. ISE: intronic splicing enhancer; ISS: intronic

splicing silencer; ESE: exonic splicing enhancer; ESS: exonic splicing silencer. SF: splicing factor. Source: Matera and Wang, Nat Rev Mol Cell Biol 2014.

Therefore, SFs regulate the activity of spliceosome, and hence the splicing process, through binding ISS, ISE, ESS or ESE regions. Briefly, U1 snRNP interact with the 5'SS, while the splicing factor 1 (SF1) bind the branch point and U2 auxiliary factor (U2AF) bind the 3'SS (146, 147). This complex, named E complex, results in the pre-spliceosomal A complex when U2 snRNP substitutes SF1 in the branch point. Then, U4, U5 and U6 form the pre-catalytic B complex associating with the formed spliceosome. When U4 is removed, U6 replaces U1 and interacts with U2 bringing the 5'SS and the branch point closer together, forming the catalytic C complex, and allowing the first reaction of trans-esterification (131, 148, 149). Finally, U5 facilitates the second trans-esterification step, approximating the two exons and allowing its junction and the removal of the intron lariat (149) (Figure 5).

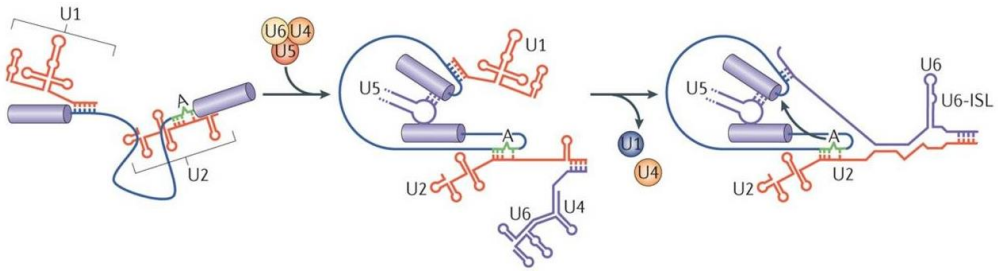

Figure 5: Intron identification by snRNPs, and subsequent intron lariat formation and release. Source: *Matera and Wang, Nat Rev Mol Cell Biol 2014.*

1.2.3. Splicing alterations in PCa

As mentioned above, dysregulation of alternative splicing has emerged as a novel hallmark of cancer, including PCa (126, 150). In fact, the expression levels of several alternative splicing variants have been found to be deeply dysregulated in tumoral tissues (125, 126, 151). Likewise, aberrant splicing variants (defined as those that have not been generated by any described splicing event) have been also described in several cancer types (125, 151). In the specific case of PCa, alteration of splicing process is especially relevant from a clinical perspective. In fact, broad differences in the global splicing pattern have been found between PCa cases with different aggressiveness status (e.g. PCa from African American vs PCa from Caucasian men) (152).

Splicing processing of specific genes has been found to be especially dysregulated and linked to relevant functional behaviours in PCa. Due to the key role that AR plays in PCa pathophysiology, AR splicing variants (especially *AR-v7*) remain the most studied splicing variants in PCa (153, 154). The first evidence indicating the existence of these variants was reported by Dhem *et al.* in 2008 (155). After that, and based on the results from many studies, *AR-v7* has arisen as the most clinically relevant AR splicing variant (156-161). Specifically, to generate *AR-v7*, AR pre-mRNA undergoes an aberrant splicing process at the cryptic exon 3, which results in a shorter protein lacking the ligand-binding domain (LBD) (Figure 6). Importantly, due to the lack of LBD, *AR-v7* remains constitutively active even in the absence of androgens, consequently playing a key role in the establishment of CRPC and in the development of abiraterone/enzalutamide resistance (155, 156). Even though several SFs have been associated to *AR-v7* generation, there are no approved drugs able to inhibit AR-v7 activity so far. Therefore, further comprehension of its biology

remains a critical issue to develop novel drugs able to downregulate or block *AR-v7* and tackle lethal CRPC.

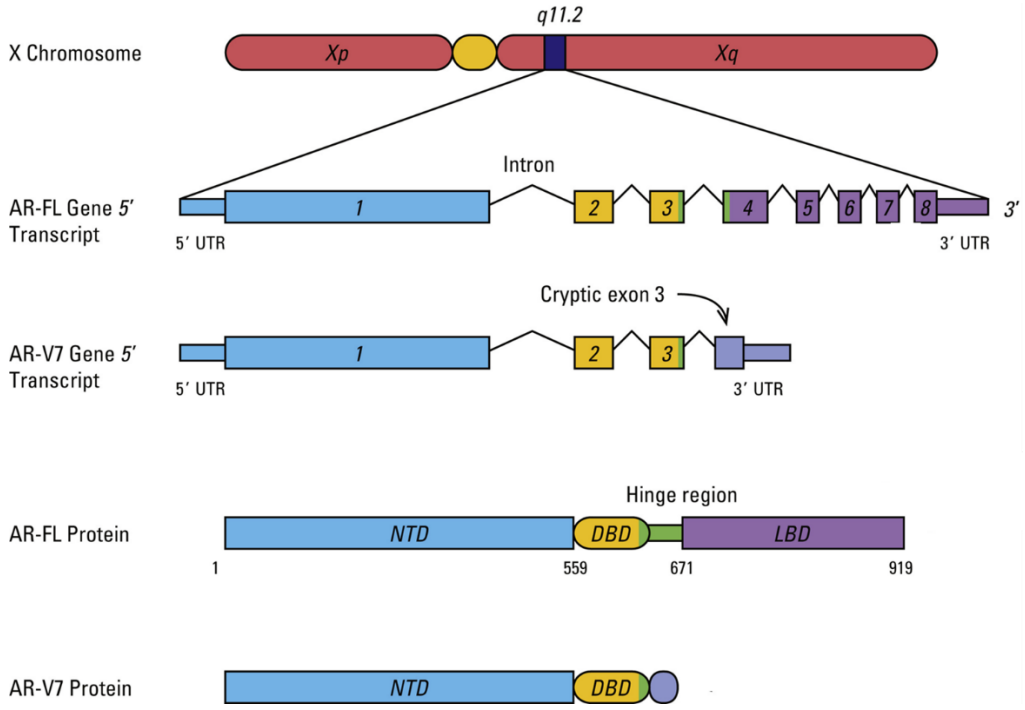

Figure 6: ***Transcript sequence and structure for the full-length AR (AR-FL) and the AR splice variant 7 (AR-V7).*** Adapted from: *Luo, Asian J Androl 2016.*

Apart from AR, the splicing processes of other genes related to the endocrine aspect of PCa are deeply altered in this disease, including somatostatin receptor 5 (*SSTR5*) and ghrelin (*GHRL*) genes. Specifically, *SST5TMD4* is an aberrant splicing variant generated from the somatostatin receptor 5 gene (*SSTR5)*, which is overexpressed in PCa and plays a relevant oncogenic role in this disease through the modulation of several tumor-related signalling pathways (162). Similarly, In1-ghrelin is an alternative splicing variant arising from the ghrelin gene (*GHRL*), which has been reported to be overexpressed in PCa, linked to aggressiveness parameters, and shows an oncogenic role in this tumor pathology (163). Interestingly, In1-ghrelin can be released to plasma, wherein its levels are higher in PCa

patients as compared to healthy individuals, suggesting a potential role as non-invasive PCa biomarker (163). Another example is REST, a transcription factor that represses the expression of genes that are involved in the development of a neuronal phenotype (164). However, the alternative splicing variant *REST4*, which is overexpressed in NEPC samples, antagonizes *REST* function (by direct binding), leading to the development of this lethal PCa phenotype (165, 166). In addition, other splicing variants have been found to be dysregulated in PCa and to show a significant clinical implication in this disease, including *FGFR2-IIIb* (167), *KLF6-SV1* (168), *VEGF165b* (169), *CCND1b* (170), among others.

In line with this, several SFs have been also found to be dysregulated in PCa (150, 171). Many of them [i.e. *U2AF2*, *SFPQ*, *SF3B2*, *KDM4B*, or *KHDRBS1* among others] have been overexpressed in PCa and related to the appearance of *AR-v7* splicing variant and, therefore, could be linked to CRPC development (158, 172-175). Likewise, *SRRM4* has been reported to be directly involved in the regulation of alternative splicing of *REST*, leading to *REST4* generation in PCa cells and therefore driving NEPC (165, 166). In addition, Munkley *et al.* recently reported that androgens are able to regulate splicing process globally through the control of *ESRP2* transcription (176), thus increasing the complexity of the relation between PCa and alternative splicing. However, these studies have been focused in specific SFs, and as far as there are more than 300 SFs described hitherto, comprehensive and further studies analysing a representative set of SFs are strongly needed to define novel PCa biomarkers and/or therapeutic targets.

Furthermore, several small molecules have been reported to target the splicing process, specifically trough the blockade of SF3B1, a key pivotal spliceosome component which is

necessary for a correct assembly of the spliceosome (177), including pladienolide-B, E7107 and spliceostatin A. However, although some of these SF3B1 inhibitors have shown antitumor effects in several cancer types, they have poorly studied in PCa and therefore, this research avenue needs to be deeply studied.

1.3. Pathophysiological relationship between metabolism dysregulation and PCa

1.3.1. Obesity and Diabetes Mellitus

Obesity has been historically defined as an excessive accumulation of adipose tissue, and more recently as a body mass index (BMI) >30, which is calculated by the following formula "weight (kg)/height^2 (m^2)". Obesity has been postulated to represent one of the most relevant pathological conditions of XXI century, not only because of the high number of affected people, but because obesity also increases the risk of developing severe endocrine pathologies [e.g. Diabetes Mellitus (DM)] and certain tumor pathologies, including PCa (178-181).

Indeed, several studies have demonstrated that PCa risk increases with obesity (180, 181). Particularly, obesity has been linked to a more aggressive disease, in terms of PCa specific mortality, biochemical recurrence and CRPC development (182-184). DM comprises a group of metabolic disorders characterized by high blood sugar levels over time. Specifically, patients with type 2 DM (T2DM) have high blood sugar levels and are resistant to insulin (185). Although some clinical studies have reported that T2DM patients were less likely to develop PCa (186, 187), some recent reports indicates that T2DM may

represent a risk factor for PCa (188, 189). Specifically, Tseng *et al*. showed, in a study comprising 494,630 Taiwan men, that T2DM was associated with an increased PCa risk independently of the duration of T2DM onset, with the highest risk ratio observed in 40–64 years old patients (189). This apparent discrepancy in the results showed in the studies exploring the association between DM and PCa could be explained by the fact that recent-onset DM increased the risk of PCa, while long-standing DM reduced it (190).

From a molecular perspective, several mechanisms have been postulated to play a relevant role in the pathophysiological interplay between obesity/DM and PCa (e.g. adipokines, IGF1, insulin or even the ghrelin system, which will be explained in detail in section 3.3) (191, 192). However, the precise molecular mechanisms underlying this pathophysiological relationship are still to be fully elucidated. Nevertheless, this pathological association between metabolic disorders and PCa may be exploited as a source for novel and more personalized diagnostic and prognostic biomarkers, as well as additional, patient-tailored therapeutic strategies based on the close interplay between these highly incident pathologies, as it is described in the following sections.

1.3.2 Influence of metformin and statins in the development/progression of PCa

Metformin is a first-line oral anti-diabetic drug commonly used to treat T2DM, while **statins** are used for the management of patients with hypercholesterolemia. Given the relation of these metabolic dysregulations (i.e. T2DM, hypercholesterolemia, obesity) with PCa risk and aggressiveness (193-195), both metformin and statins rapidly became focus of interest in the oncology field (196-199). In this sense, a widespread strategy to find

effective treatments against neglected pathological conditions is drug repositioning, which consists on the investigation of existing drugs for new therapeutic purposes (200, 201). In fact, several clinical studies have shown that metformin and statins are associated to beneficial effects in patients with several cancer types, including PCa (202-204). In addition, metformin and statins have shown antitumor actions on PCa *in vitro* and *in vivo* (205-208). However, there are some controversial results in this regard, especially related to statins (209), thus requiring further scientific evidence.

Mechanistically, direct antitumor effects of metformin and statins are mainly associated to AMPK activation and HMGCoA-reductase inhibition, respectively (210, 211). However, several independent and/or additional mechanisms of actions have been proposed to underlie the antitumor actions of metformin and/or statins, including TNFα inhibition (212), REDD1 upregulation (213) or inhibition of protein geranylgeranylation (214).

Finally, these drugs have been reported to additively reduce aggressiveness features of cancer cells *in vitro* and *in vivo,* including PCa (215-218). However, the specific molecular mechanisms underlying these additive actions remain poorly described. In addition, since all these previously mentioned studies involving PCa cells have been performed with specific statins, comprehensive studies comparing different types of biguanides and statins side-by-side are still required.

1.3.3 Implication of ghrelin system in the interplay between metabolic dysregulations an PCa

Ghrelin system is a complex and pleiotropic endocrine-metabolic axis comprised by several factors (i.e. ligands, receptors and enzymes) (219) that has been found to be closely

related to the development and progression of different tumor pathologies (219, 220) and could, therefore represent an important link between metabolic dysregulations and cancer. Specifically, ghrelin is a 28-amino acid (aa) hormone identified by reverse pharmacology as the endogenous ligand for the growth hormone secretagogue receptor (GHSR) (221). Ghrelin is expressed in several tissues where it exerts both endocrine and paracrine actions (219). Importantly, to exert its main functions [i.e. stimulation of growth hormone release, appetite and gut motility, as well as the regulation of glucose homeostasis, memory, cardiovascular- and immune-system (219, 222)], ghrelin requires to be acylated by the Ghrelin-o-acyl transferase (**GOAT**) enzyme (223). Specifically, GOAT-mediated acylation allows ghrelin to bind GHSR1a, a G protein-coupled receptor (GPCR) with seven transmembrane domains (TMD) that mediates the main ghrelin functions. Besides GHSR1a, a truncated GPCR isoform with only five TMD can also arise from GHSR gene, named GHSR1b. However, the functional activity of truncated GHSR1b remains to be fully elucidated (157, 167, 168).

Additionally, although unacylated ghrelin (Des-acyl ghrelin) is the most common form of ghrelin in plasma, its functional roles remains poorly defined (224). Apart from ghrelin, and after its discovery, several additional peptides derived from the ghrelin gene have been reported (219). In this scenario, mature ghrelin peptide results from proteolytic processing of a precursor peptide named preproghrelin, which is encoded by *GHRL* gene. Specifically, *GHRL* is composed of seven exons (from -1 to 4) that are combined through alternative splicing processes to produce different mRNAs, increasing the complexity of this system (225, 226). Among these splicing variants, **In1-ghrelin** [characterized by the retention of the intron-1 (227)] has arisen as the most clinically relevant, since its expression can be

modulated by metabolic conditions (228) and it is overexpressed in several endocrine-related cancers, including PCa, where it plays a pronounced oncogenic role (163). Indeed, beside the oncogenic activity of In1-ghrelin in PCa, it has been also suggested a potential role of this splicing variant as a non-invasive diagnostic biomarker in PCa, in that its plasma levels significantly distinguished between PCa patients and healthy individuals (163).

In1-ghrelin shares the first 5-aa with native-ghrelin, which is the minimum sequence required for ghrelin acylation by GOAT enzyme and for the binding and activation of GHSR1a (226). Remarkably, the expression of In1-ghrelin variant and GOAT, but not ghrelin, are positively correlated in several metabolic alterations (obesity, fasting, etc.) (229) and in certain endocrine-related cancers, including PCa (163, 227, 230), suggesting that In1-ghrelin variant could be a main substrate for GOAT. Indeed, GOAT has been found to be upregulated in PCa and linked to aggressiveness features (231). Likewise, GOAT has also shown a potential clinical utility as non-invasive diagnostic biomarker, in that it is secreted by PCa cells and its levels in plasma from patients with PCa are higher than those from patients with suspect of PCa but negative result in the biopsy (231, 232). Remarkably, the capacity of GOAT to diagnose PCa was even higher than that of PSA, specifically in patients with PSA in the grey zone (3-10 ng/mL) (232).

Despite of all the information presented herein, the real implication of the ghrelin system in the pathological interplay between metabolic dysregulations and PCa is still to be defined. As example, the pathophysiological role of GOAT in PCa still remains unknown and no studies have analysed the putative diagnostic capacity of In1-ghrelin and GOAT

levels in urine (a fluid enriched in prostate-secreted proteins), specially taking into consideration the metabolic status of the patients.

2. Aims of the study

The **GENERAL AIM of this Doctoral Thesis** was to determine the role of splicing-related elements (spliceosome components and splicing factors) and metabolic modulators (endogenous elements and exogenous treatments) in the development and progression of PCa, with the ultimate goal of discovering novel biomarkers and therapeutic tools to improve the diagnosis, treatment and management of PCa patients.

To achieve this main aim, we proposed the following **SPECIFIC OBJECTIVES (SO):**

SO1) To determine the expression pattern of splicing-related elements (spliceosome components and splicing factors) in PCa and explore their association with key clinical parameters.

SO2) To analyse the potential functional role and associated molecular mechanisms of specific, key splicing-related elements in PCa: SNRNP200, SRRM1, SRSF3 as well as RBM22 and SF3B1.

SO3) To investigate the functional and molecular effects of pladienolide-b (SF3B1 inhibitor) on tumor and non-tumor prostate cells, and to assess its therapeutic potential to tackle PCa.

SO4) To explore the putative contribution of the dysregulation of splicing-related elements in the antitumoral actions of metformin in PCa.

SO5) To assess the putative associations between PCa patients treatment with metformin and/or statins and the accompanying oncological aggressiveness parameters, and to explore *in vitro* in PCa cells the functional effects and mechanistic underpinnings of treatment with biguanides, statins and their combination.

SO6) To explore the diagnostic and prognostic capacity of GOAT enzyme levels in urine, as well as to interrogate its putative pathophysiological role in PCa.

SO7) To examine the capacity of urine In1-ghrelin levels to diagnose PCa in patients with low PSA (3-10 ng/mL), as well as to define their association with clinical features (metabolic and aggressiveness parameters).

3. Results and general discussion

3.1. Section I

Splicing machinery is dysregulated in prostate cancer and represents a source of prognostic biomarkers and therapeutic targets

PCa development, aggressiveness and/or resistance to pharmacological treatments (i.e. ADT, abiraterone and enzalutamide) have been associated with the presence of certain aberrantly-produced oncogenic splicing variants (SVs) (156, 162, 163, 167, 233), which could be originated by altered splicing process. In this sense, it is reasonable to envision that a dysregulation of the cellular machinery that catalyses and controls the splicing process would contribute relevantly to the extensive presence of oncogenic SVs observed in PCa. Indeed, some specific splicing factors (SFs) and spliceosome components (SCs) have been associated to PCa development and aggressiveness (150, 158, 172, 234-236). However, no studies have comprehensively explored 1) the global dysregulations of these elements in PCa, 2) their putative utility as prognostic/therapeutic targets, or 3) their implication in the antitumor effects of other drugs.

The results obtained in the first study of this section indicated that the splicing machinery is drastically dysregulated in PCa since the expression levels of more than 58% (26/45) of the SCs and SFs analysed herein were found to be altered in PCa tissues compared to non-tumor prostate tissues. In fact, an expression-based molecular fingerprint able to perfectly discriminate between PCa and non-tumor adjacent regions was generated by combining the expression levels of only 11 specific SCs and SFs. Moreover, the deranged expression levels of many of the SCs and SFs determined in our study was associated with relevant clinical and molecular features of aggressiveness, suggesting a

causal link between splicing machinery dysregulations and PCa aggressiveness. These results are consistent with and further expand previous observations pointing out the oncogenic role of certain SCs and SFs found herein to be dysregulated in PCa (e.g. *RBM3*, *U2AF2*, *ESRP1*, *ESRP2* and *NOVA1*), as well as their association to key PCa aggressiveness features (158, 234, 236, 237).

Among all the SCs and SFs analysed herein, SNRNP200, SRRM1 and SRSF3 were selected initially to be further explored in this study, due to the fact that they were not only dysregulated (i.e. overexpressed, at mRNA and protein levels), but also associated with all the relevant clinical features analysed in this study (including Gleason score, pathological stage, perineural invasion, lymphovascular invasion, biochemical recurrence, presence of metastasis at diagnosis or *AR-v7* expression). Importantly, although this is the first time that *SNRNP200* and *SRRM1* expression levels have been explored in tumor pathologies, the oncogenic role of *SRSF3* has been previously described in certain cancer types (238-240). Specifically, to the best of our knowledge, this is the first study demonstrating the antitumor functional effects of *SNRNP200*-, *SRRM1*- and *SRSF3*-silencing in PCa, which resulted in a decreased in proliferation and/or migration rates in PCa-derived cell lines.

Mechanistically, *SNRNP200*-, *SRRM1*- and *SRSF3*-silencing altered the splicing process of important genes, such as *AR*, *PKM*, *CASP2* or *XBP1*, resulting in a reduction of the mRNA levels of *AR-v7*, *PKM2*, *CASP2S*, and *XBP1s* splicing variants, which have been previously reported to be involved in tumor aggressiveness (241-244). Additionally, *SRRM1*-and *SRSF3*-silencing promoted a decrease in the phosphorylation levels of AKT and JNK proteins, respectively, probably leading to the inhibition of PI3K/AKT and JNK pathways, which have been broadly defined as oncogenic signaling pathways (245, 246).

Among the molecular changes associated with the silencing of these factors, the decrease in the expression of AR-v7 was especially relevant from a clinical perspective, since the presence of this SV has been linked to CRPC development (247) and to the lack of response to second-generation anti-hormone agents (156). Consequently, by analysing proliferation rate, we found that *SNRNP200*-, *SRRM1*- and *SRSF3*-silencing sensitized the poorly-responsive 22Rv1 cells to enzalutamide treatment, thus suggesting a potential therapeutic role of these factors in CRPC. Interestingly, the modulation of AR splicing process exerted by *SNRNP200* and *SRRM1* may be not mediated by the regulation of SFs previously reported to be involved in *AR-v7* generation such as *KHDRBS1* [21], *SFPQ* [22] or *U2AF2* [23], inasmuch as we found that the silencing of *SNRNP200* and *SRRM1* did not alter the expression levels of these AR-splicing modulators. Finally, and reinforcing the key role *SNRNP200*, *SRRM1* and *SRSF3* in PCa and CRPC, it was also found that their silencing resulted in the modulation of the expression levels of genes tightly associated to prostate oncogenesis and CRPC development, including *C-MYC*, *PTEN* and/or *TP53* (121, 248-250).

Therefore, these data demonstrate that the cellular machinery responsible for the regulation of the splicing process is drastically altered in PCa and that SNRNP200, SRRM1 and SRSF3 could represent attractive novel diagnostic and prognostic biomarkers, as well as therapeutic targets for PCa and CRPC. **These results have been published in "EBioMedicine" (Article I of this Doctoral Thesis).**

Secondly, we decided to focus on the study of the SF RBM22 in PCa inasmuch as: i) RBM22 represents a key SF due to its involvement in the activation of the spliceosome (251), ii) other proteins from the RNA Binding Motif (RBM) family have been shown to be dysregulated and to play relevant roles in PCa [e.g. RBM3 (252), RBM5 (253)], and iii) RBM22 regulates cancer-related processes (e.g. development) (254). Accordingly, this second study aimed to explore the potential dysregulation and pathological role of RBM22 in PCa. To achieve this aim, the levels of RBM22 (mRNA and protein) were analysed in PCa tissues and non-tumor regions, and both *in vitro* and *in vivo* experiments were performed after modulating the expression of *RBM22*.

Results from this study showed that the expression of RBM22 was lower (at mRNA and protein level) in PCa tissues compared to non-tumor prostate tissues in four independent cohorts of patients, and that RBM22 levels were inversely associated with key clinical parameters of aggressiveness (e.g. Gleason score, presence of metastasis, perineural and lymphovascular invasion). In addition, the analysis of prostate samples from the Transgenic Adenocarcinoma Mouse Prostate (TRAMP) mouse model, at different stages of PCa progression [i.e. mice development: i) PIN, ii) moderately differentiated PCa (MD-PCa), and iii) poorly differentiated PCa (PD-PCa) (255)], showed that both mRNA and protein levels of RBM22 were lower in TRAMP mice with PCa compared to those with PIN. Notably, these differences were even more pronounced when comparing PD-PCa with PIN samples.

In addition, we observed that the aggressiveness features (i.e. proliferation and migration rates, as well as colony and tumorspheres formation) of PCa derived cell lines significantly decreased in *RBM22* overexpression condition. Importantly, these results were validated *in*

vivo, since xenograft tumors overexpressing *RBM22* were markedly smaller than control tumors, thus suggesting a potential role of RBM22 as a tumor suppressor in PCa. Interestingly, RBM3 and RBM5 (additional members of RBM family) have been also reported to play a relevant antitumoral role in PCa (252, 253).

Mechanistically, the results derived from the analysis of 713 genes related to cancer (nCounter® PanCancer Pathway) in the xenograft tumors pointed out *MYC* as a potential hub gene in the antitumor response to *RBM22* overexpression. In addition, the analysis of an RNAseq performed in control and RBM22-overexpressing PC-3 cells showed that MYCN and MYC pathways were the top-downregulated pathways in RBM22 overexpression condition, thus further suggesting a key role for this oncogenic pathway (256) in the RBM22 antitumor actions on PCa cells.

Finally, the RNAseq analysis confirmed that RBM22 is a key regulator of the splicing process, since its overexpression resulted in the dysregulation of the splicing of 330 different genes, being exon skipping the most altered splicing event. Among all the genes with altered splicing, we found an enrichment of genes related to mitochondrial function, an interesting avenue that needs to be further explored. In this context, MYC activity is tightly linked to mitochondria function mainly due to the fact that MYC acts as a transcription factor of several genes involved in mitochondria homeostasis (257). Therefore, it is tempting to suggest that RBM22 could play its antitumor role in PCa cells through the inhibition of the MYC activity and the regulation of mitochondrial function, by directly controlling the splicing of key mitochondrial genes o indirectly via MYC inhibition. Consistently, other RBM proteins have been reported to regulate apoptosis through the control of mitochondrial membrane potential and/or MYC activity (258, 259).

Altogether, these results suggest that RBM22 plays a relevant antitumor role in PCa through the regulation of MYC activity and mitochondrial function. **These results have been already submitted to "Molecular Cancer" (Article II of this Doctoral Thesis).**

As previously mentioned in this dissertation, the splicing process is catalyzed by a complex cellular machinery, named spliceosome. Specifically, Splicing Factor 3B Subunit 1 (SF3B1) plays a key structural and functional role within the spliceosome, inasmuch as it is necessary for its correct assembly (177). In addition, SF3B1 activity can be pharmacologically blocked by currently available drugs [e.g. Pladienolide-B (260)], making this factor especially interesting from a clinical perspective.

Therefore, in the third study of this section we evaluated the levels of SF3B1 in normal and tumor prostate tissues from three independent cohorts of patients, analyzed its association to key clinical and molecular features of PCa, and explored the functional and molecular consequences triggered by pladienolide-B treatment in PCa cells.

The results obtained demonstrated that SF3B1 is overexpressed (at mRNA and protein levels) in PCa samples compared to non-tumor adjacent regions. Furthermore, *SF3B1* expression levels were associated with important aggressiveness features of PCa (i.e. Gleason score, presence of metastasis, biochemical recurrence, etc.), suggesting that SF3B1 might represent a new prognostic biomarker in PCa. Moreover, we found that the SF3B1 inhibitor pladienolide-B significantly reduced functional aggressiveness features (e.g. cell proliferation and migration rates as well as tumorsphere formation) and increased the

apoptotic rate of PCa cell lines. Importantly, pladienolide-B also decreased the viability of primary cell cultures derived from PCa tissues. Consistent with previous studies that suggested SF3B1 as a valuable therapeutic target in certain tumor types (261-263). These functional results suggest that SF3B1 inhibition could represent a potential therapeutic approach to tackle PCa. Remarkably, the antiproliferative and proapoptotic effects exerted by pladienolide-B were more pronounced in PCa cells compared to control non-tumor prostate cells, as it has been previously described for other SF3B1 inhibitors in different tumor-derived cells (264, 265), reinforcing the notion of a potential and useful therapeutic role of pladienolide-B in PCa.

In addition, this study demonstrates that *SF3B1* and *AR-v7* (but not *AR*) expression levels were correlated in PCa samples. In line with this, and as it has been observed in response to other SF3B1 inhibitors (thailanstatins), pladienolide-B altered AR splicing process by decreasing *AR-v7* levels (265). Importantly, the modulation of AR-v7 expression exerted by pladienolide-B represents a critically relevant feature from a therapeutic perspective, since AR-v7 is one of the main drivers of CRPC progression (266) and abiraterone/enzalutamide resistance (156). In addition to *AR-v7*, pladienolide-B treatment also resulted in a decrease in the expression levels of *In1-ghrelin* in PCa cells, a splicing variant that we have recently reported to play a pronounced oncogenic role in PCa (163).

We have also shown that pladienolide-B was associated with the modulation of the expression of multiple genes involved in the main processes controlling the homeostasis of splicing variants [i.e. splicing (131) and NMD (267)]. Specifically, we found that the expression levels of a relevant proportion of elements comprising the machineries involved

in the regulation of splicing and NMD processes were dramatically altered by pladienolide-B, suggesting that the restoration of the normal expression of splicing variants observed in response to SF3B1 inhibition could be due, at least in part, to the modulation of the expression of several factors involved in the control of mRNA processing. This hypothesis is reinforced by the fact that some of the SFs found to be altered by pladienolide-B treatment have been related to the generation of *AR-v7* and, therefore, associated with CRPC development, such as *SFPQ* (172), *KHDRBS1* (175) and *U2AF2* (158).

Finally, pladienolide-B treatment also reduced the activation of PI3K/AKT and JNK signaling pathways, which are involved in several oncogenic processes (245, 246). These results, together with the fact that the treatment with pladienolide-B decreased the expression of several PCa aggressiveness markers such as *KI67*, *CAV2*, and *PCA3* (268-270) in all the PCa cell lines tested herein (LNCaP, 22Rv1, PC-3 and DU145), may explain the pronounced antitumor effects of SF3B1 inhibition in AR-v7^{+} but also in AR-v7^{-} PCa cells.

Taken together, these results suggest that SF3B1 could represent a new prognostic biomarker and a therapeutic target in PCa, providing convincing evidence for the putative utility of pladienolide-B as novel therapeutic tool for the treatment of this devastating pathology. **These results have been published in "Translational Research" (Article III of this Doctoral Thesis).**

Finally, results generated in this Doctoral Thesis also shown that the splicing process is involved in the response to metformin, a metabolic drug that has been reported to exert beneficial antitumoral effects on prostate cancer progression/aggressiveness (206). However, the molecular mechanisms underlying the antitumor actions of metformin in PCa cells are not fully defined yet. In this sense, although metformin treatment has been associated to splicing dysregulation in certain cell types (271, 272), the potential effects of metformin on the modulation of splicing-related elements in PCa remain unknown. For this reason, we have analysed the expression levels of a representative set of SCs and SFs in response to metformin treatment in PCa-derived cells and in a PCa preclinical mouse model.

The results obtained showed that metformin consistently downregulated 11% of the SCs (2/18; *RBM22* and *U2AF1*) and 43% of the SFs (12/28; *CELF1*, *ESRP2*, *KHDRBS1*, *MAGOH, NOVA1*, *RAVER1, RBM3, RBM45*, *SND1*, *SRRM1*, *SRSF3*, *SRSF6*) analysed in LNCaP and PC-3 cell lines (Figure 7).

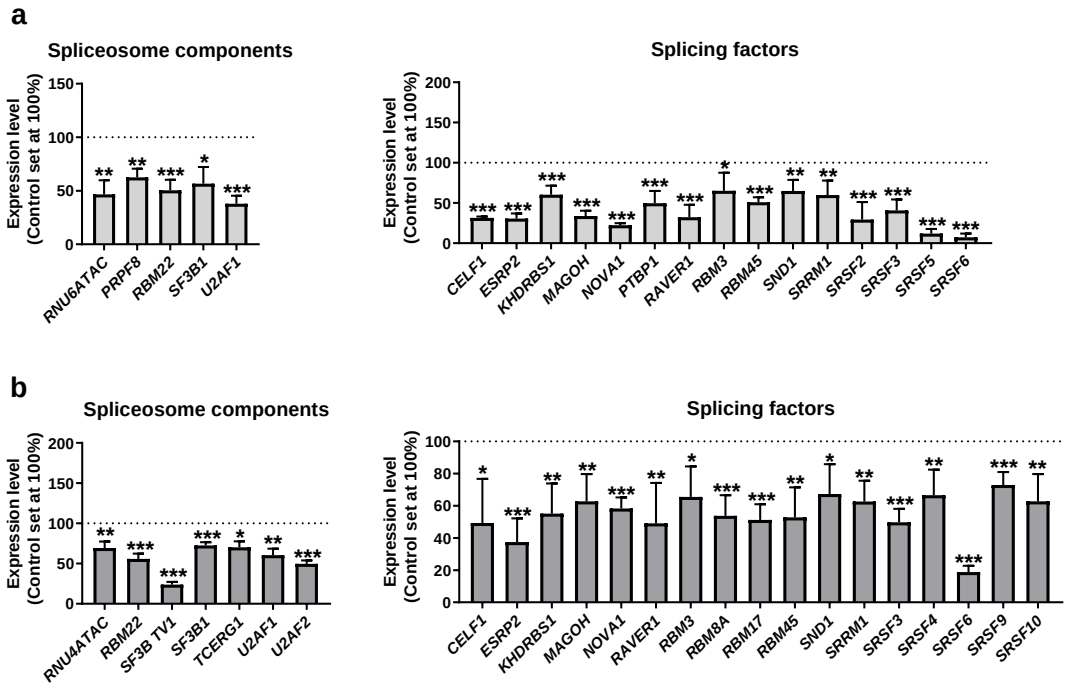

Figure 7: Expression of SCs and SFs in response to metformin (5mM) in a) LNCaP, and b) PC-3 cells. Expression levels were determined by a microfluidic-based qPCR array and adjusted by a normalization factor (calculated from ACTB and GAPDH expression levels). Data represent the mean ± SEM of mRNA expression levels. Asterisks (* $p < 0.05$; ** $p < 0.01$; *** $p < 0.001$) indicate statistically significant differences between conditions.

Additionally, since it was previously demonstrated by our group that metformin reduces tumor-growth in a diet dependent-manner, we used xenograft tumors from mice fed with Low-Fat-Diet (LFD) or High-Fat-Diet (HFD) treated with metformin or vehicle (206) to measure the mRNA levels of the 14 SCs and SFs consistently altered in LNCaP and PC-3 cells. Specifically, the downregulation of *SF3B1*, *SRRM1* and *NOVA1* was also observed in LFD- and HFD mice treated with metformin (Figure-2). On the other hand, the downregulation in response to metformin of *SND1* was observed only in HFD mice, while the downregulation of *ESRP2* and *KHDRBS1* only in LFD mice (Figure 8).

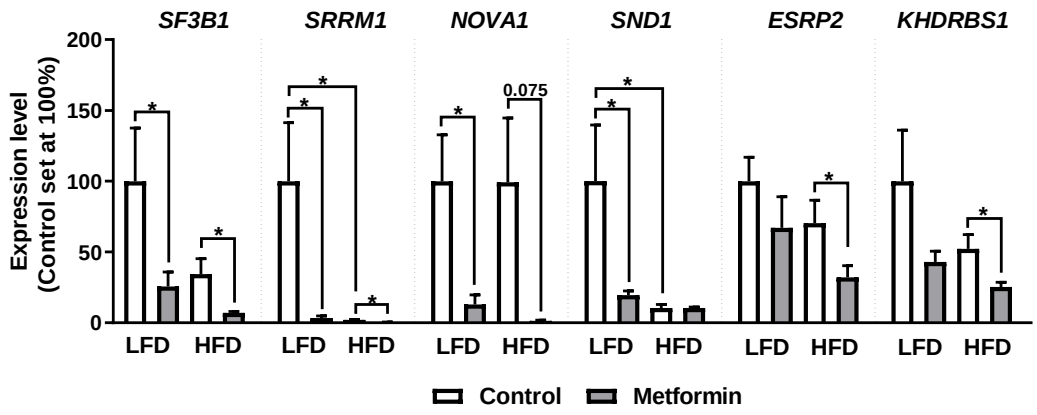

Figure 8: Expression of key SCs and SFs in response to metformin in PC-3 xenograft tumors. Expression levels were determined by qPCR and adjusted by a normalization factor (calculated from *ACTB* and *GAPDH* expression levels). Data represent the mean ± SEM of mRNA expression levels. Asterisks (* $p < 0.05$) indicate statistically significant differences between conditions.

In order to ascertain the potential contribution of the dysregulation of *SF3B1*, *SRRM1* and *NOVA1* (i.e. the three SFs consistently altered in LFD- and HFD mice treated with metformin) in the antitumor effects of metformin, proliferation rate was assessed in PC-3 cells transfected with scramble, *SF3B1*-siRNA, *SRRM1*-siRNA, and *NOVA1*-siRNA in response to metformin treatment. As results from this approach, we revealed that the antiproliferative response to metformin treatment observed in PC-3 cells was completely blocked when the expression levels of SF3B1, SRRM1 or NOVA1 was silenced (Figure 9). Importantly, it should be mentioned that we have previously reported that *SF3B1*, *SRRM1* and *NOVA1* are overexpressed in PCa and their mRNA levels are linked to PCa aggressiveness features (results from this Doctoral Thesis; Article-I). Moreover, the silencing of *SF3B1*, *SRRM1* and *NOVA1* resulted in antitumor effects in PCa cells (results from this Doctoral Thesis; Article-I, Article-II and Figure 9).

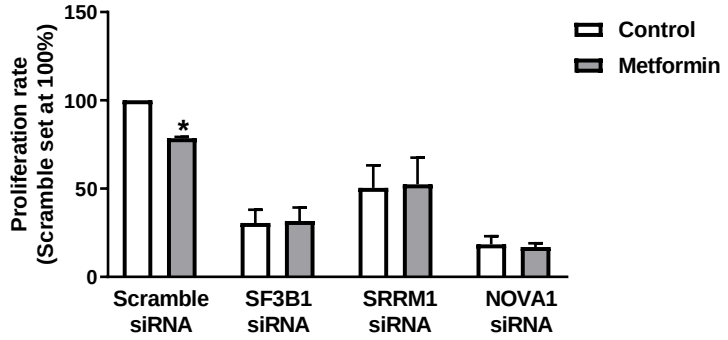

Figure 9: Effect of *SF3B1, SRRM1* and *NOVA1*-silencing on the proliferative response to metformin (5 mM). Proliferation rate was assessed by Alamar-Blue method after 72 h of incubation with metformin in PC-3 cells previously transfected with specific *SF3B1*, *SRRM1* and *NOVA1* siRNAs. Data represent the mean ± SEM of the proliferation rate. Asterisk (* $p < 0.05$) indicates statistically significant differences between metformin treatment vs control of its corresponding silencing condition.

Therefore, these results suggest that splicing dysregulation, and especially *SF3B1*, *SRRM1* and *NOVA1* downregulation, might represent an additional molecular mechanism underlying the antitumor effects of metformin in PCa**.** Of note, these results might also be clinically relevant, from a translational point of view, as they unveil, for the first time, that the antitumor actions of metformin are, in part, mediated through an alteration of the splicing machinery (spliceosome and splicing factors) which are, in turn, druggable/actionable targets. Thus, our findings unveil new opportunities to further explore the molecular mechanisms associated to the beneficial actions of metformin in other endocrine-related pathologies (e.g. diabetes). **These results are being prepared and complemented for publication in "Cancer & Metabolism" (Article IV of this Doctoral Thesis).**

3.2 Section II

Antitumor action of metformin, simvastatin and their combination in PCa

The therapeutic options to treat PCa patients have been expanded during the past decade. However, advanced stages of the disease are still difficult to manage. Therefore, the discovery and establishment of new therapeutic approaches to treat PCa are urgently needed. An emerging approach against several tumor types is based on repositioning drugs already approved for other pathologies, since they are faster and easier to translate to clinical practise than new drugs. In this scenario, treatment of patients with biguanides (e.g. metformin) and statins (e.g. simvastatin), drugs commonly used to treat metabolism-related pathologies that have been linked to PCa progression [i.e. diabetes and hypercholesterolemia (193, 195, 273)], has been associated to a lower PCa risk and aggressiveness (202-204). However, the direct antitumor effects that different biguanides (i.e. metformin, buformin and phenformin), statins (i.e. atorvastatin, simvastatin and lovastatin), and the simultaneous combination of both types of drugs, may exert on normal prostate and PCa cells, and the molecular and metabolic mechanisms and signalling pathways behind these actions, have not been yet fully compared side-by-side. For these reasons, this study was aimed to assess the putative *in vivo* association of metformin, statins and their co-treatment with clinical parameters of aggressiveness in PCa patients, as well as to explore the functional and mechanistic *in vitro* effects of the treatment with biguanides, statins and the combined treatment in PCa cells.

One of the main observations of this study was that the medical combination of metformin and statins might be associated to more beneficial effects in key clinical

parameters of aggressiveness of patients with PCa compared to the individual treatment of any of those drugs. Specifically, patients treated with metformin and statins showed lower Gleason score and longer free biochemical recurrence survival. *In vitro* studies also demonstrated that biguanides (i.e. metformin, buformin and phenformin) and statins (i.e. atorvastatin, lovastatin and simvastatin) significantly decreased functional parameters of tumor aggressiveness in PCa cells, being these antitumor effects especially pronounced (i.e. additive) when combining both treatments (e.g. metformin and simvastatin) compared to the individual treatment of any of those drugs. Interestingly, the additive antitumor effects of biguanides and statins *in vitro* have been previously reported in other cancer types (215).

In addition, from a mechanistic perspective, we found that treatment with metformin, simvastatin and especially their combination reduced the expression levels as well as the activity of AR gene. Since AR plays a pivotal role in prostate tumorigenesis (274), and it is the most common amplified gene in CRPC (121), these results pave the way to further study the potential value of metformin, simvastatin and especially their combined treatment as novel therapeutic approaches for the treatment of PCa and especially of CRPC. Moreover, as expected, metformin increased the activity of AMPK, its main molecular target (275). On the other hand, simvastatin decreased the activity of PI3K/AKT and MAPK/ERK signalling pathways, which have been associated to the antitumor actions of different drugs in PCa cells (276, 277). Additionally, we found that the combination of metformin and simvastatin was also able to alter the activity (i.e. inactivation) of mTOR, an oncogenic route that represents a key downstream effector of AMPK, PI3K/AKT, and MAPK/ERK signalling pathways (278-280). Notably, this study also revealed that relevant cyclin-dependent kinase inhibitors (CKIs; i.e. *CDKN1A*, *CDKN1B*, *CDKN2A* and

CDKN2D) that play a pronounced antitumor role in PCa (281-291), and has been shown to be regulated by the signalling pathways previously altered in response to metformin and/or simvastatin (i.e. AR, mTOR, AMPK, PI3K/AKT and MAPK/ERK pathways), were upregulated *in vitro* in response to the combined treatment of metformin and simvastatin, but not in response to metformin or simvastatin alone, thus emerging as potential key mechanisms underlying the additive antitumor effects exerted by metformin and simvastatin. Remarkably, the upregulation of *CDKN1B* and *CDKN2A* was also observed *in vivo*, in samples from patients treated with metformin and statins as compared to those from untreated patients. Hence, based on the molecular results reported, we can conclude that co-administration of metformin and simvastatin might exert additive antitumor actions in PCa cells through an inactivation of mTOR and AR, as well to an increase of the levels of CKIs.

Altogether, this study demonstrates that metformin and simvastatin exert additive antitumor effects in PCa, thus suggesting that this combination might be a novel and attractive therapeutic approach to tackle PCa. **These results have been submitted and are under review in "Journal of Clinical Endocrinology & Metabolism" (Article V of this Doctoral Thesis).**

3.3 Section III

Specific components of the ghrelin system as potential diagnostic, prognostic and/or therapeutic tools in prostate cancer

The discovery of PSA and its use as a non-invasive diagnostic biomarker for PCa has undoubtedly improved the management of this disease (292). Unfortunately, PCa screening with PSA has been also associated to overtreatment, overdiagnosis and unnecessary biopsies (293). Moreover, PSA has proven arguable specificity (since its levels are increased in response to non-tumor conditions (41, 42)], especially in the lower range of levels [< 10 ng/mL, known as grey-zone (56)]. Therefore, novel diagnostic biomarkers that overcome or complement the diagnostic capability of PSA, are strongly needed in clinical practise.

In this sense, our group has reported that some factors belonging to the complex regulatory ghrelin system [specially, Ghrelin-O-Acyl transferase (GOAT) enzyme and its potential substrate in various pathological conditions, the In1-ghrelin variant (294)] are overexpressed in PCa tissues and associated to PCa aggressive features (295, 296). Importantly, we have previously reported that both GOAT and In1-ghrelin are released into the plasma and their levels are higher in patients with PCa compared to healthy individuals, representing potential non-invasive diagnostic biomarkers of PCa (232, 295, 296). Moreover, plasma GOAT levels have been found to be altered in patients with adverse metabolic conditions (e.g. diabetes, dyslipidaemia), thus influencing the diagnostic ability of GOAT in plasma and highlighting the well-known pathologic association between obesity and PCa (297).

However, the potential diagnostic capacity of the urine levels of both GOAT and In1-ghrelin remains nowadays unknown. Likewise, although we have recently demonstrated that In1-ghrelin can exert an important oncogenic role in PCa (296), and that GOAT mRNA-, protein- and secreted-levels are overexpressed in and linked to PCa aggressive features (232, 295), to date, the putative pathophysiological role of GOAT enzyme in PCa remains unknown. In addition, although ghrelin system is markedly altered by endocrine-metabolic dysregulations (298), no studies have been performed to date focusing on In1-ghrelin levels in the context of altered endocrine-metabolic conditions.

Therefore, this section has been firstly focused on expanding the knowledge on the diagnostic ability of GOAT (using plasma and urine samples from a cohort of almost 1,000 patients), as well as on exploring its potential pathophysiological role (using *in vitro* and *in vivo* models) in PCa. Secondly, we interrogated the diagnostic ability of urine In1-ghrelin, as well as its potential involvement in the pathophysiological association between OB and PCa, using a cohort of 604 patients with PSA ranging 3-10 ng/mL.

The results from the first study (using ~1000 patients) corroborated the diagnostic ability of GOAT in plasma, and demonstrated that the accuracy of this biomarker to distinguish between PCa and non-PCa patients was even higher when analysing urine samples. This improvement could be due to the fact that urine is enriched in prostate-derived proteins compared to the plasma (299). Specifically, urine GOAT levels outperformed the capacity of PSA to diagnose PCa, especially clinically significant PCa (SigPCa; defined as Gleason score ≥7) in patients with PSA in the grey zone. In addition, high urine GOAT levels were associated to a higher risk of developing PCa and SigPCa, independently of other parameters clinically relevant for PCa diagnosis [i.e. Gleason score (52), PSA (300), age

and DRE (301)]. Likewise, and as we found in a previous study wherein plasma GOAT levels were examined, urine GOAT levels were positively correlated to clinical parameters associated to PCa risk and aggressiveness, including Gleason score (52), age (302) and CRP (303). Moreover, reinforcing the idea that urine GOAT levels are associated to PCa aggressiveness, significant correlations were also found between urine GOAT levels and the expression, in PCa tissues, of molecular markers of PCa aggressiveness, including *CDK6* (304), *CDKN2A* (305), *EZH2* (306) and *SIRT1* (307).

Finally, this study also provides, for the first time, primary evidence demonstrating that GOAT plays an oncogenic role in PCa *in vitro* and *in vivo*, since its overexpression resulted in an increase of PCa aggressiveness *in vitro* (i.e. cell proliferation) and *in vivo* (i.e. tumor growth, KI67- and mitotic-index). On the other hand, *GOAT* silencing and the inhibition of its activity (using a GOAT inhibitor) significantly decreased the aggressiveness of PCa cells *in vitro*, thus suggesting a potential therapeutic role for GOAT in PCa.

Altogether, these results demonstrated that GOAT represents an additional non-invasive diagnostic biomarker, as well as a potential prognostic and therapeutic tool for PCa. **These results have been published in "Journal of Clinical Medicine" (Article VI of this Doctoral Thesis).**

The second study of this section aimed to further explore the putative capacity of In1-ghrelin as non-invasive (urine) diagnostic and/or prognostic biomarkers in PCa. Indeed, plasma In1-ghrelin levels have been reported to be able to discriminate between patients

with PCa and healthy individuals in a discrete cohort of patients (pilot study) (296). Therefore, since we have previously suggested that In1-ghrelin (but not native ghrelin) seems to be the oncogenic substrate of GOAT enzyme in PCa (296), and that the first study of this section has demonstrated the capacity of urine GOAT levels to distinguish between PCa and patients with negative biopsy result outperforming the diagnostic capacity of PSA when analysing patients with low levels of PSA (3-10 ng/mL), we decided to analyse urine In1-ghrelin levels in PCa patients with low levels of PSA and determine its diagnostic and/or prognostic capacity. To achieve this aim, a commercial radioimmunoassay kit to detect In1-ghrelin (RK-032–42; Phoenix, Burlingame, CA, USA) was used in urine samples from patients with PSA ranging 3-10 ng/mL (n=604).

The results of this analysis indicated that urine In1-ghrelin levels (but not plasma PSA levels) were higher in PCa patients compared to patients with negative biopsy result (Figure 10a). Indeed, urine In1-ghrelin levels, but not plasma PSA levels, were able to significantly distinguish between PCa and patients with negative biopsy result (Figure 10b). Moreover, similar to the results found with urine GOAT enzyme levels (reported in the first study of this section), elevated urine In1-ghrelin levels in PCa patients were associated with an increased PCa risk (Table 3).

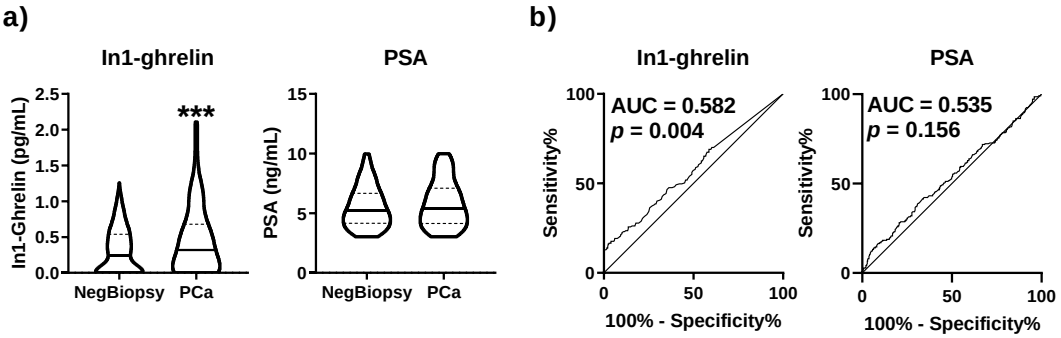

Figure 10: Comparison between the diagnostic capacity of urine In1-ghrelin levels and plasma PSA levels. A) Urine levels of In1-ghrelin (left panel) and plasma PSA levels (right panel) in patients with negative biopsy result (NegBiopsy) and patients with PCa. **B)** ROC curves showing the capacity of urine In1-ghrelin levels (left panel) and plasma PSA levels (right panel) to identify PCa. Asterisks (***, p<0.001) indicate statistically significant differences between groups. AUC represents the area under the curve and the p-value is represented by *p*.

Table 3. Univariate analysis showing the influence of plasma PSA and urine In1-ghrelin levels on the diagnosis of PCa. OR: Odds ratio; CI: Confidence interval.

	PCa		
Variable	**OR**	***p-Value***	**95% CI (OR)**
PSA	1.09	0.068	0.99-1.20
In1-ghrelin	2.93	<0.0001	1.85-4.64

Given the pathophysiological relationship between metabolic disorders (e.g. obesity, diabetes) and PCa (297), and the pronounced influence that adverse metabolic conditions exert on the expression of several components of the ghrelin system (308), we next explored the associations between urine In1-ghrelin levels and key factors commonly dysregulated in obese and diabetic patients (e.g. insulin, triglycerides, Hb1Ac). Firstly, we observed that urine In1-ghrelin levels were higher in obese and overweight patients

compared to normo-weight patients (Figure 11a), and that obese patients had higher urine In1-ghrelin levels than overweight patients (Figure 11a). In addition, diabetic patients had higher urine In1-ghrelin levels compared to non-diabetic patients (Figure 11b). Consistently, urine In1-ghrelin levels were positively correlated with body mass index (BMI) and waist circumference (WC) in our cohort of patients (Figure 11c-d). Interestingly, urine In1-ghrelin levels also showed a positive correlation with circulating levels of several factors commonly upregulated in plasma of diabetic and/or obese patients, including insulin, glucose, triglycerides, homocysteine and HbA1c (309-311) (Figure 11e-i). Furthermore, high urine In1-ghrelin levels were associated with higher risk of overweight (defined as BMI≥25), obesity (defined as BMI≥30) and diabetes mellitus (Table 4).

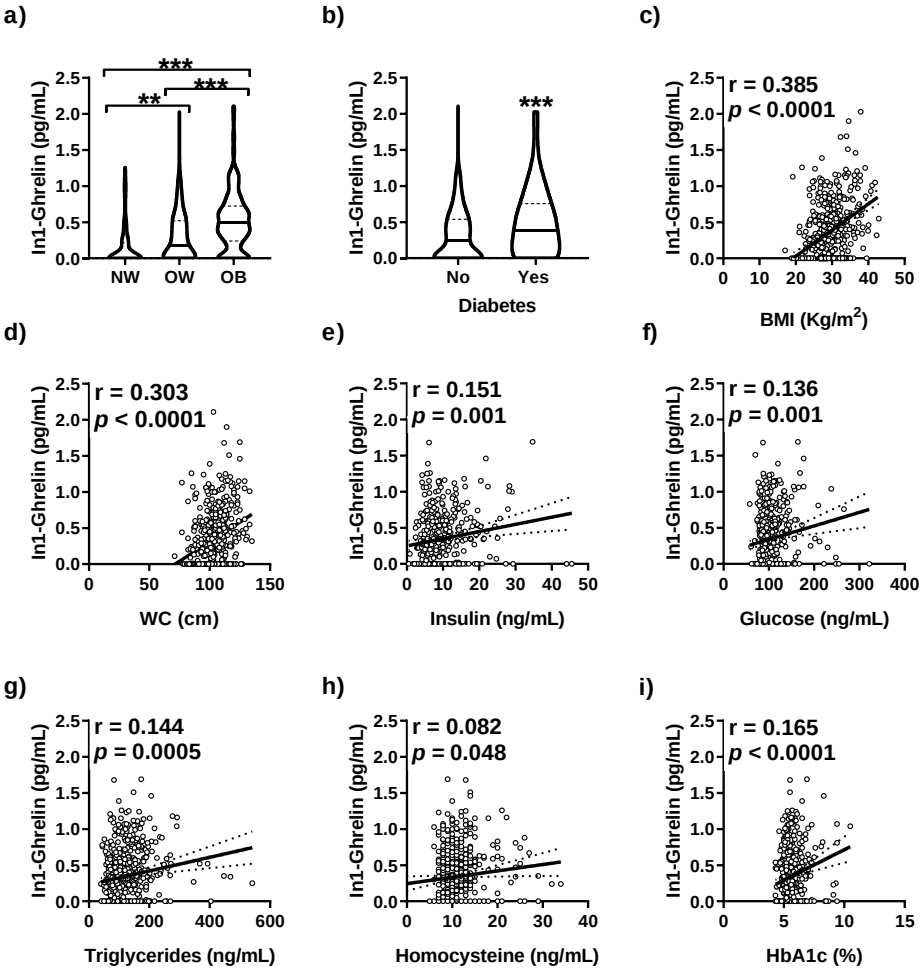

Figure 11: Relationship between urine In1-ghrelin levels and relevant metabolic parameters. Urine In1-ghrelin levels in patients categorized according to: a) body mass index (BMI) [normo-weight (NW), overweight (OW), obese (OB), and b) the presence of diabetes mellitus (DM). Correlations of urine In1-ghrelin levels with metabolic parameters including: c) BMI, d) waist circumference (WC), e) insulin, f) glucose, g) triglycerides, h) homocysteine, and i) glycosylated haemoglobin (HbA1c). The regression coefficient is indicated as "r" and the *p*-value as "p". Asterisks (**, p <0.01; ***, p <0.001) indicate statistically significant differences between groups.

Table 4. Univariate analysis showing the influence of plasma PSA and urine In1-ghrelin levels on the risk of overweight, obesity and diabetes mellitus (DM). Overweight was defined as BMI ≥25, and obesity as BMI ≥30. OR: Odds ratio; CI: Confidence interval.

	Overweight			**Obesity**			**DM**		
Variable	**OR**	***p-Value***	**95% CI (OR)**	**OR**	***p-Value***	**95% CI (OR)**	**OR**	***p-Value***	**95% CI (OR)**
PSA	5.24	0.915	4.14-6.80	1.01	0.932	0.87-1.16	1.08	0.333	0.96-1.21
In1-ghrelin	10.09	<0.001	4.38-27.0	35.3	<0.001	12.3-101	2.96	0.001	1.76-4.99

Given the relationship of In1-ghrelin with obesity and DM, we next categorized the cohort according to BMI and DM status. Firstly, it was observed that the ability of urine In1-ghrelin levels to distinguish between PCa and patients with negative biopsy result was higher when analysing only obese patients as compared to that observed when analysing normo-weight, overweight or the full cohort (results from Figure 12a-c compared to results from Figure 10). These results indicate that In1-ghrelin might serve as a potential non-invasive diagnostic biomarker of PCa, especially for obese patients. Furthermore, these findings suggest that In1-ghrelin could be a potentially relevant player involved in the association between obesity and PCa risk. On the other hand, the diagnostic capacity of urine In1-ghrelin levels did not improve when the cohort was categorized based on the presence of DM compared to the analysis of the full cohort (Figure 12d-e).

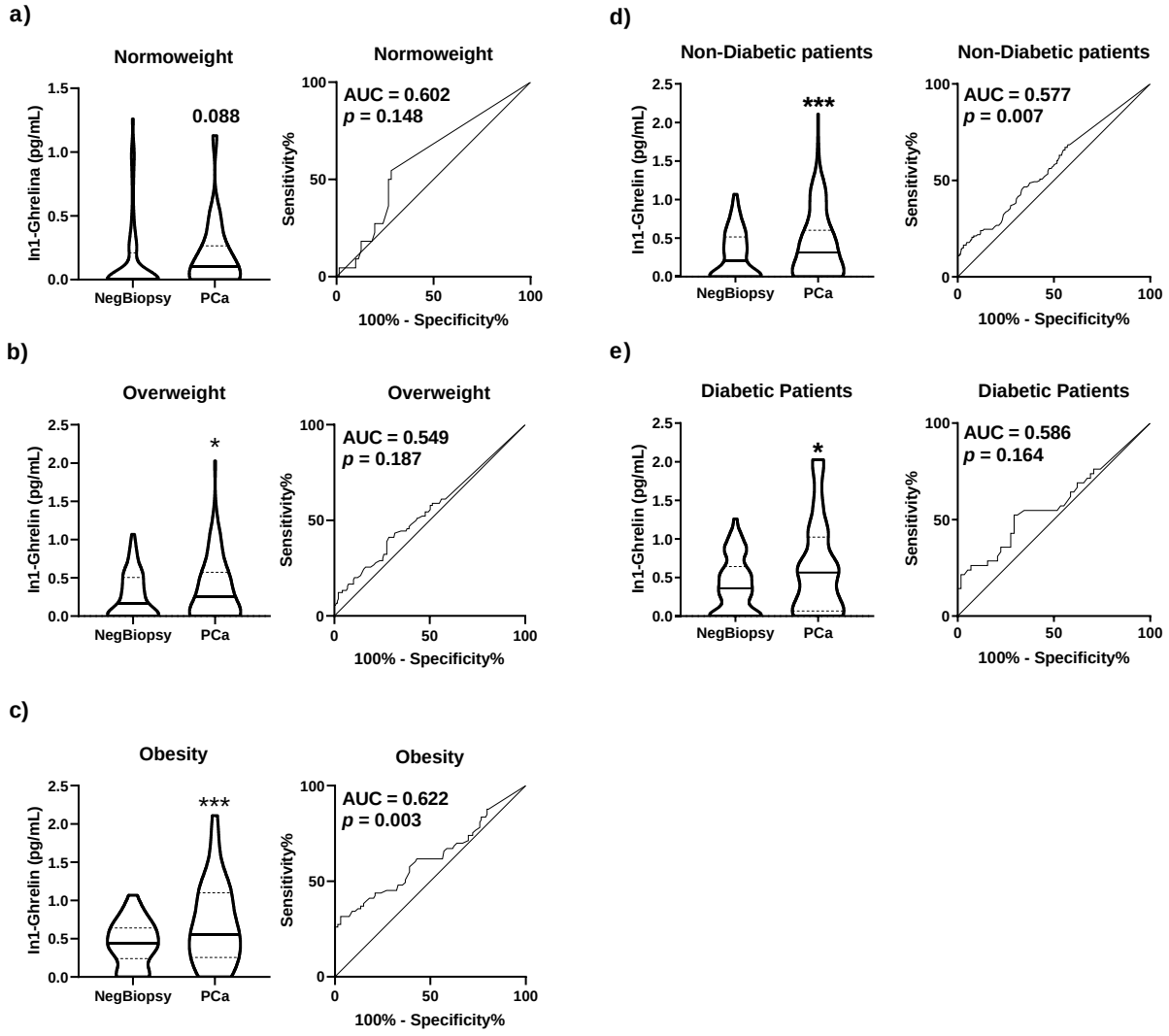

Figure 12: Diagnostic capacity of urinary In1-ghrelin levels according to metabolic status. Comparison of the urine In1-ghrelin levels between NegBiopsy and PCa in patients with: a) normoweight, b) overweight, c) obesity, d) without diabetes, and e) with diabetes. Asterisks (* p <0.05; ** p <0.01), indicate statistically significant differences between groups. AUC represents the area under the curve and p-value is represented by "p".

In this cohort, we also observed a positive correlation of urine In1-ghrelin levels with plasma PSA levels (Figure 13a), but most importantly, with urine GOAT levels (Figure 13b), reinforcing the putative functional association between these two components of the

ghrelin system in PCa (228, 295, 296). Likewise, urine In1-ghrelin levels were inversely correlated with circulating testosterone levels (Figure 13c), and positively correlated with circulating beta-2 microglobulin and C-reactive protein (CRP) levels (Figure 13d-e). Remarkably, low testosterone levels and high beta-2 microglobulin and CRP levels have been related to PCa progression (312-315), thus reinforcing the idea that urine In1-ghrelin levels might be associated to PCa aggressiveness, even in patients with low levels of PSA. This hypothesis is supported by the fact that the treatment with In1-ghrelin derived peptides increases aggressiveness features (e.g. proliferation and migration rate) in PCa-derived cells (296). In line with this, we also found that high urine In1-ghrelin levels were associated to higher levels of pathological PCa stage and tumors with lymphovascular invasion capacity (Figure 13f-g), and tended to be associated with perineural invasion capacity (Figure 13h).

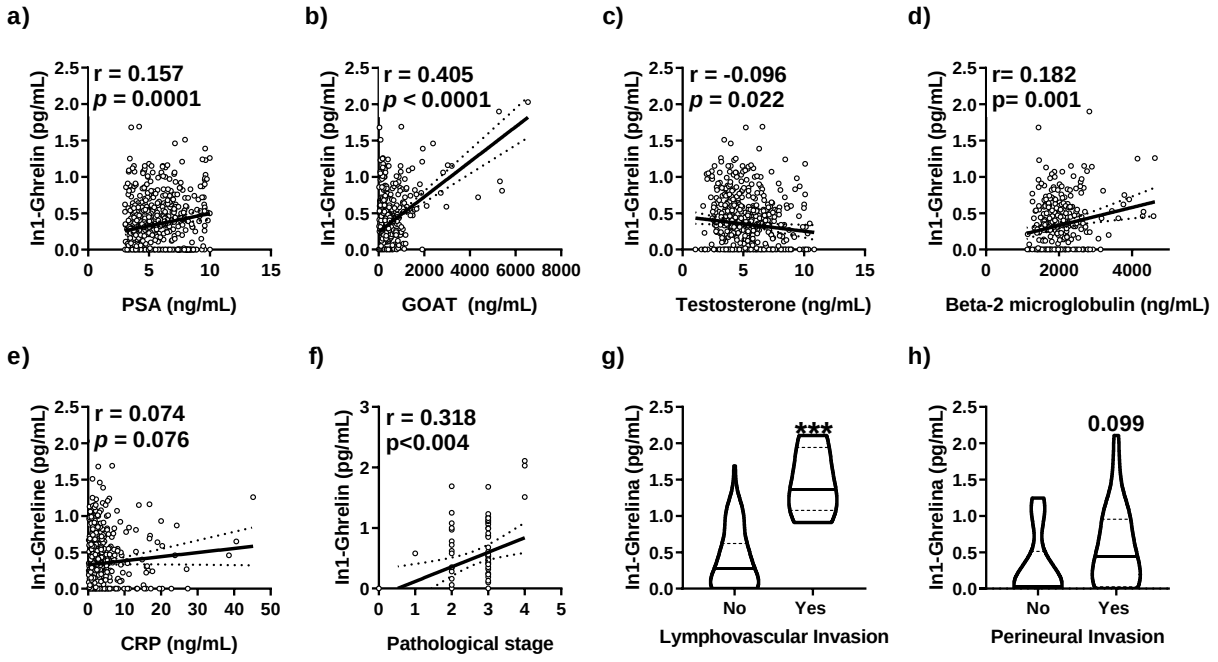

Figure 13: Relationship between urine In1-ghrelin levels and key clinical-pathological parameters. Correlations of urine In1-ghrelin levels with clinical-pathological parameters including: **a)** plasma PSA, **b)** urine GOAT levels, **c)** testosterone, **d)** beta-2 microglobulin,

e) CRP, **f)** pathological stage, **g)** Lymphovascular invasion, and **h)** perineural invasion. The regression coefficient is indicated as "r" and the p-value as "p". Asterisks (*** $p < 0.001$), indicate statistically significant differences between groups.

On the other hand, no correlation was found between plasma PSA levels and urine GOAT (Figure 14a) or testosterone levels (Figure 14b). In contrast, plasma PSA levels were found to be positively correlated with circulating levels of beta-2 microglobulin and CRP (Figure 14c-d). Finally, high PSA levels presented a tendency to be associated with the pathological stage of the tumors (Figure 14e), and were significantly associated with tumors with limphovascular invasion capacity (Figure 14g). Therefore, since the relationship between PCa aggressiveness features and In1-ghrelin urine levels was more pronounced than the observed with PSA plasma levels, we might speculate that urine In1-ghrelin levels could also represent a potential non-invasive biomarker for aggressiveness status of PCa in the PSA range 3-10 ng/mL.

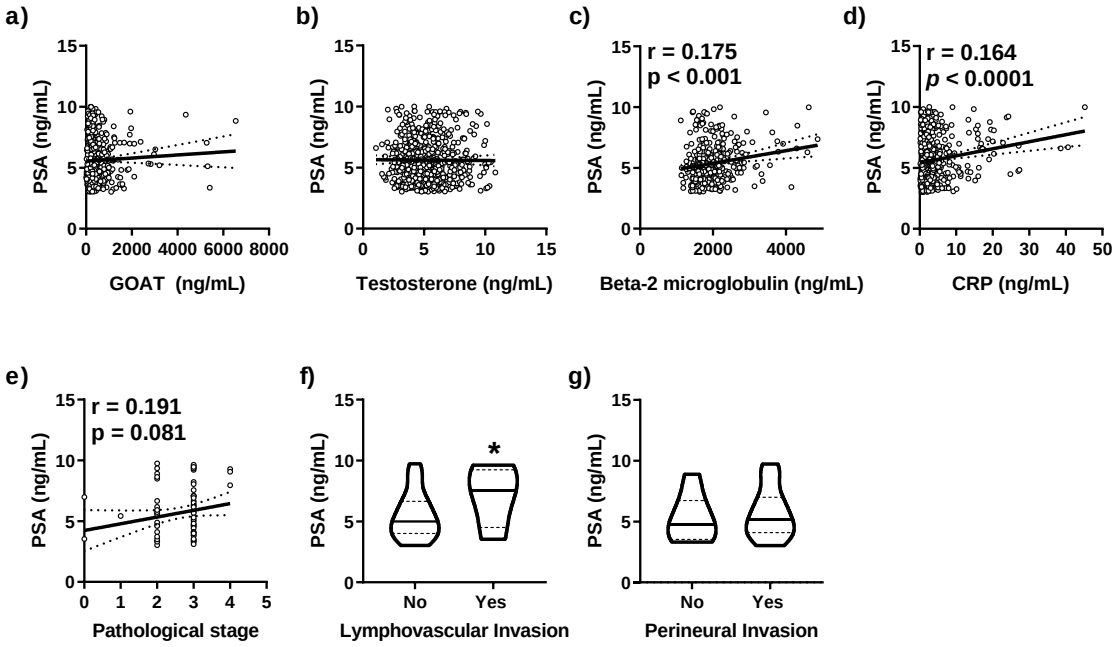

Figure 14: Relation between plasma PSA levels and key clinical-pathological parameters. Correlations of plasma PSA levels with clinical-pathological parameters including: **a)** urine GOAT levels, b**)** testosterone, **c)** beta-2 microglobulin, **d)** CRP, **e)** pathological stage, **f)** Lymphovascular invasion, and **g)** perineural invasion. The regression coefficient is indicated as "r" and the *p*-value as "p". Asterisk (* p <0.05), indicates statistically significant differences between groups.

Taken together, these results indicate that urine In1-ghrelin levels might represent a novel non-invasive diagnostic and prognostic tool in PCa in the PSA grey zone, especially for obese patients. **These results are being prepared and complemented for publication in "Cancers" (Article VII of this Doctoral Thesis).**

4. General conclusions

The main conclusions associated to each section/article of this Doctoral Thesis are described below:

Section I:

1) The cellular machinery that regulates the splicing process is drastically altered in PCa and provides a source of novel potential diagnostic and prognostic biomarkers, as well as putative targets to develop new therapeutic strategies against PCa (**article I**).

2) SNRNP200, SRRM1, SRSF3 and SF3B1 are upregulated while RBM22 is downregulated in PCa tissues, being their levels tightly coupled to relevant clinical features of tumor aggressiveness, and becoming thereby attractive novel diagnostic and prognostic biomarkers for PCa (**articles I-III**).

3) The silencing of *SNRNP200*, *SRRM1*, *SRSF3* and *SF3B1*, as well as the overexpression of *RBM22*, decreased key functional features and altered relevant molecular parameters associated with PCa aggressiveness, thus suggesting their added potential also as novel therapeutic targets to tackle the development and/or aggressiveness of this disease (**articles I-III**).

4) Pladienolide-B, a selective inhibitor of SF3B1 activity, exerts potent anti-tumor actions in PCa cells, through the modulation of an ample repertoire of molecular events (signaling pathways, tumor markers, splicing variants and mRNA homeostasis-associated machineries), providing convincing evidence for its putative utility as a novel therapeutic tool for the treatment of PCa (**article II**).

5) The dysregulation of the splicing process, especially *SF3B1*, *SRRM1* and *NOVA1* downregulation, might represent an additional molecular mechanism underlying the antitumor effects of metformin in PCa (**article IV**).

Section II:

6) Treatments with metformin and/or statins are inversely associated with clinical and molecular features of tumor aggressiveness in PCa patients, being these effects more pronounced when patients were co-treated with both drugs (**article V**).

7) Metformin and statins reduce the aggressiveness of PCa cells *in vitro*, being these effects significantly more pronounced when combining both treatments. Hence, combination of these compounds could represent an attractive therapeutic approach in PCa (**article V**).

8) The additive antitumor actions of metformin and statins in PCa could be mediated, at least in part, by AR and mTOR hyper-inactivation and by the upregulation of CKIs expression (**article V**).

Section III:

9) GOAT enzyme overexpression increased PCa cells aggressiveness, whereas its silencing or blockade of its activity reduced it, thus unveiling an oncogenic role and therapeutic potential for GOAT in this disease (**article VI**).

10) The diagnostic capacity of GOAT was higher in urine than in plasma samples, and outperformed the capacity of PSA to diagnose PCa, especially significant PCa, in patients with PSA in the grey zone (**article VI**).

11) Urine GOAT levels are directly associated to key clinical and molecular parameters of aggressiveness, representing a potential non-invasive prognostic biomarker for PCa patients (**article VI**).

12) Urine In1-ghrelin levels are elevated and associated with multiple metabolic parameters (e.g. BMI, diabetes, insulin and glucose levels), as well as PCa aggressive features in PCa patients, thus emerging as a potentially relevant player in the pathological association between obesity and PCa risk (**article VII**).

13) Urine In1-ghrelin levels outperformed the capacity of PSA to diagnose PCa in patients with PSA in the grey zone, especially when considering obese patients. Consequently, measuring urine In1-ghrelin levels may provide a novel non-invasive diagnostic and prognostic tool, particularly in obese PCa patients with PSA in the grey zone (**article VII**).

Altogether, these results demonstrate that the **alteration of the splicing process and the dysregulation of certain endocrine-metabolic systems could contribute to the development and progression of PCa, representing a source of novel diagnostic, prognostic and therapeutic targets that could be used to improve the diagnosis and management of PCa patients, as well as new therapeutic tools to be implemented in PCa**.

5. References

1. Patel P, Nayak JG, Biljetina Z, Donnelly B, Trpkov K. Prostate cancer after initial high-grade prostatic intraepithelial neoplasia and benign prostate biopsy. The Canadian journal of urology. 2015;22(6):8056-62.
2. Zhang C, Li HR, Fan JB, Wang-Rodriguez J, Downs T, Fu XD, et al. Profiling alternatively spliced mRNA isoforms for prostate cancer classification. BMC bioinformatics. 2006;7:202.
3. Stoyanova T, Cooper AR, Drake JM, Liu X, Armstrong AJ, Pienta KJ, et al. Prostate cancer originating in basal cells progresses to adenocarcinoma propagated by luminal-like cells. Proceedings of the National Academy of Sciences of the United States of America. 2013;110(50):20111-6.
4. Marcus DM, Goodman M, Jani AB, Osunkoya AO, Rossi PJ. A comprehensive review of incidence and survival in patients with rare histological variants of prostate cancer in the United States from 1973 to 2008. Prostate cancer and prostatic diseases. 2012;15(3):283-8.
5. Parimi V, Goyal R, Poropatich K, Yang XJ. Neuroendocrine differentiation of prostate cancer: a review. American journal of clinical and experimental urology. 2014;2(4):273-85.
6. Grignon DJ. Unusual subtypes of prostate cancer. Modern pathology : an official journal of the United States and Canadian Academy of Pathology, Inc. 2004;17(3):316-27.
7. Denmeade SR, Isaacs JT. A history of prostate cancer treatment. Nat Rev Cancer. 2002;2(5):389-96.
8. Attard G, Parker C, Eeles RA, Schröder F, Tomlins SA, Tannock I, et al. Prostate cancer. Lancet (London, England). 2016;387(10013):70-82.
9. Villers A, McNeal JE, Freiha FS, Stamey TA. Multiple cancers in the prostate. Morphologic features of clinically recognized versus incidental tumors. Cancer. 1992;70(9):2313-8.
10. Boutros PC, Fraser M, Harding NJ, de Borja R, Trudel D, Lalonde E, et al. Spatial genomic heterogeneity within localized, multifocal prostate cancer. Nature genetics. 2015;47(7):736-45.
11. Bray F, Ferlay J, Soerjomataram I, Siegel RL, Torre LA, Jemal A. Global cancer statistics 2018: GLOBOCAN estimates of incidence and mortality worldwide for 36 cancers in 185 countries. CA: a cancer journal for clinicians. 2018;68(6):394-424.
12. Arnold M, Karim-Kos HE, Coebergh JW, Byrnes G, Antilla A, Ferlay J, et al. Recent trends in incidence of five common cancers in 26 European countries since 1988: Analysis of the European Cancer Observatory. Eur J Cancer. 2015;51(9):1164-87.
13. De Angelis R, Sant M, Coleman MP, Francisci S, Baili P, Pierannunzio D, et al. Cancer survival in Europe 1999-2007 by country and age: results of EUROCARE--5-a population-based study. The Lancet Oncology. 2014;15(1):23-34.
14. Sartor O, de Bono JS. Metastatic Prostate Cancer. The New England journal of medicine. 2018;378(7):645-57.
15. Bell KJ, Del Mar C, Wright G, Dickinson J, Glasziou P. Prevalence of incidental prostate cancer: A systematic review of autopsy studies. International journal of cancer. 2015;137(7):1749-57.
16. Warner HR. Superoxide dismutase, aging, and degenerative disease. Free radical biology & medicine. 1994;17(3):249-58.
17. Stadtman ER. Protein oxidation and aging. Free radical research. 2006;40(12):1250-8.
18. He P, Yasumoto K. Dietary butylated hydroxytoluene counteracts with paraquat to reduce the rate of hepatic DNA single strand breaks in senescence-accelerated mice. Mechanisms of ageing and development. 1994;76(1):43-8.
19. Hartman TJ, Albanes D, Rautalahti M, Tangrea JA, Virtamo J, Stolzenberg R, et al. Physical activity and prostate cancer in the Alpha-Tocopherol, Beta-Carotene (ATBC) Cancer Prevention Study (Finland). Cancer causes & control : CCC. 1998;9(1):11-8.

20. Heinonen OP, Albanes D, Virtamo J, Taylor PR, Huttunen JK, Hartman AM, et al. Prostate cancer and supplementation with alpha-tocopherol and beta-carotene: incidence and mortality in a controlled trial. Journal of the National Cancer Institute. 1998;90(6):440-6.
21. Giovannucci E, Ascherio A, Rimm EB, Stampfer MJ, Colditz GA, Willett WC. Intake of carotenoids and retinol in relation to risk of prostate cancer. Journal of the National Cancer Institute. 1995;87(23):1767-76.
22. Zeegers MP, Jellema A, Ostrer H. Empiric risk of prostate carcinoma for relatives of patients with prostate carcinoma: a meta-analysis. Cancer. 2003;97(8):1894-903.
23. Johns LE, Houlston RS. A systematic review and meta-analysis of familial prostate cancer risk. BJU international. 2003;91(9):789-94.
24. Stone SN, Hoffman RM, Tollestrup K, Stidley CA, Witter JL, Gilliland FD. Family history, Hispanic ethnicity, and prostate cancer risk. Ethnicity & disease. 2003;13(2):233-9.
25. Carter BS, Bova GS, Beaty TH, Steinberg GD, Childs B, Isaacs WB, et al. Hereditary prostate cancer: epidemiologic and clinical features. The Journal of urology. 1993;150(3):797-802.
26. Lichtenstein P, Holm NV, Verkasalo PK, Iliadou A, Kaprio J, Koskenvuo M, et al. Environmental and heritable factors in the causation of cancer--analyses of cohorts of twins from Sweden, Denmark, and Finland. The New England journal of medicine. 2000;343(2):78-85.
27. Hemminki K. Familial risk and familial survival in prostate cancer. World journal of urology. 2012;30(2):143-8.
28. Lynch HT, Kosoko-Lasaki O, Leslie SW, Rendell M, Shaw T, Snyder C, et al. Screening for familial and hereditary prostate cancer. International journal of cancer. 2016;138(11):2579-91.
29. Bancroft EK, Page EC, Castro E, Lilja H, Vickers A, Sjoberg D, et al. Targeted prostate cancer screening in BRCA1 and BRCA2 mutation carriers: results from the initial screening round of the IMPACT study. European urology. 2014;66(3):489-99.
30. Bancroft EK, Eeles RA. Corrigendum to "Targeted Prostate Cancer Screening in BRCA1 and BRCA2 Mutation Carriers: Results from the Initial Screening Round of the IMPACT Study" [Eur Urol 2014;66:489-99]. European urology. 2015;67(6):e126.
31. Odedina FT, Akinremi TO, Chinegwundoh F, Roberts R, Yu D, Reams RR, et al. Prostate cancer disparities in Black men of African descent: a comparative literature review of prostate cancer burden among Black men in the United States, Caribbean, United Kingdom, and West Africa. Infectious agents and cancer. 2009;4 Suppl 1(Suppl 1):S2.
32. Siegel RL, Miller KD, Jemal A. Cancer statistics, 2020. CA: a cancer journal for clinicians. 2020;70(1):7-30.
33. Chornokur G, Dalton K, Borysova ME, Kumar NB. Disparities at presentation, diagnosis, treatment, and survival in African American men, affected by prostate cancer. The Prostate. 2011;71(9):985-97.
34. Morrison BF, Aiken WD, Mayhew R. Current state of prostate cancer treatment in Jamaica. Ecancermedicalscience. 2014;8:456.
35. Morrison BF, Aiken WD, Mayhew R, Gordon Y, Odedina FT. Prostate Cancer Knowledge, Prevention, and Screening Behaviors in Jamaican Men. Journal of cancer education : the official journal of the American Association for Cancer Education. 2017;32(2):352-6.
36. Cotter MP, Gern RW, Ho GY, Chang RY, Burk RD. Role of family history and ethnicity on the mode and age of prostate cancer presentation. The Prostate. 2002;50(4):216-21.
37. Robert M, Gibbs BF, Jacobson E, Gagnon C. Characterization of prostate-specific antigen proteolytic activity on its major physiological substrate, the sperm motility inhibitor precursor/semenogelin I. Biochemistry. 1997;36(13):3811-9.
38. Balk SP, Ko YJ, Bubley GJ. Biology of prostate-specific antigen. Journal of clinical oncology : official journal of the American Society of Clinical Oncology. 2003;21(2):383-91.
39. Diamandis EP, Yu H. Nonprostatic sources of prostate-specific antigen. The Urologic clinics of North America. 1997;24(2):275-82.

40. Schröder FH, Hugosson J, Roobol MJ, Tammela TL, Zappa M, Nelen V, et al. Screening and prostate cancer mortality: results of the European Randomised Study of Screening for Prostate Cancer (ERSPC) at 13 years of follow-up. Lancet (London, England). 2014;384(9959):2027-35.
41. Oesterling JE. Prostate specific antigen: a critical assessment of the most useful tumor marker for adenocarcinoma of the prostate. The Journal of urology. 1991;145(5):907-23.
42. Sölétormos G, Semjonow A, Sibley PE, Lamerz R, Petersen PH, Albrecht W, et al. Biological variation of total prostate-specific antigen: a survey of published estimates and consequences for clinical practice. Clinical chemistry. 2005;51(8):1342-51.
43. Hennigan TW, Franks PJ, Hocken DB, Allen-Mersh TG. Rectal examination in general practice. BMJ (Clinical research ed). 1990;301(6750):478-80.
44. Richie JP, Catalona WJ, Ahmann FR, Hudson MA, Scardino PT, Flanigan RC, et al. Effect of patient age on early detection of prostate cancer with serum prostate-specific antigen and digital rectal examination. Urology. 1993;42(4):365-74.
45. Carvalhal GF, Smith DS, Mager DE, Ramos C, Catalona WJ. Digital rectal examination for detecting prostate cancer at prostate specific antigen levels of 4 ng./ml. or less. The Journal of urology. 1999;161(3):835-9.
46. Okotie OT, Roehl KA, Han M, Loeb S, Gashti SN, Catalona WJ. Characteristics of prostate cancer detected by digital rectal examination only. Urology. 2007;70(6):1117-20.
47. Humphrey PA. Diagnosis of adenocarcinoma in prostate needle biopsy tissue. Journal of clinical pathology. 2007;60(1):35-42.
48. Ohori M, Wheeler TM, Scardino PT. The New American Joint Committee on Cancer and International Union Against Cancer TNM classification of prostate cancer. Clinicopathologic correlations. Cancer. 1994;74(1):104-14.
49. Minervini A, Vittori G, Siena G, Carini M. Morbidity and psychological impact of prostate biopsy: the future calls for a change. Asian journal of andrology. 2014;16(3):415-7.
50. Gleason DF. Classification of prostatic carcinomas. Cancer chemotherapy reports. 1966;50(3):125-8.
51. Al-Maghrabi JA, Bakshi NA, Farsi HM. Gleason grading of prostate cancer in needle core biopsies: a comparison of general and urologic pathologists. Annals of Saudi medicine. 2013;33(1):40-4.
52. Epstein JI, Egevad L, Amin MB, Delahunt B, Srigley JR, Humphrey PA. The 2014 International Society of Urological Pathology (ISUP) Consensus Conference on Gleason Grading of Prostatic Carcinoma: Definition of Grading Patterns and Proposal for a New Grading System. The American journal of surgical pathology. 2016;40(2):244-52.
53. Montironi R, Santoni M, Mazzucchelli R, Burattini L, Berardi R, Galosi AB, et al. Prostate cancer: from Gleason scoring to prognostic grade grouping. Expert review of anticancer therapy. 2016;16(4):433-40.
54. Leapman MS, Cowan JE, Simko J, Roberge G, Stohr BA, Carroll PR, et al. Application of a Prognostic Gleason Grade Grouping System to Assess Distant Prostate Cancer Outcomes. European urology. 2017;71(5):750-9.
55. Buyyounouski MK, Choyke PL, McKenney JK, Sartor O, Sandler HM, Amin MB, et al. Prostate cancer - major changes in the American Joint Committee on Cancer eighth edition cancer staging manual. CA: a cancer journal for clinicians. 2017;67(3):245-53.
56. Ross T, Ahmed K, Raison N, Challacombe B, Dasgupta P. Clarifying the PSA grey zone: The management of patients with a borderline PSA. International journal of clinical practice. 2016;70(11):950-9.
57. Stenman UH, Abrahamsson PA, Aus G, Lilja H, Bangma C, Hamdy FC, et al. Prognostic value of serum markers for prostate cancer. Scandinavian journal of urology and nephrology Supplementum. 2005(216):64-81.

58. Draisma G, Etzioni R, Tsodikov A, Mariotto A, Wever E, Gulati R, et al. Lead time and overdiagnosis in prostate-specific antigen screening: importance of methods and context. Journal of the National Cancer Institute. 2009;101(6):374-83.
59. Etzioni R, Cha R, Feuer EJ, Davidov O. Asymptomatic incidence and duration of prostate cancer. American journal of epidemiology. 1998;148(8):775-85.
60. Loeb S, Catalona WJ. The Prostate Health Index: a new test for the detection of prostate cancer. Therapeutic advances in urology. 2014;6(2):74-7.
61. Bryant RJ, Sjoberg DD, Vickers AJ, Robinson MC, Kumar R, Marsden L, et al. Predicting high-grade cancer at ten-core prostate biopsy using four kallikrein markers measured in blood in the ProtecT study. Journal of the National Cancer Institute. 2015;107(7).
62. Nordström T, Vickers A, Assel M, Lilja H, Grönberg H, Eklund M. Comparison Between the Four-kallikrein Panel and Prostate Health Index for Predicting Prostate Cancer. European urology. 2015;68(1):139-46.
63. Lazzeri M, Haese A, Abrate A, de la Taille A, Redorta JP, McNicholas T, et al. Clinical performance of serum prostate-specific antigen isoform [-2]proPSA (p2PSA) and its derivatives, %p2PSA and the prostate health index (PHI), in men with a family history of prostate cancer: results from a multicentre European study, the PROMEtheuS project. BJU international. 2013;112(3):313-21.
64. Marks LS, Fradet Y, Deras IL, Blase A, Mathis J, Aubin SM, et al. PCA3 molecular urine assay for prostate cancer in men undergoing repeat biopsy. Urology. 2007;69(3):532-5.
65. Hessels D, Klein Gunnewiek JM, van Oort I, Karthaus HF, van Leenders GJ, van Balken B, et al. DD3(PCA3)-based molecular urine analysis for the diagnosis of prostate cancer. European urology. 2003;44(1):8-15; discussion -6.
66. Van Neste L, Hendriks RJ, Dijkstra S, Trooskens G, Cornel EB, Jannink SA, et al. Detection of High-grade Prostate Cancer Using a Urinary Molecular Biomarker-Based Risk Score. European urology. 2016;70(5):740-8.
67. Tomlins SA, Day JR, Lonigro RJ, Hovelson DH, Siddiqui J, Kunju LP, et al. Urine TMPRSS2:ERG Plus PCA3 for Individualized Prostate Cancer Risk Assessment. European urology. 2016;70(1):45-53.
68. McKiernan J, Donovan MJ, Margolis E, Partin A, Carter B, Brown G, et al. A Prospective Adaptive Utility Trial to Validate Performance of a Novel Urine Exosome Gene Expression Assay to Predict High-grade Prostate Cancer in Patients with Prostate-specific Antigen 2-10ng/ml at Initial Biopsy. European urology. 2018;74(6):731-8.
69. Cullen J, Rosner IL, Brand TC, Zhang N, Tsiatis AC, Moncur J, et al. A Biopsy-based 17-gene Genomic Prostate Score Predicts Recurrence After Radical Prostatectomy and Adverse Surgical Pathology in a Racially Diverse Population of Men with Clinically Low- and Intermediate-risk Prostate Cancer. European urology. 2015;68(1):123-31.
70. Léon P, Cancel-Tassin G, Drouin S, Audouin M, Varinot J, Comperat E, et al. Comparison of cell cycle progression score with two immunohistochemical markers (PTEN and Ki-67) for predicting outcome in prostate cancer after radical prostatectomy. World journal of urology. 2018;36(9):1495-500.
71. Glass AG, Leo MC, Haddad Z, Yousefi K, du Plessis M, Chen C, et al. Validation of a Genomic Classifier for Predicting Post-Prostatectomy Recurrence in a Community Based Health Care Setting. The Journal of urology. 2016;195(6):1748-53.
72. Ross AE, Feng FY, Ghadessi M, Erho N, Crisan A, Buerki C, et al. A genomic classifier predicting metastatic disease progression in men with biochemical recurrence after prostatectomy. Prostate cancer and prostatic diseases. 2014;17(1):64-9.
73. Adolfsson J. Watchful waiting and active surveillance: the current position. BJU international. 2008;102(1):10-4.

74. Binder J, Jones J, Bentas W, Wolfram M, Bräutigam R, Probst M, et al. [Robot-assisted laparoscopy in urology. Radical prostatectomy and reconstructive retroperitoneal interventions]. Der Urologe Ausg A. 2002;41(2):144-9.
75. Ling CC, Yorke E, Fuks Z. From IMRT to IGRT: frontierland or neverland? Radiotherapy and oncology : journal of the European Society for Therapeutic Radiology and Oncology. 2006;78(2):119-22.
76. Skowronek J. Current status of brachytherapy in cancer treatment - short overview. Journal of contemporary brachytherapy. 2017;9(6):581-9.
77. Pagliarulo V, Bracarda S, Eisenberger MA, Mottet N, Schröder FH, Sternberg CN, et al. Contemporary role of androgen deprivation therapy for prostate cancer. European urology. 2012;61(1):11-25.
78. Klotz L, Boccon-Gibod L, Shore ND, Andreou C, Persson BE, Cantor P, et al. The efficacy and safety of degarelix: a 12-month, comparative, randomized, open-label, parallel-group phase III study in patients with prostate cancer. BJU international. 2008;102(11):1531-8.
79. Sciarra A, Fasulo A, Ciardi A, Petrangeli E, Gentilucci A, Maggi M, et al. A meta-analysis and systematic review of randomized controlled trials with degarelix versus gonadotropin-releasing hormone agonists for advanced prostate cancer. Medicine. 2016;95(27):e3845.
80. Iversen P. Antiandrogen monotherapy: indications and results. Urology. 2002;60(3 Suppl 1):64-71.
81. Potter GA, Barrie SE, Jarman M, Rowlands MG. Novel steroidal inhibitors of human cytochrome P45017 alpha (17 alpha-hydroxylase-C17,20-lyase): potential agents for the treatment of prostatic cancer. Journal of medicinal chemistry. 1995;38(13):2463-71.
82. Tran C, Ouk S, Clegg NJ, Chen Y, Watson PA, Arora V, et al. Development of a second-generation antiandrogen for treatment of advanced prostate cancer. Science (New York, NY). 2009;324(5928):787-90.
83. Clegg NJ, Wongvipat J, Joseph JD, Tran C, Ouk S, Dilhas A, et al. ARN-509: a novel antiandrogen for prostate cancer treatment. Cancer Res. 2012;72(6):1494-503.
84. de Bono JS, Oudard S, Ozguroglu M, Hansen S, Machiels JP, Kocak I, et al. Prednisone plus cabazitaxel or mitoxantrone for metastatic castration-resistant prostate cancer progressing after docetaxel treatment: a randomised open-label trial. Lancet (London, England). 2010;376(9747):1147-54.
85. Kantoff PW, Higano CS, Shore ND, Berger ER, Small EJ, Penson DF, et al. Sipuleucel-T immunotherapy for castration-resistant prostate cancer. The New England journal of medicine. 2010;363(5):411-22.
86. Parker C, Nilsson S, Heinrich D, Helle SI, O'Sullivan JM, Fosså SD, et al. Alpha emitter radium-223 and survival in metastatic prostate cancer. The New England journal of medicine. 2013;369(3):213-23.
87. Sanda MG, Dunn RL, Michalski J, Sandler HM, Northouse L, Hembroff L, et al. Quality of life and satisfaction with outcome among prostate-cancer survivors. The New England journal of medicine. 2008;358(12):1250-61.
88. de Bono J, Mateo J, Fizazi K, Saad F, Shore N, Sandhu S, et al. Olaparib for Metastatic Castration-Resistant Prostate Cancer. The New England journal of medicine. 2020;382(22):2091-102.
89. de Bono JS, Logothetis CJ, Molina A, Fizazi K, North S, Chu L, et al. Abiraterone and increased survival in metastatic prostate cancer. The New England journal of medicine. 2011;364(21):1995-2005.
90. Ryan CJ, Smith MR, Fizazi K, Saad F, Mulders PF, Sternberg CN, et al. Abiraterone acetate plus prednisone versus placebo plus prednisone in chemotherapy-naive men with metastatic castration-resistant prostate cancer (COU-AA-302): final overall survival analysis of a randomised, double-blind, placebo-controlled phase 3 study. The Lancet Oncology. 2015;16(2):152-60.

91. Scher HI, Fizazi K, Saad F, Taplin ME, Sternberg CN, Miller K, et al. Increased survival with enzalutamide in prostate cancer after chemotherapy. The New England journal of medicine. 2012;367(13):1187-97.
92. Hussain M, Fizazi K, Saad F, Rathenborg P, Shore N, Ferreira U, et al. Enzalutamide in Men with Nonmetastatic, Castration-Resistant Prostate Cancer. The New England journal of medicine. 2018;378(26):2465-74.
93. Ramsay CR, Adewuyi TE, Gray J, Hislop J, Shirley MD, Jayakody S, et al. Ablative therapy for people with localised prostate cancer: a systematic review and economic evaluation. Health technology assessment (Winchester, England). 2015;19(49):1-490.
94. Murai J, Huang SY, Das BB, Renaud A, Zhang Y, Doroshow JH, et al. Trapping of PARP1 and PARP2 by Clinical PARP Inhibitors. Cancer Res. 2012;72(21):5588-99.
95. Bryce AH, Sartor O, de Bono J. DNA Repair and Prostate Cancer: A Field Ripe for Harvest. European urology. 2020.
96. Barbieri CE, Baca SC, Lawrence MS, Demichelis F, Blattner M, Theurillat JP, et al. Exome sequencing identifies recurrent SPOP, FOXA1 and MED12 mutations in prostate cancer. Nature genetics. 2012;44(6):685-9.
97. Lawrence MS, Stojanov P, Polak P, Kryukov GV, Cibulskis K, Sivachenko A, et al. Mutational heterogeneity in cancer and the search for new cancer-associated genes. Nature. 2013;499(7457):214-8.
98. Lawrence MS, Stojanov P, Mermel CH, Robinson JT, Garraway LA, Golub TR, et al. Discovery and saturation analysis of cancer genes across 21 tumour types. Nature. 2014;505(7484):495-501.
99. The Molecular Taxonomy of Primary Prostate Cancer. Cell. 2015;163(4):1011-25.
100. Tomlins SA, Bjartell A, Chinnaiyan AM, Jenster G, Nam RK, Rubin MA, et al. ETS gene fusions in prostate cancer: from discovery to daily clinical practice. European urology. 2009;56(2):275-86.
101. Nguyen LT, Tretiakova MS, Silvis MR, Lucas J, Klezovitch O, Coleman I, et al. ERG Activates the YAP1 Transcriptional Program and Induces the Development of Age-Related Prostate Tumors. Cancer Cell. 2015;27(6):797-808.
102. Leslie NR, Kriplani N, Hermida MA, Alvarez-Garcia V, Wise HM. The PTEN protein: cellular localization and post-translational regulation. Biochem Soc Trans. 2016;44(1):273-8.
103. Leslie NR, Downes CP. PTEN function: how normal cells control it and tumour cells lose it. Biochem J. 2004;382(Pt 1):1-11.
104. Taylor BS, Schultz N, Hieronymus H, Gopalan A, Xiao Y, Carver BS, et al. Integrative genomic profiling of human prostate cancer. Cancer cell. 2010;18(1):11-22.
105. Kwak MK, Johnson DT, Zhu C, Lee SH, Ye DW, Luong R, et al. Conditional deletion of the Pten gene in the mouse prostate induces prostatic intraepithelial neoplasms at early ages but a slow progression to prostate tumors. PloS one. 2013;8(1):e53476.
106. Barbieri CE, Bangma CH, Bjartell A, Catto JW, Culig Z, Gronberg H, et al. The mutational landscape of prostate cancer. Eur Urol. 2013;64(4):567-76.
107. Vinall RL, Chen JQ, Hubbard NE, Sulaimon SS, Shen MM, Devere White RW, et al. Initiation of prostate cancer in mice by Tp53R270H: evidence for an alternative molecular progression. Disease models & mechanisms. 2012;5(6):914-20.
108. Blattner M, Liu D, Robinson BD, Huang D, Poliakov A, Gao D, et al. SPOP Mutation Drives Prostate Tumorigenesis In Vivo through Coordinate Regulation of PI3K/mTOR and AR Signaling. Cancer cell. 2017;31(3):436-51.
109. Zhang C, Wang L, Wu D, Chen H, Chen Z, Thomas-Ahner JM, et al. Definition of a FoxA1 Cistrome that is crucial for G1 to S-phase cell-cycle transit in castration-resistant prostate cancer. Cancer Res. 2011;71(21):6738-48.

110. Adams EJ, Karthaus WR, Hoover E, Liu D, Gruet A, Zhang Z, et al. FOXA1 mutations alter pioneering activity, differentiation and prostate cancer phenotypes. Nature. 2019;571(7765):408-12.
111. Di Cristofano A, De Acetis M, Koff A, Cordon-Cardo C, Pandolfi PP. Pten and p27KIP1 cooperate in prostate cancer tumor suppression in the mouse. Nature genetics. 2001;27(2):222-4.
112. Song H, Zhang B, Watson MA, Humphrey PA, Lim H, Milbrandt J. Loss of Nkx3.1 leads to the activation of discrete downstream target genes during prostate tumorigenesis. Oncogene. 2009;28(37):3307-19.
113. Thangapazham R, Saenz F, Katta S, Mohamed AA, Tan SH, Petrovics G, et al. Loss of the NKX3.1 tumorsuppressor promotes the TMPRSS2-ERG fusion gene expression in prostate cancer. BMC Cancer. 2014;14:16.
114. Kim MJ, Cardiff RD, Desai N, Banach-Petrosky WA, Parsons R, Shen MM, et al. Cooperativity of Nkx3.1 and Pten loss of function in a mouse model of prostate carcinogenesis. Proc Natl Acad Sci U S A. 2002;99(5):2884-9.
115. Zhou H, Kim S, Ishii S, Boyer TG. Mediator modulates Gli3-dependent Sonic hedgehog signaling. Molecular and cellular biology. 2006;26(23):8667-82.
116. Barbieri C, Baca S, Lawrence M, Demichelis F, Blattner M, Theurillat J, et al. Exome sequencing identifies recurrent SPOP, FOXA1 and MED12 mutations in prostate cancer. Nature genetics. 2012;44:685-9.
117. Heidenreich A, Bastian PJ, Bellmunt J, Bolla M, Joniau S, van der Kwast T, et al. EAU guidelines on prostate cancer. Part II: Treatment of advanced, relapsing, and castration-resistant prostate cancer. European urology. 2014;65(2):467-79.
118. Shafi AA, Yen AE, Weigel NL. Androgen receptors in hormone-dependent and castration-resistant prostate cancer. Pharmacol Ther. 2013;140(3):223-38.
119. Gundem G, Van Loo P, Kremeyer B, Alexandrov LB, Tubio JMC, Papaemmanuil E, et al. The evolutionary history of lethal metastatic prostate cancer. Nature. 2015;520(7547):353-7.
120. Grasso CS, Wu YM, Robinson DR, Cao X, Dhanasekaran SM, Khan AP, et al. The mutational landscape of lethal castration-resistant prostate cancer. Nature. 2012;487(7406):239-43.
121. Robinson D, Van Allen EM, Wu YM, Schultz N, Lonigro RJ, Mosquera JM, et al. Integrative clinical genomics of advanced prostate cancer. Cell. 2015;161(5):1215-28.
122. Sun S, Sprenger CC, Vessella RL, Haugk K, Soriano K, Mostaghel EA, et al. Castration resistance in human prostate cancer is conferred by a frequently occurring androgen receptor splice variant. The Journal of clinical investigation. 2010;120(8):2715-30.
123. Ferraldeschi R, Nava Rodrigues D, Riisnaes R, Miranda S, Figueiredo I, Rescigno P, et al. PTEN protein loss and clinical outcome from castration-resistant prostate cancer treated with abiraterone acetate. European urology. 2015;67(4):795-802.
124. Baca SC, Prandi D, Lawrence MS, Mosquera JM, Romanel A, Drier Y, et al. Punctuated evolution of prostate cancer genomes. Cell. 2013;153(3):666-77.
125. Ladomery M. Aberrant alternative splicing is another hallmark of cancer. International journal of cell biology. 2013;2013:463786.
126. Oltean S, Bates DO. Hallmarks of alternative splicing in cancer. Oncogene. 2014;33(46):5311-8.
127. Scotti MM, Swanson MS. RNA mis-splicing in disease. Nat Rev Genet. 2016;17(1):19-32.
128. Barta A, Schümperli D. Editorial on alternative splicing and disease. RNA biology. 2010;7(4):388-9.
129. Cooper TA, Wan L, Dreyfuss G. RNA and disease. Cell. 2009;136(4):777-93.
130. Chen M, Manley JL. Mechanisms of alternative splicing regulation: insights from molecular and genomics approaches. Nature reviews Molecular cell biology. 2009;10(11):741-54.
131. Matera AG, Wang Z. A day in the life of the spliceosome. Nature reviews Molecular cell biology. 2014;15(2):108-21.

132. Kelemen O, Convertini P, Zhang Z, Wen Y, Shen M, Falaleeva M, et al. Function of alternative splicing. Gene. 2013;514(1):1-30.
133. Wang Y, Liu J, Huang BO, Xu YM, Li J, Huang LF, et al. Mechanism of alternative splicing and its regulation. Biomedical reports. 2015;3(2):152-8.
134. Nilsen TW, Graveley BR. Expansion of the eukaryotic proteome by alternative splicing. Nature. 2010;463(7280):457-63.
135. Patel AA, Steitz JA. Splicing double: insights from the second spliceosome. Nature reviews Molecular cell biology. 2003;4(12):960-70.
136. Dvinge H. Regulation of alternative mRNA splicing: old players and new perspectives. FEBS letters. 2018;592(17):2987-3006.
137. Sharp PA, Burge CB. Classification of introns: U2-type or U12-type. Cell. 1997;91(7):875-9.
138. Cartegni L, Chew SL, Krainer AR. Listening to silence and understanding nonsense: exonic mutations that affect splicing. Nat Rev Genet. 2002;3(4):285-98.
139. Jeong S. SR Proteins: Binders, Regulators, and Connectors of RNA. Molecules and cells. 2017;40(1):1-9.
140. Lee Y, Rio DC. Mechanisms and Regulation of Alternative Pre-mRNA Splicing. Annual review of biochemistry. 2015;84:291-323.
141. Chaudhury A, Chander P, Howe PH. Heterogeneous nuclear ribonucleoproteins (hnRNPs) in cellular processes: Focus on hnRNP E1's multifunctional regulatory roles. RNA (New York, NY). 2010;16(8):1449-62.
142. Weighardt F, Biamonti G, Riva S. The roles of heterogeneous nuclear ribonucleoproteins (hnRNP) in RNA metabolism. BioEssays : news and reviews in molecular, cellular and developmental biology. 1996;18(9):747-56.
143. Schlautmann LP, Gehring NH. A Day in the Life of the Exon Junction Complex. Biomolecules. 2020;10(6).
144. Mure F, Corbin A, Benbahouche NEH, Bertrand E, Manet E, Gruffat H. The splicing factor SRSF3 is functionally connected to the nuclear RNA exosome for intronless mRNA decay. Scientific reports. 2018;8(1):12901.
145. Kurosaki T, Popp MW, Maquat LE. Quality and quantity control of gene expression by nonsense-mediated mRNA decay. Nature reviews Molecular cell biology. 2019;20(7):406-20.
146. Berget SM. Exon recognition in vertebrate splicing. The Journal of biological chemistry. 1995;270(6):2411-4.
147. Schneider M, Will CL, Anokhina M, Tazi J, Urlaub H, Lührmann R. Exon definition complexes contain the tri-snRNP and can be directly converted into B-like precatalytic splicing complexes. Mol Cell. 2010;38(2):223-35.
148. Sterne-Weiler T, Sanford JR. Exon identity crisis: disease-causing mutations that disrupt the splicing code. Genome Biol. 2014;15(1):201.
149. Valadkhan S, Manley JL. Splicing-related catalysis by protein-free snRNAs. Nature. 2001;413(6857):701-7.
150. Paschalis A, Sharp A, Welti JC, Neeb A, Raj GV, Luo J, et al. Alternative splicing in prostate cancer. Nature reviews Clinical oncology. 2018;15(11):663-75.
151. Venables JP. Aberrant and alternative splicing in cancer. Cancer Res. 2004;64(21):7647-54.
152. Wang BD, Ceniccola K, Hwang S, Andrawis R, Horvath A, Freedman JA, et al. Alternative splicing promotes tumour aggressiveness and drug resistance in African American prostate cancer. Nat Commun. 2017;8:15921.
153. Wadosky KM, Koochekpour S. Androgen receptor splice variants and prostate cancer: From bench to bedside. Oncotarget. 2017;8(11):18550-76.
154. Lu C, Luo J. Decoding the androgen receptor splice variants. Translational andrology and urology. 2013;2(3):178-86.

155. Dehm SM, Schmidt LJ, Heemers HV, Vessella RL, Tindall DJ. Splicing of a novel androgen receptor exon generates a constitutively active androgen receptor that mediates prostate cancer therapy resistance. Cancer Res. 2008;68(13):5469-77.
156. Antonarakis ES, Lu C, Wang H, Luber B, Nakazawa M, Roeser JC, et al. AR-V7 and resistance to enzalutamide and abiraterone in prostate cancer. The New England journal of medicine. 2014;371(11):1028-38.
157. Efstathiou E, Titus M, Wen S, Hoang A, Karlou M, Ashe R, et al. Molecular characterization of enzalutamide-treated bone metastatic castration-resistant prostate cancer. European urology. 2015;67(1):53-60.
158. Liu LL, Xie N, Sun S, Plymate S, Mostaghel E, Dong X. Mechanisms of the androgen receptor splicing in prostate cancer cells. Oncogene. 2014;33(24):3140-50.
159. Hörnberg E, Ylitalo EB, Crnalic S, Antti H, Stattin P, Widmark A, et al. Expression of androgen receptor splice variants in prostate cancer bone metastases is associated with castration-resistance and short survival. PloS one. 2011;6(4):e19059.
160. Scher HI, Lu D, Schreiber NA, Louw J, Graf RP, Vargas HA, et al. Association of AR-V7 on Circulating Tumor Cells as a Treatment-Specific Biomarker With Outcomes and Survival in Castration-Resistant Prostate Cancer. JAMA oncology. 2016;2(11):1441-9.
161. Scher HI, Graf RP, Schreiber NA, McLaughlin B, Lu D, Louw J, et al. Nuclear-specific AR-V7 Protein Localization is Necessary to Guide Treatment Selection in Metastatic Castration-resistant Prostate Cancer. European urology. 2017;71(6):874-82.
162. Hormaechea-Agulla D, Jiménez-Vacas JM, Gómez-Gómez E, F LL, Carrasco-Valiente J, Valero-Rosa J, et al. The oncogenic role of the spliced somatostatin receptor sst5TMD4 variant in prostate cancer. FASEB journal : official publication of the Federation of American Societies for Experimental Biology. 2017;31(11):4682-96.
163. Hormaechea-Agulla D, Gahete MD, Jiménez-Vacas JM, Gómez-Gómez E, Ibáñez-Costa A, F LL, et al. The oncogenic role of the In1-ghrelin splicing variant in prostate cancer aggressiveness. Molecular cancer. 2017;16(1):146.
164. Raj B, Irimia M, Braunschweig U, Sterne-Weiler T, O'Hanlon D, Lin ZY, et al. A global regulatory mechanism for activating an exon network required for neurogenesis. Mol Cell. 2014;56(1):90-103.
165. Zhang X, Coleman IM, Brown LG, True LD, Kollath L, Lucas JM, et al. SRRM4 Expression and the Loss of REST Activity May Promote the Emergence of the Neuroendocrine Phenotype in Castration-Resistant Prostate Cancer. Clinical cancer research : an official journal of the American Association for Cancer Research. 2015;21(20):4698-708.
166. Li Y, Donmez N, Sahinalp C, Xie N, Wang Y, Xue H, et al. SRRM4 Drives Neuroendocrine Transdifferentiation of Prostate Adenocarcinoma Under Androgen Receptor Pathway Inhibition. European urology. 2017;71(1):68-78.
167. Carstens RP, Eaton JV, Krigman HR, Walther PJ, Garcia-Blanco MA. Alternative splicing of fibroblast growth factor receptor 2 (FGF-R2) in human prostate cancer. Oncogene. 1997;15(25):3059-65.
168. Narla G, DiFeo A, Yao S, Banno A, Hod E, Reeves HL, et al. Targeted inhibition of the KLF6 splice variant, KLF6 SV1, suppresses prostate cancer cell growth and spread. Cancer Res. 2005;65(13):5761-8.
169. Woolard J, Wang WY, Bevan HS, Qiu Y, Morbidelli L, Pritchard-Jones RO, et al. VEGF165b, an inhibitory vascular endothelial growth factor splice variant: mechanism of action, in vivo effect on angiogenesis and endogenous protein expression. Cancer Res. 2004;64(21):7822-35.
170. Augello MA, Burd CJ, Birbe R, McNair C, Ertel A, Magee MS, et al. Convergence of oncogenic and hormone receptor pathways promotes metastatic phenotypes. The Journal of clinical investigation. 2013;123(1):493-508.
171. Takeiwa T, Mitobe Y, Ikeda K, Horie-Inoue K, Inoue S. Roles of Splicing Factors in Hormone-Related Cancer Progression. International journal of molecular sciences. 2020;21(5).

172. Takayama KI, Suzuki T, Fujimura T, Yamada Y, Takahashi S, Homma Y, et al. Dysregulation of spliceosome gene expression in advanced prostate cancer by RNA-binding protein PSF. Proceedings of the National Academy of Sciences of the United States of America. 2017;114(39):10461-6.
173. Kawamura N, Nimura K, Saga K, Ishibashi A, Kitamura K, Nagano H, et al. SF3B2-Mediated RNA Splicing Drives Human Prostate Cancer Progression. Cancer Res. 2019;79(20):5204-17.
174. Duan L, Chen Z, Lu J, Liang Y, Wang M, Roggero CM, et al. Histone lysine demethylase KDM4B regulates the alternative splicing of the androgen receptor in response to androgen deprivation. Nucleic acids research. 2019;47(22):11623-36.
175. Stockley J, Markert E, Zhou Y, Robson CN, Elliott DJ, Lindberg J, et al. The RNA-binding protein Sam68 regulates expression and transcription function of the androgen receptor splice variant AR-V7. Scientific reports. 2015;5:13426.
176. Munkley J, Li L, Krishnan SRG, Hysenaj G, Scott E, Dalgliesh C, et al. Androgen-regulated transcription of ESRP2 drives alternative splicing patterns in prostate cancer. eLife. 2019;8.
177. Kramer A, Gruter P, Groning K, Kastner B. Combined biochemical and electron microscopic analyses reveal the architecture of the mammalian U2 snRNP. The Journal of cell biology. 1999;145(7):1355-68.
178. Smith KB, Smith MS. Obesity Statistics. Primary care. 2016;43(1):121-35, ix.
179. Lobstein T, Jackson-Leach R, Moodie ML, Hall KD, Gortmaker SL, Swinburn BA, et al. Child and adolescent obesity: part of a bigger picture. Lancet (London, England). 2015;385(9986):2510-20.
180. MacInnis RJ, English DR. Body size and composition and prostate cancer risk: systematic review and meta-regression analysis. Cancer causes & control : CCC. 2006;17(8):989-1003.
181. Bergström A, Pisani P, Tenet V, Wolk A, Adami HO. Overweight as an avoidable cause of cancer in Europe. International journal of cancer. 2001;91(3):421-30.
182. Calle EE, Rodriguez C, Walker-Thurmond K, Thun MJ. Overweight, obesity, and mortality from cancer in a prospectively studied cohort of U.S. adults. The New England journal of medicine. 2003;348(17):1625-38.
183. Andersson SO, Wolk A, Bergström R, Adami HO, Engholm G, Englund A, et al. Body size and prostate cancer: a 20-year follow-up study among 135006 Swedish construction workers. Journal of the National Cancer Institute. 1997;89(5):385-9.
184. Wright ME, Chang SC, Schatzkin A, Albanes D, Kipnis V, Mouw T, et al. Prospective study of adiposity and weight change in relation to prostate cancer incidence and mortality. Cancer. 2007;109(4):675-84.
185. Kharroubi AT, Darwish HM. Diabetes mellitus: The epidemic of the century. World journal of diabetes. 2015;6(6):850-67.
186. Kasper JS, Liu Y, Giovannucci E. Diabetes mellitus and risk of prostate cancer in the health professionals follow-up study. International journal of cancer. 2009;124(6):1398-403.
187. Häggström C, Van Hemelrijck M, Zethelius B, Robinson D, Grundmark B, Holmberg L, et al. Prospective study of Type 2 diabetes mellitus, anti-diabetic drugs and risk of prostate cancer. International journal of cancer. 2017;140(3):611-7.
188. Choi JB, Moon HW, Park YH, Bae WJ, Cho HJ, Hong SH, et al. The Impact of Diabetes on the Risk of Prostate Cancer Development according to Body Mass Index: A 10-year Nationwide Cohort Study. Journal of Cancer. 2016;7(14):2061-6.
189. Tseng CH. Diabetes and risk of prostate cancer: a study using the National Health Insurance. Diabetes care. 2011;34(3):616-21.
190. Darbinian JA, Ferrara AM, Van Den Eeden SK, Quesenberry CP, Jr., Fireman B, Habel LA. Glycemic status and risk of prostate cancer. Cancer epidemiology, biomarkers & prevention : a

publication of the American Association for Cancer Research, cosponsored by the American Society of Preventive Oncology. 2008;17(3):628-35.
191. Mistry T, Digby JE, Desai KM, Randeva HS. Obesity and prostate cancer: a role for adipokines. European urology. 2007;52(1):46-53.
192. Westley RL, May FE. A twenty-first century cancer epidemic caused by obesity: the involvement of insulin, diabetes, and insulin-like growth factors. International journal of endocrinology. 2013;2013:632461.
193. Polesel J, Gini A, Dal Maso L, Stocco C, Birri S, Taborelli M, et al. The impact of diabetes and other metabolic disorders on prostate cancer prognosis. Journal of diabetes and its complications. 2016;30(4):591-6.
194. Maj-Hes AB, Mathieu R, Özsoy M, Soria F, Moschini M, Abufaraj M, et al. Obesity is associated with biochemical recurrence after radical prostatectomy: A multi-institutional extended validation study. Urologic oncology. 2017;35(7):460.e1-.e8.
195. Jamnagerwalla J, Howard LE, Allott EH, Vidal AC, Moreira DM, Castro-Santamaria R, et al. Serum cholesterol and risk of high-grade prostate cancer: results from the REDUCE study. Prostate cancer and prostatic diseases. 2018;21(2):252-9.
196. Kato K, Iwama H, Yamashita T, Kobayashi K, Fujihara S, Fujimori T, et al. The anti-diabetic drug metformin inhibits pancreatic cancer cell proliferation in vitro and in vivo: Study of the microRNAs associated with the antitumor effect of metformin. Oncology reports. 2016;35(3):1582-92.
197. Quinn BJ, Kitagawa H, Memmott RM, Gills JJ, Dennis PA. Repositioning metformin for cancer prevention and treatment. Trends in endocrinology and metabolism: TEM. 2013;24(9):469-80.
198. Thompson JS, Sood A, Arora R. Statins and cancer: a potential link? American journal of therapeutics. 2010;17(4):e100-4.
199. Osmak M. Statins and cancer: current and future prospects. Cancer letters. 2012;324(1):1-12.
200. Kirtonia A, Gala K, Fernandes SG, Pandya G, Pandey AK, Sethi G, et al. Repurposing of drugs: An attractive pharmacological strategy for cancer therapeutics. Seminars in cancer biology. 2020.
201. Ashburn TT, Thor KB. Drug repositioning: identifying and developing new uses for existing drugs. Nature reviews Drug discovery. 2004;3(8):673-83.
202. Spratt DE, Zhang C, Zumsteg ZS, Pei X, Zhang Z, Zelefsky MJ. Metformin and prostate cancer: reduced development of castration-resistant disease and prostate cancer mortality. European urology. 2013;63(4):709-16.
203. Yu O, Eberg M, Benayoun S, Aprikian A, Batist G, Suissa S, et al. Use of statins and the risk of death in patients with prostate cancer. Journal of clinical oncology : official journal of the American Society of Clinical Oncology. 2014;32(1):5-11.
204. Tan N, Klein EA, Li J, Moussa AS, Jones JS. Statin use and risk of prostate cancer in a population of men who underwent biopsy. The Journal of urology. 2011;186(1):86-90.
205. Ben Sahra I, Laurent K, Giuliano S, Larbret F, Ponzio G, Gounon P, et al. Targeting cancer cell metabolism: the combination of metformin and 2-deoxyglucose induces p53-dependent apoptosis in prostate cancer cells. Cancer Res. 2010;70(6):2465-75.
206. Sarmento-Cabral A, F LL, Gahete MD, Castaño JP, Luque RM. Metformin Reduces Prostate Tumor Growth, in a Diet-Dependent Manner, by Modulating Multiple Signaling Pathways. Molecular cancer research : MCR. 2017;15(7):862-74.
207. Wang C, Tao W, Wang Y, Bikow J, Lu B, Keating A, et al. Rosuvastatin, identified from a zebrafish chemical genetic screen for antiangiogenic compounds, suppresses the growth of prostate cancer. European urology. 2010;58(3):418-26.
208. Xie F, Liu J, Li C, Zhao Y. Simvastatin blocks TGF-β1-induced epithelial-mesenchymal transition in human prostate cancer cells. Oncology letters. 2016;11(5):3377-83.

209. Caro-Maldonado A, Camacho L, Zabala-Letona A, Torrano V, Fernandez-Ruiz S, Zamacola-Bascaran K, et al. Low-dose statin treatment increases prostate cancer aggressiveness. Oncotarget. 2018;9(2):1494-504.
210. Rena G, Hardie DG, Pearson ER. The mechanisms of action of metformin. Diabetologia. 2017;60(9):1577-85.
211. Alberts AW, Chen J, Kuron G, Hunt V, Huff J, Hoffman C, et al. Mevinolin: a highly potent competitive inhibitor of hydroxymethylglutaryl-coenzyme A reductase and a cholesterol-lowering agent. Proceedings of the National Academy of Sciences of the United States of America. 1980;77(7):3957-61.
212. Arai M, Uchiba M, Komura H, Mizuochi Y, Harada N, Okajima K. Metformin, an antidiabetic agent, suppresses the production of tumor necrosis factor and tissue factor by inhibiting early growth response factor-1 expression in human monocytes in vitro. The Journal of pharmacology and experimental therapeutics. 2010;334(1):206-13.
213. Ben Sahra I, Regazzetti C, Robert G, Laurent K, Le Marchand-Brustel Y, Auberger P, et al. Metformin, independent of AMPK, induces mTOR inhibition and cell-cycle arrest through REDD1. Cancer Res. 2011;71(13):4366-72.
214. Xia Z, Tan MM, Wong WW, Dimitroulakos J, Minden MD, Penn LZ. Blocking protein geranylgeranylation is essential for lovastatin-induced apoptosis of human acute myeloid leukemia cells. Leukemia. 2001;15(9):1398-407.
215. Kim JS, Turbov J, Rosales R, Thaete LG, Rodriguez GC. Combination simvastatin and metformin synergistically inhibits endometrial cancer cell growth. Gynecologic oncology. 2019;154(2):432-40.
216. Chen HH, Lin MC, Muo CH, Yeh SY, Sung FC, Kao CH. Combination Therapy of Metformin and Statin May Decrease Hepatocellular Carcinoma Among Diabetic Patients in Asia. Medicine. 2015;94(24):e1013.
217. Babcook MA, Shukla S, Fu P, Vazquez EJ, Puchowicz MA, Molter JP, et al. Synergistic simvastatin and metformin combination chemotherapy for osseous metastatic castration-resistant prostate cancer. Molecular cancer therapeutics. 2014;13(10):2288-302.
218. Wang ZS, Huang HR, Zhang LY, Kim S, He Y, Li DL, et al. Mechanistic Study of Inhibitory Effects of Metformin and Atorvastatin in Combination on Prostate Cancer Cells in Vitro and in Vivo. Biological & pharmaceutical bulletin. 2017;40(8):1247-54.
219. Gahete MD, Rincón-Fernández D, Villa-Osaba A, Hormaechea-Agulla D, Ibáñez-Costa A, Martínez-Fuentes AJ, et al. Ghrelin gene products, receptors, and GOAT enzyme: biological and pathophysiological insight. The Journal of endocrinology. 2014;220(1):R1-24.
220. Chopin LK, Seim I, Walpole CM, Herington AC. The ghrelin axis--does it have an appetite for cancer progression? Endocrine reviews. 2012;33(6):849-91.
221. Kojima M, Hosoda H, Date Y, Nakazato M, Matsuo H, Kangawa K. Ghrelin is a growth-hormone-releasing acylated peptide from stomach. Nature. 1999;402(6762):656-60.
222. van der Lely AJ, Tschop M, Heiman ML, Ghigo E. Biological, physiological, pathophysiological, and pharmacological aspects of ghrelin. Endocr Rev. 2004;25(3):426-57.
223. Al Massadi O, Tschop MH, Tong J. Ghrelin acylation and metabolic control. Peptides. 2011;32(11):2301-8.
224. Delhanty PJ, Neggers SJ, van der Lely AJ. Des-acyl ghrelin: a metabolically active peptide. Endocr Dev. 2013;25:112-21.
225. Sato T, Nakamura Y, Shiimura Y, Ohgusu H, Kangawa K, Kojima M. Structure, regulation and function of ghrelin. J Biochem. 2012;151(2):119-28.
226. Seim I, Herington AC, Chopin LK. New insights into the molecular complexity of the ghrelin gene locus. Cytokine & growth factor reviews. 2009;20(4):297-304.
227. Gahete MD, Córdoba-Chacón J, Hergueta-Redondo M, Martínez-Fuentes AJ, Kineman RD, Moreno-Bueno G, et al. A novel human ghrelin variant (In1-ghrelin) and ghrelin-O-acyltransferase

are overexpressed in breast cancer: potential pathophysiological relevance. PloS one. 2011;6(8):e23302.
228. Gahete MD, Cordoba-Chacon J, Salvatori R, Castano JP, Kineman RD, Luque RM. Metabolic regulation of ghrelin O-acyl transferase (GOAT) expression in the mouse hypothalamus, pituitary, and stomach. Molecular and cellular endocrinology. 2010;317(1-2):154-60.
229. Gahete MD, Córdoba-Chacón J, Salvatori R, Castaño JP, Kineman RD, Luque RM. Metabolic regulation of ghrelin O-acyl transferase (GOAT) expression in the mouse hypothalamus, pituitary, and stomach. Molecular and cellular endocrinology. 2010;317(1-2):154-60.
230. Luque RM, Sampedro-Nuñez M, Gahete MD, Ramos-Levi A, Ibáñez-Costa A, Rivero-Cortés E, et al. In1-ghrelin, a splice variant of ghrelin gene, is associated with the evolution and aggressiveness of human neuroendocrine tumors: Evidence from clinical, cellular and molecular parameters. Oncotarget. 2015;6(23):19619-33.
231. Hormaechea-Agulla D, Gómez-Gómez E, Ibáñez-Costa A, Carrasco-Valiente J, Rivero-Cortés E, F LL, et al. Ghrelin O-acyltransferase (GOAT) enzyme is overexpressed in prostate cancer, and its levels are associated with patient's metabolic status: Potential value as a non-invasive biomarker. Cancer letters. 2016;383(1):125-34.
232. Gomez-Gomez E, Jimenez-Vacas JM, Carrasco-Valiente J, Herrero-Aguayo V, Blanca-Pedregosa AM, Leon-Gonzalez AJ, et al. Plasma ghrelin O-acyltransferase (GOAT) enzyme levels: A novel non-invasive diagnosis tool for patients with significant prostate cancer. Journal of cellular and molecular medicine. 2018;22(11):5688-97.
233. Narla G, DiFeo A, Fernandez Y, Dhanasekaran S, Huang F, Sangodkar J, et al. KLF6-SV1 overexpression accelerates human and mouse prostate cancer progression and metastasis. The Journal of clinical investigation. 2008;118(8):2711-21.
234. Grupp K, Wilking J, Prien K, Hube-Magg C, Sirma H, Simon R, et al. High RNA-binding motif protein 3 expression is an independent prognostic marker in operated prostate cancer and tightly linked to ERG activation and PTEN deletions. Eur J Cancer. 2014;50(4):852-61.
235. Yamamoto R, Osawa T, Sasaki Y, Yamamoto S, Anai M, Izumi K, et al. Overexpression of p54(nrb)/NONO induces differential EPHA6 splicing and contributes to castration-resistant prostate cancer growth. Oncotarget. 2018;9(12):10510-24.
236. Gerhauser C, Favero F, Risch T, Simon R, Feuerbach L, Assenov Y, et al. Molecular Evolution of Early-Onset Prostate Cancer Identifies Molecular Risk Markers and Clinical Trajectories. Cancer cell. 2018;34(6):996-1011.e8.
237. Lu ZX, Huang Q, Park JW, Shen S, Lin L, Tokheim CJ, et al. Transcriptome-wide landscape of pre-mRNA alternative splicing associated with metastatic colonization. Molecular cancer research : MCR. 2015;13(2):305-18.
238. Peiqi L, Zhaozhong G, Yaotian Y, Jun J, Jihua G, Rong J. Expression of SRSF3 is Correlated with Carcinogenesis and Progression of Oral Squamous Cell Carcinoma. International journal of medical sciences. 2016;13(7):533-9.
239. Gautrey H, Jackson C, Dittrich AL, Browell D, Lennard T, Tyson-Capper A. SRSF3 and hnRNP H1 regulate a splicing hotspot of HER2 in breast cancer cells. RNA biology. 2015;12(10):1139-51.
240. Lin JC, Lee YC, Tan TH, Liang YC, Chuang HC, Fann YC, et al. RBM4-SRSF3-MAP4K4 splicing cascade modulates the metastatic signature of colorectal cancer cell. Biochimica et biophysica acta Molecular cell research. 2018;1865(2):259-72.
241. Wong N, Yan J, Ojo D, De Melo J, Cutz JC, Tang D. Changes in PKM2 associate with prostate cancer progression. Cancer investigation. 2014;32(7):330-8.
242. Han C, Zhao R, Kroger J, Qu M, Wani AA, Wang QE. Caspase-2 short isoform interacts with membrane-associated cytoskeleton proteins to inhibit apoptosis. PloS one. 2013;8(7):e67033.
243. Sheng X, Nenseth HZ, Qu S, Kuzu OF, Frahnow T, Simon L, et al. IRE1α-XBP1s pathway promotes prostate cancer by activating c-MYC signaling. Nat Commun. 2019;10(1):323.

244. Cato L, de Tribolet-Hardy J, Lee I, Rottenberg JT, Coleman I, Melchers D, et al. ARv7 Represses Tumor-Suppressor Genes in Castration-Resistant Prostate Cancer. Cancer cell. 2019;35(3):401-13.e6.
245. Chen H, Zhou L, Wu X, Li R, Wen J, Sha J, et al. The PI3K/AKT pathway in the pathogenesis of prostate cancer. Frontiers in bioscience (Landmark edition). 2016;21:1084-91.
246. Hubner A, Mulholland DJ, Standen CL, Karasarides M, Cavanagh-Kyros J, Barrett T, et al. JNK and PTEN cooperatively control the development of invasive adenocarcinoma of the prostate. Proceedings of the National Academy of Sciences of the United States of America. 2012;109(30):12046-51.
247. Qu Y, Dai B, Ye D, Kong Y, Chang K, Jia Z, et al. Constitutively active AR-V7 plays an essential role in the development and progression of castration-resistant prostate cancer. Scientific reports. 2015;5:7654.
248. Bai S, Cao S, Jin L, Kobelski M, Schouest B, Wang X, et al. A positive role of c-Myc in regulating androgen receptor and its splice variants in prostate cancer. Oncogene. 2019;38(25):4977-89.
249. Jamaspishvili T, Berman DM, Ross AE, Scher HI, De Marzo AM, Squire JA, et al. Clinical implications of PTEN loss in prostate cancer. Nature reviews Urology. 2018;15(4):222-34.
250. Hamid AA, Gray KP, Shaw G, MacConaill LE, Evan C, Bernard B, et al. Compound Genomic Alterations of TP53, PTEN, and RB1 Tumor Suppressors in Localized and Metastatic Prostate Cancer. European urology. 2019;76(1):89-97.
251. Rasche N, Dybkov O, Schmitzova J, Akyildiz B, Fabrizio P, Luhrmann R. Cwc2 and its human homologue RBM22 promote an active conformation of the spliceosome catalytic centre. The EMBO journal. 2012;31(6):1591-604.
252. Zeng Y, Wodzenski D, Gao D, Shiraishi T, Terada N, Li Y, et al. Stress-response protein RBM3 attenuates the stem-like properties of prostate cancer cells by interfering with CD44 variant splicing. Cancer Res. 2013;73(13):4123-33.
253. Zhao L, Li R, Shao C, Li P, Liu J, Wang K. 3p21.3 tumor suppressor gene RBM5 inhibits growth of human prostate cancer PC-3 cells through apoptosis. World journal of surgical oncology. 2012;10:247.
254. He F, Wang CT, Gou LT. RNA-binding motif protein RBM22 is required for normal development of zebrafish embryos. Genetics and molecular research : GMR. 2009;8(4):1466-73.
255. Gingrich JR, Barrios RJ, Foster BA, Greenberg NM. Pathologic progression of autochthonous prostate cancer in the TRAMP model. Prostate cancer and prostatic diseases. 1999;2(2):70-5.
256. Dang CV. MYC on the path to cancer. Cell. 2012;149(1):22-35.
257. Dang CV, Le A, Gao P. MYC-induced cancer cell energy metabolism and therapeutic opportunities. Clinical cancer research : an official journal of the American Association for Cancer Research. 2009;15(21):6479-83.
258. Ge Y, Schuster MB, Pundhir S, Rapin N, Bagger FO, Sidiropoulos N, et al. The splicing factor RBM25 controls MYC activity in acute myeloid leukemia. Nat Commun. 2019;10(1):172.
259. Jung JH, Lee H, Cao B, Liao P, Zeng SX, Lu H. RNA-binding motif protein 10 induces apoptosis and suppresses proliferation by activating p53. Oncogene. 2020;39(5):1031-40.
260. Yokoi A, Kotake Y, Takahashi K, Kadowaki T, Matsumoto Y, Minoshima Y, et al. Biological validation that SF3b is a target of the antitumor macrolide pladienolide. The FEBS journal. 2011;278(24):4870-80.
261. Sato M, Muguruma N, Nakagawa T, Okamoto K, Kimura T, Kitamura S, et al. High antitumor activity of pladienolide B and its derivative in gastric cancer. Cancer science. 2014;105(1):110-6.
262. Hepburn LA, McHugh A, Fernandes K, Boag G, Proby CM, Leigh IM, et al. Targeting the spliceosome for cutaneous squamous cell carcinoma therapy: a role for c-MYC and wild-type p53 in determining the degree of tumour selectivity. Oncotarget. 2018;9(33):23029-46.

263. Kashyap MK, Kumar D, Villa R, La Clair JJ, Benner C, Sasik R, et al. Targeting the spliceosome in chronic lymphocytic leukemia with the macrolides FD-895 and pladienolide-B. Haematologica. 2015;100(7):945-54.
264. Huang Y, Hale J, Wang Y, Li W, Zhang S, Zhang J, et al. SF3B1 deficiency impairs human erythropoiesis via activation of p53 pathway: implications for understanding of ineffective erythropoiesis in MDS. Journal of hematology & oncology. 2018;11(1):19.
265. Wang B, Lo UG, Wu K, Kapur P, Liu X, Huang J, et al. Developing new targeting strategy for androgen receptor variants in castration resistant prostate cancer. International journal of cancer. 2017;141(10):2121-30.
266. Hu R, Dunn TA, Wei S, Isharwal S, Veltri RW, Humphreys E, et al. Ligand-independent androgen receptor variants derived from splicing of cryptic exons signify hormone-refractory prostate cancer. Cancer Res. 2009;69(1):16-22.
267. Lykke-Andersen S, Jensen TH. Nonsense-mediated mRNA decay: an intricate machinery that shapes transcriptomes. Nature reviews Molecular cell biology. 2015;16(11):665-77.
268. Richardsen E, Andersen S, Al-Saad S, Rakaee M, Nordby Y, Pedersen MI, et al. Evaluation of the proliferation marker Ki-67 in a large prostatectomy cohort. PloS one. 2017;12(11):e0186852.
269. Sugie S, Mukai S, Yamasaki K, Kamibeppu T, Tsukino H, Kamoto T. Significant Association of Caveolin-1 and Caveolin-2 with Prostate Cancer Progression. Cancer genomics & proteomics. 2015;12(6):391-6.
270. Wang Y, Liu XJ, Yao XD. Function of PCA3 in prostate tissue and clinical research progress on developing a PCA3 score. Chinese journal of cancer research = Chung-kuo yen cheng yen chiu. 2014;26(4):493-500.
271. Laustriat D, Gide J, Barrault L, Chautard E, Benoit C, Auboeuf D, et al. In Vitro and In Vivo Modulation of Alternative Splicing by the Biguanide Metformin. Molecular therapy Nucleic acids. 2015;4(11):e262.
272. Matsumoto E, Akiyama K, Saito T, Matsumoto Y, Kobayashi KI, Inoue J, et al. AMP-activated protein kinase regulates alternative pre-mRNA splicing by phosphorylation of SRSF1. The Biochemical journal. 2020;477(12):2237-48.
273. Maj-Hes AB, Mathieu R, Ozsoy M, Soria F, Moschini M, Abufaraj M, et al. Obesity is associated with biochemical recurrence after radical prostatectomy: A multi-institutional extended validation study. Urologic oncology. 2017;35(7):460.e1-.e8.
274. Heinlein CA, Chang C. Androgen receptor in prostate cancer. Endocrine reviews. 2004;25(2):276-308.
275. Zaidi S, Gandhi J, Joshi G, Smith NL, Khan SA. The anticancer potential of metformin on prostate cancer. Prostate cancer and prostatic diseases. 2019;22(3):351-61.
276. Nickols NG, Nazarian R, Zhao SG, Tan V, Uzunangelov V, Xia Z, et al. MEK-ERK signaling is a therapeutic target in metastatic castration resistant prostate cancer. Prostate cancer and prostatic diseases. 2019;22(4):531-8.
277. Bitting RL, Armstrong AJ. Targeting the PI3K/Akt/mTOR pathway in castration-resistant prostate cancer. Endocrine-related cancer. 2013;20(3):R83-99.
278. Edlind MP, Hsieh AC. PI3K-AKT-mTOR signaling in prostate cancer progression and androgen deprivation therapy resistance. Asian journal of andrology. 2014;16(3):378-86.
279. Shaw RJ. LKB1 and AMP-activated protein kinase control of mTOR signalling and growth. Acta physiologica (Oxford, England). 2009;196(1):65-80.
280. Mendoza MC, Er EE, Blenis J. The Ras-ERK and PI3K-mTOR pathways: cross-talk and compensation. Trends in biochemical sciences. 2011;36(6):320-8.
281. Bott SR, Arya M, Kirby RS, Williamson M. p21WAF1/CIP1 gene is inactivated in metastatic prostatic cancer cell lines by promoter methylation. Prostate cancer and prostatic diseases. 2005;8(4):321-6.

282. Sirma H, Broemel M, Stumm L, Tsourlakis T, Steurer S, Tennstedt P, et al. Loss of CDKN1B/p27Kip1 expression is associated with ERG fusion-negative prostate cancer, but is unrelated to patient prognosis. Oncology letters. 2013;6(5):1245-52.
283. Steiner MS, Wang Y, Zhang Y, Zhang X, Lu Y. p16/MTS1/INK4A suppresses prostate cancer by both pRb dependent and independent pathways. Oncogene. 2000;19(10):1297-306.
284. Pencik J, Schlederer M, Gruber W, Unger C, Walker SM, Chalaris A, et al. STAT3 regulated ARF expression suppresses prostate cancer metastasis. Nat Commun. 2015;6:7736.
285. Katayama K, Nakamura A, Sugimoto Y, Tsuruo T, Fujita N. FOXO transcription factor-dependent p15(INK4b) and p19(INK4d) expression. Oncogene. 2008;27(12):1677-86.
286. Qi H, Liu Y, Li S, Chen Y, Li L, Cao Y, et al. Activation of AMPK Attenuated Cardiac Fibrosis by Inhibiting CDK2 via p21/p27 and miR-29 Family Pathways in Rats. Molecular therapy Nucleic acids. 2017;8:277-90.
287. Ciccarelli C, Marampon F, Scoglio A, Mauro A, Giacinti C, De Cesaris P, et al. p21WAF1 expression induced by MEK/ERK pathway activation or inhibition correlates with growth arrest, myogenic differentiation and onco-phenotype reversal in rhabdomyosarcoma cells. Mol Cancer. 2005;4:41.
288. Moss SC, Lightell DJ, Jr., Marx SO, Marks AR, Woods TC. Rapamycin regulates endothelial cell migration through regulation of the cyclin-dependent kinase inhibitor p27Kip1. The Journal of biological chemistry. 2010;285(16):11991-7.
289. Chen B, Xu X, Luo J, Wang H, Zhou S. Rapamycin Enhances the Anti-Cancer Effect of Dasatinib by Suppressing Src/PI3K/mTOR Pathway in NSCLC Cells. PloS one. 2015;10(6):e0129663.
290. Ye D, Mendelsohn J, Fan Z. Androgen and epidermal growth factor down-regulate cyclin-dependent kinase inhibitor p27Kip1 and costimulate proliferation of MDA PCa 2a and MDA PCa 2b prostate cancer cells. Clinical cancer research : an official journal of the American Association for Cancer Research. 1999;5(8):2171-7.
291. Hessenkemper W, Roediger J, Bartsch S, Houtsmuller AB, van Royen ME, Petersen I, et al. A natural androgen receptor antagonist induces cellular senescence in prostate cancer cells. Molecular endocrinology (Baltimore, Md). 2014;28(11):1831-40.
292. De Angelis G, Rittenhouse HG, Mikolajczyk SD, Blair Shamel L, Semjonow A. Twenty Years of PSA: From Prostate Antigen to Tumor Marker. Reviews in urology. 2007;9(3):113-23.
293. Loeb S, Bjurlin MA, Nicholson J, Tammela TL, Penson DF, Carter HB, et al. Overdiagnosis and overtreatment of prostate cancer. European urology. 2014;65(6):1046-55.
294. Gahete MD, Rincon-Fernandez D, Villa-Osaba A, Hormaechea-Agulla D, Ibanez-Costa A, Martinez-Fuentes AJ, et al. Ghrelin gene products, receptors, and GOAT enzyme: biological and pathophysiological insight. The Journal of endocrinology. 2014;220(1):R1-24.
295. Hormaechea-Agulla D, Gomez-Gomez E, Ibanez-Costa A, Carrasco-Valiente J, Rivero-Cortes E, F LL, et al. Ghrelin O-acyltransferase (GOAT) enzyme is overexpressed in prostate cancer, and its levels are associated with patient's metabolic status: Potential value as a non-invasive biomarker. Cancer letters. 2016;383(1):125-34.
296. Hormaechea-Agulla D, Gahete MD, Jimenez-Vacas JM, Gomez-Gomez E, Ibanez-Costa A, F LL, et al. The oncogenic role of the In1-ghrelin splicing variant in prostate cancer aggressiveness. Mol Cancer. 2017;16(1):146.
297. Allott EH, Masko EM, Freedland SJ. Obesity and prostate cancer: weighing the evidence. European urology. 2013;63(5):800-9.
298. Scerif M, Goldstone AP, Korbonits M. Ghrelin in obesity and endocrine diseases. Molecular and cellular endocrinology. 2011;340(1):15-25.
299. Principe S, Kim Y, Fontana S, Ignatchenko V, Nyalwidhe JO, Lance RS, et al. Identification of prostate-enriched proteins by in-depth proteomic analyses of expressed prostatic secretions in urine. Journal of proteome research. 2012;11(4):2386-96.

300. Ilic D, Djulbegovic M, Jung JH, Hwang EC, Zhou Q, Cleves A, et al. Prostate cancer screening with prostate-specific antigen (PSA) test: a systematic review and meta-analysis. BMJ (Clinical research ed). 2018;362:k3519.
301. Merriel SWD, Funston G, Hamilton W. Prostate Cancer in Primary Care. Advances in therapy. 2018;35(9):1285-94.
302. Calvocoressi L, Uchio E, Ko J, Radhakrishnan K, Aslan M, Concato J. Prostate cancer aggressiveness and age: Impact of p53, BCL-2 and microvessel density. Journal of investigative medicine : the official publication of the American Federation for Clinical Research. 2018;66(8):1142-6.
303. Thurner EM, Krenn-Pilko S, Langsenlehner U, Stojakovic T, Pichler M, Gerger A, et al. The elevated C-reactive protein level is associated with poor prognosis in prostate cancer patients treated with radiotherapy. Eur J Cancer. 2015;51(5):610-9.
304. Deshpande A, Sicinski P, Hinds PW. Cyclins and cdks in development and cancer: a perspective. Oncogene. 2005;24(17):2909-15.
305. Cao Z, Wei L, Zhu W, Yao X. Meta-analysis of CDKN2A methylation to find its role in prostate cancer development and progression, and also to find the effect of CDKN2A expression on disease-free survival (PRISMA). Medicine. 2018;97(12):e0182.
306. Liu X, Wu Q, Li L. Functional and therapeutic significance of EZH2 in urological cancers. Oncotarget. 2017;8(23):38044-55.
307. Jung-Hynes B, Nihal M, Zhong W, Ahmad N. Role of sirtuin histone deacetylase SIRT1 in prostate cancer. A target for prostate cancer management via its inhibition? The Journal of biological chemistry. 2009;284(6):3823-32.
308. Wiedmer P, Nogueiras R, Broglio F, D'Alessio D, Tschöp MH. Ghrelin, obesity and diabetes. Nature clinical practice Endocrinology & metabolism. 2007;3(10):705-12.
309. Chobot A, Górowska-Kowolik K, Sokołowska M, Jarosz-Chobot P. Obesity and diabetes-Not only a simple link between two epidemics. Diabetes/metabolism research and reviews. 2018;34(7):e3042.
310. Klop B, Elte JW, Cabezas MC. Dyslipidemia in obesity: mechanisms and potential targets. Nutrients. 2013;5(4):1218-40.
311. Huang T, Ren J, Huang J, Li D. Association of homocysteine with type 2 diabetes: a meta-analysis implementing Mendelian randomization approach. BMC genomics. 2013;14:867.
312. Tu H, Gu J, Meng QH, Kim J, Strom S, Davis JW, et al. Low serum testosterone is associated with tumor aggressiveness and poor prognosis in prostate cancer. Oncology letters. 2017;13(3):1949-57.
313. Gross M, Top I, Laux I, Katz J, Curran J, Tindell C, et al. Beta-2-microglobulin is an androgen-regulated secreted protein elevated in serum of patients with advanced prostate cancer. Clinical cancer research : an official journal of the American Association for Cancer Research. 2007;13(7):1979-86.
314. Lehrer S, Diamond EJ, Mamkine B, Droller MJ, Stone NN, Stock RG. C-reactive protein is significantly associated with prostate-specific antigen and metastatic disease in prostate cancer. BJU international. 2005;95(7):961-2.
315. Gomez-Gomez E, Carrasco-Valiente J, Campos-Hernandez JP, Blanca-Pedregosa AM, Jimenez-Vacas JM, Ruiz-Garcia J, et al. Clinical association of metabolic syndrome, C-reactive protein and testosterone levels with clinically significant prostate cancer. Journal of cellular and molecular medicine. 2019;23(2):934-42.

6. Articles

This Thesis is based on the research articles listed below, which will be referred in the test by their Roman numerals.

Article I: Juan M. Jimenez-Vacas, Vicente Herrero-Aguayo, Antonio J. Montero-Hidalgo, Enrique Gómez-Gómez, Antonio C. Fuentes-Fayos, Antonio J. Leon-Gonzalez, Prudencio Saez-Martínez, Emilia Alors-Perez, Sergio Pedraza-Arevalo, Teresa Gonzalez-Serrano, Oscar Reyes, Ana Martínez-Lopez, Rafael Sánchez-Sánchez, Sebastian Ventura, Elena M. Yubero-Serrano, María J. Requena-Tapia, Justo P. Castaño, Manuel D. Gahete, Raul M. Luque. *Dysregulation of the splicing machinery is directly associated to aggressiveness of prostate cancer*. 2020. EBioMedicine 51:102547. doi:10.1016/j.ebiom.2019.11.008.

Article II: Juan M. Jiménez-Vacas, Antonio J. Montero-Hidalgo, Enrique Gómez-Gómez, Vicente Herrero-Aguayo, Antonio C. Fuentes-Fayos, Prudencio Saéz-Martínez, Antonio J. León-González, Rafael Sánchez-Sánchez, Teresa González-Serrano, María J. Requena-Tapia, Justo P. Castaño, Manuel D. Gahete, Raúl M. Luque. *RBM22 plays an antitumor role in prostate cancer trough splicing dysregulation and MYC inhibition*. Manuscript submitted on 23/07/2020 to "Molecular Cancer".

Article III: Juan M. Jimenez-Vacas, Vicente Herrero-Aguayo, Enrique Gómez-Gómez, Antonio J. León-González, Prudencio Sáez-Martínez, Emilia Alors-Pérez, Antonio C. Fuentes-Fayos, Ana Martínez-López, Rafael Sánchez-Sánchez, Teresa González-Serrano, Daniel J. López-Ruiz, María J. Requena-Tapia, Justo P. Castaño, Manuel D. Gahete, Raúl M. Luque. *Spliceosome Component SF3B1 as Novel Prognostic Biomarker and Therapeutic Target for Prostate Cancer*. 2019. Translational Research 212:89-103. doi: 10.1016/j.trsl.2019.07.001.

Article IV: Juan M. Jiménez-Vacas, Antonio Montero-Hidalgo, André Sarmento-Cabral, Enrique Gómez-Gómez, Miguel López, Manuel D. Gahete, Raúl M. Luque. *Alterations in the splicing machinery as a key molecular mechanism underlying the antitumor effects of metformin in prostate cancer*. Manuscript in preparation for "Cancer & Metabolism".

Article V: Juan M. Jiménez-Vacas, Vicente Herrero-Aguayo, Antonio J. Montero-Hidalgo, Prudencio Sáez-Martínez, Enrique Gómez-Gómez, Antonio J. León-González, Antonio C. Fuentes-Fayos, Elena M. Yubero-Serrano, María J. Requena-Tapia, Miguel Lopez, Justo P. Castaño, Manuel D. Gahete, Raúl M. Luque. *Clinical, cellular and molecular evidence of the additive antitumor effects of biguanides and statins in prostate cancer*. Manuscript submitted on 11/07/2020 to "Journal of Clinical Endocrinology & Metabolism".

Article VI: Juan M. Jiménez-Vacas, Enrique Gómez-Gómez, Antonio J. Montero-Hidalgo, Vicente Herrero-Aguayo, Fernando L-López, Rafael Sánchez-Sánchez, Ipek Guler, Ana Blanca, María José Méndez-Vidal, Julia Carrasco, José Lopez-Miranda, María

J. Requena-Tapia, Justo P. Castaño, Manuel D. Gahete, and Raúl M. Luque. *Clinical Utility of Ghrelin-O-Acyltransferase (GOAT) Enzyme as a Diagnostic Tool and Potential Therapeutic Target in Prostate Cancer*. Journal of Clinical Medicine. 8(12):2056. doi: 10.3390/jcm8122056.

Article VII: Juan M. Jiménez-Vacas, Enrique Gómez-Gómez, Antonio Montero-Hidalgo, Ipek Guler, Jesús Delgado-Luque, Francisco Ruiz-Pino, María J. Requena-Tapia, Manuel Tena-Sempere, Justo P. Castaño, Manuel D. Gahete, Raúl M. Luque. *Pathophysiological relation between obesity and prostate cancer: role of In1-ghrelin as a novel non-invasive diagnostic and prognostic biomarker.* Manuscript in preparation for "Cancer Letters".

Article I

EBioMedicine 51 (2020) 102547

Contents lists available at ScienceDirect

EBioMedicine

journal homepage: www.elsevier.com/locate/ebiom

Research paper

Dysregulation of the splicing machinery is directly associated to aggressiveness of prostate cancer

Juan M. Jiménez-Vacas[a,b,c,d], Vicente Herrero-Aguayo[a,b,c,d], Antonio J. Montero-Hidalgo[a,b,c,d], Enrique Gómez-Gómez[a,b,c,e], Antonio C. Fuentes-Fayos[a,b,c,d], Antonio J. León-González[a,b,c,d], Prudencio Sáez-Martínez[a,b,c,d], Emilia Alors-Pérez[a,b,c,d], Sergio Pedraza-Arévalo[a,b,c,d], Teresa González-Serrano[a,c,f], Oscar Reyes[a,c,g], Ana Martínez-López[a,c,f], Rafael Sánchez-Sánchez[a,c,f], Sebastián Ventura[a,c,g], Elena M. Yubero-Serrano[a,b,c,d,h], María J. Requena-Tapia[a,c,e], Justo P. Castaño[a,b,c,d], Manuel D. Gahete[a,b,c,d], Raúl M. Luque[a,b,c,d,*]

[a] Maimonides Institute for Biomedical Research of Córdoba (IMIBIC), Córdoba, Spain
[b] Department of Cell Biology, Physiology, and Immunology, University of Córdoba, Córdoba, Spain
[c] Hospital Universitario Reina Sofía (HURS), Córdoba, Spain
[d] Centro de Investigación Biomédica en Red de Fisiopatología de la Obesidad y Nutrición, (CIBERobn), Córdoba, Spain
[e] Urology Service, HURS/IMIBIC, Córdoba, Spain
[f] Anatomical Pathology Service, HURS, Córdoba, Spain
[g] Department of Computer Sciences, University of Córdoba, Córdoba, Spain
[h] Lipids and Atherosclerosis Unit, Reina Sofia University Hospital, Córdoba, Spain

ARTICLE INFO

Article History:
Received 24 July 2019
Revised 28 October 2019
Accepted 7 November 2019
Available online 3 January 2020

Keywords:
Prostate cancer
Splicing
Spliceosome
SNRNP200
SRSF3
SRRM1
Therapeutic target

ABSTRACT

Background: Dysregulation of splicing variants (SVs) expression has recently emerged as a novel cancer hallmark. Although the generation of aberrant SVs (e.g. AR-v7/sst5TMD4/etc.) is associated to prostate-cancer (PCa) aggressiveness and/or castration-resistant PCa (CRPC) development, whether the molecular reason behind such phenomena might be linked to a dysregulation of the cellular machinery responsible for the splicing process [spliceosome-components (SCs) and splicing-factors (SFs)] has not been yet explored.

Methods: Expression levels of 43 key SCs and SFs were measured in two cohorts of PCa-samples: 1) Clinically-localized formalin-fixed paraffin-embedded PCa-samples ($n = 84$), and 2) highly-aggressive freshly-obtained PCa-samples ($n = 42$).

Findings: A profound dysregulation in the expression of multiple components of the splicing machinery (i.e. 7 SCs/19 SFs) were found in PCa compared to their non-tumor adjacent-regions. Notably, overexpression of *SNRNP200, SRSF3* and *SRRM1* (mRNA and/or protein) were associated with relevant clinical (e.g. Gleason score, T-Stage, metastasis, biochemical recurrence, etc.) and molecular (e.g. *AR-v7* expression) parameters of aggressiveness in PCa-samples. Functional (cell-proliferation/migration) and mechanistic [gene-expression (qPCR) and protein-levels (western-blot)] assays were performed in normal prostate cells (PNT2) and PCa-cells (LNCaP/22Rv1/PC-3/DU145 cell-lines) in response to *SNRNP200, SRSF3* and/or *SRRM1* silencing (using specific siRNAs) revealed an overall decrease in proliferation/migration-rate in PCa-cells through the modulation of key oncogenic SVs expression levels (e.g. *AR-v7*/*PKM2*/*XBP1s*) and alteration of oncogenic signaling pathways (e.g. p-AKT/p-JNK).

Interpretation: These results demonstrate that the spliceosome is drastically altered in PCa wherein SNRNP200, SRSF3 and SRRM1 could represent attractive novel diagnostic/prognostic and therapeutic targets for PCa and CRPC.

1. Introduction

Dysregulation of the alternative splicing process is considered a key hallmark of cancer and could represent a novel source for the identification of diagnostic, prognostic and therapeutic targets in highly prevalent tumor pathologies [1]. Specifically, alternative splicing represents an essential biological process by which the introns of an immature pre-mRNA are excised, and the exons are fused to generate mature mRNAs capable to be translated into functional proteins [2]. Indeed, most eukaryotic genes undergo alternative splicing, leading to a higher molecular flexibility through the increase of

* Correspondence author.
E-mail addresses: raul.luque@uco.es, bc2luhur@uco.es (R.M. Luque).

https://doi.org/10.1016/j.ebiom.2019.11.008

Research in context

Evidence before this study

Early studies have demonstrated that the dysregulation of the expression of several splicing variants [e.g. Androgen receptor variant-7 (AR-v7), truncated somatostatin receptor SST_5TMD4, In1-ghrelin, etc.) increases prostate cancer (PCa) aggressiveness and/or promotes resistance to the available drugs currently used in clinical practice (e.g. antiandrogens), hampering the treatment and the management of PCa patients. In this context, it is well known that this process is catalyzed by a macromolecular machinery (i.e. spliceosome) and regulated by specific proteins (i.e. splicing factors; SFs). However, the putative dysregulation of spliceosome components (SCs) and splicing factors in PCa as well as the potential of these elements as diagnostic, prognostic and/or therapeutic tools for this pathology remain poorly known.

Added value of this study

Our study demonstrates that the expression of several SCs and SFs are drastically dysregulated in PCa tissues compared with control (non-tumoral) tissues. Of particular importance is the demonstration that the changes in the expression of SNRNP200, SRSF3 and SRRM1 (at the mRNA and protein level) are associated to key clinical features of aggressiveness (e.g. Gleason score, biochemical recurrence, presence of metastasis, vascular and perineural invasion) in PCa patients as well as to important molecular phenotypes (e.g. *AR-v7* expression) of PCa. Notably, this study also shows that the silencing of the expression of *SNRNP200*, *SRRM1* and *SRSF3*: 1) evoked clear antitumor actions in PCa cells (e.g. inhibition of proliferation, migration) through the modulation of key oncogenic signaling pathways (e.g. PI3K/AKT, ERK, JNK) and splicing variants (e.g. *AR-v7*, *PKM2*, *XBP1s*), and, 2) was able to re-sensitizes PCa cells to enzalutamide treatment, pointing out the potential therapeutic utility of these elements for the most aggressive phenotype of PCa, castration resistant PCa, which remains lethal nowadays.

Implications of all the available evidence

Altered expression of splicing machinery elements (spliceosome components and splicing factors) might be associated with the development, progression and aggressiveness of PCa. Our data demonstrate the existence of a splicing machinery-associated molecular dysregulation that could be potentially considered as a source of novel diagnostic and prognostic biomarkers as well as therapeutic targets for PCa. Specifically, our results reveal that three components of the splicing machinery (SNRNP200, SRSF3 and SRRM1) could represent potential, global and effective therapeutic targets to tackle this devastating pathology.

transcripts generated from a given gene [2]. Unfortunately, dysregulations of this process are associated to the appearance of diverse protein isoforms that could exhibit strong pathological potential [1]. In eukaryotes, the control of the appropriate splicing process is orchestrated by the spliceosome, a complex cellular machinery comprised by different small nuclear ribonucleoproteins (RNU1, RNU2, etc.) and core spliceosome-associated proteins (PRPF8, PRPF40A, U2AF2, SF3B1, etc.). The spliceosome dynamically interacts with additional proteins (splicing factors; SFs) to finely recognize the introns and exons to be processed and to catalyze the splicing process of the pre-RNAs [1]. The appropriate functioning of this cellular machinery is essential to maintain the cellular, tissue and body homeostasis and, therefore, the dysregulation of this process has been associated to different diseases, including endocrine-metabolic and tumor pathologies [2].

In this scenario, it has been shown that alternative splicing contributes to the heterogeneity, aggressiveness and resistance to medical treatment of prostate cancer (PCa), one of the most important public health problems worldwide with numbers of cases increasing significantly every year [3]. In this context, several studies have demonstrated that the androgen receptor (*AR*) gene is a source of splicing variants (SVs), especially AR-v7, which is a key driver for PCa progression (e.g. increased risk of biochemical relapse and inferior overall survival outcomes). In addition, a number of cancer-specific SVs has been identified in PCa, including SST_5TMD4 [4], PKM2 [5], REST4 [6], XBP1s [7], In1-Ghrelin [8] etc., which also play an oncogenic role in this tumor pathology. In fact, it has been proposed that the "splicing signature" represents a more accurate parameter to stratify patients than the "transcriptome signature", which is typically analysed by conventional microarray analyses [9]. Thus, the understanding of the regulation of splicing in normal and pathological prostate cells may help to identify novel biomarkers and therapeutic targets for this devastating tumor pathology. However, to the best of our knowledge, to date no studies have been focused on the mechanisms driving the generation of the SVs (i.e. the regulation of the splicing machinery), which might provide new contexts for the development of novel strategies to tackle PCa, since targeting the activity of selected spliceosome components that may be dysregulated in PCa could serve to inhibit the generation of oncogenic SVs (e.g. AR-v7), representing an attractive therapeutic strategy for PCa. Therefore, in this study we aimed to determine for the first time the expression levels of a representative set of spliceosome components (SCs) and SFs and their relationship with clinical and molecular features of PCa-aggressiveness, as well as its pathological role in this disease.

2. Material and methods

2.1. Patients and samples

This study was approved by the Reina Sofia University Hospital Ethics Committee and was conducted in accordance with the principles of the Declaration of Helsinki. The regional Biobank coordinated the collection, processing, management and assignment of the biological samples used in the present study according to the standard procedures established for this purpose. Written informed consent was obtained from all patients. Two different cohorts of prostate samples were included in this study:

- **Cohort 1**) formalin-fixed, paraffin-embedded (FFPE) PCa tissues ($n = 84$) and their non-tumor adjacent region (N-TAR; used as control tissues; $n = 84$), taken from radical prostatectomies from patients diagnosed with clinically localized PCa (Table 1).
- **Cohort 2**) fresh PCa samples ($n = 42$) that were obtained by core needle biopsies from patients with suspect of presenting significant PCa [defined as Gleason score (GS) $\geq$ 7; highly aggressive PCa], which was further confirmed histologically by uro-pathologists (Table 2).

The clinical parameters collected from each patient were GS (analysed by uro-pathologists following the modified 2005, 2010 and 2014 ISUP criteria, based on the sample collection date), T-Stage, perineural invasion, lymphovascular invasion, presence of metastases at diagnose (determined by computed tomography and bone scan) and biochemical recurrence (defined by two consecutive PSA values $>$ 0.2 ng/mL and rising, after radical prostatectomy).

Table 1
Demographic, biochemical and clinical parameters of the patients with clinically localized PCa (Cohort 1). PSA: Prostate specific antigen; SigPCa: Significant PCa, defined as Gleason score ≥ 7; pT: Pathological primary tumor staging; PI: Perineural invasion; VI: Vascular invasion.

Parameter	
Patients [*n*]	84
Age, years [median (IQR)]	61 (57–66)
PSA levels, ng/mL [median (IQR)]	5.2 (4.2–8.0)
Sig PCa [*n* (%)]	76 (90.5%)
pT ≥ 3a [*n* (%)]	59 (70.2%)
PI [*n* (%)]	72 (85.7%)
VI [*n* (%)]	8 (9.52%)
Recurrence [*n* (%)]	35 (41.7%)
Metastasis [*n* (%)]	0 (0%)

2.2. Cell cultures

PCa cell lines (LNCaP, 22Rv1, PC-3 and DU145) were obtained from American Type Culture Collection (ATCC; Manassas, VA, USA) while normal prostate cell line PNT2 was a kind gift from Dr. J. De Bono. These cell lines were cultured according to manufacturer instructions as previously described [4,8,10], validated by analysis of short tandem repeats (STRs) sequences using GenePrint 10 System (Promega, Barcelona, Spain) and checked for mycoplasma contamination by PCR as previously reported [4]. For functional assays, LNCaP, 22Rv1 and DU145 cell lines were used. For mechanistic assays, 22Rv1 cells were used since this cell line represents a PCa model with AR and AR-v7 expression.

2.3. Transfection with specific siRNAs

For silencing assays, LNCaP, 22Rv1 and DU145 cell lines were used. Specifically, 200,000 cells were seeded in 6-well plates and grown until 70% of confluence was reached. Then, cells were transfected with specific siRNAs against *SNRNP200* (#124735; Thermo Fisher Scientific, Madrid, Spain), *SRRM1* (s20018; Thermo Fisher Scientific) and *SRSF3* (s12733; Thermo Fisher Scientific) at 100 nM, using Lipofectamine-RNAiMAX (Thermo Fisher Scientific) as previously reported [22]. After 24h, cells were collected for quantitative-PCR (qPCR), western blot, cell proliferation and/or cell migration assays.

2.4. Cell proliferation

In order to determine the effect of the silencing of *SNRNP200, SRRM1* and *SRSF3* on cell proliferation, Alamar-Blue assay (Bio-Source International, Camarillo, CA, USA) was performed in LNCaP, 22Rv1 and DU145 cell lines, as previously reported [4]. Briefly, cells were seeded in 96-well plates at a density of 3,000–5,000 cells/well and serum-starved for 24h, then cell proliferation was evaluated using the FlexStation III system (Molecular Devices, Sunnyvale, CA, USA) until 72 h.

Table 2
Demographic, biochemical and clinical parameters of the patients with highly aggressive PCa (Cohort 2). PSA: Prostate specific antigen; SigPCa: Significant PCa defined as Gleason score ≥ 7.

Parameter	
Patients [*n*]	42
Age, years [median (IQR)]	75 (69–81)
PSA levels, ng/mL [median (IQR)]	62.0 (36.2–254.5)
SigPCa [*n* (%)]	42 (100%)
Metastasis [*n* (%)]	28 (66.7%)

2.5. Enzalutamide-sensitization assay

To test the role of *SNRNP200, SRRM1* and *SRSF3* on the response to enzalutamide treatment (#1613, Axon Medchem, Groningen, The Netherlands), cell proliferation was evaluated. Specifically, LNCaP and 22Rv1 cells were acclimated during 24h to RPMI 1640 without phenol-red supplemented with charcoal-stripped serum (#A3382101; Thermo Fisher Scientific). Then, scrambled- or siRNA-transfected cells were treated with enzalutamide at 1 μM. All cells were treated with 5α-dihydrotestosterone (DHT; # D-073; Merck, Madrid, Spain) at 10 nM. Cell proliferation was calculated, after 24h of treatment, as described above. Results were expressed as percentage referred to scramble treated with vehicle (DMSO) plus DHT treatment.

2.6. Cell migration

Cell migration was evaluated by wound-healing assay in DU145 cell line in response to *SNRNP200, SRRM1, SRSF3* silencing, due to the inability of LNCaP and 22Rv1 cells to migrate. Specifically, images of the scratch were taken at 0 and 12 h and wound healing was calculated as the area observed 12 h after the wound was made vs. the area observed just after wounding, as previously described [4]. Results were expressed as percentage referred to scramble.

2.7. Western blot

Protein levels of several PCa-related genes were analysed in 22Rv1 cells as previously reported [4]. Briefly, 200,000 cells were seeded in 12-well plates and after two days, proteins were extracted using pre-warmed (65 °C) SDS-DTT buffer (62.5 mM Tris–HCl, 2% SDS, 20% glycerol, 100 mM DTT, and 0.005% bromophenol blue). Then, proteins were sonicated for 10 s and boiled for 5 min at 95 °C. Proteins were separated by SDS-PAGE and transferred to nitrocellulose membranes (Millipore, Billerica, MA, USA). Membranes were blocked with 5% non-fat dry milk in Tris-buffered saline/0.05% Tween 20 and incubated overnight with the specific antibodies for phospho-AKT (#4060S; Cell Signaling, Leiden, NLD), phospho-ERK (#4370S; Cell Signaling), phospho-JNK (AF1205; R&D-Systems, Minneapolis, MN, USA), AKT (#9272S; Cell Signaling), ERK (sc-154; Santa Cruz Biotechnology, Dallas, TX, USA), JNK (AF1387; R&D Systems), SNRNP200 (ab241589; Abcam, Camdridge, UK), SRRM1 (PA5-69086; Thermo Fisher Scientific), SRSF3 (ab198291; Abcam) and the secondary antibody HRP-conjugated goat anti-rabbit IgG (#7074 s; Cell Signaling). Specifically, the specificity of SNRNP200 and SRSF3 antibodies was validated in our laboratory by western blot and ICC (only 1 band was recognized by western blot and depletion of protein quantity was observed in response to specific siRNAs using western blot and ICC approaches). SRRM1 specificity was not completely validated since more than 1 band was recognized in western blot (however, depletion of protein quantity was observed in response to a specific siRNAs using western blot and ICC approaches). Proteins were detected using an enhanced chemiluminescence detection system (GEHealthcare, Madrid, Spain) with dyed molecular weight markers (Bio-Rad, Madrid, Spain). A densitometry analysis of the bands obtained was carried out with ImageJ software, using total AKT, ERK and JNK protein levels as normalizing factor for phospho-AKT, phospho-ERK and phospho-JNK, respectively.

2.8. RNA extraction

Total RNA from FFPE samples was isolated and DNase-treated using the Maxwell 16 LEVRNA FFPE Kit (Promega, Madison, WI, USA) according to manufacturer instructions in the Maxwell MDx 16 Instrument (Promega, Madrid, Spain). Additionally, total RNA was extracted from fresh samples using the AllPrep DNA/RNA/Protein

Mini Kit (Qiagen) and from PCa cell lines using TRIzol Reagent (Thermo Fisher Scientific, Waltham, MA, USA), followed, in both cases, by DNase treatment using RNase-Free DNase Kit (Qiagen, Hilden, DEU). Total RNA concentration and purity was assessed using Nanodrop One Spectrophotometer (Thermo Fisher Scientific). Total RNA was retrotranscribed using random hexamer primers and the cDNA First Strand Synthesis kit (Thermo Fisher Scientific).

2.9. qPCR dynamic array based on microfluidic technology

A qPCR dynamic array based on microfluidic technology that allows the determination of the expression of 45 transcripts in 48 samples, simultaneously, (Fluidigm, San Francisco, CA, USA) was implemented. Specific primers for human transcripts including components of the major spliceosome ($n = 10$), minor spliceosome ($n = 4$), associated SFs ($n = 25$) and three housekeeping genes (*ACTB*, *GAPDH* and *HPRT*) were specifically designed with the Primer3 software and StepOne™ Real-Time PCR System software v2.3 (Applied Biosystems, Foster City, CA, USA) (Supplemental Table 1). Preamplification, exonuclease treatment and qPCR dynamic array based on microfluidic technology were implemented as recently reported [11,12], following manufacturer's instructions using the Biomark System and the Real-Time PCR Analysis Software (Fluidigm). To control for variations in the efficiency of the retro-transcription reaction, mRNA copy numbers of the different transcripts analysed were adjusted by normalization factor, calculated with the expression levels of *ACTB* and *GAPDH* using GeNorm 3.3 [13].

2.10. RNA retrotranscription and quantitative real-time PCR

Details regarding the development, validation, and application of the quantitative real-time PCR to measure expression levels of the transcripts of interest have been previously reported by our laboratory [14–17]. Specific primers set used to measure the expression levels of the genes of interest in this study are described in Supplemental Table 2. Specifically, primers for *KLF6-SV1, KLF6, PKM2, PKM1, REST4* and *REST* transcripts were obtained from previous studies [18–20]. To control for variations in the efficiency of the retro-transcription reaction, mRNA copy numbers of the different transcripts analysed were adjusted by a normalization factor which was calculated with the expression levels of *ACTB* and *GAPDH* using GeNorm 3.3 [13].

2.11. Immunohistochemistry (IHC) analysis

IHC analysis was performed on FFPE prostate samples that were obtained by core needle biopsies from patients of cohort 2, since they represent the most aggressive cohort of our study (GS $\geq$ 7). Samples of benign prostatic hyperplasia (BPH), prostatic intraepithelial neoplasia (PIN) and non-significant PCa with GS =6 ($n = 7$, 6 and 5, respectively) also taken by core needle biopsies were included in this analysis as control samples and low aggressive PCa, respectively. Briefly, deparaffinized sections were incubated overnight (4 °C) with the primary antibodies against the proteins of interest [i.e. SNRNP200 (ab241589; Abcam), SRRM1 (PA5-69086; Thermo Fisher Scientific) or SRSF3 (ab198291; Abcam)] at 1:250 dilution, followed by incubation with an anti-rabbit horseradish peroxidase–conjugated secondary antibody (#7074; Cell Signaling). Finally, sections were developed with 3,39-diaminobenzidine (Envision system 2-Kit Solution DAB) and contrasted with haematoxylin. Two independent pathologists performed histopathologic analyses indicating low, moderate, and high intensities of staining, following a blinded protocol.

2.12. Statistical and bioinformatic analyses

Statistical differences between two groups were calculated by unpaired parametric *t*-test or nonparametric Mann Whitney U test, according to normality, assessed by Kolmogorov-Smirnov test. For differences among three groups, One-Way ANOVA analysis was performed. Spearman's or Pearson's bivariate correlations were performed for quantitative variables according to normality. Significant relation between categorized mRNA expression and biochemical PCa recurrence was studied using the long-rank-p-value method. Predictive models were constructed by Random Forest algorithm (with R language) as classifier as previously reported [11,12]. The rest of the statistical analyses were assessed using GraphPad Prism 7 (GraphPad Software, La Jolla, CA) or SPSS version 17.0. All the experiments were performed in, at least, 3 independent times ($n \geq 3$), and with at least 2 technical replicates. Statistical significance was considered when $p < 0.05$. A trend for significance was indicated when p-values ranged between > 0.05 and < 0.1.

3. Results

3.1. Expression levels of spliceosome components and splicing factors are dysregulated in PCa and are associated with clinical and molecular aggressiveness features

The expression levels of 26 out of 45 (58%) genes involved in the pre-RNA splicing process were found to be significantly dysregulated in PCa-tissues compared to their respective control-tissues (N-TAR) from a cohort of patients with clinically-localized PCa ($n = 84$; Table 1; Fig. 1a/b). Specifically, the SCs *RNU4, RNU6, PRPF40A, SF3B1, SNRNP200, U2AF2* and *RNU12* were overexpressed in PCa-tissues (Fig. 1a). Additionally, the SFs *ESRP1, ESRP2, KHDRBS1, MAGOH, NOVA1, PTBP1, RBM3, RBM45, SND1, SRSF2, SRSF3, SRSF4, SRSF5, SRSF9, SRSF10, SRRM1, TIA1* and *TRA2A* were also overexpressed while the SF *SRRM4* was down-regulated in PCa-tissues (Fig. 1b). No statistically significant differences were observed in the expression levels of the rest of SCs and SFs analysed (Supplemental Figure 1). Non-supervised clustering bioinformatic approaches (Random Forest algorithm) revealed that the molecular fingerprint comprised by the combination of the expression of *SNRNP200, SRRM1, SRSF3, TIA1, SRSF10, U2AF2, SRSF9, SRRM4, SND1, ESRP1*, and *KHDRBS1* perfectly discriminated between PCa and N-TARs samples with an AUC =1 (Fig. 1c). This was further supported by cross-validation analysis of this molecular fingerprint (AUC =0.83, $p < 0.0001$; Fig. 1d).

Notably, the expression levels of the 85% (22 out of 26) SCs and SFs found dysregulated herein were significantly associated and/or correlated with at least one clinical parameter of PCa-aggressiveness (Tables 3 and 4). Remarkably, *SNRNP200, SRRM1* and *SRSF3* were the only genes whose expression was directly associated/correlated with all the clinical parameters of aggressiveness (Gleason score, T-Stage, perineural- and lymphovascular-invasion; Table 3; Fig. 1e) and progression (biochemical recurrence; Table 4; Fig. 1f) available in this cohort of patients. In addition, *in silico* data showed the overexpression in PCa samples of *SNRNP200* in Singh, Wallace and Welsh datasets. Moreover, *SRRM1* was found to be overexpressed in PCa samples in Welsh and Tomlins datasets, while a trend was observed in Wallace dataset ($p = 0.089$). On the other hand, an overexpression of *SRSF3* in PCa samples was found in Singh and Tomlins datasets (Supplemental Figure 2).

Based on these results, we further analysed the expression levels of *SNRNP200, SRRM1* and *SRSF3* in an independent and more aggressive cohort of PCa-samples (Table 2). These analyses revealed an association between the elevated expression levels of *SNRNP200, SRRM1* and *SRSF3* in PCa-samples and the presence of metastases at the moment of diagnosis (Fig. 2a). *SNRNP200* and *SRSF3* expression tended to be positively correlated with Gleason score ($p = 0.053$,

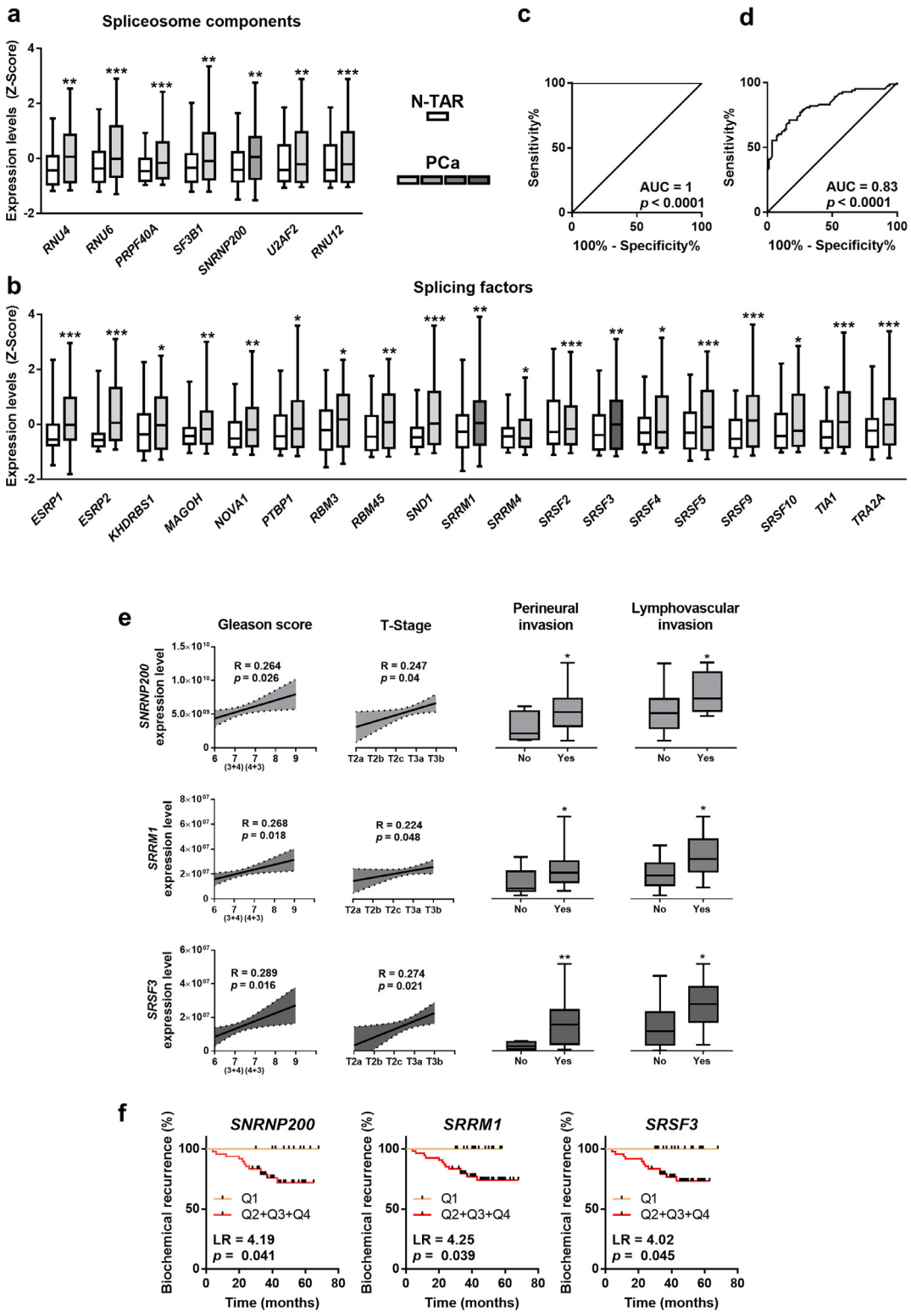

Fig. 1. Expression of spliceosome components and splicing factors in prostate cancer (PCa) samples. (a–b) Comparison of mRNA levels of spliceosome components (a) and splicing factors (b) between formalin-fixed paraffin embedded (FFPE) samples from PCa samples and non-tumor adjacent regions (N-TAR) ($n = 84$) determined by a microfluidic-based qPCR array. Data represent the mean ± SEM of mRNA expression levels adjusted by normalization factor (calculated from *ACTB* and *GAPDH* expression levels) and standardized by Z-score. c-d) ROC curves of a subset of spliceosome components and splicing factors generated by Random Forest computational algorithm (c) followed by cross validation analysis (d) to distinguish between tumor and N-TAR samples. e) Association between the expression levels of selected spliceosome components and splicing factors (*SNRNP200*, *SRRM1* and *SRSF3*) and clinical parameters (Gleason score, T-Stage, perineural and lymphovascular invasion) in the same cohort of FFPE samples ($n = 84$). Correlations are represented by mean (connecting line) and error bands (pointed line) of expression levels. Data of associations represent the mean ± SEM of mRNA expression levels adjusted by normalization factor (calculated from *ACTB* and *GAPDH* expression levels). f) Association between *SNRNP200*, *SRRM1* and *SRSF3* expression levels and biochemical PCa recurrence in 67 samples from FFPE cohort (samples from patients who underwent adjuvant radiotherapy were not included), calculated by Log Rank analysis (LR). mRNA levels were determined by a microfluidic-based qPCR array and adjusted by normalization factor calculated from *ACTB* and *GAPDH* expression levels. Asterisks (* $p < 0.05$; ** $p < 0.01$; *** $p < 0.001$) indicate statistically significant differences between groups.

Table 3
Correlation and association of *SNRNP200, SRRM1* and *SRSF3* expression levels with clinical features of prostate cancer aggressiveness. Data of correlations represent the coefficient "r". Data of associations represent the difference between means of each group ± standard deviation. Significant prostate cancer (SigPCa) is defined as Gleason score ≥ 7. Asterisks (* $p < 0.05$; ** $p < 0.01$; ** $p < 0.001$) indicate statistically significant differences between groups.

	Correlations		Associations		
	Gleason score	T- Stage	Perineural Invasion	Lymphovascular Invasion	SigPca
RNU4	0.122	**0.239***	**9,664,718,823 ± 3,162,530,673 ****	**7,730,140,948 ± 3,078,119,236 ***	**7,526,218,231 ± 3,298,861,131 ***
RNU6	**0.235***	0.075	**230,034,826 ± 72,616,606 ****	119,362,920 ± 102,513,311	**163,738,961 ± 75,084,561 ***
PRPF40A	0.184	0.214	**1,801,231 ± 878,336 ***	1,669,010 ± 855,998	**1,789,300 ± 832,618 ***
SF3B1	**0.312****	0.121	**9,003,875 ± 3,487,752 ***	**10,853,954 ± 4,783,529 ****	5,808,930 ± 3,941,225
U2AF2	0.09	0.083	**714,287 ± 348,778 ***	807,889 ± 481,128	347,329 ± 370,880
SNRNP200	**0.264***	**0.247***	**2,681,185,105 ± 1,175,955,224 ***	**2,812,777,484 ± 1,275,566,115 ***	**2,125,357,393 ± 1,042,911,480 ***
RNU12	**0.321****	0.178	**395,441 ± 132,486 ****	133,816 ± 149,579	208,236 ± 139,628
ESRP1	**0.319****	0.166	1,658,118 ± 916,550	2,151,271 ± 1,084,569	**1,874,015 ± 936,328 ***
ESRP2	**0.281***	**0.254***	1,953,298 ± 1,179,570	**3,964,985 ± 1,266,549 ****	**2,941,102 ± 1,300,974 ***
KHDRBS1	0.128	0.215	**8,816,079 ± 4,355,945 ***	7,047,264 ± 5,942,380	**10,326,770 ± 4,988,242 ***
MAGOH	**0.331****	0.173	572,836 ± 376,052	**1,036,475 ± 489,737 ***	772,768 ± 395,132
NOVA1	0.131	0.211	1,375,554 ± 1,240,422	**2,891,594 ± 1,397,232 ***	1,968,158 ± 1,417,671
PTB	0.189	0.197	462,842 ± 504,081	707,443 ± 685,520	923,496 ± 547,502
RBM3	0.141	0.139	1,831,860 ± 1,133,513	**2,948,642 ± 1,333,148 ***	2,051,801 ± 1,189,264
RBM45	0.145	0.159	2,144,099 ± 1,086,705	2,444,946 ± 1,430,495	1,613,514 ± 1,237,865
SND1	**0.236***	0.167	**6,829,797 ± 3,127,408 ***	**8,116,316 ± 3,698,131 ***	**7,483,290 ± 3,461,207 ***
SRSF2	**0.284***	0.161	**903,780 ± 409,990 ***	**1,099,682 ± 533,886 ***	914,182 ± 460,892
SRSF3	**0.289***	**0.274***	**13,698,858 ± 5,050,576 ****	**12,653,631 ± 5,712,504 ***	**10,070,038 ± 5,031,330 ***
SRSF4	0.139	0.169	**2,131,612 ± 857,251 ***	**3,422,072 ± 1,068,338 ****	941,268 ± 902,489
SRSF5	0.055	0.129	**105,348,741 ± 37,924,790 ****	**141,185,003 ± 48,026,387 ****	35,477,260 ± 37,643,655
SRSF9	0.088	0.211	**33,397,890 ± 12,917,648 ***	28,501,453 ± 15,538,733	26,539,564 ± 14,468,693
SRSF10	0.057	0.218	**10,135,257 ± 4,077,596 ***	10,622,878 ± 5,604,567	4,248,356 ± 4,293,783
SRRM1	**0.211***	**0.224***	**9,522,292 ± 4,314,271 ***	**9,444,197 ± 4,007,860 ***	**9,478,531 ± 4,760,093 ***
SRRM4	−0.154	0.107	53,981 ± 33,971	-2375 ± 34,689	47,458 ± 36,610
TIA1	0.114	**0.246***	**5,965,156 ± 2,459,924 ***	6,334,929 ± 2,989,097	**5,493,989 ± 2,630,409***
TRA2A	0.141	0.191	**27,361,791 ± 12,693,441 ***	39,100,412 ± 15,368,002	29,010,940 ± 15,801,444

R = 0.308; $p = 0.086$, R = 0.290; respectively; Fig. 2b). Furthermore, *SNRNP200, SRRM1* and/or *SRSF3* expression directly correlated with the expression levels of the oncogenic SV *AR-v7* [(Fig. 2c); but not with *AR* expression (Fig. 2d)], with *MKI67* (Fig. 2e) and *KLK3* (i.e. *SRSF3* and *SRRM1*, but not *SNRNP200;* Fig. 2f).

3.2. Protein levels of SNRNP200, SRRM1 and SRSF3 are elevated in PCa samples and associated with clinical aggressiveness features

IHC analyses using FFPE samples from the cohort of patients with highly-aggressive PCa (Table 2) revealed that SNRNP200, SRSF3 and SRRM1 protein levels were significantly higher in PCa-samples compared to controls samples (FFPE samples of patients with PIN and/or BPH). Specifically, nuclear staining of SNRNP200 was higher in PCa samples compared to PIN and BPH samples. Low levels of cytoplasmic SNRNP200 protein were detected, while no changes were observed among groups (data not shown). Furthermore, although cytoplasmic protein level of SRRM1 was not detected, SRRM1-nuclear levels were significantly higher in PCa-samples compared to BPH and PIN samples (Fig. 3b). In contrast, no differences among SRSF3-nuclear staining were found between PCa, BPH and PIN samples (data not shown); however, SRSF3-cytoplasmic staining was significantly higher in PCa and PIN samples compared to BPH samples (Fig. 3c). Finally, SNRNP200, SRRM1 and SRSF3 protein levels were associated with clinically significant PCa (SigPCa; Gleason score ≥ 7) and, in the case of SRRM1 and SRSF3, tended to be associated with the presence of metastasis ($p = =0.077$, $p = =0.067$, respectively).

3.3. Silencing of SNRNP200, SRRM1 and SRSF3 expression decreases functional parameters of aggressiveness in PCa cells

The analysis of the expression levels of *SNRNP200, SRRM1* and *SRSF3* in prostate-derived cell lines showed that: 1) *SNRNP200* was overexpressed in the PCa-derived cell lines 22Rv1, LNCaP and DU145 compared to the normal-like prostate cell line PNT2 (Fig. 4a, left-panel); 2) *SRRM1* was significantly overexpressed in all the PCa cell lines compared to PNT2 (Fig. 4a, middle-panel); and, 3) that *SRSF3* was overexpressed in 22Rv1, DU145 and PC-3 compared to PNT2 (Fig. 4a, right-panel). Therefore, we selected an androgen-dependent AR^+/AR-$v7^-$ model (LNCaP), an androgen-independent AR^+/AR-$v7^+$model (22Rv1) and an androgen independent AR^-/AR-$v7^-$ model (DU145) to perform functional experiments in response to the silencing of these three genes. The silencing of *SNRNP200, SRRM1* and *SRSF3* in response to specific siRNAs was validated at mRNA levels in LNCaP, 22Rv1 and DU145 cells (Fig. 4b), as well as at protein levels in DU145 cells (Supplemental Figure 3). Remarkably, no effects in proliferation rate were observed in response to scramble-siRNA in LNCaP, 22Rv1 and DU145 as compared to non-transfected cells (Supplemental Figure 4). Specifically, proliferation rate of LNCaP cells significantly decreased at 48 and 72 h in response to *SNRNP200*- and *SRRM1*-silencing, as well as at 24, 48 and 72 h in response to *SRSF3*-silencing (Fig. 4c) compared to scramble-transfected cells. Moreover, the silencing of *SNRNP200, SRRM1* and *SRSF3* significantly decreased proliferation rate (at 48 and 72 h) in 22Rv1 and DU145 (Fig. 4c). In addition, silencing of *SNRNP200, SRSF3*, but not *SRRM1*, reduced migration rate in DU145 cells (Fig. 4d).

3.4. Silencing of SNRNP200, SRRM1 and SRSF3 modulates relevant signaling pathways and the expression of oncogenic splicing variants in PCa

The silencing of *SRRM1* significantly decreased the phosphorylation levels of AKT, while silencing of *SRSF3* increased phosphorylation levels of ERK and decreased that of JNK (Fig. 5a). In contrast, no statistically significant changes in the phosphorylation levels of AKT, ERK or JNK were observed in response to *SNRNP200*-silencing (Fig. 5a).

Table 4
Association of expression levels of spliceosome components and splicing factors with the development of biochemical recurrence of prostate cancer.

Factor	LongRank	*p* value
RNU4	1.822	0.177
RNU6	5.046	0.025
PRPF40A	4.938	0.026
SF3B1	4.012	0.045
U2AF2	4.222	0.040
RNU12	2.844	0.092
ESRP1	3.201	0.074
ESRP2	5.049	0.025
KHDRBS1	4.455	0.035
MAGOH	2.540	0.111
NOVA1	4.758	0.029
PTBP1	4.407	0.036
RBM3	1.631	0.202
RBM45	5.075	0.024
SND1	4.992	0.025
SRSF2	4.632	0.031
SRSF4	3.722	0.054
SRSF5	3.944	0.047
SRSF9	4.349	0.037
SRSF10	3.971	0.046
SRRM4	1.703	0.192
TIA1	4.551	0.033
TRA2A	4.702	0.030

The silencing of the expression of *SNRNP200, SRRM1* and *SRSF3* reduced the expression levels of the oncogenic splicing variants *PKM2, CASP2S* and *XBP1s*, without altering the expression of *PKM1, CASP2* and *XBP1*u. Therefore, *SNRNP200*-, *SRRM1*- and *SRSF3*-silencing decreased *PKM2*/*PKM1, CASP2S*/*CASP2* and *XBP1s*/*XBP1u* ratio (Fig. 5b). Moreover, only *SRRM1*-silencing resulted in a decrease in the *REST4*/*REST* expression ratio (by a reduction of *REST4* without alteration of *REST*) and in a reduction of *KLF6-SV1* expression (Fig. 5b). In the case of *AR* splicing process, silencing of *SNRNP200* and *SRRM1* (but not *SRSF3*) evoked a decrease in the ratio of the *AR-v7*/*AR* expression, by a reduction of *AR-v7* without altering *AR* expression; while the silencing of *SRSF3* decreased both *AR-v7* and *AR* expression. Due to the importance of AR-v7 on PCa aggressiveness, we determined whether *SNRNP200* and *SRRM1* could control the expression levels of splicing factors previously associated to the modulation of *AR* gene splicing and with *AR-v7* generation [i.e. *KHDRBS1* [21], *SFPQ* [22] and *U2AF2* [23]]. However, the expression levels of *KHDRBS1, SFPQ* and *U2AF2* were not significantly altered in response to the silencing of *SNRNP200* or *SRRM1* (Fig. 5c). In addition, no statistically significant changes were observed in the expression of additional splicing variants, such as SST_5TMD4 and *In1-ghrelin*, in response to *SNRNP200*-, *SRRM1*- and *SRSF3*-silencing (Fig. 5b).

Finally, expression levels of classical markers of PCa aggressiveness were analysed in response to *SNRNP200*-, *SRRM1*- and *SRSF3*-silencing. Specifically, *C-MYC* expression levels were reduced in response to *SRSF3*-silencing, while those of *TP53* were increased in response to *SNRNP200*-silencing (Fig. 5d). In addition, the silencing of *SNRNP200, SRRM1* and *SRSF3* resulted in a significantly increase of the expression levels of *PTEN* (Fig. 5d).

3.5. Silencing of SNRNP200, SRRM1 and SRSF3 enhanced the antitumor actions of enzalutamide in PCa cells

In order to test the effects of *SNRNP200*-, *SRRM1*- and *SRSF3*-silencing on androgens and enzalutamide responsiveness, we evaluated proliferation rate of 22Rv1 and LNCaP cells after 24h. We used this experimental paradigm in that cell proliferation was not significantly

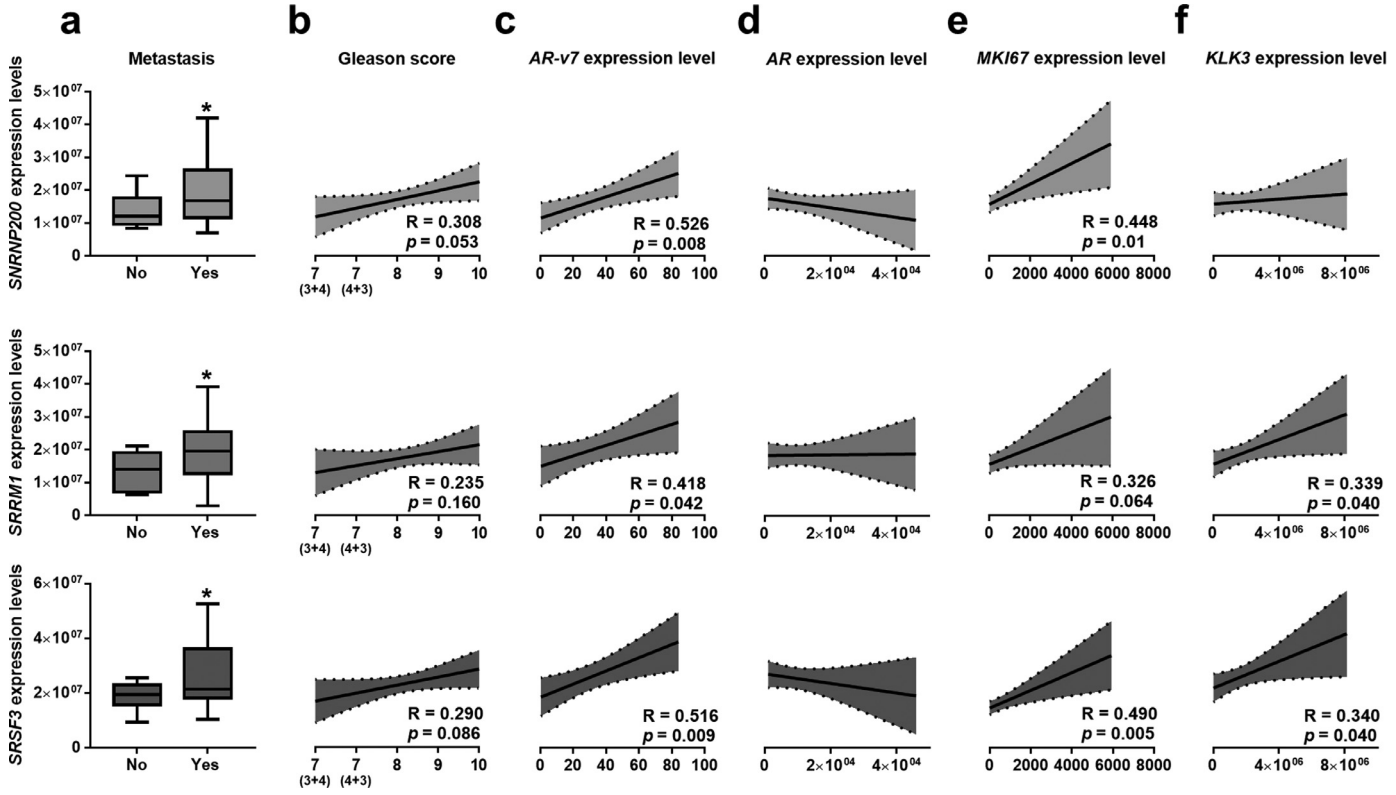

Fig. 2. Expression of *SNRNP200, SRRM1* and *SRSF3* in a highly aggressive cohort of prostate cancer (PCa) samples. (a) *SNRNP200, SRRM1* and *SRSF3* expression levels in a battery of highly-aggressive PCa samples, with or without the presence of metastasis ($n = 42$). represent the mean ± SEM of mRNA expression levels. b-f) Correlation between *SNRNP200, SRRM1* and *SRSF3* expression levels and Gleason score (b), expression levels of *AR-v7* (c), *AR* (d) *MKI67* (e) and *KLK3* (f). mRNA levels were determined by a microfluidic-based qPCR array and adjusted by normalization factor calculated from *ACTB* and *GAPDH* expression levels. Asterisk (* $p < 0.05$) indicates statistically significant differences between groups.

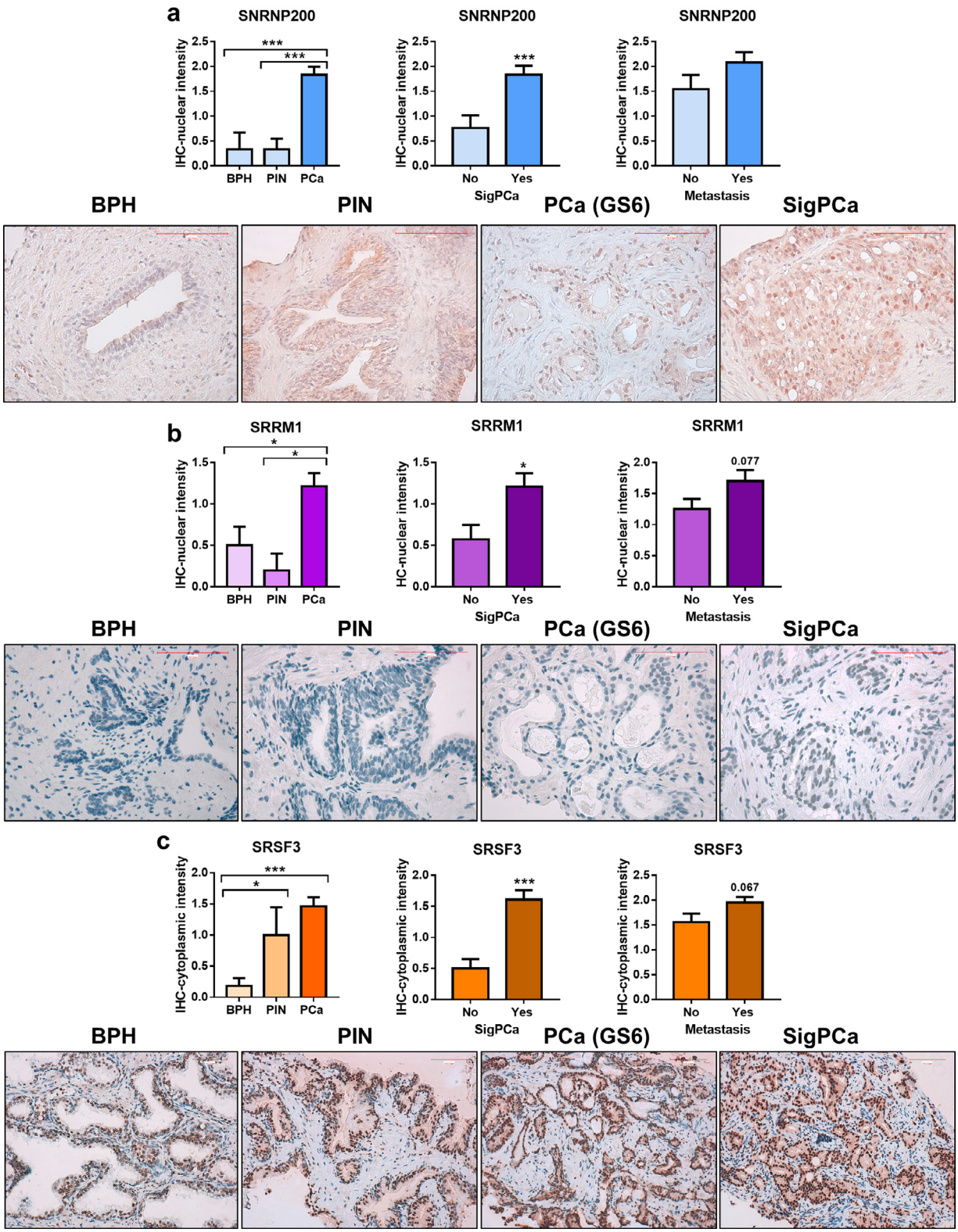

Fig. 3. Immunohistochemical analysis of SNRNP200, SRRM1 and SRSF3 in prostate cancer (PCa) samples. a) Comparison of SNRNP200, SRRM1 (b) and SRSF3 (c) protein levels by immunohistochemistry (IHC) between a representative set of PCa samples ($n = 47$), prostatic intraepithelial neoplasia (PIN; $n = 6$) and benign prostatic hyperplasia (BPH; $n = 7$). Association of protein levels with clinically significant PCa (SigPCa; defined as Gleason score higher than 7) and the presence of metastasis at diagnosis (central panel and right panel, respectively). Representative images of BPH, PIN, PCa with Gleason score = 6 and SigPCa stained with SNRNP200 (400× magnification), SRRM1 (400× magnification) and SRSF3 (200× magnification) antibodies are showed below a, b and c panels, respectively. Scale bar indicates 100 μm. Data are expressed as mean ± SEM of IHC staining scaled from low [1] to high [3] intensity. Asterisks (* $p < 0.05$; ** $p < 0.01$; *** $p < 0.001$) indicate statistically significant differences between groups.

compromised after 24h of enzalutamide treatment nor by 24h of *SNRNP200*-, *SRRM1*- and *SRSF3*-silencing (Fig. 6a, open bars) in 22Rv1 cells. Firstly, we observed that the silencing of *SNRNP200*, *SRRM1* or *SRSF3* did not alter the normal (scramble-treated) response to DHT as a similar decrease of proliferation rate was found compared to DHT-treated cells, independently of the siRNA used (i.e. scramble,

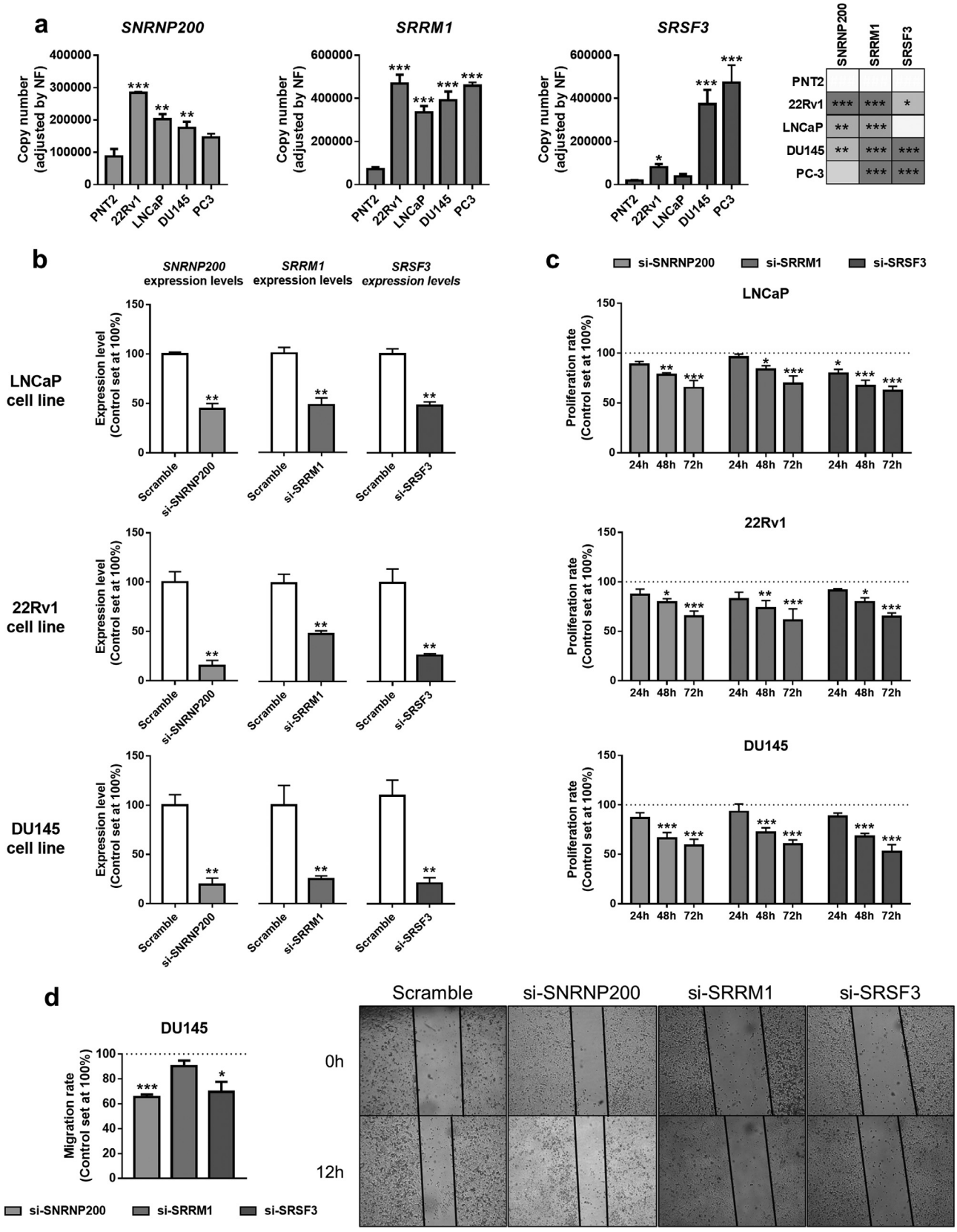

Fig. 4. Functional consequences of *SNRNP200, SRRM1* and *SRSF3* silencing in prostate-derived cell lines. a) Comparison of *SNRNP200, SRRM1* and *SRSF3* expression levels between a non-tumor prostate cell line (PNT2) and PCa cell lines LNCaP, 22Rv1, DU145 and PC-3 ($n = 5$). mRNA levels were determined by qPCR and adjusted by normalization factor calculated from *ACTB* and *GAPDH* expression levels. b) Validation by qPCR of *SNRNP200, SRRM1* and *SRSF3* silencing (si-SNRNP200, si-SRRM1 and si-SRSF3, respectively). mRNA levels were determined by qPCR and adjusted by normalization factor calculated from *ACTB* and *GAPDH* expression levels. Data were represented as percent of scramble cells (mean ± SEM). c) Proliferation rate of LNCaP (upper panel), 22Rv1 (middlepanel) and DU145 (bottom panel) cell lines after 24-, 48- and 72 h of *SNRNP200*-, *SRRM1*- and *SRSF3*-silencing ($n = 4$). d) Effect of *SNRNP200*-, *SRRM1*- and *SRSF3*-silencing on the migration rate of DU145 cell line was determined by wound-healing assay (12 h; $n \geq 3$). Representative images are depicted in right panel. Data were represented as percent of scramble cells (mean ± SEM). Asterisks (* $p < 0.05$; ** $p < 0.01$; *** $p < 0.001$) indicate statistically significant differences between groups.

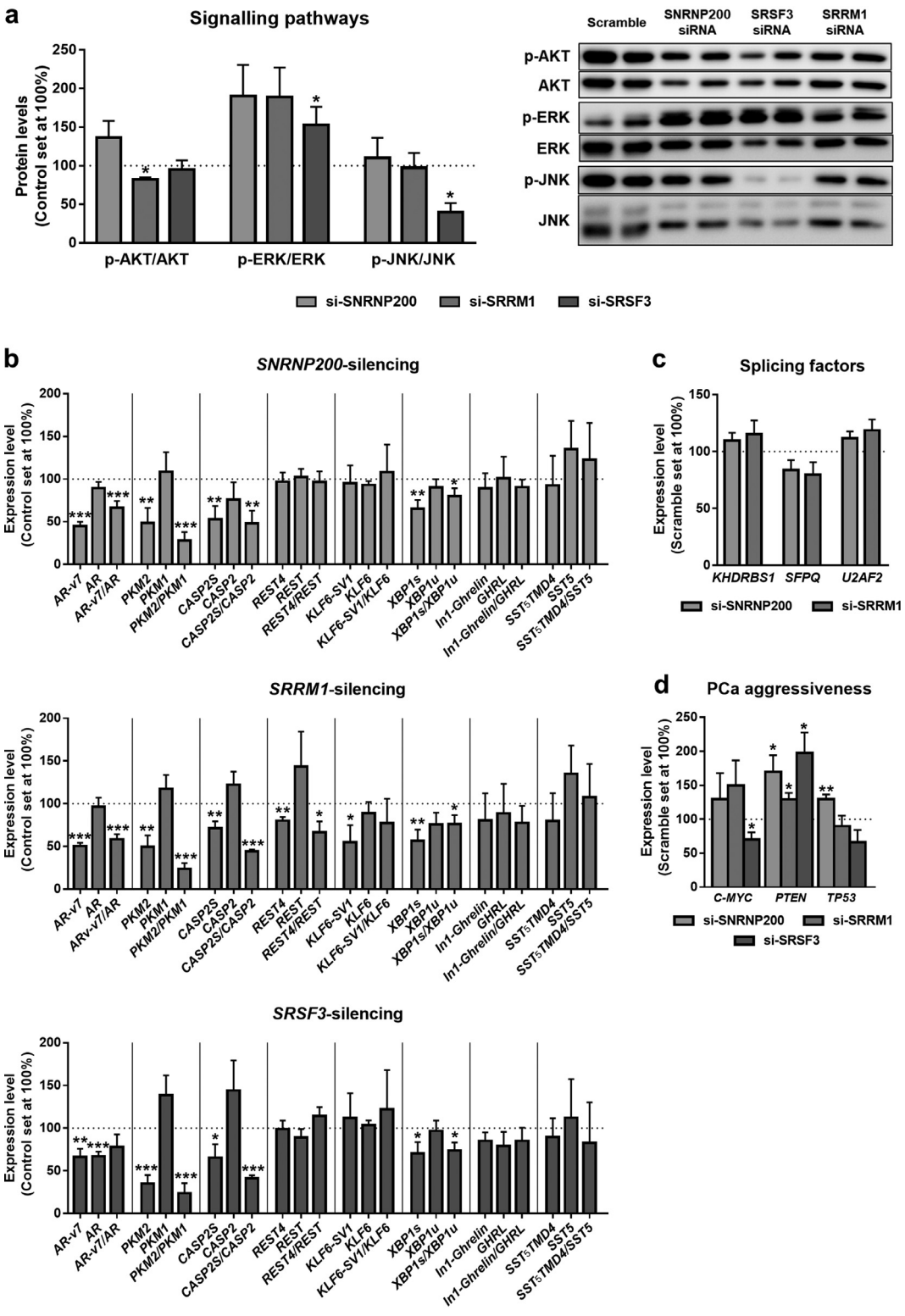

Fig. 5. Molecular consequences of *SNRNP200, SRRM1* and *SRSF3* silencing in 22Rv1 cell line. a) Basal phospho-AKT, phospho-ERK1/2 and phospho-JNK levels in *SNRNP200-*, *SRRM1-* and *SRSF3* silenced 22Rv1 cells (si-SNRNP200, si-SRRM1 and si-SRSF3, respectively; 24 h; $n \geq 3$). Protein levels were normalized by total AKT, ERK and JNK protein levels. Representative images are shown in right panel. Protein data were represented as percent of scramble cells. b) Expression levels of selected transcripts in response to *SNRNP200* (upper panel), *SRRM1* (central panel) and *SRSF3* (bottom panel) silencing (24 h) in 22Rv1 cells. Ratio between the expression of splicing variants is shown in bars with dotted pattern. c) Expression levels of *KHDRBS1, SFPQ* and *U2AF2* in response to *SNRNP200-* and *SRRM1*-silencing in 22Rv1 cells. d) Expression levels of *C-MYC, PTEN* and *TP53* in response to *SNRNP200-*, *SRRM1-* and *SRSF3*-silencing in 22Rv1 cells. mRNA levels were determined by qPCR and adjusted by normalization factor calculated from *ACTB* and *GAPDH* expression levels. Data were represented as percent of scramble-treated control cells (mean ± SEM). Asterisks (* $p < 0.05$; ** $p < 0.01$; *** $p < 0.001$) indicate statistically significant differences between groups.

si-SNRNP200, si-SRRM1 or si-SRSF3) in 22Rv1 and LNCaP cell lines (Fig. 6a/b). However, the silencing of *SNRNP200, SRRM1* and *SRSF3* combined with enzalutamide treatment resulted in an additive, statistically significant antiproliferative effect in 22Rv1 cells at 24h of incubation, indicating that silencing of *SNRNP200, SRRM1* or *SRSF3* sensitized 22Rv1 cells to enzalutamide (Fig. 6a). Additionally, although no differences

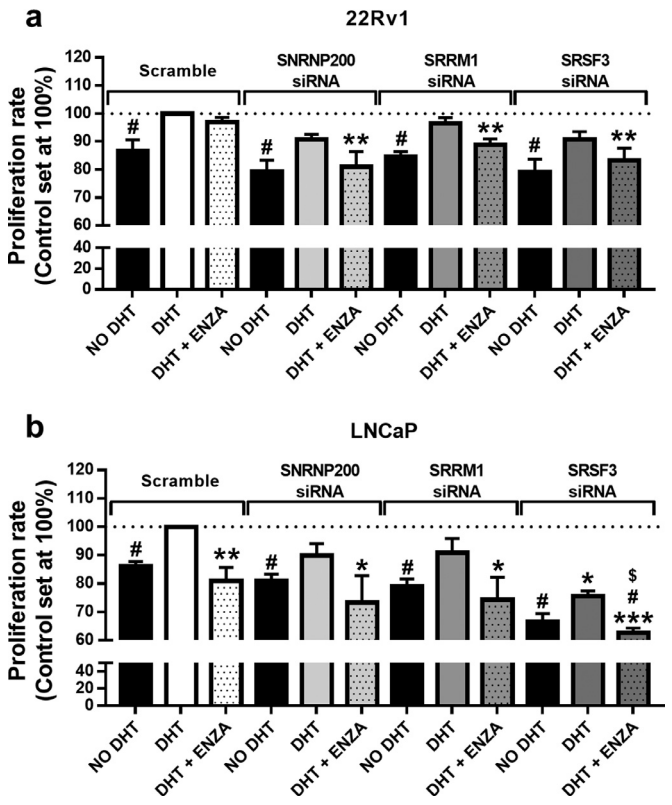

Fig. 6. Cell proliferation assay in response to enzalutamide treatment combined with *SNRNP200, SRRM1* and *SRSF3* silencing. Proliferation rate of 22Rv1 (a) and LNCaP (b) cell line was measured after 24 h of *SNRNP200*-, *SRRM1*- and *SRSF3*-silencing in the presence (DHT) or absence (no DHT) of 5α-dihydrotestosterone with or without enzalutamide (ENZA; $n = 4$). Results were expressed as percentage referred to scramble vehicle-treated control with DHT (mean ± SEM). Asterisks (* $p < 0.05$; ** $p < 0.01$), dash ($^{\#}$ $p < 0.05$) and dollar sign ($^{\$}$ $p < 0.05$) indicate statistically significant differences compared to DHT of scramble, DHT of each condition and DHT+ENZA of scramble, respectively.

were observed when analysing 22Rv1 scramble-treated cells in response to enzalutamide at 24h, we found a significantly decrease in the proliferation rate of scramble-treated LNCaP cells in response to enzalutamide (Fig. 6a/b). Interestingly, the pattern of response of *SNRNP200*- and *SRRM1*-silenced LNCaP cells was similar to scramble-treated LNCaP cells (Fig. 6b), wherein the response to non-DHT and to enzalutamide was comparable in scramble-, si-SNRNP200- and si-SRRM1-treated LNCaP cells. In striking contrast, the response of *SRSF3*-silenced cells was markedly different. Specifically, the proliferation rate of *SRSF3*-silenced LNCaP cells in the presence of DHT was significantly lower compared to scramble-treated LNCaP cells in the presence of DHT. In addition, we observed that enzalutamide treatment and *SRSF3*-silencing exerted an additive antiproliferative effect in LNCaP cells, inasmuch as the proliferation rate of enzalutamide-treated *SRSF3*-silenced LNCaP cells was significantly lower than that of enzalutamide-treated scramble-treated cells (in presence of DHT) and than that of *SRSF3*-silenced cells (in presence of DHT) (Fig. 6b).

4. Discussion

PCa is one of the tumor pathologies whose development and, specially, progression is mostly influenced by the alteration of the normal gene expression pattern and the aberrant presence of oncogenic SVs [24]. Indeed, PCa is drastically influenced by the appearance of the AR splicing variant-7 (AR-v7), inasmuch as it has been strongly associated with PCa aggressiveness [25], as well as with the resistance to conventional therapies such as antiandrogens and chemotherapy [26,27]. Similarly, the altered expression pattern of additional SVs, such as *SST$_5$TMD4* [4], *PKM2* [5], *REST4* [6], *XBP1s* [7], *In1-Ghrelin* [8] among others, has also been found to be associated to PCa development and progression. In this sense, it is reasonable to think that a dysregulation of the cellular machinery involved in the control of splicing process would be responsible for the broad alteration of oncogenic SVs observed in PCa. However, although some specific SFs and SCs have been associated with PCa development and aggressiveness [22,23,28–30], to the best of our knowledge, no studies have comprehensively explored the global dysregulations of these elements in PCa.

In our study, we have demonstrated for the first time a profound and overt dysregulation of the expression levels of a representative set of SCs and associated SFs in PCa. In particular, more than 50% of the SCs and SFs analysed herein displayed an altered expression pattern, demonstrating that the components of the cellular machinery responsible for the processing of the splicing process are drastically dysregulated in PCa. Indeed, we have bioinformatically defined an expression-based molecular fingerprint (combining the mRNA expression levels of 11 SCs and SFs) able to perfectly discriminate between PCa and non-tumor adjacent regions, which further reinforces this contention and demonstrate that PCa curses with a global dysregulation of the splicing machinery. Even more important is the fact that the expression levels of many of the SCs and SFs determined in this study were associated or correlated with relevant clinical and molecular features of aggressiveness (e.g. Gleason score, presence of metastasis and *AR-v7* expression), suggesting a causal link between the dysregulations of the splicing machinery and the aggressiveness of PCa. These results are consistent with and further expand previous observations indicating that high expression of specifics SFs, including *RBM3*, *U2AF2*, *ESRP1*, *ESRP2* and *NOVA1* among others, is associated to clinical and/or molecular PCa aggressiveness features [23,28,30,31].

Among all the SCs and SFs analysed herein, SNRNP200, SRRM1 and SRSF3 seemed to have special relevance in PCa pathophysiology in that their expression levels were significantly up-regulated and associated with all the relevant clinical features analysed in this study, including Gleason score, pathological stage, perineural invasion, lymphovascular invasion, biochemical recurrence, presence of metastasis at diagnosis or *AR-v7* expression. Importantly, data available *in silico* further validated the overexpression of *SNRNP200*, *SRRM1* and *SRSF3* in PCa as compared to non-tumoral prostate tissues [i.e. Singh, Wallace, Tomlins and/or Welsh-dataset [32–35]]. In addition, these splicing machinery components could represent novel biomarkers and/or therapeutic targets in PCa inasmuch as their dysregulation has not been previously described in this tumor pathology and their expression levels showed a potential utility as prognostic markers, since these levels were associated with biochemical recurrence. It should to be noted that, although *SRSF3* has been defined as an oncogene in different tumor pathologies [36–38], this is the first description of the overexpression of this SF in PCa. Specifically, it has been shown that SRSF3 can enhance aggressiveness features of several tumor types through the control of splicing process in the nucleus [37,39,40], but also through the alteration of translational efficiency of certain mRNAs in the cytoplasm [41]. This suggests that overexpression of *SRSF3* mRNA can exert oncogenic actions either by increasing SRSF3 protein levels in the nucleus or in the cytoplasm, as found herein in the case of PCa cells. On the other hand, the protein overexpression of SRRM1 and SNRNP200 was observed in the nucleus of PCa cells, suggesting an enhancement of their putative activity as splicing modulators in these cells.

Due to the increasing body of evidence pointing toward a strong dysregulation of the splicing process in cancer, many therapeutic strategies to prevent the expression of oncogenic SVs and/or to modulate the activity of the spliceosome have been reported hitherto [42]. In particular, during the last years, many spliceosome inhibitors (e.g. Pladienolide-B, spliceostatin-A) have been reported and suggested as therapeutic targets in different pathologies wherein the dysregulated splicing process has been shown to be relevant [43,44].

However, while blocking the activity of the spliceosome could be less specific, targeting specific SCs and/or SFs could represent a novel and more specific approach to tackle cancer diseases in that a more reduced number but better-defined splicing events may be altered. In this sense, we have demonstrated for the first time herein that the silencing of the expression of *SNRNP200*, *SRRM1* and *SRSF3* using specific siRNAs clearly decreased key functional parameters of aggressiveness, including proliferation and migration, in PCa-derived cell lines. These clinically relevant antitumor actions seemed to be associated to the modulation of key signaling pathways and the expression of certain oncogenic SVs. Indeed, *SRRM1*-and *SRSF3*-silencing evoked a decrease in phosphorylation levels of AKT and JNK proteins, respectively, probably leading to the inhibition of PI3K/AKT and JNK pathways, which have been broadly defined as oncogenic signaling pathways [45,46]. Intriguingly, the silencing of *SRSF3* increased ERK-phosphorylation, presumably leading to a higher activation of MAPK/ERK pathway, which has been reported to be highly susceptible to be dysregulated in response to splicing changes [47]. Remarkably, despite its well-known oncogenic role, MAPK/ERK-pathway has been postulated as a regulator of cell senescence, thus also exerting antitumor effects [48]. As expected, and providing a mechanistic explanation, *SNRNP200*-, *SRRM1*- and *SRSF3*-silencing dysregulated the splicing process of several genes involved in tumor aggressiveness, such as *AR*, *PKM*, *CASP2* or *XBP1*. Among them, especially relevant are the results obtained in *AR* splicing, due to its well-known role in the development and aggressiveness of PCa [49]. Specifically, a decrease in the expression of *AR-v7* (but not *AR*) was observed in response to *SNRNP200*- and *SRRM1*-silencing, thus altering the normal splicing process of *AR*. Interestingly, the modulation of *AR* splicing process exerted by SNRNP200 and SRRM1 may be not mediated by the regulation of splicing factors previously reported to be involved in *AR-v7* generation such as KHDRBS1 [21], SFPQ [22] or U2AF2 [23], inasmuch as we found that the silencing of *SNRNP200* and *SRRM1* did not alter the expression levels of these *AR*-splicing modulators. On the other hand, the silencing of *SRSF3* decreased the expression levels of both *AR* and *AR-v7*. In any case, these results postulate these three factors as potential therapeutic target candidates to tackle castration resistant PCa (CRPC), since AR-v7 has been reported as a driver of CRPC-development [50]. Reinforcing the oncogenic role of *SNRNP200*, *SRRM1* and *SRSF3* in PCa, we found that the silencing of these genes resulted in the modulation of the expression of key genes involved in CRPC aggressiveness, including *C-MYC, PTEN* and/or *TP53* [51–53]. Consistently, *SNRNP200-, SRRM1*- and *SRSF3*-silencing sensitized 22Rv1 cells to enzalutamide by showing additive effects in the inhibition of proliferation rate in these cells, possibly through AR-v7 down-regulation. This hypothesis was reinforced by the fact that *SNRNP200*- or *SRRM1*-silencing did not alter the normal response to enzalutamide in LNCaP cell line (which express AR but lack AR-v7), while *SRSF3*-silencing (which is associated to a reduction in full-length *AR* expression) in combination with enzalutamide treatment resulted in an additive antiproliferative effect in these cells.

Therefore, the data presented herein indicate that the cellular machinery responsible for the regulation of the splicing process is drastically altered in PCa and that certain SCs and SVs could represent novel candidates as potential diagnostic and prognostic biomarkers, as well as putative targets to develop novel therapeutic strategies against PCa. Specifically, our results demonstrated that SNRNP200, SRRM1 and SRSF3 could represent attractive novel diagnostic/prognostic and therapeutic targets for PCa and CRPC.

5. Role of the funding sources

This work was funded by Instituto de Salud Carlos III, co-funded by European Union (ERDF/ESF, “Investing in your future”) [PI16/00264, PI17-02287, CM16/00180, FI17/00282, CD16/00092], FEDER (CCB.030PM), MINECO/MECD (BFU2016-80360-R; FPU16/06190, FPU18/02485, FPU16/05059, FPU17/00263, FPU14/04290), Junta de Andalucía (BIO-0139), Spanish Association Against Cancer (AECC; INVES18057YUBE) and CIBERobn. CIBER is an initiative of Instituto de Salud Carlos III, Ministerio de Sanidad, Servicios Sociales e Igualdad, Spain. The biological samples repository node (Córdoba, Spain) is gratefully acknowledged for coordination tasks in the selection of samples.

All the funding sources were essential for data collection, analysis, interpretation and patient recruitment. The corresponding author declare that he had full access to all the data in the study and had the final responsibility for the decision to submit for publication.

Author’s contributions

Juan Manuel Jiménez-Vacas: Conceptualization, Data curation, Formal analysis, Investigation, Methodology, Validation, Visualization, Writing - original draft, Writing - review & editing. *Vicente Herrero-Aguayo, Antonio Jesús Montero-Hidalgo*: Conceptualization, Data curation, Formal analysis, Investigation, Methodology, Validation, Visualization, Writing - review & editing. *Enrique Gómez-Gómez*: Conceptualization, Data curation, Formal analysis, Investigation, Methodology, Validation, Resources, Writing - review & editing. *Antonio C. Fuentes-Fayos, Antonio José León-González, Prudencio Sáez-Martínez, Emilia Alors-Pérez, Sergio Pedraza-Arévalo, Teresa González-Serrano, Oscar Reyes, Ana Martínez-López, Rafael Sánchez-Sánchez* and *Elena M Yubero-Serrano*: Data curation, Formal analysis, Investigation, Writing - review and editing. *Sebastián Ventura*: Data curation, Formal analysis, Investigation, Software, Writing - review and editing. *María J. Requena-Tapia, Justo P. Castaño* and *Manuel D. Gahete*: Formal analysis, Methodology, Resources, Writing - original draft, Writing - original draft, Writing - review & editing. *Raúl M. Luque*: Conceptualization, Data curation, Formal analysis, Funding acquisition, Investigation, Methodology, Project administration, Resources, Supervision, Visualization, Writing - original draft, Writing - review & editing.

Declaration of Competing Interest

The authors declare that they have no conflict of interest.

Supplementary materials

Supplementary material associated with this article can be found in the online version at doi:10.1016/j.ebiom.2019.11.008.

References

[1] Matera AG, Wang Z. A day in the life of the spliceosome. Nat Rev Mol Cell Biol 2014;15(2):108–21.
[2] Scotti MM, Swanson MS. RNA mis-splicing in disease. Nat Rev Genet 2016;17(1):19–32.
[3] Bray F, Ferlay J, Soerjomataram I, Siegel RL, Torre LA, Jemal A. Global cancer statistics 2018: GLOBOCAN estimates of incidence and mortality worldwide for 36 cancers in 185 countries. CA Cancer J Clin 2018;68(6):394–424.
[4] Hormaechea-Agulla D, Jimenez-Vacas JM, Gomez-Gomez E, F LL, Carrasco-Valiente J, Valero-Rosa J, et al. The oncogenic role of the spliced somatostatin receptor sst5TMD4 variant in prostate cancer. Faseb J 2017;31(11):4682–96.
[5] Wong N, Yan J, Ojo D, De Melo J, Cutz JC, Tang D. Changes in PKM2 associate with prostate cancer progression. Cancer Invest 2014;32(7):330–8.
[6] Zhang X, Coleman IM, Brown LG, True LD, Kollath L, Lucas JM, et al. SRRM4 expression and the loss of rest activity may promote the emergence of the neuroendocrine phenotype in castration-resistant prostate cancer. Clin Cancer Res 2015;21(20):4698–708.
[7] Sheng X, Nenseth HZ, Qu S, Kuzu OF, Frahnow T, Simon L, et al. IRE1α-XBP1s pathway promotes prostate cancer by activating c-MYC signaling. Nat Commun 2019;10(1):323.
[8] Hormaechea-Agulla D, Gahete MD, Jimenez-Vacas JM, Gomez-Gomez E, Ibanez-Costa A, F LL, et al. The oncogenic role of the In1-ghrelin splicing variant in prostate cancer aggressiveness. Mol Cancer 2017;16(1):146.
[9] Zhang C, Li HR, Fan JB, Wang-Rodriguez J, Downs T, Fu XD, et al. Profiling alternatively spliced mRNA isoforms for prostate cancer classification. BMC Bioinformat 2006;7:202.

[10] Pedraza-Arevalo S, Hormaechea-Agulla D, Gomez-Gomez E, Requena MJ, Selth LA, Gahete MD, et al. Somatostatin receptor subtype 1 as a potential diagnostic marker and therapeutic target in prostate cancer. Prostate 2017;77(15):1499–511.
[11] Del Rio-Moreno M, Alors-Perez E, Gonzalez-Rubio S, Ferrin G, Reyes O, Rodriguez-Peralvarez M, et al. Dysregulation of the splicing machinery is associated to the development of non-alcoholic fatty liver disease. J Clin Endocrinol Metab 2019.
[12] Gahete MD, Del Rio-Moreno M, Camargo A, Alcala-Diaz JF, Alors-Perez E, Delgado-Lista J, et al. Changes in splicing machinery components influence, precede, and early predict the development of type 2 diabetes: from the cordioprev study. EBioMedicine 2018;37:356–65.
[13] Vandesompele J, De Preter K, Pattyn F, Poppe B, Van Roy N, De Paepe A, et al. Accurate normalization of real-time quantitative rt-pcr data by geometric averaging of multiple internal control genes. Genome Biol 2002;3(7) research0034.1.
[14] Luque RM, Ibanez-Costa A, Neto LV, Taboada GF, Hormaechea-Agulla D, Kasuki L, et al. Truncated somatostatin receptor variant sst5TMD4 confers aggressive features (proliferation, invasion and reduced octreotide response) to somatotropinomas. Cancer Lett 2015;359(2):299–306.
[15] Ibanez-Costa A, Gahete MD, Rivero-Cortes E, Rincon-Fernandez D, Nelson R, Beltran M, et al. In1-ghrelin splicing variant is overexpressed in pituitary adenomas and increases their aggressive features. Sci Rep 2015;5:8714.
[16] Duran-Prado M, Gahete MD, Hergueta-Redondo M, Martinez-Fuentes AJ, Cordoba-Chacon J, Palacios J, et al. The new truncated somatostatin receptor variant sst5TMD4 is associated to poor prognosis in breast cancer and increases malignancy in MCF-7 cells. Oncogene 2012;31(16):2049–61.
[17] Sampedro-Nunez M, Luque RM, Ramos-Levi AM, Gahete MD, Serrano-Somavilla A, Villa-Osaba A, et al. Presence of sst5TMD4, a truncated splice variant of the somatostatin receptor subtype 5, is associated to features of increased aggressiveness in pancreatic neuroendocrine tumors. Oncotarget 2016;7(6):6593–608.
[18] Hatami R, Sieuwerts AM, Izadmehr S, Yao Z, Qiao RF, Papa L, et al. KLF6-SV1 drives breast cancer metastasis and is associated with poor survival. Sci Transl Med 2013;5(169) 169ra12.
[19] Kuranaga Y, Sugito N, Shinohara H, Tsujino T, Taniguchi K, Komura K, et al. SRSF3, a splicer of the PKM gene, regulates cell growth and maintenance of cancer-specific energy metabolism in colon cancer cells. Int J Molecular Sci 2018;19(10).
[20] Li Y, Donmez N, Sahinalp C, Xie N, Wang Y, Xue H, et al. SRRM4 drives neuroendocrine transdifferentiation of prostate adenocarcinoma under androgen receptor pathway inhibition. Eur Urol 2017;71(1):68–78.
[21] Stockley J, Markert E, Zhou Y, Robson CN, Elliott DJ, Lindberg J, et al. The RNA-binding protein Sam68 regulates expression and transcription function of the androgen receptor splice variant AR-V7. Sci Rep 2015;5:13426.
[22] Takayama KI, Suzuki T, Fujimura T, Yamada Y, Takahashi S, Homma Y, et al. Dysregulation of spliceosome gene expression in advanced prostate cancer by RNA-binding protein PSF. PNAS 2017;114(39):10461–6.
[23] Liu LL, Xie N, Sun S, Plymate S, Mostaghel E, Dong X. Mechanisms of the androgen receptor splicing in prostate cancer cells. Oncogene 2014;33(24):3140–50.
[24] Paschalis A, Sharp A, Welti JC, Neeb A, Raj GV, Luo J, et al. Alternative splicing in prostate cancer. Nat Rev Clin Oncol 2018;15(11):663–75.
[25] Kong D, Sethi S, Li Y, Chen W, Sakr WA, Heath E, et al. Androgen receptor splice variants contribute to prostate cancer aggressiveness through induction of EMT and expression of stem cell marker genes. Prostate 2015;75 (2):161–74.
[26] Antonarakis ES, Lu C, Wang H, Luber B, Nakazawa M, Roeser JC, et al. AR-V7 and resistance to enzalutamide and abiraterone in prostate cancer. N Engl J Med 2014;371(11):1028–38.
[27] Antonarakis ES, Lu C, Luber B, Wang H, Chen Y, Nakazawa M, et al. Androgen receptor splice variant 7 and efficacy of taxane chemotherapy in patients with metastatic castration-resistant prostate cancer. JAMA Oncol 2015;1(5):582–91.
[28] Grupp K, Wilking J, Prien K, Hube-Magg C, Sirma H, Simon R, et al. High RNA-binding motif protein 3 expression is an independent prognostic marker in operated prostate cancer and tightly linked to ERG activation and PTEN deletions. Eur J Cancer 2014;50(4):852–61.
[29] Yamamoto R, Osawa T, Sasaki Y, Yamamoto S, Anai M, Izumi K, et al. Overexpression of p54(nrb)/NONO induces differential EPHA6 splicing and contributes to castration-resistant prostate cancer growth. Oncotarget 2018;9 (12):10510–24.
[30] Gerhauser C, Favero F, Risch T, Simon R, Feuerbach L, Assenov Y, et al. Molecular evolution of early-onset prostate cancer identifies molecular risk markers and clinical trajectories. Cancer Cell 2018;34(6) 996-1011.e8.
[31] Lu ZX, Huang Q, Park JW, Shen S, Lin L, Tokheim CJ, et al. Transcriptome-wide landscape of pre-mRNA alternative splicing associated with metastatic colonization. Mol Cancer Res 2015;13(2):305–18.
[32] Singh D, Febbo PG, Ross K, Jackson DG, Manola J, Ladd C, et al. Gene expression correlates of clinical prostate cancer behavior. Cancer Cell 2002;1(2):203–9.
[33] Wallace TA, Prueitt RL, Yi M, Howe TM, Gillespie JW, Yfantis HG, et al. Tumor immunobiological differences in prostate cancer between African-American and European-American men. Cancer Res 2008;68(3):927–36.
[34] Kim JH, Dhanasekaran SM, Mehra R, Tomlins SA, Gu W, Yu J, et al. Integrative analysis of genomic aberrations associated with prostate cancer progression. Cancer Res 2007;67(17):8229–39.
[35] Welsh JB, Sapinoso LM, Su AI, Kern SG, Wang-Rodriguez J, Moskaluk CA, et al. Analysis of gene expression identifies candidate markers and pharmacological targets in prostate cancer. Cancer Res 2001;61(16):5974–8.
[36] Peiqi L, Zhaozhong G, Yaotian Y, Jun J, Jihua G, Rong J. Expression of SRSF3 is correlated with carcinogenesis and progression of oral squamous cell carcinoma. Int J Med Sci 2016;13(7):533–9.
[37] Gautrey H, Jackson C, Dittrich AL, Browell D, Lennard T, Tyson-Capper A. SRSF3 and hnRNP H1 regulate a splicing hotspot of HER2 in breast cancer cells. RNA Biol 2015;12(10):1139–51.
[38] Lin JC, Lee YC, Tan TH, Liang YC, Chuang HC, Fann YC, et al. RBM4-SRSF3-MAP4K4 splicing cascade modulates the metastatic signature of colorectal cancer cell. Biochimica et Biophysica Acta Molecular Cell Res 2018;1865(2):259–72.
[39] Wang H, Zhang CZ, Lu SX, Zhang MF, Liu LL, Luo RZ, et al. A coiled-coil domain containing 50 splice variant is modulated by serine/arginine-rich splicing factor 3 and promotes hepatocellular carcinoma in mice by the ras signaling pathway. Hepatology (Baltimore, Md) 2019;69(1):179–95.
[40] Zhu S, Chen Z, Katsha A, Hong J, Belkhiri A, El-Rifai W. Regulation of CD44E by DARPP-32-dependent activation of SRp20 splicing factor in gastric tumorigenesis. Oncogene 2016;35(14):1847–56.
[41] Kim J, Park RY, Chen JK, Kim J, Jeong S, Ohn T. Splicing factor SRSF3 represses the translation of programmed cell death 4 mRNA by associating with the 5′-UTR region. Cell Death Differ 2014;21(3):481–90.
[42] Jyotsana N, Heuser M. Exploiting differential RNA splicing patterns: a potential new group of therapeutic targets in cancer. Expert Opin Ther Targets 2018;22 (2):107–21.
[43] Sato M, Muguruma N, Nakagawa T, Okamoto K, Kimura T, Kitamura S, et al. High antitumor activity of pladienolide B and its derivative in gastric cancer. Cancer Sci 2014;105(1):110–6.
[44] Larrayoz M, Blakemore SJ, Dobson RC, Blunt MD, Rose-Zerilli MJ, Walewska R, et al. The SF3B1 inhibitor spliceostatin a (SSA) elicits apoptosis in chronic lymphocytic leukaemia cells through downregulation of Mcl-1. Leukemia 2016;30(2):351–60.
[45] Chen H, Zhou L, Wu X, Li R, Wen J, Sha J, et al. The PI3K/AKT pathway in the pathogenesis of prostate cancer. Front Biosci (Landmark Ed) 2016;21: 1084–91.
[46] Hubner A, Mulholland DJ, Standen CL, Karasarides M, Cavanagh-Kyros J, Barrett T, et al. JNK and pten cooperatively control the development of invasive adenocarcinoma of the prostate. PNAS 2012;109(30):12046–51.
[47] Siegfried Z, Bonomi S, Ghigna C, Karni R. Regulation of the Ras-MAPK and PI3K-mTOR signalling pathways by alternative splicing in cancer. Int J Cell Biol 2013;2013:568931.
[48] Deschenes-Simard X, Gaumont-Leclerc MF, Bourdeau V, Lessard F, Moiseeva O, Forest V, et al. Tumor suppressor activity of the erk/mapk pathway by promoting selective protein degradation. Genes Dev. 2013;27(8):900–15.
[49] Tan MH, Li J, Xu HE, Melcher K, Yong EL. Androgen receptor: structure, role in prostate cancer and drug discovery. Acta Pharmacol Sin 2015;36(1):3–23.
[50] Qu Y, Dai B, Ye D, Kong Y, Chang K, Jia Z, et al. Constitutively active AR-V7 plays an essential role in the development and progression of castration-resistant prostate cancer. Sci Rep 2015;5:7654.
[51] Bai S, Cao S, Jin L, Kobelski M, Schouest B, Wang X, et al. A positive role of c-Myc in regulating androgen receptor and its splice variants in prostate cancer. Oncogene 2019;38(25):4977–89.
[52] Jamaspishvili T, Berman DM, Ross AE, Scher HI, De Marzo AM, Squire JA, et al. Clinical implications of PTEN loss in prostate cancer. Nat Rev Urol 2018;15 (4):222–34.
[53] Hamid AA, Gray KP, Shaw G, MacConaill LE, Evan C, Bernard B, et al. Compound genomic alterations of TP53, PTEN, and RB1 tumor suppressors in localized and metastatic prostate cancer. Eur Urol 2019;76(1):89–97.

Supplemental Table 1.

	Gene	Accession number	Primer sequence (Sense. Se)	Primer sequence (Antisense. As)	Product size
Spliceosome Components	PRPF40A	NM_017892.3	GCTCGGAAGATGAAACGAAA	TGTCCTCAAATGCTGGCTCT	130
	PRPF8	NM_006445.3	TGCCCACTACAACCGAGAA	AGGCCCGTCCTTCAGGTA	139
	RNU11	NR_004407.1	AAGGGCTTCTGTCGTGAGTG	CCAGCTGCCCAAATACCA	108
	RNU12	NR_029422.1	ATAACGATTCGGGGTGACG	CAGGCATCCCGCAAAGTA	106
	RNU2	NR_002716.3	CTCGGCCTTTTGGCTAAGAT	TATTCCATCTCCCTGCTCCA	116
	RNU4	NR_003925.1	TCGTAGCCAATGAGGTCTATCC	AAAATTGCCAGTGCCGACTA	103
	RNU4ATAC	NR_023343.1	GTTGCGCTACTGTCCAATGA	CAAAAATTGCACCAAAATAA	85
	RNU6	NR_004394.1	CGCTTCGGCAGCACATATA	AAAATATGGAACGCTTCACGAA	101
	RNU6atac	NR_023344.1	TGAAAGGAGAGAAGGTTAGCACTC	CGATGGTTAGATGCCACGA	112
	SF3B1	NM_012433.3	CAGTTCCGTCTGTGTGTTCG	GCTGCCTTCTTGCCTTGA	101
	RNU1	NM_001301069.1	ATCACGAAGGTGGTTTTCC	GCAGTCGAGTTTCCCACA	114
	SNRNP200	NM_014014.4	GGTGCTGTCCCTTGTTGG	CTTTCTTCGCTTGGCTCTTCT	103
	TCERG1	NM_006706.3	GAGGAGCCCAAAGAAGAGGA	CACCAGTCCAAACGACACAC	112
	U2AF1	NM_006758.2	GAAGTATGGGGAAGTAGAGGAGATG	TTCAAGTCAATCACAGCCTTTTC	120
	U2AF2	NM_007279.2	CTTTGACCAGAGGCGCTAAA	TACTGCATTGGGGTGATGTG	130
Splicing Factors	CELF1	NM_006560.3	AACAGAAGAGAATGGCCCAGC	TGCTGAAGGAGTGCTAAATACTG	121
	ESRP1	NM_020180.3	TTTTGGGATCACTGCTGGGG	TGTCCCACCTTCTTGTTGGC	108
	ESRP2	NM_024939.2	AGAGCCCAGCAGTCAATTGTT	GTCTCACTGTCCACCACATCAG	96
	KHDRBS1	NM_006559.2	GAGCGAGTGCTGATACCTGTC	CACCAGTCTCTTCCTGCAGTC	106
	MAGOH	NM_002370.3	GCCAACAACAGCAATTACAAGA	TTATTCTCTTCAGTTCCTCCATCAC	88
	NOVA1	NM_002515.2	TACCCAGGTACTACTGAGCGAG	CTGGTTCTGTCTTGGCCACAT	124
	PTBP1	NM_002819.4	TGGGTCGGTTCCTGCTATT	CAGATCCCCGCTTTGTAC	111
	RAVER1	NM_133452.2	GTAACCGCCGCAAGATACTG	CGAAGGCTGTCCCTTTGTATT	126
	RBM17	NM_032905.4	CAAAGAGCCAAAGGACGAAA	TACATGCGGTGGAGTGTCC	107
	RBM3	NM_006743.4	AAGCTCTTCGTGGGAGGG	TTGACAACGACCACCTCAGA	98
	RBM45	NM_152945.3	CCCATCAAGGTTTTCATTGC	TTCCCGCAGATCTTCTTCTG	123
	SFPQ	NM_005066.2	TGGTAGGGGGTGAAAGTG	TTAAAAACAAGAAATGGGGAAATG	125
	SND1	NM_014390.3	ACTACGGCAACAGAGAGGTCC	GAAGGCATACTCCGTGGCT	101
	SNW1	NM_001318844.1	ATGCGTGCCCAAGTAGAGAG	TCCCCATCCTCTTTTTCCA	134
	SRRM1	NM_001303448.1	GTAGCCCAAGAAGACGCAAA	TGGTTCTGTGACGGGGAG	108
	SRRM4	NM_194286.3	CCTTCACCACCTCCTCAC	TTCGGCACATTCCAGACA	113
	SRSF1	NM_006924.4	TGTCTCTGGACTGCCTCCA	TGCCATCTCGGTAAACATCA	98
	SRSF2	NM_003016.4	TGTCCAAGAGGGAATCCAAA	GTTTACACTGCTTGCCGATACA	113
	SRSF3	NM_003017.4	TAACCCTAGATCTCGAAATGCATC	CATAGTAGCCAAAAGCCCGTT	117
	SRSF4	NM_005626.4	GGAACTGAAGTCAATGGGAGAA	CTTCGAGAGCGAGACCTTGA	110
	SRSF5	NM_001039465.1	GCAAAAGGCACAGTAGGTCAA	TTTGCGACTACGGGAACG	92
	SRSF9	NM_003769.2	CCCTGCGTAAACTGGATGAC	AGCTGGTGCTTCTCTCAGGA	87
	SRSF10	NM_006625.5	CTACACTCGCCGTCCAAGAG	CCGTCCACAAATCCACTTTC	103
	TIA1	NM_022037.2	TAAATCCCGTGCAACAGCAGA	TATGCAGGAACTTGCCAACCA	124
	TRA2A	NM_013293.4	TCAAAGGAGGCTATGGAAAGG	TGTGTGCGCTCTCTTGGTTA	90
	TRA2B	NM_004593.2	GATGATGCCAAGGAAGCTAAAG	AGGTAGGTCTCCCCATGTAAATTC	130
Hk	ACTB	NM_001101	ACTCTTCCAGCCTTCCTTCCT	CAGTGATCTCCTTCTGCATCCT	176
	GAPDH	NM_002046	AATCCCATCACCATCTTCCA	AAATGAGCCCCAGCCTTC	122
	HPRT	NM_000194.2	CTGAGGATTTGGAAAGGGTGT	TAATCCAGCAGGTCAGCAAAG	157

Supplemental Table 1. Specific primers for human transcripts used in this study, including spliceosome components, associated splicing factors and three housekeeping genes (Hk) that were specifically designed and used in qPCR-based microfluidic assays. Official name of the genes, NCBI accession number of the transcripts, primers sequences and product sizes of the amplification products are included.

Supplemental Table 2.

Gene	Accession number	Primer sequence (Sense)	Primer sequence (Antisense)	Product size (bp)
AR-v7	NM_001348061.1	CAGGGATGACTCTGGGAAAA	TGAGGCAAGTCAGCCTTTCT	87
AR	NM_000044.4	GCAGGAAGCAGTATCCGAAG	GTTGTCAGAAATGGTCGAAGTG	112
CASP2-S	NM_001224.4	CACCTCCTTCTGTTCACTGCT	ATCCTGCGTGGTTCTTTCC	92
CASP2	NM_032982.4	AGCTGGCATATAGGTTGCAGTC	ATCCCCTCCAGAGCGAAAT	104
In1-Ghrelin	GU942497.1	TCTGGGCTTCAGTCTTCTCC	GTTCATCCTCTGCCCCTTCT	215
GHRL	NM_016362.3	CACCAGAGAGTCCAGCAGAGA	CCGGACTTCCAGTTCATC	215
sst5TMD4	NM_001172560.1	TACCTGCAACCGTCTGCC	AGCCTGGGCCTTTCTCCT	98
SSTR5	NM_001053.3	CTGGTGTTTGCGGGATGTT	GAAGCTCTGGCGGAAGTTGT	183
XBP1-S	NM_001079539.1	TGGATGCCCTGGTTGCT	CACCTGCTGCGGACTCA	87
XBP1-U	NM_005080.3	CGCAGCACTCAGACTACGTG	CTGGGTCCAAGTTGTCCAGA	147
ACTB	NM_001101	ACTCTTCCAGCCTTCCTTCCT	CAGTGATCTCCTTCTGCATCCT	176

Supplemental Table 2. Specific primers for human transcripts were specifically designed and used in RT-qPCR assays. Official name of the genes, NCBI accession number of the transcripts, primers sequences and product sizes of the amplification products are included.

Supplemental Figure 1

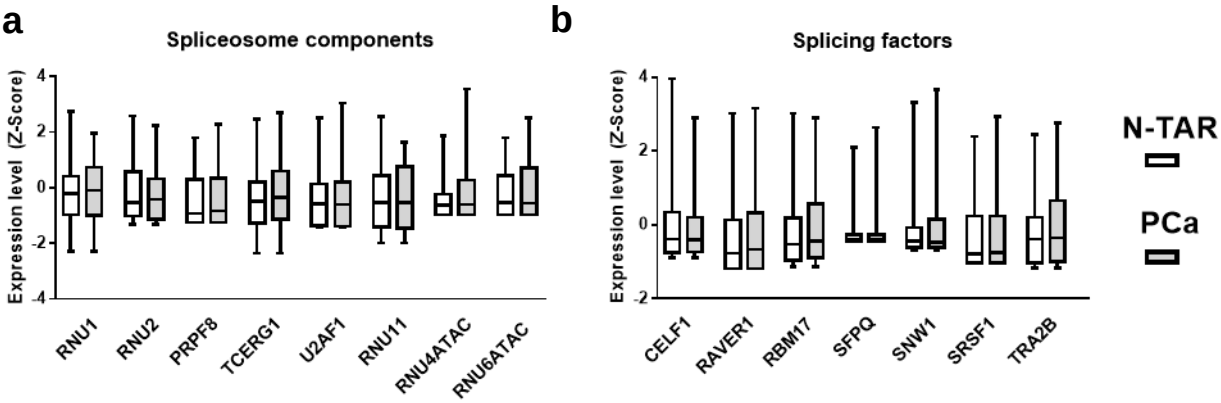

Supplemental Figure 1. Expression of spliceosome components and splicing factors in prostate cancer (PCa) samples. (a–b) Comparison of mRNA levels of spliceosome components (a) and splicing factors (b) between formalin-fixed paraffin embedded (FFPE) samples from PCa samples and non-tumor adjacent regions (N-TAR) (n = 84) determined by a microfluidic-based qPCR array. Data represent the mean ± SEM of mRNA expression levels adjusted by normalization factor (calculated from ACTB and GAPDH expression levels) and standardized by Z-score.

Supplemental Figure 2

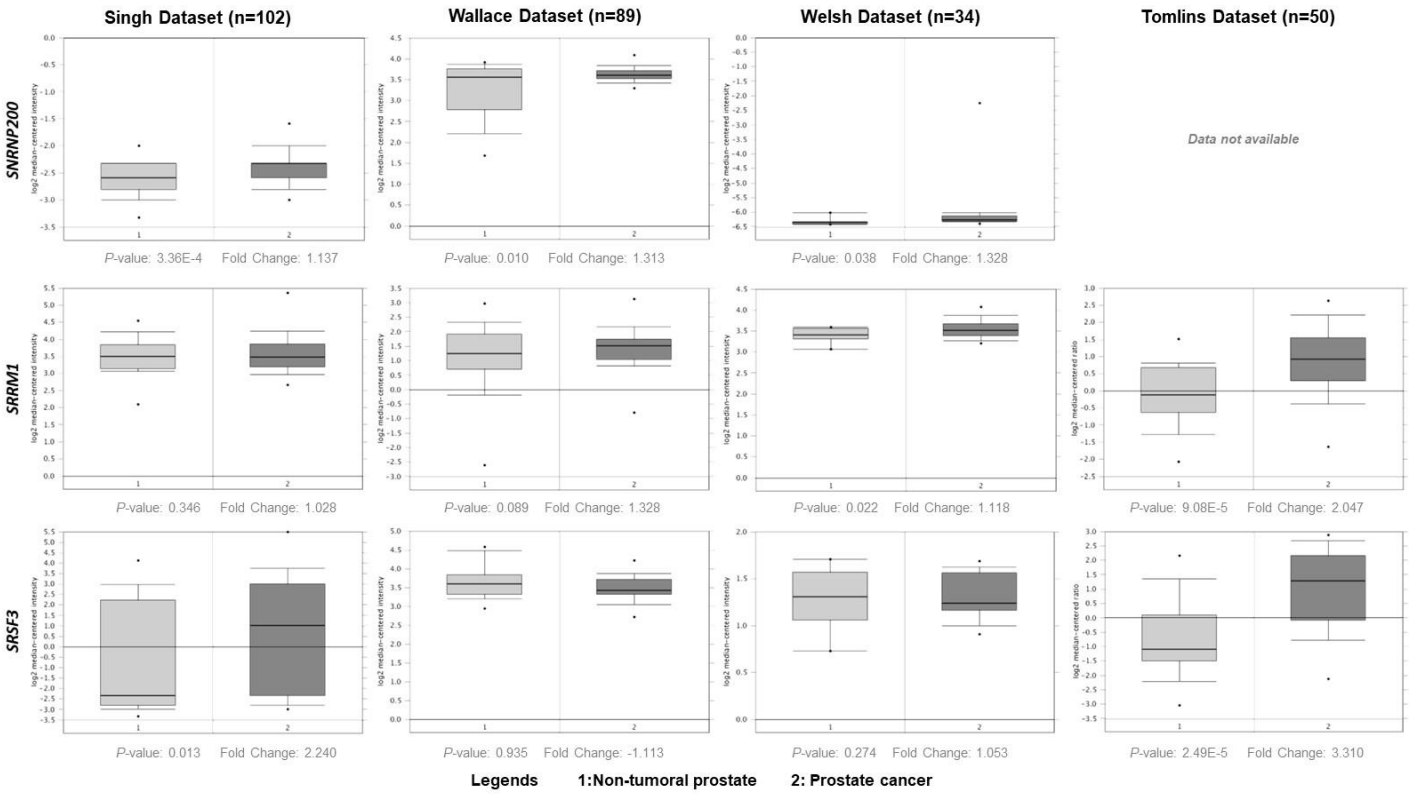

Supplemental Figure 2. Expression of *SNRNP200*, *SRRM1* and *SRSF3* in Singh, Wallace, Welsh and Tomlins Dataset (n=102, n=89, n=34 and n=50, respectively). mRNA levels of selected genes in PCa samples and non-tumour prostate tissues were available at Oncomine (ThermoFisher). Data represent the $\log_2$ median-centered intensity. P-value and fold change was indicated for each condition.

Supplemental Figure 3

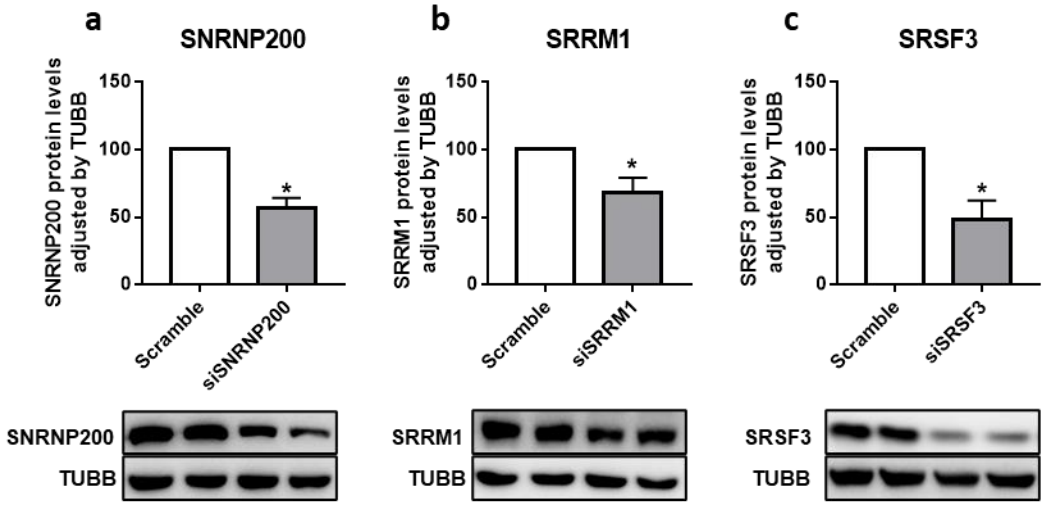

Supplemental Figure 3. **Validation of SNRNP200, SRRM1 and SRSF3 silencing**. Protein levels of SNRNP200, SRRM1 and SRSF3 after siRNA transfection (si-SNRNP200, si-SRRM1 and si-SRSF3, respectively) compared to scramble transfection (n=3). Data were normalized by β-Tubulin (TUBB) protein levels. Representative images of western blot results were located at below panel. Asterisk (* $p < 0.05$) indicates statistically significant differences between groups.

Supplemental Figure 4

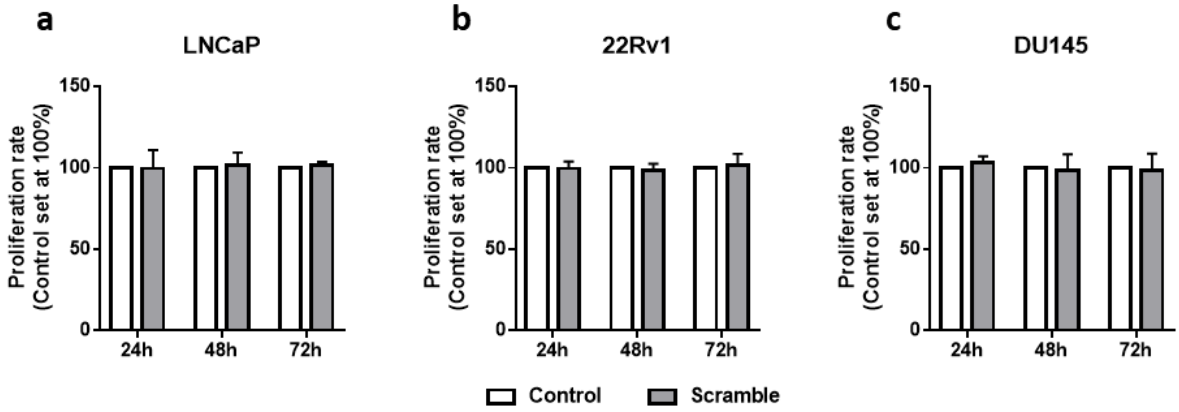

Supplemental Figure 4. Proliferation rate of LNCaP, 22Rv1 and DU145 cell lines after 24-, 48- and 72 h of transfection with scramble siRNA compared to non-transfected cells (n=3). Data were represented as percent of vehicle-treated control cells (mean ± SEM).

Article II

Title: RBM22 plays an antitumor role in prostate cancer trough splicing dysregulation and MYC inhibition.

Authors: Jiménez-Vacas JM[1,2,3,4], Montero-Hidalgo AJ[1,2,3,4], Gómez-Gómez E[1,3,5], Herrero-Aguayo V[1,2,3,4], Fuentes-Fayos AC[1,2,3,4], Saéz-Martínez P[1,2,3,4], León-González A[1,2,3,4], Sánchez-Sánchez R[1,3,6], González-Serrano T[1,3,6], Requena-Tapia MJ[1,3,5], Castaño JP[1,2,3,4], Gahete MD[1,2,3,4], Luque RM[1,2,3,4].

Affiliations: [1]Maimonides Institute for Biomedical Research of Córdoba (IMIBIC), Cordoba, Spain; [2]Department of Cell Biology, Physiology, and Immunology, University of Córdoba, Cordoba, Spain; [3]Hospital Universitario Reina Sofía (HURS), Cordoba, Spain; [4]Centro de Investigación Biomédica en Red de Fisiopatología de la Obesidad y Nutrición, (CIBERobn), Cordoba, Spain; [5]Urology Service, HURS/IMIBIC, Cordoba, Spain; [6]Anatomical Pathology Service, HURS, Cordoba, Spain.

Keywords: RBM22, spliceosome, splicing, prostate cancer, MYC, MYCN, E2F.

Corresponding Author: Raúl M. Luque. Department of Cell Biology, Physiology and Immunology, University of Cordoba; Maimonides Institute of Biomedical Research of Cordoba (IMIBIC), Menéndez Pidal s/n, first floor; E-14004 Cordoba, Spain. Email: raul.luque@uco.es

Disclosure Statement: The authors have nothing to disclose.

Acknowledgements: This research was funded by Instituto de Salud Carlos III, co-funded by European Union (ERDF/ESF, "Investing in your future") [PI16/00264, PI17/02287, CD16/00092], MINECO/MECD (PID2019-105564RB-I00, FPU16/06190, FPU17/00263, FPU18/02485, BFU2016-80360-R), Junta de Andalucia (BIO-0139), and CIBERobn. Elena M Yubero-Serrano was the recipient of the Nicolas Monardes Programme from the "Servicio Andaluz de Salud, Junta de Andalucia", Spain (C1-0005-2019). CIBER is an initiative of Instituto de Salud Carlos III, Ministerio de Sanidad, Servicios Sociales e Igualdad, Spain.

Abstract

Prostate cancer (PCa) is one the leading causes of cancer-related deaths among men in developed countries. Therefore, identification of novel molecular and therapeutic approaches to tackle this pathology are urgently needed. In this scenario, our group have recently reported that elements of the cellular machinery controlling alternative splicing processes might be used as potential novel therapeutic tools against PCa and castration-resistant PCa (CRPC). In this context, RBM22 has been identified as a key spliceosome component, playing a crucial role for normal development; however, the potential dysregulation and functional role of RBM22 in cancer still remain unknown. Here, we identify for the first time a profound downregulation of RBM22 (at mRNA/protein-levels) in two well-characterized cohorts of PCa patients, compared to non-tumor control samples, which was inversely associated to key clinical aggressiveness features (i.e. extraprostatic extension and perineural invasion). Results were confirmed in two additional, independent *in silico* human cohorts. Overexpression of RBM22 in PCa cells decreased aggressiveness parameters *in vitro* (e.g. proliferation, migration, tumorsphere- and colony-formation, etc.), and drastically decreased tumor development and progression *in vivo* (using a preclinical mouse model), which would underlie a relevant direct association of lower RBM22 levels with enhanced tumor progression. This was corroborated using the TRAMP model, wherein gradual reduction of RBM22 from PIN to moderately differentiated PCa and to poorly differentiated PCa was observed. These actions are likely mediated through the modulation of key signaling pathways (i.e. cycle-apoptosis, PI3K pathways, etc) and critical molecular regulators (i.e. MYC, MCYN and E2F), and may involve the alteration of alternative splicing events of key genes involved in these pathways. Therefore, our study demonstrates that RBM22 plays a critical functional role in the pathophysiology of PCa and invites to suggest that the targeting of RBM22 expression/activity could represent a novel potential therapeutic tool to tackle this devastating pathology.

Introduction

Prostate cancer (PCa) is the most diagnosed tumor pathology and remains one the leading causes of cancer-related deaths among men in developed countries (1). Although PCa might represent a slow-growing disease, it can also arise as or evolve to an aggressive form, called castration-resistant PCa (CRPC) (2). Thus, despite the advances achieved in the therapy of PCa during the last years (3, 4), CRPC remains a lethal disease and, therefore, additional molecular and therapeutic approaches to tackle this pathology are urgently needed.

In this scenario, due to the key role that aberrantly produced or dysregulated alternative splicing variants [AR-v7 (5), XBP1s (6), sst5TMD4 (7), In1-ghrelin (8)] play in PCa/CRPC development and/or progression, the elements regulating this process [i.e. spliceosome components (SCs) and splicing factors (SFs)] have become a focus of interest in PCa field (9). Indeed, recent data from our group and others have suggested many SCs and SFs (e.g. SNRNP200, SRRM1, SRSF3, SF3B1, ESRP2) as potential therapeutic targets that could be used for the development of novel therapeutic tools against PCa and CRPC (10-12). Specifically, several members of the RNA binding motif (RBM) family have been found to be dysregulated in PCa and to play either an oncogenic or antitumor role in this pathology, including RBM3, RBM5, NONO and PSF/SFPQ (13-16). Among these RBM family members, RBM22 plays a crucial role in the activation of the spliceosome (17), through the interaction with U6 internal stem-loop, regions of U6 and the pre-mRNA intron (18). In addition, RBM22 has been demonstrated that is required for normal development (19), a biological process tightly linked to tumorigenesis (20). Likewise, calcium signalling, a molecular pathway related to several cancer types, including PCa, has been found to be altered in response to RBM22 presence (21, 22). Therefore, all these data may suggest that RBM22 might be a relevant component of the splicing process with a key role in cancer biology, including PCa. However, the potential dysregulation and functional role of RBM22 in PCa (nor any others tumor pathologies) still remain unknown. Consequently, in this study we aim to determine the levels of RBM22, as well as its functional and molecular actions, in PCa, in order to define RBM22 as a potential diagnostic and/or prognostic biomarker and/or therapeutic target of this disease.

Materials and methods

Patients and samples

This study was approved by the Reina Sofia University Hospital Ethics Committee and was conducted in accordance with the principles of the Declaration of Helsinki. The regional Biobank coordinated the collection, processing, management and assignment of the biological samples used in the present study according to the standard procedures established for this purpose. Written informed consent was obtained from all patients. Two different cohorts of prostate samples previously described (11, 23) were analysed:

- **Cohort 1**) formalin-fixed, paraffin-embedded (FFPE) PCa tissues (n=84) and their non-tumor adjacent region (N-TAR; used as control tissues; n=84), taken from radical prostatectomies from patients diagnosed with clinically localized PCa (Table 1).
- **Cohort 2**) fresh samples that were obtained: i) by core needle biopsies from patients with suspect of significant PCa (n=42); and ii) from non-tumor prostates taken from patients who underwent cystoprostatectomy (n=9) (Table 2). The presence or the absence of tumor was histologically confirmed by expert uro-pathologists.

The clinical parameters collected from each patient were Gleason Score (GS; analysed by uro-pathologists following the modified 2014 ISUP criteria), T-Stage, perineural invasion, lymphovascular invasion and presence of metastases at diagnose (determined by computed tomography and bone scan). In addition, gene expression and clinical data of interest from two *in silico* available cohorts (i.e. TCGA and Lapointe) were downloaded from cBioPortal and GEO datasets, respectively (24-27).

Cell lines

Cell lines derived from normal prostate (RWPE-1) and PCa (LNCaP, 22Rv1, DU145 and PC-3) were obtained from the American Type Culture Collection (Manassas, VA, USA) and cultured in a humidified incubator with 5% CO_2 at 37 °C according to manufacturer

instructions, as previously described (7, 8, 10). Analyses of short tandem repeats sequences (STRs) were performed to validate these cell lines by using GenePrint 10 System (Promega, Barcelona, Spain), and the absence of mycoplasma was confirmed by PCR as previously reported (7, 8, 10).

RNA-isolation, retrotranscription and real-time qPCR

RNA from FFPE samples, fresh tissues and cell-lines was isolated as previously reported (28-30). Briefly, Maxwell 16 LEVRNA FFPE Kit (Promega, Madison, USA) was used in the Maxwell MDx 16 Instrument (Promega, Madrid, Spain) to isolate RNA from FFPE samples. Additionally, AllPrep DNA/RNA/Protein Mini Kit (Qiagen) and TRIzol Reagent (Thermo Fisher Scientific, Waltham, MA, USA) were used to isolate RNA from fresh tissues and PCa cell lines, respectively. RNA from fresh tissues and PCa cell lines was then DNase-treated using RNase-Free DNase Kit (Qiagen). Total RNA concentration and purity was assessed using Nanodrop One Spectrophotometer (Thermo Fisher Scientific, Madrid, Spain). Total RNA was retrotranscribed using random hexamer primers and the cDNA First Strand Synthesis kit (Thermo Scientific). Details regarding the development, validation, and application of the quantitative real-time PCR to measure the expression levels of the transcripts of interest have been previously reported by our laboratory (28-30). Specifically, the following primers were used to measure the expression levels of human genes [*RBM22* (Sense: CTCTGGGTTCCAACACCTACA; Antisense: GGCACAGATTTTGCATTCCT), *ACTB* (Sense: ACTCTTCCAGCCTTCCTTCCT; Antisense: CAGTGATCTCCTTCTGCATCCT) and *GAPDH* (Sense: AATCCCATCACCATCTTCCA; Antisense: AAATGAGCCCCAGCCTTC] and mouse genes [Rbm22 (Sense: TGTCTGATCCCTTCCCACTC; Antisense: CCGCCCAAAAAGATACAAAA), *Ciclophylin* (Sense: TGGTCTTTGGGAAGGTGAAAG; Antisense: TGTCCACAGTCGGAAATGGT). A normalization factor [calculated with *ACTB* and *GAPDH* expression levels, using GeNorm 3.3 (31)] and *Ciclophylin* expression levels were used to adjust mRNA expression levels of the human and mouse RBM22 genes, respectively,

wherein the expression levels of the housekeeping genes were stable among experimental conditions (data not shown).

Immunohistochemistry

Immunohistochemistry (IHC) analysis was performed on fresh prostate samples that were obtained by core needle biopsies from patients of cohort 2. Moreover, additional samples of benign prostatic hyperplasia (BPH), prostatic intraepithelial neoplasia (PIN) and non-significant PCa with GS=6 (n=7, 6 and 5, respectively) were also taken by core needle biopsies to be used in this analysis as control samples and low aggressive PCa, respectively. The IHC protocol followed in this study was previously described (10). Briefly, deparaffinized sections were incubated overnight (4°C) with the anti-RBM22 antibody (ab59157, Abcam Camdridge,UK) at 1:250 dilution, followed by incubation with an anti-rabbit horseradish peroxidase–conjugated secondary antibody (#7074; Cell Signalling). Finally, sections were developed with 3,39-diaminobenzidine (Envision system 2-Kit Solution DAB) and contrasted with haematoxylin. Two independent pathologists performed histopathologic analyses indicating low, moderate, and high intensities of staining, following a blinded protocol.

Stable transfection of RBM22

LNCaP and PC-3 cell lines were stably transfected as previously reported (7, 8). Specifically, cells were transfected with 1μg of RBM22 plasmid (OHu02939, GenScript) using Lipofectamine-2000 (Gibco, Barcelona, Spain) following manufacturer's instructions, and selected by addition of geneticin at 1% (Gibco).

Cell proliferation

Cell proliferation was assessed by alamar-blue assay (Bio-Source International, Camarillo, CA, USA) as previously reported (7, 8, 10), in response to *RBM22* overexpression in LNCaP and PC-3. Briefly, 3000 cells per well were seeded in 96-well plates, serum-starved overnight, and then fluorescence (540 nm excitation and 590 nm emission) was measured (after 3h incubation with 10% resazurin) at 24, 48 and 72 h using the FlexStation III system (Molecular Devices, Sunnyvale, CA, USA).

Cell migration

Cell migration was evaluated in PC-3, given its high invasiveness nature (32). Specifically, 500.000 cells were seeded in 12-well plates. Then, when confluence was reached, a wound was made in each well with a 100uL tip and images of the scratch were taken at 0 and after 12 h. Wound healing was calculated as the area observed 12 h after the wound was made vs. the area observed just after wounding.

Tumorspheres formation assay

Tumorsphere formation assay was carried out in LNCaP and PC-3 in response to RBM22 overexpression, as previously reported (11, 33). Briefly, 2000 cells/well were seeded in Corning Costar 24-well ultra-low attachment plates (Merck, Madrid, Spain) with DMEM F-12 medium supplemented with 20 ng/mL EGF (Sigma-Aldrich, Madrid, Spain). The number of tumorspheres was determined after 14 days of incubation with ImageJ software.

Colony formation assay

To determine the clonogenic capacity of LNCaP and PC-3 cells in response to RBM22 overexpression, 2,000 cells were seeded into 6-well plates. Then, the medium was removed, the

colonies washed with PBS and stained with crystal violet for 30 min and air-dried. The number of individual colonies and the percent of area covered with colonies by colony area were determined by ImageJ software (colony area plugin).

RNA sequencing (RNAseq) in RBM22-overexpressing PCa cells

RNA integrity of total RNA (500ng) from RBM22-overexpressing PC-3 cells (n=3) and mock PC-3 cells (n=3) was assessed using the Agilent 2100 Bioanalyzer. RNAseq was performed at the Genomics Core Unit of The National Centre for Cancer Research (CNIO), Madrid, Spain. Briefly, PolyA+ fraction was purified and randomly fragmented, converted to double stranded cDNA and processed through subsequent enzymatic treatments of end-repair, dA-tailing, and ligation to adapters (NEBNext Ultra II Directional RNA Library Prep Kit for Illumina, NEB #E7760) as recommended by the kit manufacturer. This kit generates directional libraries stranded in the antisense orientation [the read1 (the only read in single read format) has the antisense orientation]. Adapter-ligated library was completed by PCR with Illumina PE primers. The resulting purified cDNA libraries, with an average size of 400bp, were applied to an Illumina flow cell for cluster generation and sequenced on an Illumina instrument following manufacturer's protocols. Image analysis, per-cycle basecalling and quality score assignment was performed with Illumina HiSeq Control Software. Conversion of BCL files to FASTQ format was performed with the bcl2fastq Software (Illumina). Differentially expressed genes (DEGs) were analysed using SALMON method (34). Alternative splicing events and variants were analysed using SUPPA2 method (35). *In silico a*vailable data from a CLIP-seq analysis in response to *RBM22* depletion were used to determine the SVs potentially regulated by direct interaction with RBM22 (36). Hallmark gene sets (37) were evaluated in patients with high RBM22 expression (first quartile vs. other quartiles) from TCGA and Lapointe datasets, using single-sample Gene Set Enrichment Analysis Projection from GenePattern (38).

nCOUNTER analysis

nCounter PanCancer Pathways Panel kit (GXA-PATH1-12; NanoString Technologies) was used and performed at the Laboratory of Genetics at UCAIB (IMIBIC) as previously described (39). Briefly, the quality of all samples [RBM22-overexpressing PC-3 cells (n=3) and mock PC-3 cells (n=3)] was analysed using the Agilent 2100 Bioanalyzer. Then, 100 ng of RNA from all the samples were loaded in the nCounter PanCancer Pathways Panel kit and the experiment was run in the nCounter Analisys System (NanoString Technologies), following manufacturer's protocol. The data were analysed using the nSolverAnalysisSoftware 3.0.22 from NanoStringTechnologies. Data were normalised using 40 genes as housekeeping genes as previously described (39). All specific target sequences and panel details are available on the manufacture's webpage.

Preclinical models of PCa

Experiments with mice were carried out according to the European Regulations for Animal Care under the approval of the university/regional government research ethics committees. For tumor growth experiments, ten-week-old male athymic BALB/cAnNRj-Foxn1nu mice (Janvier Labs, Le Genest-Saint-Isle, France) were subcutaneously grafted in both flanks with $3x10^6$ mock-transfected (n=5 mice;10 tumors) or RBM22-stably transfected PC-3 cells (n=5 mice; n=10 tumors) that were resuspended in 100 ml of basement membrane extract (Trevigen, Gaithersburg, MD, USA). Tumor growth was monitored once per week for two months using a digital caliper. After euthanization of mice, each tumor was kept at -80°C for later RNA extraction by using Trizol reagent (Thermo Fisher Scientific) or protein extraction using SDS-DTT buffer as previously reported (7, 8).

Additionally, in order to determine the expression of RBM22 during PCa progression, we used the transgenic adenocarcinoma of mouse prostate (TRAMP) mice, heterozygous for the PB-Tag transgene, maintained in a C57BL/6 background and crossed with non-transgenic FVB

mice to obtain transgenic [C57BL/6 × FVB] F1 males. TRAMP mice genotype was validated by PCR screening using primers recommended by The Jackson Laboratory (Sense: TACAACTGCCAACTGGGATG; Antisense: CAGGCACTCCTTTCAAGACC). Mice were sacrificed at 13, 21, and 30 weeks of age, when it has been demonstrated that these mice develop PIN, moderately differentiated PCa and poorly differentiated PCa, respectively (40). Prostate tissues were stored at −80°C and used for gene expression and protein analysis.

Statistical analysis

All the experiments were performed in at least 3 independent experiments ($n \geq 3$). Statistical differences between two variables were calculated by unpaired parametric t-test and nonparametric Mann Whitney U test, according to normality, assessed by Kolmogorov-Smirnov test. For differences among three variables, One-Way ANOVA analysis was performed. Statistical significance was considered when $p<0.05$. A trend for significance was indicated when P values ranged between >0.05 and <0.1. All the analyses were assessed using GraphPad Prism 8 (GraphPad Software, La Jolla, CA, USA).

Results

RBM22 is downregulated in PCa and associated to clinical features of aggressiveness

Expression levels of *RBM22* were significantly lower in PCa tissues compared to non-tumor prostate tissues in two independent, retrospective cohorts of samples (PCa prostatectomies vs. N-TAR, and positive biopsies vs. non-tumor prostates, respectively; Figure 1a). Consistently, the downregulation of *RBM22* in PCa samples compared to non-tumor tissues was also observed in two independent cohorts of patients available *in silico* (Lapointe and TCGA datasets; Figure 1b). To explore the potential association between *RBM22* expression levels and key clinical/molecular features of PCa aggressiveness, we further interrogated biopsy samples (the most aggressive cohort analysed herein) and found that tumors with extraprostatic extension as well as those with perineural invasion capacity were associated to lower levels of *RBM22* (Figure 1c). Moreover, the expression levels of RBM22 tended to be inversely correlated to those of *KLK3* and *PCA3* in the biopsies cohort (Figure 1d). On the other hand, neither statistically significant correlations nor associations were found between RBM22 expression levels and Gleason score, plasma PSA levels, age or presence of metastasis (Supplemental Figure 1a-b). Likewise, RBM22 expression levels were not significantly correlated to those of AR, AR-v7 or MKI67 (Supplemental Figure 1c).

Complementary, the TRAMP mouse model was used to determine the expression levels of RBM22 during PCa progression (from PIN to poorly differentiated PCa; Figure 1e). Interestingly, *RBM22* expression levels were significantly lower in moderately differentiated PCa and poorly differentiated PCa samples compared to PIN samples (Figure 1f).

Protein levels of RBM22 are altered in PCa and associated to tumor aggressiveness.

To examine the protein levels of RBM22 in healthy, non-tumor but pathological, and tumor prostate tissues, IHC analysis were performed in FFPE samples from the biopsies cohort as well as from an additional set of samples (i.e. PIN, BPH and GS6 PCa samples). First, the results showed that RBM22-staining was exclusively detected in the nucleus of the cells, and that this RBM22 nuclear staining was significantly lower in PCa samples compared to non-tumor and BPH tissues (Figures 2a-b). In addition, RBM22 nuclear staining was significantly lower in PCa samples with GS $\geq$ 7 compared to those with GS 6 (Figures 2c and 2e). Moreover, RBM22 staining tended (p = 0.082) to be lower in primary PCa samples from patients with metastasis compared with those from patients without metastasis (Figures 2d-e).

Consistently, a progressive decrease in RBM22 protein levels was observed when comparing PIN, moderately differentiated PCa, and poorly differentiated PCa samples from TRAMP mice (Figure 2f-g).

Overexpression of RBM22 reduced relevant functional parameters of PCa aggressiveness in vitro

Similar to that previously found in PCa tissues, expression levels of *RBM22* were significantly lower in all the PCa cell lines analysed herein (LNCaP, 22Rv1, PC-3 and DU145) compared to the normal-like prostate cell line (RWPE-1) (Figure 3a). To test the functional role of RBM22 in PCa cells, LNCaP and PC-3 cell lines were used as representative models of hormone-sensitive and hormone-refractory PCa. Specifically, PCa cells were stably transfected with RBM22-overexpression plasmid (Supplemental Figure 2a-b) which resulted in a significantly decreased in proliferation rate at 48- and 72-h (Figure 3b). Likewise, RBM22-overexpressing LNCaP and PC-3 cells generated less and smaller colonies than mock-transfected control cells (Figure 3c-d). Moreover, the number of tumorspheres was also significantly decreased in response to *RBM22* overexpression (Figure 3e). Finally, RBM22-overexpressing PC-3 cells showed a lower migration capacity compared to mock-transfected PC-3 cells after 12 h of incubation (Figure 3f).

RBM22 overexpression induces the dysregulation of the splicing process

To unveil the molecular mechanisms underlying the antitumor role of RBM22 in PCa cells, an RNAseq was performed in RBM22-overexpressing and mock-transfected PC-3 cells. Since it has been reported that the main known function of RBM22 is to control splicing process, we first focused on the potential splicing dysregulation in response to RBM22-overexpression. We found that 856 genes underwent an altered splicing process in RBM22-overexpressing as compared to mock-transfected PC-3 cells (Supplemental Table 1). Specifically, an increase of exon skipping and decrease of alternative last exon were the most dysregulated splicing events observed in response to *RBM22* overexpression (Figure 4a). We then took advantage of an available CLIP-seq dataset of RBM22-silenced HepG2 cells (36) and found that RBM22 protein can physically bind to the pre-RNA of 8002 genes. Among those genes, 358 genes (of the 856 previously found that underwent an altered splicing process in RBM22-overexpressing) showed a dysregulated splicing pattern (based on the alteration of the expression of, at least, one splicing variant) in response to RBM22 overexpression (Figure 4b). Among these 358 genes producing splicing variants potentially altered by the direct actions of RBM22, STRING analysis showed an enrichment of genes involved in key pathophysiologic cellular processes

such as splicing (cluster-1:orange), translation (cluster-2:pale blue), mitochondrial translation (cluster-3: purple), ubiquitination and proteasome-dependent degradation (cluster-4: dark blue), transcription (cluster-5:light green), scaffolding (cluster-6: dark green) and vesicle trafficking (cluster-7: emerald green) (Figure 4c).

Overexpression of RBM22 drastically reduced tumor growth in vivo by the modulation of critical molecular/signaling *pathways in PCa*

To validate the RBM22 antitumor actions *in vivo*, the growth of xenograft tumors generated by RBM22-overexpressing and mock-transfected PC-3 cells (Figure 5a) was monitored. Specifically, RBM22-overexpressing tumors showed a dramatic slower growth than mock-tumors (Figure 5b). Consistently, overexpression of RBM22 *in vivo* resulted in smaller tumors as compared to mock-cells induced tumors (Figure 5c-d).

Mechanistically, overexpression of RBM22 *in vivo* resulted in an alteration in the expression of 154 out of 770 genes analysed with the nCounter PanCancer Pathways Panel kit compared to mock-transfected tumors (Figure 5e). Specifically, cell cycle-apoptosis pathway was the most altered signaling pathway (i.e. 44 genes: 20 upregulated/24 downregulated; Figure 5f), followed by the PI3K pathway (i.e. 36 genes: 26 upregulated/10 downregulated; Figure 5f). Additionally, other key signaling pathways were also altered (e.g. Driver gene, MAPK, Ras, Transcription misregulation, Wnt, JAK-STAT, etc.; Figure 5f). Finally, PPI (Protein-Protein Interaction) functional association analysis, carried out using Network Analyst software, pointed out MYC as a potential hub gene in response to RBM22 overexpression (Figure 5g).

Overexpression of RBM22 leads to a major dysregulation of oncogenic molecular pathways in PCa cells

To further explore the mechanistic changes potentially driving RBM22 antitumor actions, we used the RNAseq performed in RBM22-overexpressing and mock-transfected PC-3 cells and analysed the data using IPA software. Specifically, the expression levels of 5466 were found to be dysregulated (p-value < 0.05 and FC ≥ 0.5) in response to RBM22 overexpression in PC-3 cells (Figure 6a). Additionally, IPA upstream regulator analysis pointed out MYCN, MYC and E2F-family, critical oncogenic genes frequently overexpressed in aggressive forms of PCa and other tumors, as three of the five most altered RBM22 ‘upstream regulator' in response to *RBM22* overexpression (Figure 6b), suggesting that MYCN, MYC and E2F-family proteins might be key mediators of RBM22-antitumor effects. Moreover, analysis using the IPA software indicated that these three elements (MYCN, MYC and E2F) are functionally related (Figure 6c). Reinforcing this hypothesis, RBM22-induced gene expression profile was

associated with ‘E2F targets”, “MYC-targets” hallmarks in TCGA and Lapointe datasets (Figure 6d).

Discussion

Given the oncogenic role that several splicing variants play in a variety of tumor pathologies, the dysregulation of the alternative splicing process has arisen as a novel hallmark of cancer (41, 42). In the case of PCa, the alteration of the expression of alternative, as well as the generation of aberrant, splicing variants have pave the way to study the potential dysregulation of regulatory elements of the splicing process (9). In this sense, we and others have reported that the levels of a number of spliceosome components (SCs) and splicing factors (SFs) are dysregulated in PCa, associated to relevant clinical parameters and implicated in the modulation of critical functional features of tumor aggressiveness, thus representing attractive therapeutic targets for this disease (9-11). However, the splicing process is controlled by more than 350 SCs and SFs, and the implication of many of them in cancer has not been yet explored. In this scenario, although RBM22 is a SC that plays a crucial role in the activation of the spliceosome and in embryo development (17, 19), its role in cancer is still completely unknown. In this study, we demonstrate for the first time that *RBM22* expression is significantly downregulated in PCa (using 4 independent cohorts of patients), and that its mRNA levels are inversely associated to key clinical parameters of PCa aggressiveness (i.e. extraprostatic extension and perineural invasion). Remarkably, these results were corroborated and even more evident and pronounced at protein level, inasmuch as aggressive PCa samples (i.e. tumors with high Gleason score from patients with metastasis at diagnosis) showed dramatically low protein levels of nucleic RBM22. Indeed, although RBM22 can shuttle between the nucleus and the cytoplasm in response to cellular stress conditions, wherein it can be partially involved in different processes such as calcium signalling (21, 22), in the case of PCa cells, RBM22 was principally located at nucleic level, thus suggesting that the potential role of this SF in PCa may be related to its function as a key regulator of the splicing process (17). Consistently, mRNA and protein levels of RBM22 were found to be gradually reduced from PIN to poorly differentiated PCa samples taken from the TRAMP mice model, thus supporting the novel link between RBM22 and PCa aggressiveness.

Further studies to investigate the direct potential role of RBM22 in PCa demonstrated a pronounced decrease of several functional parameters of PCa aggressiveness (i.e. proliferation, migration, number and area of colonies as well as number of tumorspheres) in response to RBM22 overexpression in PCa-derived cells,

thus suggesting a potential tumor suppressor role of RBM22 in PCa. Consistently, the antitumor actions of RBM22 were also observed *in vivo*, in that tumor growth of xenografted RBM22-overexpressing tumors was dramatically slower than mock-transfected control tumors. These results are consistent with previously reported studies demonstrating the antitumor role of other SCs and SFs belonging to the RBM family [e.g. *RBM3*, *RBM5*, *RBM25*] (13, 14, 43). In fact, it has been previously proposed that the RBM family could serve as a potential source of anti-apoptotic proteins (44), but to the best of our knowledge, this is the first report identifying a relevant tumor-associated role for RBM22 in cancer.

According to a pivotal role of RBM22 in the activation of the spliceosome (17), this study demonstrates that RBM22 modulation in PCa cells triggers a profound alteration of the splicing pattern of hundreds of genes (i.e. 856), being "exon skipping" and "alternative last exon" the most common splicing events altered in response to RBM22 overexpression. Interestingly, analysis of available Clip-seq data [performed in HepG2 cells in response to RBM22 knockdown (36)] revealed that RBM22 can physically bind to the pre-mRNA of 358 of those genes identified in the RNAseq, suggesting that RBM22 can directly regulate the splicing of certain genes by binding their nascent mRNA, while the splicing process of many other genes can be indirectly influenced by altering the spliceosome function or the expression/activity of other SCs and SFs. Indeed, enrichment analysis performed with those genes whose splicing pattern is directly altered in response to RBM22 overexpression revealed that the most dysregulated pathways are spliceosome, translation, mitochondrial translation, ubiquitination, proteasome-dependent degradation and transcription pathways, all of which are pathophysiological events strongly associated to PCa development and progression (9, 45-49). Although further studies would be necessary before a precise and unequivocal conclusion can be reached in this regard, these results suggest that RBM22 could play its antitumor role through the direct or indirect regulation of the splicing of key genes involved in these pathways and/or processes.

Remarkably, several pieces of evidence included in this work also indicate that MYC may be a hub gene in the molecular/functional response observed in response to RBM22 modulation in PCa cells. Firstly, a more directed analysis of the expression of 713 genes related to cancer (nCounter® PanCancer Pathway) in RBM22-overexpressing and mock-transfected xenograft tumors pointed out MYC as a central

regulator of the functional alterations observed in response to RBM22 overexpression. Secondly, IPA analysis of upstream regulators of the DEGs observed in RBM22-overexpressing PC-3 cells estimated that the activity of MYC, as well as other upstream regulators critically involved in PCa progression [such as MYCN, E2F (50, 51)], was pronouncedly inhibited in response to RBM22 overexpression. Third, the relationship of RBM22 with MYC, MYCN and E2F activity was also validated in PCa patients (from TCGA and Lapointe cohorts), inasmuch as PCa samples with high expression levels of *RBM22* showed an enrichment of c-MYC, MYCN and E2F target genes. And finally, other members of the RBM family such as RBM25 (another RBM protein that enhances U1 snRNP recruitment, as RBM22) has been reported to exert antitumor actions trough the decrease of MYC signalling (43). Importantly, MYC overexpression and the amplification of the chromosomal region that encodes MYC (8q24) are common alterations of PCa (52, 53). MYC promotes oncogenic signaling in PCa (54, 55) through multiple mechanisms including the activation of the ribosomal RNA synthesis (56-58) or the coordination of cell-metabolism [e.g. glucolysis, oxidative phosphorylation, fatty acid metabolism (59)] among others. On the other hand, MYCN exclusively arise with CRPC [the most aggressive PCa phenotype, which remains lethal and is characterized by the lack of response to hormonal therapy (3)], being commonly overexpressed (up to 40%) in CRPC samples with neuroendocrine features (60, 61). Finally, E2F-proteins comprise a complex pleiotropic family (62). As an example, in advanced PCa, when RB1 is phosphorylated or lost [a common CRPC feature (63, 64)] E2F1 dissociates from RB1, and consequently triggers the transcription of its target genes, regulating several cell processes involved in tumor development and progression (apoptosis, cell migration, invasion, and metabolism as well as cell cycle, among others) (65, 66). For that reason, targeting MYC, MYCN and E2F proteins has become focus of interest in the oncology field to tackle several tumor types driven by MYC, MYCN and RB, including PCa/CRPC. Unfortunately, despite the progress achieved during the last years, substantial structural and functional challenges still remain which have hampered a direct MYC/MYCN-targeted drug development and pan-inhibition of E2Fs (67, 68). In this scenario, although it is still to be fully defined if RMB22 can control MYC, MYCN and EF2 activity through the modulation of the splicing of key genes or vice versa, these results pave the way to further study RBM22 in order to develop novel approaches able to target MYC, MCYN and E2F activity and tackle MYC, MYCN and EF2/RB driven tumors, including PCa/CRPC.

Taken together, our results unveiled new conceptual and functional avenues in PCa/CRPC, with potential therapeutic implications, by demonstrating for the first time a drastic down-regulation of RBM22 in PCa. This is likely relevant clinically, because RBM22 expression directly associates to key aggressiveness features of PCa (i.e. extraprostatic extension and perineural invasion), and its *in vitro* and *in vivo* modulation significantly decreased critical pathophysiological processes of PCa cells (i.e. tumor growth, cell proliferation, migration as well as tumorsphere and colonies formation), which would underlie a relevant direct association of lower RBM22 levels with enhanced tumor progression, as was directly corroborated using the TRAMP model (i.e. gradual down-regulation of RBM22 expression from PIN to moderately differentiated PCa and to poorly differentiated PCa). These actions are likely mediated through the modulation of key signaling pathways (i.e. cycle-apoptosis, PI3K pathways, etc.) and critical molecular regulators (i.e. MYC, MCYN and E2F), and may probably involve the alteration of alternative splicing events of key genes involved in these pathways. Therefore, our study provides solid, convincing evidence demonstrating that RBM22 has a critical functional role in the pathophysiology of PCa, and invites to suggest that the development and use of drugs targeting RBM22 expression could represent a potential therapeutic tool for PCa patients, offering a clinical relevant opportunity that should be soon tested for their use in humans.

References

1. Bray F, Ferlay J, Soerjomataram I, Siegel RL, Torre LA, Jemal A. Global cancer statistics 2018: GLOBOCAN estimates of incidence and mortality worldwide for 36 cancers in 185 countries. CA: a cancer journal for clinicians. 2018;68(6):394-424.
2. Tolkach Y, Kristiansen G. The Heterogeneity of Prostate Cancer: A Practical Approach. Pathobiology : journal of immunopathology, molecular and cellular biology. 2018;85(1-2):108-16.
3. Sartor O, de Bono JS. Metastatic Prostate Cancer. The New England journal of medicine. 2018;378(7):645-57.
4. Bryce AH, Sartor O, de Bono J. DNA Repair and Prostate Cancer: A Field Ripe for Harvest. European urology. 2020.
5. Cato L, de Tribolet-Hardy J, Lee I, Rottenberg JT, Coleman I, Melchers D, et al. ARv7 Represses Tumor-Suppressor Genes in Castration-Resistant Prostate Cancer. Cancer cell. 2019;35(3):401-13.e6.
6. Sheng X, Nenseth HZ, Qu S, Kuzu OF, Frahnow T, Simon L, et al. IRE1α-XBP1s pathway promotes prostate cancer by activating c-MYC signaling. Nature Communications. 2019;10(1):323.
7. Hormaechea-Agulla D, Jimenez-Vacas JM, Gomez-Gomez E, F LL, Carrasco-Valiente J, Valero-Rosa J, et al. The oncogenic role of the spliced somatostatin receptor sst5TMD4 variant in prostate cancer. Faseb j. 2017;31(11):4682-96.
8. Hormaechea-Agulla D, Gahete MD, Jimenez-Vacas JM, Gomez-Gomez E, Ibanez-Costa A, F LL, et al. The oncogenic role of the In1-ghrelin splicing variant in prostate cancer aggressiveness. Mol Cancer. 2017;16(1):146.
9. Paschalis A, Sharp A, Welti JC, Neeb A, Raj GV, Luo J, et al. Alternative splicing in prostate cancer. Nature reviews Clinical oncology. 2018;15(11):663-75.
10. Jimenez-Vacas JM, Herrero-Aguayo V, Montero-Hidalgo AJ, Gomez-Gomez E, Fuentes-Fayos AC, Leon-Gonzalez AJ, et al. Dysregulation of the splicing machinery is directly associated to aggressiveness of prostate cancer. EBioMedicine. 2020:102547.
11. Jimenez-Vacas JM, Herrero-Aguayo V, Gomez-Gomez E, Leon-Gonzalez AJ, Saez-Martinez P, Alors-Perez E, et al. Spliceosome Component SF3B1 as Novel Prognostic Biomarker and Therapeutic Target for Prostate Cancer. Translational research : the journal of laboratory and clinical medicine. 2019.
12. Munkley J, Li L, Krishnan SRG, Hysenaj G, Scott E, Dalgliesh C, et al. Androgen-regulated transcription of ESRP2 drives alternative splicing patterns in prostate cancer. eLife. 2019;8.
13. Zeng Y, Wodzenski D, Gao D, Shiraishi T, Terada N, Li Y, et al. Stress-response protein RBM3 attenuates the stem-like properties of prostate cancer cells by interfering with CD44 variant splicing. Cancer Res. 2013;73(13):4123-33.
14. Zhao L, Li R, Shao C, Li P, Liu J, Wang K. 3p21.3 tumor suppressor gene RBM5 inhibits growth of human prostate cancer PC-3 cells through apoptosis. World journal of surgical oncology. 2012;10:247.
15. Yamamoto R, Osawa T, Sasaki Y, Yamamoto S, Anai M, Izumi K, et al. Overexpression of p54(nrb)/NONO induces differential EPHA6 splicing and contributes to castration-resistant prostate cancer growth. Oncotarget. 2018;9(12):10510-24.
16. Takayama KI, Suzuki T, Fujimura T, Yamada Y, Takahashi S, Homma Y, et al. Dysregulation of spliceosome gene expression in advanced prostate cancer by RNA-binding protein PSF. Proceedings of the National Academy of Sciences of the United States of America. 2017;114(39):10461-6.
17. Rasche N, Dybkov O, Schmitzova J, Akyildiz B, Fabrizio P, Luhrmann R. Cwc2 and its human homologue RBM22 promote an active conformation of the spliceosome catalytic centre. The EMBO journal. 2012;31(6):1591-604.
18. Rasche N, Dybkov O, Schmitzová J, Akyildiz B, Fabrizio P, Lührmann R. Cwc2 and its human homologue RBM22 promote an active conformation of the spliceosome catalytic centre. The EMBO journal. 2012;31(6):1591-604.
19. He F, Wang CT, Gou LT. RNA-binding motif protein RBM22 is required for normal development of zebrafish embryos. Genetics and molecular research : GMR. 2009;8(4):1466-73.
20. Manzo G. Similarities Between Embryo Development and Cancer Process Suggest New Strategies for Research and Therapy of Tumors: A New Point of View. Frontiers in cell and developmental biology. 2019;7:20.
21. Janowicz A, Michalak M, Krebs J. Stress induced subcellular distribution of ALG-2, RBM22 and hSlu7. Biochimica et biophysica acta. 2011;1813(5):1045-9.
22. Montaville P, Dai Y, Cheung CY, Giller K, Becker S, Michalak M, et al. Nuclear translocation of the calcium-binding protein ALG-2 induced by the RNA-binding protein RBM22. Biochimica et biophysica acta. 2006;1763(11):1335-43.

23. Jimenez-Vacas JM, Herrero-Aguayo V, Montero-Hidalgo AJ, Gomez-Gomez E, Fuentes-Fayos AC, Leon-Gonzalez AJ, et al. Dysregulation of the splicing machinery is directly associated to aggressiveness of prostate cancer. EBioMedicine. 2020;51:102547.
24. Gao J, Aksoy BA, Dogrusoz U, Dresdner G, Gross B, Sumer SO, et al. Integrative analysis of complex cancer genomics and clinical profiles using the cBioPortal. Science signaling. 2013;6(269):pl1.
25. Cerami E, Gao J, Dogrusoz U, Gross BE, Sumer SO, Aksoy BA, et al. The cBio cancer genomics portal: an open platform for exploring multidimensional cancer genomics data. Cancer discovery. 2012;2(5):401-4.
26. Lapointe J, Li C, Higgins JP, van de Rijn M, Bair E, Montgomery K, et al. Gene expression profiling identifies clinically relevant subtypes of prostate cancer. Proceedings of the National Academy of Sciences of the United States of America. 2004;101(3):811-6.
27. The Molecular Taxonomy of Primary Prostate Cancer. Cell. 2015;163(4):1011-25.
28. Sáez-Martínez P, Jiménez-Vacas JM, León-González AJ, Herrero-Aguayo V, Montero Hidalgo AJ, Gómez-Gómez E, et al. Unleashing the Diagnostic, Prognostic and Therapeutic Potential of the Neuronostatin/GPR107 System in Prostate Cancer. Journal of clinical medicine. 2020;9(6).
29. Jimenez-Vacas JM, Gomez-Gomez E, Montero-Hidalgo AJ, Herrero-Aguayo V, F LL, Sanchez-Sanchez R, et al. Clinical Utility of Ghrelin-O-Acyltransferase (GOAT) Enzyme as a Diagnostic Tool and Potential Therapeutic Target in Prostate Cancer. Journal of clinical medicine. 2019;8(12).
30. Gómez-Gómez E, Jiménez-Vacas JM, Pedraza-Arévalo S, López-López F, Herrero-Aguayo V, Hormaechea-Agulla D, et al. Oncogenic Role of Secreted Engrailed Homeobox 2 (EN2) in Prostate Cancer. Journal of clinical medicine. 2019;8(9).
31. Vandesompele J, De Preter K, Pattyn F, Poppe B, Van Roy N, De Paepe A, et al. Accurate normalization of real-time quantitative RT-PCR data by geometric averaging of multiple internal control genes. Genome Biology. 2002;3(7):research0034.1.
32. Su ZZ, Lin J, Shen R, Fisher PE, Goldstein NI, Fisher PB. Surface-epitope masking and expression cloning identifies the human prostate carcinoma tumor antigen gene PCTA-1 a member of the galectin gene family. Proceedings of the National Academy of Sciences of the United States of America. 1996;93(14):7252-7.
33. Del Rio-Moreno M, Alors-Perez E, Borges de Souza P, Prados-Gonzalez ME, CastaNo JP, Luque RM, et al. Peptides derived from the extracellular domain of the somatostatin receptor splicing variant SST5TMD4 increase malignancy in multiple cancer cell types. Translational research : the journal of laboratory and clinical medicine. 2019;211:147-60.
34. Patro R, Duggal G, Love MI, Irizarry RA, Kingsford C. Salmon provides fast and bias-aware quantification of transcript expression. Nature methods. 2017;14(4):417-9.
35. Trincado JL, Entizne JC, Hysenaj G, Singh B, Skalic M, Elliott DJ, et al. SUPPA2: fast, accurate, and uncertainty-aware differential splicing analysis across multiple conditions. Genome Biol. 2018;19(1):40.
36. Van Nostrand EL, Freese P, Pratt GA, Wang X, Wei X, Xiao R, et al. A Large-Scale Binding and Functional Map of Human RNA Binding Proteins. bioRxiv. 2018:179648.
37. Liberzon A, Birger C, Thorvaldsdóttir H, Ghandi M, Mesirov JP, Tamayo P. The Molecular Signatures Database (MSigDB) hallmark gene set collection. Cell systems. 2015;1(6):417-25.
38. Reich M, Liefeld T, Gould J, Lerner J, Tamayo P, Mesirov JP. GenePattern 2.0. Nature genetics. 2006;38(5):500-1.
39. Sarmento-Cabral A, F LL, Gahete MD, Castano JP, Luque RM. Metformin Reduces Prostate Tumor Growth, in a Diet-Dependent Manner, by Modulating Multiple Signaling Pathways. Molecular cancer research : MCR. 2017;15(7):862-74.
40. Gelman IH. How the TRAMP Model Revolutionized the Study of Prostate Cancer Progression. Cancer Res. 2016;76(21):6137-9.
41. Oltean S, Bates DO. Hallmarks of alternative splicing in cancer. Oncogene. 2014;33(46):5311-8.
42. Ladomery M. Aberrant alternative splicing is another hallmark of cancer. International journal of cell biology. 2013;2013:463786.
43. Ge Y, Schuster MB, Pundhir S, Rapin N, Bagger FO, Sidiropoulos N, et al. The splicing factor RBM25 controls MYC activity in acute myeloid leukemia. Nat Commun. 2019;10(1):172.
44. Sutherland LC, Rintala-Maki ND, White RD, Morin CD. RNA binding motif (RBM) proteins: a novel family of apoptosis modulators? Journal of cellular biochemistry. 2005;94(1):5-24.
45. Hernández G, Ramírez JL, Pedroza-Torres A, Herrera LA, Jiménez-Ríos MA. The Secret Life of Translation Initiation in Prostate Cancer. Frontiers in genetics. 2019;10:14.
46. Bader DA, Hartig SM, Putluri V, Foley C, Hamilton MP, Smith EA, et al. Mitochondrial pyruvate import is a metabolic vulnerability in androgen receptor-driven prostate cancer. Nature Metabolism. 2019;1(1):70-85.

47. Bajpai P, Koc E, Sonpavde G, Singh R, Singh KK. Mitochondrial localization, import, and mitochondrial function of the androgen receptor. The Journal of biological chemistry. 2019;294(16):6621-34.
48. Chen Z, Lu W. Roles of ubiquitination and SUMOylation on prostate cancer: mechanisms and clinical implications. International journal of molecular sciences. 2015;16(3):4560-80.
49. Baumgart SJ, Nevedomskaya E, Haendler B. Dysregulated Transcriptional Control in Prostate Cancer. International journal of molecular sciences. 2019;20(12).
50. Berger A, Brady NJ, Bareja R, Robinson B, Conteduca V, Augello MA, et al. N-Myc-mediated epigenetic reprogramming drives lineage plasticity in advanced prostate cancer. The Journal of clinical investigation. 2019;129(9):3924-40.
51. Davis JN, Wojno KJ, Daignault S, Hofer MD, Kuefer R, Rubin MA, et al. Elevated E2F1 inhibits transcription of the androgen receptor in metastatic hormone-resistant prostate cancer. Cancer Res. 2006;66(24):11897-906.
52. Gurel B, Iwata T, Koh CM, Jenkins RB, Lan F, Van Dang C, et al. Nuclear MYC protein overexpression is an early alteration in human prostate carcinogenesis. Modern pathology : an official journal of the United States and Canadian Academy of Pathology, Inc. 2008;21(9):1156-67.
53. Chen H, Liu W, Roberts W, Hooker S, Fedor H, DeMarzo A, et al. 8q24 allelic imbalance and MYC gene copy number in primary prostate cancer. Prostate cancer and prostatic diseases. 2010;13(3):238-43.
54. Dang CV, O'Donnell KA, Zeller KI, Nguyen T, Osthus RC, Li F. The c-Myc target gene network. Seminars in cancer biology. 2006;16(4):253-64.
55. Koh CM, Bieberich CJ, Dang CV, Nelson WG, Yegnasubramanian S, De Marzo AM. MYC and Prostate Cancer. Genes & cancer. 2010;1(6):617-28.
56. Grandori C, Gomez-Roman N, Felton-Edkins ZA, Ngouenet C, Galloway DA, Eisenman RN, et al. c-Myc binds to human ribosomal DNA and stimulates transcription of rRNA genes by RNA polymerase I. Nature cell biology. 2005;7(3):311-8.
57. Grewal SS, Li L, Orian A, Eisenman RN, Edgar BA. Myc-dependent regulation of ribosomal RNA synthesis during Drosophila development. Nature cell biology. 2005;7(3):295-302.
58. Dang CV. MYC on the path to cancer. Cell. 2012;149(1):22-35.
59. Goetzman ES, Prochownik EV. The Role for Myc in Coordinating Glycolysis, Oxidative Phosphorylation, Glutaminolysis, and Fatty Acid Metabolism in Normal and Neoplastic Tissues. Frontiers in endocrinology. 2018;9:129.
60. Beltran H, Rickman DS, Park K, Chae SS, Sboner A, MacDonald TY, et al. Molecular characterization of neuroendocrine prostate cancer and identification of new drug targets. Cancer discovery. 2011;1(6):487-95.
61. Beltran H, Prandi D, Mosquera JM, Benelli M, Puca L, Cyrta J, et al. Divergent clonal evolution of castration-resistant neuroendocrine prostate cancer. Nat Med. 2016;22(3):298-305.
62. Dimova DK, Dyson NJ. The E2F transcriptional network: old acquaintances with new faces. Oncogene. 2005;24(17):2810-26.
63. Robinson D, Van Allen EM, Wu YM, Schultz N, Lonigro RJ, Mosquera JM, et al. Integrative clinical genomics of advanced prostate cancer. Cell. 2015;161(5):1215-28.
64. Macleod KF. The RB tumor suppressor: a gatekeeper to hormone independence in prostate cancer? The Journal of clinical investigation. 2010;120(12):4179-82.
65. Polager S, Ginsberg D. E2F - at the crossroads of life and death. Trends in cell biology. 2008;18(11):528-35.
66. Poppy Roworth A, Ghari F, La Thangue NB. To live or let die - complexity within the E2F1 pathway. Molecular & cellular oncology. 2015;2(1):e970480.
67. Rebello RJ, Pearson RB, Hannan RD, Furic L. Therapeutic Approaches Targeting MYC-Driven Prostate Cancer. Genes. 2017;8(2).
68. Kent LN, Leone G. The broken cycle: E2F dysfunction in cancer. Nat Rev Cancer. 2019;19(6):326-38.

Table 1. Demographic, biochemical and clinical parameters of the patients from cohort 1. PSA: Prostate specific antigen; pT: Pathological primary tumor staging; PI: Perineural invasion; VI: Vascular invasion. GS: Gleason score.

Table 2. Demographic, biochemical and clinical parameters of the patients from cohort 2. PSA: Prostate specific antigen; GS: Gleason score.

Figure 1. Expression levels of *RBM22* in human and mice prostate samples. (a) Comparison of *RBM22* mRNA levels from two cohorts of patients: i) formalin-fixed paraffin embedded (FFPE) samples from PCa tissues and non-tumor adjacent regions (N-TAR) (left panel; n=84); and, ii) biopsy samples of patients with suspect of significant PCa (n=42) and non-tumor prostates (n=9) (right panel). mRNA levels were determined by qPCR. Data are represented as mean ± SEM of mRNA levels adjusted by a normalization factor (calculated from *ACTB* and *GAPDH* expression levels) and standardized by Z-score. (b) Comparison of *RBM22* mRNA levels from Lapointe (left panel; n=112) and TCGA (right panel; n=376) datasets. Data are represented as mean ± SEM of mRNA levels and standardized by Z-score. (c) Association between *RBM22* mRNA levels and clinical parameters (extraprostatic extension and perineural invasion) in PCa samples from cohort ii (n=42). Data are represented as mean ± SEM of mRNA levels adjusted by a normalization factor (calculated from *ACTB* and *GAPDH* expression levels). (d) Correlation between *RBM22* mRNA levels and expression levels of *KLK3* and *PCA3*. Correlations are represented by mean (connecting line) and error bands (pointed line) of expression levels. (e) Comparison of *RBM22* mRNA levels from prostatic intraepithelial neoplasia (PIN; n=5), moderately differentiated PCa (MD-PCa; n=4) and poorly differentiated PCa (PD-PCa; n=5) derived from TRAMP mice. Data are represented as mean ± SEM of mRNA levels adjusted by *CICLO* expression levels. Asterisks (* $p<0.05$; ** $p<0.01$; *** $p<0.001$) indicate statistically significant differences between groups.

Figure 2. Protein levels of RBM22 in human and mice prostate samples. (a) Comparison of RBM22 protein levels by immunohistochemistry (IHC) between a representative set of normal prostate (NP; n=9), benign prostatic hyperplasia (BPH; n=7), prostatic intraepithelial neoplasia (PIN; n=6) and prostate cancer (PCa; n=47) samples. Data are represented as mean ± SEM of IHC staining scaled from low (1) to high (3) intensity. (b) Representative images of NP, PIN, BPH, and PCa stained with RBM22. Association of RBM22 protein levels with: (c) Gleason score [GS 6 (n=5) and GS≥7 (n=42)], and (d) presence of metastasis at diagnosis [no metastasis (n=19) and metastasis (n=28)]. Data are represented as mean ± SEM of IHC staining scaled from low (1) to high (3) intensity. (e) Representative images of non-metastatic GS 6 (left panel), and metastatic GS≥7 (right panel) samples stained with RBM22 staining. (f) Comparison of RBM22 protein levels from prostatic intraepithelial neoplasia (PIN; n=5), moderately differentiated PCa (MD-PCa; n=4) and poorly differentiated PCa (PD-PCa; n=5) derived from TRAMP mice. Protein levels were normalized by total protein loading (Ponceau staining). (g) Representative images of RBM22 protein level measurement by Western-Blot (upper panel) on PIN, MD-PCa and PD-PCa samples from TRAMP mice. Asterisks (** $p<0.01$; *** $p<0.001$) indicate statistically significant differences between groups.

Figure 3. Functional consequences of *RBM22* overexpression in prostate cancer-derived cell lines. (a) Comparison of *RBM22* mRNA expression levels between non-tumor (RWPE-1)

and tumor (22Rv1, LNCaP, DU145 and PC-3) prostate-derived cell lines. mRNA levels were determined by qPCR. Data are represented as mean ± SEM of mRNA levels adjusted by a normalization factor (calculated from *ACTB* and *GAPDH* expression levels). (b) Proliferation rate of LNCaP (left panel) and PC-3 (right panel) cells in response to *RBM22* overexpression. Effect of *RBM22* overexpression in: (c) LNCaP (left panel) and PC-3 (right panel) colony number, and (d) colony area. Representative images of LNCaP and PC-3 cells are depicted on lower panel. (e) Tumorsphere formation of LNCaP (left panel) and PC-3 (right panel) cells in response to *RBM22* overexpression. (f) Migration rate of PC-3 cells in response to *RBM22* overexpression. Representative images are depicted on lower panel. Data are represented as percentage of mock-transfected cells. Asterisks (* $p<0.05$; ** $p<0.01$; *** $p<0.001$) indicate statistically significant differences between groups.

Figure 4. Impact of *RBM22* overexpression in RNA splicing in PCa cells. (a) Comparison of splicing events distribution in response to *RBM22* overexpression in PC-3 cells. (b) Venn-diagram of pre-RNAs that physically bind to RBM22 identified by CLIP-seq analysis (green) and whose splicing process is altered in response to *RBM22* (pink). (c) Functional association network of genes whose splicing pattern is potentially and directly altered by RBM22. These significantly altered genes were clustered using k-means network clustering from STRING database. Action types and action effects are explained in the bottom panel.

Figure 5. *In vivo* functional and molecular response to *RBM22* overexpression in a PC-3 xenograft model. (a) Validation of *RBM22* overexpression by qPCR. mRNA levels were adjusted by a normalization factor (calculated from *ACTB* and *GAPDH* expression levels). Data (mean ± SEM) are represented as percentage of mock-transfected xenograft tumors. Comparison between the tumor growth (b) and tumor weight (c) of xenograft tumors derived from mock-transfected cells (blank line) and *RBM22*-overexpressing cells (blue line) over time. (d) Representative images of tumor size of mock-transfected and *RBM22*-overexpressing xenograft tumors. (e) Hierarchical heatmap generated using the mRNA expression levels of significantly altered cancer-related genes (154 genes) in mock-transfected (red) and *RBM22*-overexpressing (green) xenograft tumors. These expression levels were obtained by the nCounter PanCancer platform. (f) Number of hits of significantly altered cancer-related genes in response to *RBM22* overexpression in cancer-related pathways or processes. (g) Protein-Protein Interaction (PPI) association analysis carried out within genes altered in response to *RBM22* overexpression. Asterisks (*** $p<0.001$) indicate statistically significant differences between groups.

Figure 6. Molecular consequences of *RBM22* overexpression in PCa cells. (a) Volcano plot highlighting differentially expressed genes in response to *RBM22* overexpression in PC-3 cells (blue). (b) Upstream regulator analysis of the most dysregulated pathways in response to *RBM22* overexpression, using IPA software. (c) Funcional association network of upstream regulator genes whose activity is altered in response to *RBM22* overexpression. Hallmark gene sets enriched in patients with high RBM22 expression (first quartile vs. other quartiles) obtained from the TCGA (d) and Lapointe (e) datasets, performed using GenePattern software.

Table 1

Parameter	
Patients [*n*]	84
Age, years [median (IQR)]	61 (57-66)
PSA levels, ng/mL [median (IQR)]	5.2 (4.2-8.0)
GS ≥ 7 [*n* (%)]	76 (90.5%)
PI [*n* (%)]	72 (85.7%)
VI [*n* (%)]	8 (9.52%)
Metastasis [*n* (%)]	0 (0%)

Table 2

Parameter	
Patients [*n*]	42
Age, years [median (IQR)]	75 (69-81)
PSA levels, ng/mL [median (IQR)]	62.0 (36.2-254.5)
EE [*n* (%)]	16 (38%)
GS ≥ 7 [*n* (%)]	42 (100%)
Metastasis [*n* (%)]	28 (66.7%)

Figure 1

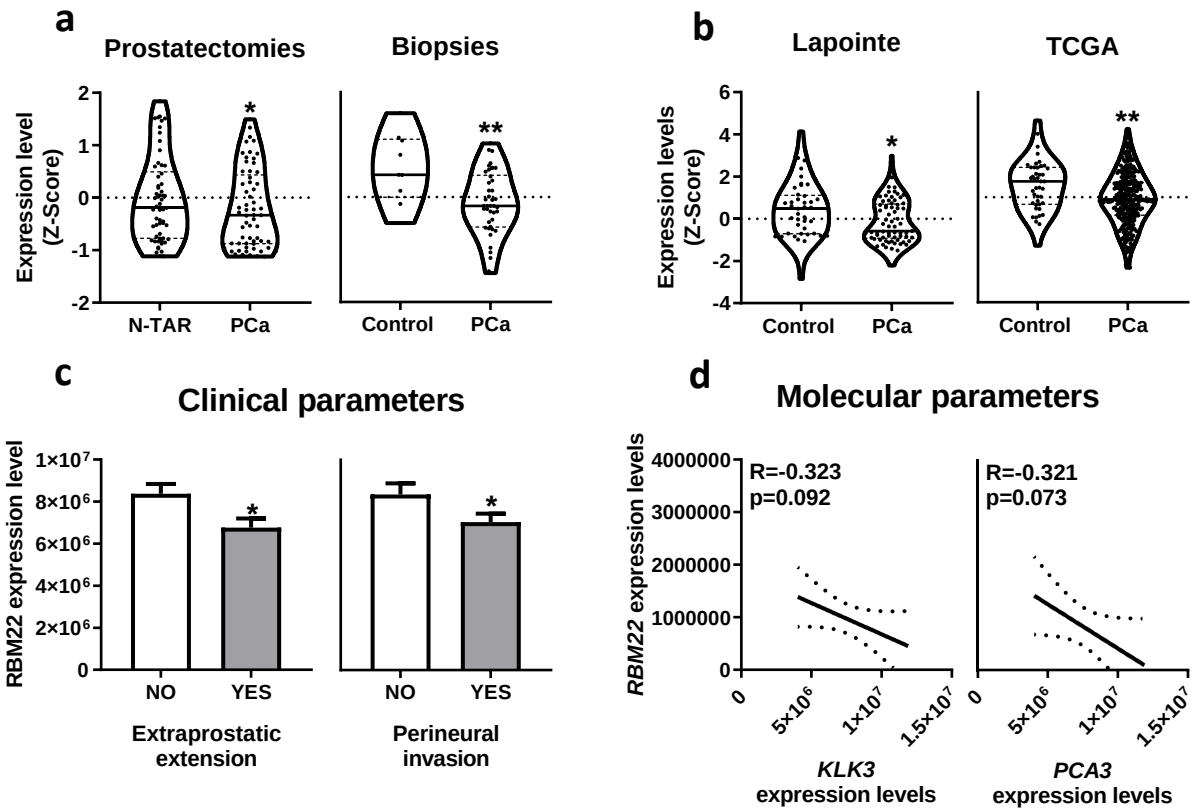
a
Prostatectomies
Biopsies
Expression level (Z-Score)
N-TAR
PCa
Control
PCa
b
Lapointe
TCGA
Expression levels (Z-Score)
Control
PCa
c
Clinical parameters
RBM22 expression level
NO
YES
Extraprostatic extension
Perineural invasion
d
Molecular parameters
RBM22 expression levels
R=-0.323
p=0.092
R=-0.321
p=0.073
KLK3 expression levels
PCA3 expression levels

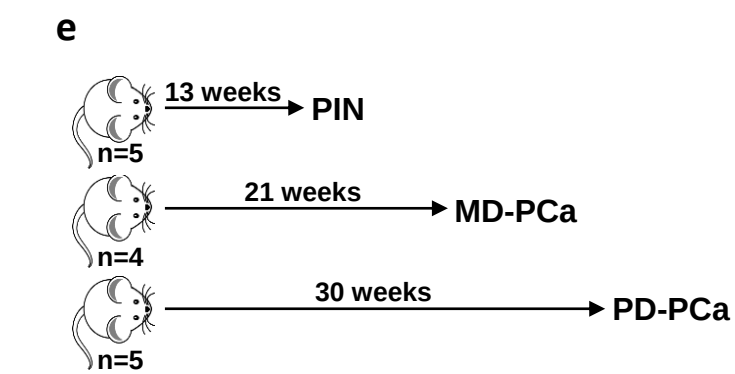
e
13 weeks
PIN
n=5
21 weeks
MD-PCa
n=4
30 weeks
PD-PCa
n=5

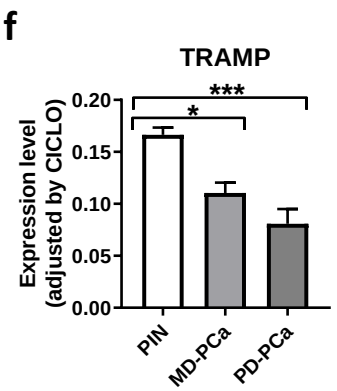
f
TRAMP
Expression level (adjusted by CICLO)
PIN
MD-PCa
PD-PCa

Figure 2

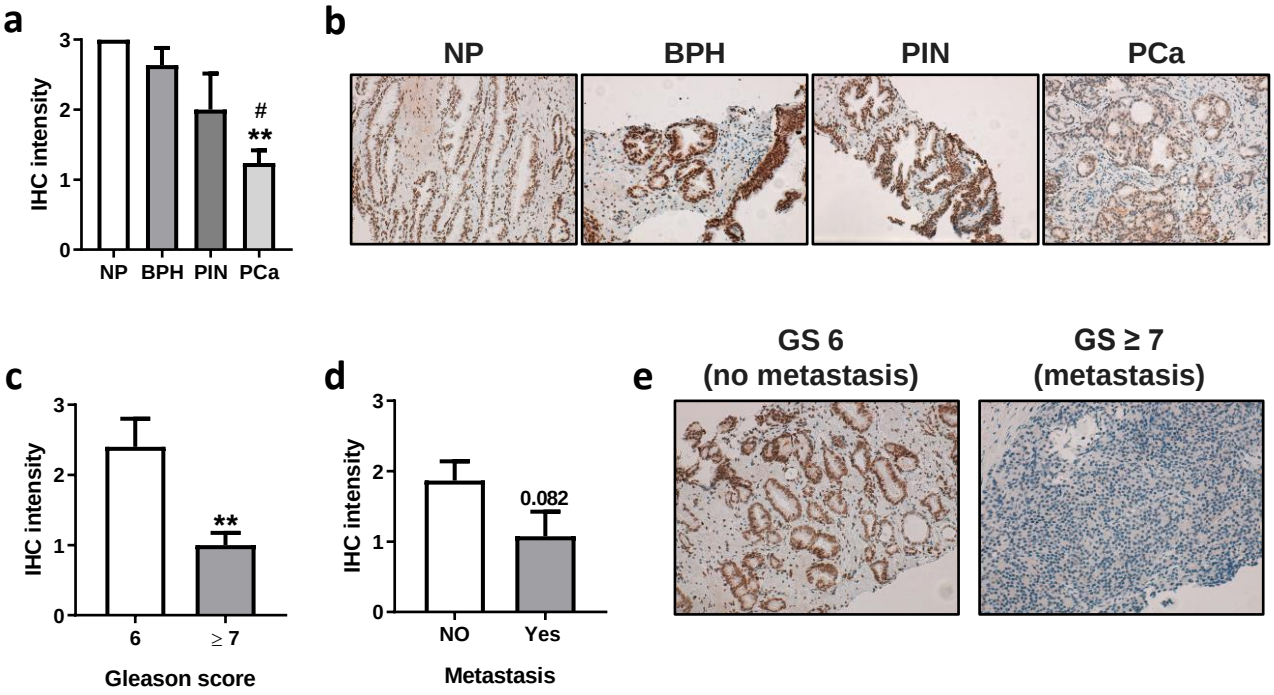
a
IHC intensity
3
2
1
0
#
**
NP BPH PIN PCa
b
NP
BPH
PIN
PCa
c
IHC intensity
3
2
1
0
**
6
≥ 7
Gleason score
d
IHC intensity
3
2
1
0
0.082
NO
Yes
Metastasis
e
GS 6
(no metastasis)
GS ≥ 7
(metastasis)

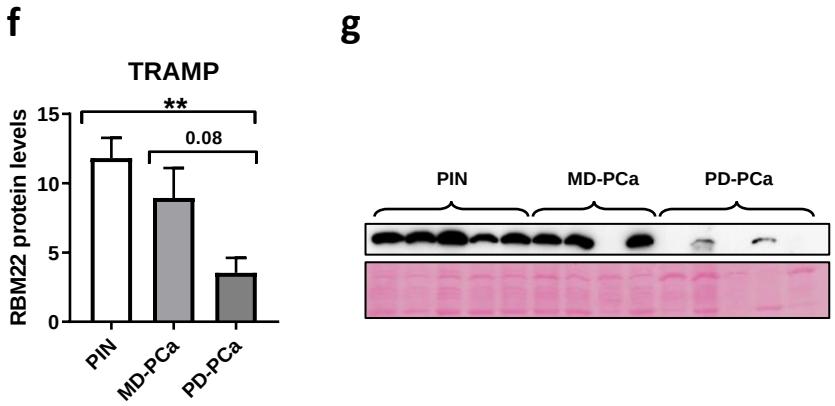
f
TRAMP
RBM22 protein levels
15
10
5
0
**
0.08
PIN
MD-PCa
PD-PCa
g
PIN
MD-PCa
PD-PCa

Figure 3

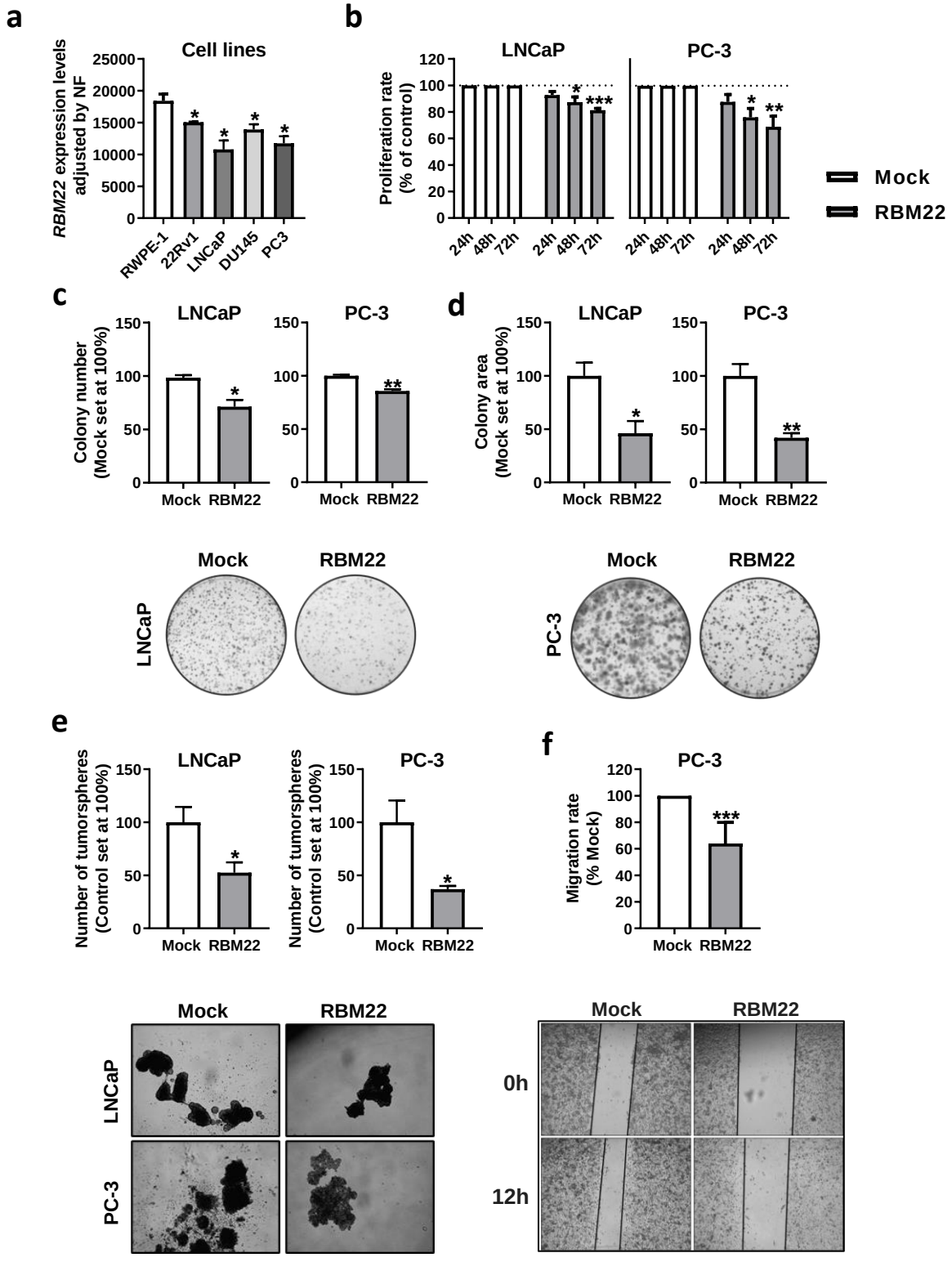
a
Cell lines
RBM22 expression levels adjusted by NF
25000
20000
15000
10000
5000
0
RWPE-1
22Rv1
LNCaP
DU145
PC3
b
LNCaP
PC-3
Proliferation rate (% of control)
120
100
80
60
40
20
0
24h
48h
72h
Mock
RBM22
c
LNCaP
PC-3
Colony number (Mock set at 100%)
150
100
50
0
Mock
RBM22
d
LNCaP
PC-3
Colony area (Mock set at 100%)
Mock
RBM22
LNCaP
PC-3
e
LNCaP
PC-3
Number of tumorspheres (Control set at 100%)
Mock
RBM22
f
PC-3
Migration rate (% Mock)
Mock
RBM22
0h
12h

Figure 4

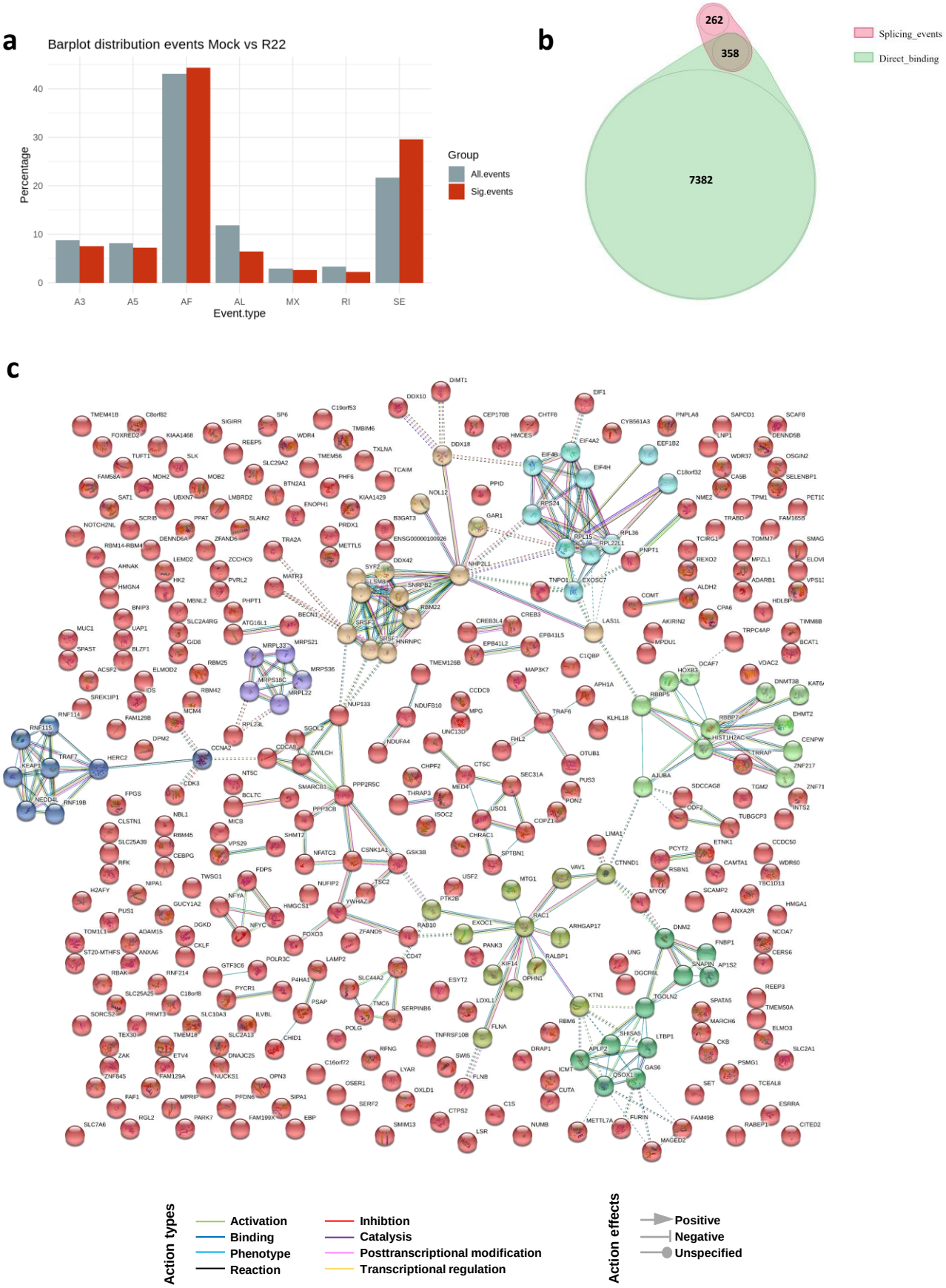
a
Barplot distribution events Mock vs R22
Percentage
Event.type
A3
A5
AF
AL
MX
RI
SE
Group
All.events
Sig.events
b
262
358
7382
Splicing_events
Direct_binding
c
Action types
Activation
Binding
Phenotype
Reaction
Inhibtion
Catalysis
Posttranscriptional modification
Transcriptional regulation
Action effects
Positive
Negative
Unspecified

Figure 5

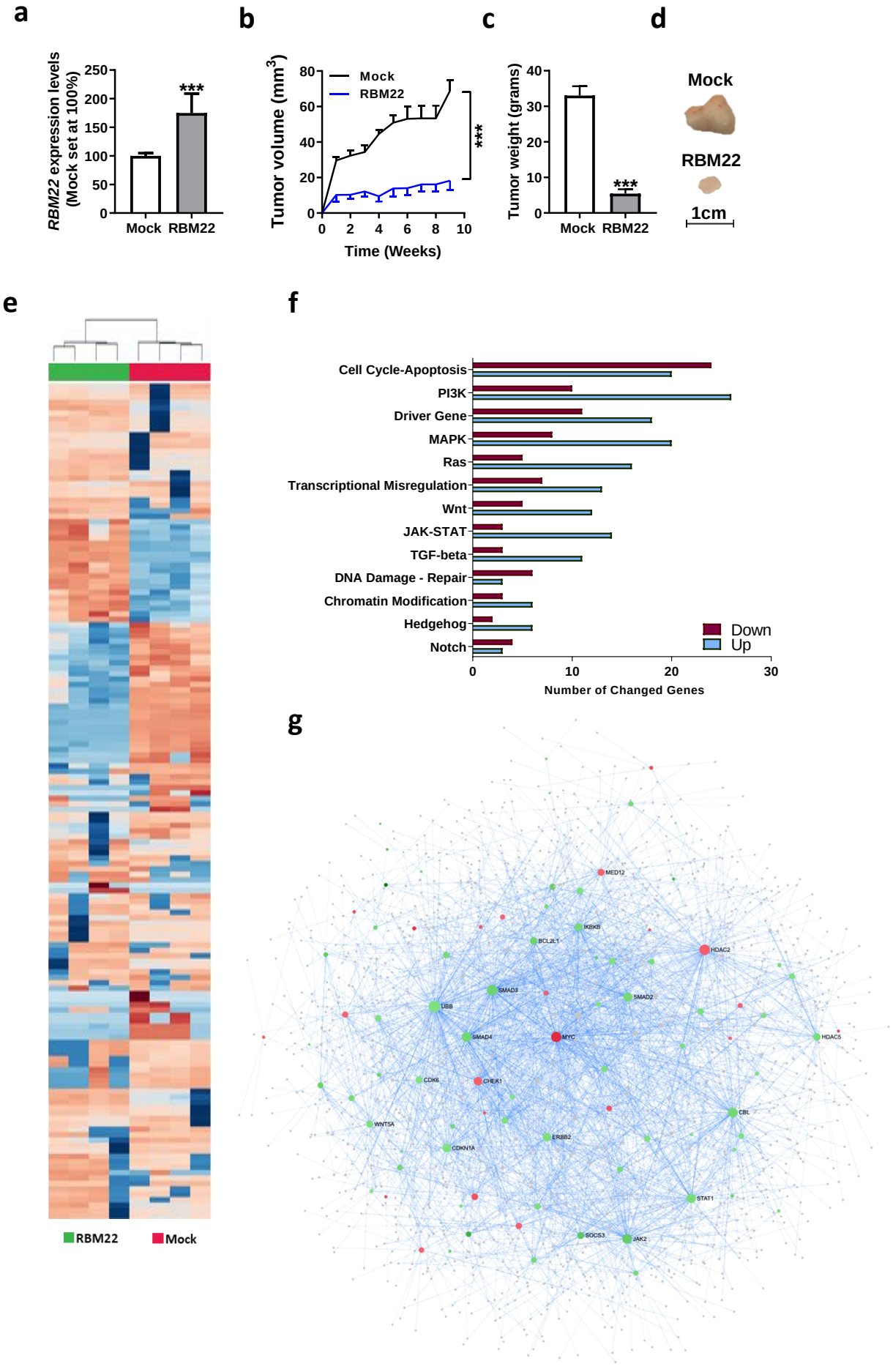
a
RBM22 expression levels (Mock set at 100%)
250
200
150
100
50
0
***
Mock
RBM22
b
Tumor volume (mm3)
80
60
40
20
0
Mock
RBM22
***
0
2
4
6
8
10
Time (Weeks)
c
Tumor weight (grams)
40
30
20
10
0
***
Mock
RBM22
d
Mock
RBM22
1cm
e
RBM22
Mock
f
Cell Cycle-Apoptosis
PI3K
Driver Gene
MAPK
Ras
Transcriptional Misregulation
Wnt
JAK-STAT
TGF-beta
DNA Damage - Repair
Chromatin Modification
Hedgehog
Notch
Down
Up
0
10
20
30
Number of Changed Genes
g
MED12
IKBKB
BCL2L1
HDAC2
SMAD3
SMAD2
UBB
SMAD4
MYC
HDAC5
CDK6
CHEK1
CBL
WNT5A
ERBB2
CDKN1A
STAT1
SOCS3
JAK2

Figure 6

a

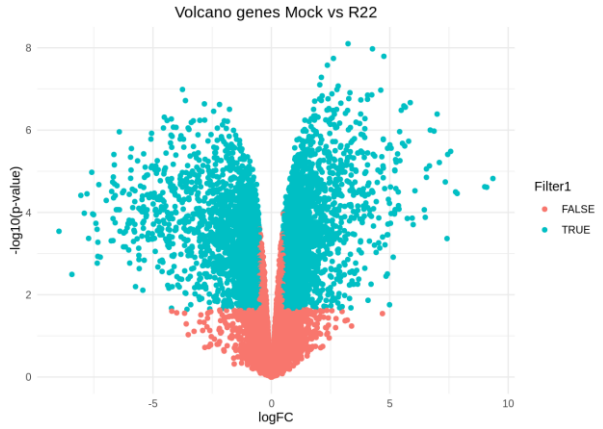

b

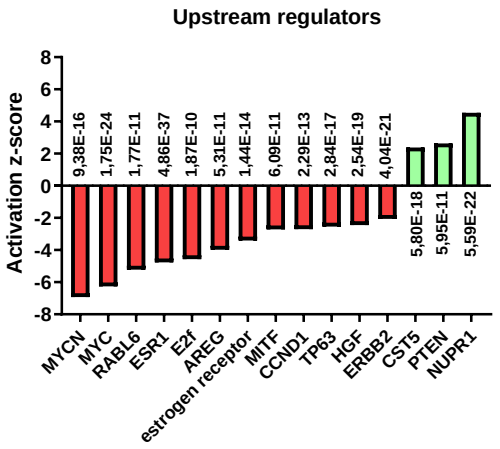

c

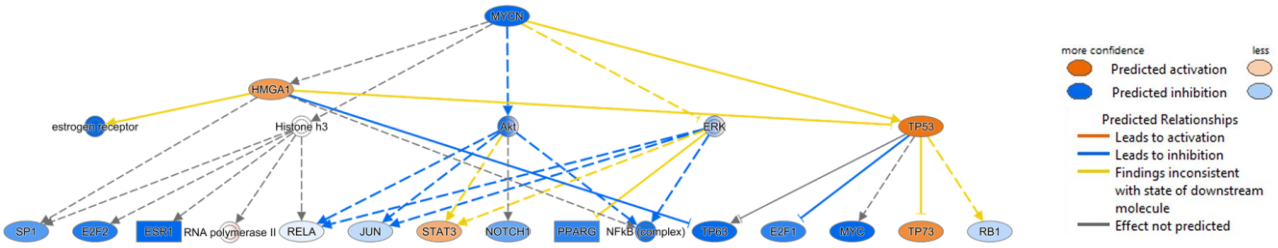

d

TCGA

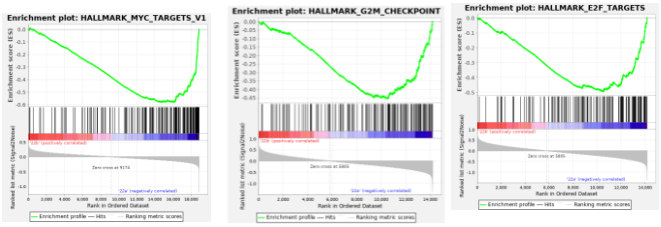

e

Lapointe

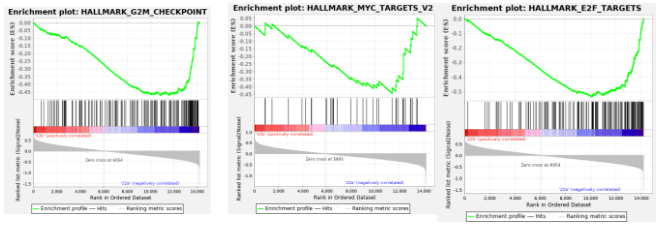

Supplemental Figure 1

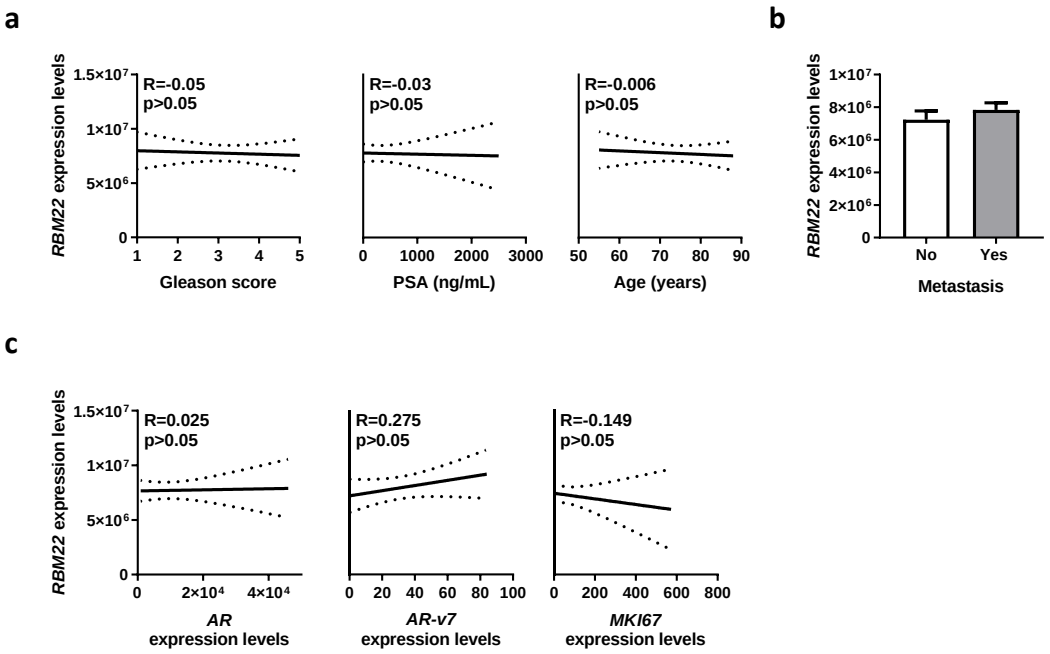

Supplemental Figure 1. Non-significant correlations between *RBM22* expression levels and parameters of PCa aggressiveness. (a) Correlations of *RBM22* expression levels and Gleason score (left panel), circulant PSA levels (central panel) and age (right panel) in PCa patients from cohort 2. (b) Association between *RBM22* expression levels and the presence of metastasis at diagnosis of PCa patients from cohort 2. (c) Correlations of *RBM22* expression levels and *AR* (left panel), *AR-v7* (central panel) and *MKI67* (right panel) expression levels of PCa patients from cohort 2. Correlations are represented by mean (connecting line) and error bands (pointed line) of expression levels.

Supplemental Figure 2

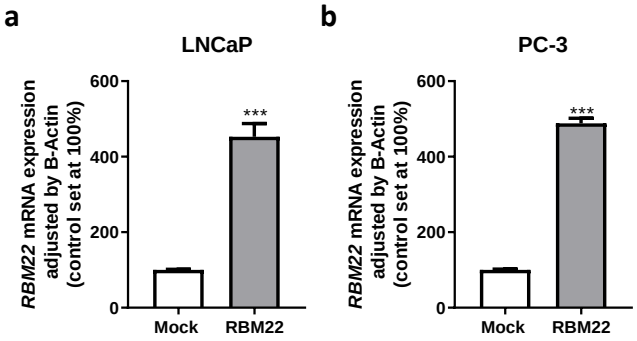

Supplemental Figure 2. Validation of *RBM22* overexpression in PCa cell-lines. Validation of *RBM22* overexpression in LNCaP (a) and PC-3 (b) cell-lines. mRNA levels were adjusted by a normalization factor (calculated from *ACTB* and *GAPDH* expression levels). Data (mean ± SEM) are represented as percentage of mock-transfected cells. Asterisks (*** $p<0.001$) indicate statistically significant differences between groups.

Article III

Spliceosome component SF3B1 as novel prognostic biomarker and therapeutic target for prostate cancer

JUAN M. JIMÉNEZ-VACAS, VICENTE HERRERO-AGUAYO, ENRIQUE GÓMEZ-GÓMEZ, ANTONIO J. LEÓN-GONZÁLEZ, PRUDENCIO SÁEZ-MARTÍNEZ, EMILIA ALORS-PÉREZ, ANTONIO C. FUENTES-FAYOS, ANA MARTÍNEZ-LÓPEZ, RAFAEL SÁNCHEZ-SÁNCHEZ, TERESA GONZÁLEZ-SERRANO, DANIEL J. LÓPEZ-RUIZ, MARÍA J. REQUENA-TAPIA, JUSTO P. CASTAÑO, MANUEL D. GAHETE, and RAÚL M. LUQUE

CORDOBA, SPAIN

Prostate cancer (PCa) is one of the most common cancers types among men. Development and progression of PCa is associated with aberrant expression of oncogenic splicing-variants (eg, AR-v7), suggesting that dysregulation of the splicing process might represent a potential actionable target for PCa. Expression levels (mRNA and protein) of SF3B1, one of the main components of the splicing machinery, were analyzed in different cohorts of PCa patients (clinically localized (n = 84), highly aggressive PCa (n = 42), and TCGA dataset (n = 497)). Functional and mechanistic assays were performed in response to pladienolide-B in nontumor and tumor-derived prostate cells. Our results revealed that *SF3B1* was overexpressed in PCa tissues and its levels were associated with clinically relevant PCa-aggressive features (eg, metastasis/*AR-v7* expression). Moreover, inhibition of SF3B1 activity by pladienolide-B reduced functional parameters of aggressiveness (proliferation/migration/tumorspheres-formation/apoptosis) in PCa cell lines, irrespective of *AR-v7* expression, and reduced viability of primary PCa cells. Antitumor actions of pladienolide-B involved: (1) inhibition of PI3K/AKT and JNK signaling pathways, (2) modulation of tumor markers and splicing variants (AR-v7/In1-ghrelin), and (3) regulation of key components of mRNA homeostasis-associated machineries (spliceosome/SURF/EJC). Altogether, our results demonstrated that *SF3B1* is overexpressed and associated with malignant features in PCa, and its inhibition reduces PCa aggressiveness, suggesting that SF3B1 could represent a novel prognostic biomarker and a therapeutic target in PCa. (Translational Research 2019; 212:89–103)

Abbreviations: CRPC = castration-resistant prostate cancer; cSCC = cutaneous squamous cell carcinoma; EJC = exon-junction complex; EMT = epithelial mesenchymal transition; FFPE = formalin-fixed paraffin-embedded; IHC = immunohistochemistry; ISUP = International Society of Urological Pathology; NMD = nonsense-mediated mRNA decay; N-TAR = non-tumoral adjacent region; PCa = prostate cancer; PIRADS = Prostate Imaging—Reporting and Data System;

From the Maimonides Institute for Biomedical Research of Córdoba (IMIBIC), Córdoba, Spain; Department of Cell Biology, Physiology, and Immunology, University of Córdoba, Córdoba, Spain; Hospital Universitario Reina Sofía (HURS), Córdoba, Spain; Centro de Investigación Biomédica en Red de Fisiopatología de la Obesidad y Nutrición, (CIBERobn), Córdoba, Spain; Urology Service, HURS/IMIBIC, Córdoba, Spain; Ana-Anatomical Pathology Service, HURS, Córdoba, Spain; Radiology Service, HURS/IMIBIC.

Submitted for Publication April 10, 2019; received submitted June 19, 2019; accepted for publication July 5, 2019.

Reprint requests: Raúl M. Luque, Edificio IMIBIC, Av. Menéndez Pidal s/n, 14004 Córdoba, Spain. e-mail: bc2luhur@uco.es.

1931-5244/$ - see front matter

https://doi.org/10.1016/j.trsl.2019.07.001

PSA = prostate-specific antigen; SF = splicing factor; snRNP = small nuclear ribonucleoprotein; STR = short tandem repeat; SURF = SMG-1-Upf1–eRF1–eRF3 complex; TCGA = The Cancer Genome Atlas

AT A GLANCE COMMENTARY

Juan M. J-V, et al.

Background

Dysregulation of various oncogenic splicing variants is associated with an increase in prostate cancer (PCa) aggressiveness and resistance to medical treatment. The control of the appropriate splicing process is catalyzed by a complex cellular machinery, the spliceosome, wherein SF3B1 is a main structural/functional component. However, the pathologic role of SF3B1 and its potential as diagnostic/prognostic biomarker and therapeutic target in PCa remain unknown.

Translational Significance

SF3B1 is overexpressed in PCa tissues and linked to relevant aggressiveness features, indicating that could represent a novel prognostic biomarker for PCa. Additionally, blockade of SF3B1 activity exerts strong antitumoral effects in PCa cells suggesting that SF3B1 might be considered as a potential therapeutic target for PCa.

INTRODUCTION

Prostate cancer (PCa) is the most diagnosed tumor pathology among men in more than 50% of the countries worldwide and represents one of the leading causes of cancer-related death among male population in developed countries.[1] The high mortality rate associated with PCa is mainly due to the most aggressive phenotype of this endocrine-related cancer, called castration-resistant PCa (CRPC).[2] In fact, although the development of novel drugs (eg, Abiraterone and Enzalutamide) has significantly improved the overall survival of PCa patients, this devastating pathology remains a lethal disease.[3,4] A common hallmark of most cancers, including PCa, is the alteration of the appropriate regulation of gene expression,[5] which leads to the aberrant expression of mRNA species and, particularly, to the appearance of splicing variants with oncogenic potential.[6] Indeed, PCa aggressiveness, CRPC development, and resistance to medical treatment are associated with the dysregulation of the expression of aberrant splicing variants, especially the androgen receptor variant 7 (AR-v7),[7] but also other oncogenic splicing variants as In1-ghrelin,[8] sst5TMD4,[9] KLF6-SV1,[10] FGFR2IIIc,[11] etc. Expression of the adequate pattern of splicing variants is mainly controlled by 2 intricate and tightly intertwined processes, namely, alternative splicing[12] and nonsense-mediated mRNA decay (NMD),[13] which are precisely catalyzed and regulated by different molecular machineries, the spliceosome, and the exon-junction (EJC) and SMG-1Upf1–eRF1–eRF3 (SURF) complexes, respectively.[12,13] Unfortunately, although many efforts have been implemented to counteract the expression of some oncogenic splicing variants (eg, AR-v7), there is a lack of available drugs for this purpose in the current clinical practice. Thus, novel drugs and therapeutic targets to manipulate the splicing process and reduce PCa aggressiveness (including AR-v7 and other oncogenic splicing variants) are strongly necessary.

The splicing factor (SF) 3B subunit 1 (SF3B1) is a key spliceosome component that could represent a valuable tool to modulate the splicing process. SF3B1 composes, together with SF3a and a 12S RNA unit, the U2 small nuclear ribonucleoprotein (snRNP) complex, which binds pre-mRNA upstream of the intron branch site in a sequence-independent manner.[14] *SF3B1* mutations have been recently reported in certain tumor pathologies such as breast cancer,[15] uveal carcinoma,[16] pancreatic ductal adenocarcinoma,[17] myelodysplastic syndromes,[18] and with a low frequency (1.1%) in PCa,[19] suggesting its putative role in tumor initiation. Remarkably, SF3B1 activity can be pharmacologically blocked by available drugs, as is the case of pladienolide-B,[20] a compound with reported antitumor effects in certain tumor pathologies, such as gastric cancer,[21] cutaneous squamous cell carcinoma (cSCC),[22] or leukaemia.[23] To date, however, the expression of *SF3B1* in normal prostate, its putative alteration in PCa, as well as the functional and molecular consequence of blocking its activity by pladienolide-B in PCa cells remains unknown. Therefore, in this study, we aimed to determine the expression levels of *SF3B1* in PCa samples and their relationship with clinical and molecular features. Moreover, we assessed the potential antitumor effects of reducing SF3B1 activity by pladienolide-B in PCa cells (proliferation, migration, etc.), and explored the molecular/signaling pathways modulated by pladienolide-B to exert its actions, by analyzing the expression of splicing variants (eg, *AR-v7*) and a representative set of splicing-associated genes and mRNA regulatory machineries. Our ultimate goal is to define whether *SF3B1* acts as a novel diagnostic and/or prognostic biomarker and as an actionable therapeutic target to manage PCa and CRPC.

MATERIALS AND METHODS

Patients and samples. The SSPA Biobank has coordinated the collection, processing, management, and assignment of the biological samples used in this study, according to the standard procedures established for this purpose. This study was approved by the Reina Sofia University Hospital Ethics Committee (Approval 2461) and was conducted in accordance with the principles of the Declaration of Helsinki. Written informed consent was obtained from all patients. Two different cohorts of prostate samples were included:

- **Cohort 1**) formalin-fixed, paraffin-embedded (FFPE) PCa tissues (n = 84) and their nontumor adjacent region (N-TAR; used as control tissues; n = 84), which were obtained from radical prostatectomies from patients who were diagnosed with clinically localized PCa (Table 1).
- **Cohort 2**) fresh PCa samples (n = 42) that were obtained by core needle biopsies from patients with suspect of presenting significant PCa (highly aggressive PCa), which was further confirmed histologically by a specialized pathologist (Table 2).

Computed tomography scan and bone scan were performed in these patients to determine the presence of metastasis. Available clinical parameters of tumor aggressiveness were collected from each patient, such as presence of metastases, Gleason score (analyzed by specialist uropathologists following the modified 2005, 2010, and 2014 ISUP criteria, based on the sample collection date) and prostatic-specific antigen (PSA) levels. In addition, expression and clinical data of interest for this study were downloaded from "The Cancer Genome Atlas" (TCGA) database using cBioPortal.[24,25]

Cell cultures. Normal prostate (RWPE-1) and PCa (LNCaP, 22Rv1, PC-3, and DU145) cell lines were obtained from the American Type Culture Collection (ATCC; Manassas, VA) and cultured according to manufacturer instructions as previously described.[8,9,26] These cell lines were validated by analysis of short tandem repeats sequences (STRs) using GenePrint 10 System (Promega, Barcelona, Spain) and checked for mycoplasma contamination by PCR as previously reported.[9] For functional assays, all cell lines described above were used unless otherwise stated. For mechanistic assays, LNCaP, 22Rv1, and PC-3 were used as representative models of androgen-dependence, androgen-independence with AR and AR-v7 expression and androgen-independence without AR expression, respectively. Pladienolide-B (Santa Cruz Biotechnology, Bergheimer, Germany) was resuspended in DMSO and was initially used in the 10^{-11} M to 10^{-7} M range.

Primary cultures. Normal and tumor prostate tissues were dispersed into single cells by mechanic and enzymatic digestion using the protocol described by Goldstein et al[27] with modifications.[28] Tumor prostate tissues for dispersion were taken following an adapted protocol from Ugalde-Olano et al.[29] Briefly, a 4-mm tissue cylinder was taken by using a dermatological punch (Clinicord, Córdoba, Spain) from the prostatectomy specimen in the area indicated by the PIRADS v2 map,[30] which was previously confirmed by prostate biopsy. The cylinder was longitudinally divided using a scalpel; one piece was included in paraffin to be analyzed by an expert anatomo-pathologist in order to ensure the presence of tumor tissue and, the other piece was immediately placed in sterile cold (4°C) DMEM High Glucose with D-valine (Seralab, Oviedo, Spain) and immediately transported to the laboratory for dispersion and primary culture experiments.

Cell proliferation and migration. Cell proliferation and migration were measured as previously reported.[9] Briefly, cell proliferation/viability was assessed by Alamar-Blue Reagent (Bio-Source International, Camarillo, CA) in response to pladienolide-B treatment and SF3B1-siRNA (100 nM; #9284S, Cell Signaling, Barcelona, Spain). Cells were seeded in 96-well plates at a density of 3000−5000 cells/well and serum-starved for 24 hours.

Table 1. Demographic, biochemical, and clinical parameters of the patients with clinically localized PCa (cohort 1)

Parameter	
Patients (n)	84
Age, y (median (IQR))	61 (57-66)
PSA levels, ng/mL (median (IQR))	5.2 (4.2-8.0)
Sig PCa (n (%))	76 (90.5%)
pT ≥3a (n (%))	59 (70.2%)
PI (n (%))	72 (85.7%)
VI (n (%))	8 (9.52%)
Recurrence (n (%))	35 (41.7%)
Metastasis (n (%))	0 (0%)

Abbreviations: PI, perineural invasion; PSA, prostate-specific antigen; pT, pathological primary tumor staging; VI, vascular invasion.
SigPCa is defined as Gleason score ≥7.

Table 2. Demographic, biochemical, and clinical parameters of the patients with highly aggressive PCa (cohort 2)

Parameter	
Patients (n)	42
Age, y (median (IQR))	75 (69-81)
PSA levels, ng/mL (median (IQR))	62.0 (36.2-254.5)
Sig PCa (n (%))	42 (100%)
Metastasis (n (%))	28 (66.7%)

Abbreviations: EE, extraprostatic extension; PI, perineural invasion; PSA, prostate-specific antigen; pT, pathological primary tumor staging; VI, vascular invasion.
SigPCa is defined as Gleason score ≥7.

Then, cell proliferation/viability was evaluated every 24 hours using FlexStation III system (Molecular Devices, Sunnyvale, CA) until 72 hours. Cell migration was evaluated by wound-healing assay in all cell lines except for 22Rv1, due to its inability to migrate. Briefly, images of the scratch were taken at 0 and 12 hours and wound healing was calculated as the area observed 12 hours after the wound was made *vs* the area observed just after wounding. Results were expressed as percentage referred to control.

Tumorsphere formation. Tumorsphere formation assay was carried out in representative cell models of advanced PCa (22Rv1, PC-3, and DU145). Briefly, 2000 cells were seeded in a 24-well Corning Costar ultra-low attachment plate (Merck, Madrid, Spain) with DMEM F-12 medium supplemented with 20 ng/mg EGF (Sigma-Aldrich, Madrid, Spain). Treatments were added at the moment of plating and refreshed every 3 days. The number of tumorspheres was determined using an inverted microscope after 10 days of incubation.

Apoptosis assay. Apoptosis rate was determined by the Caspase-Glo 3/7 assay (Promega) according to manufacturer's instructions. Briefly, 6000 cells/well were plated in a 96-well white microplate and cultured for 24 hours at 37˚C in an atmosphere containing 5% CO_2. Then, cells were treated with pladienolide-B or vehicle and incubated for 24 hours. Next, 100 μL of Caspase-Glo 3/7 reagent was added to each well and after 30 minutes of incubation, luminescence was measured at room temperature using the FlexStation III system. Results were expressed as percentage of relative luminescence units referred to control.

RNA extraction and quantitative real-time PCR (qPCR). Total RNA from FFPE samples was isolated and DNase-treated using the Maxwell 16 LEVRNA FFPE Kit (Promega) according to manufacturer instructions in the Maxwell MDx 16 Instrument (Promega). Additionally, total RNA was extracted from fresh samples using the AllPrep DNA/RNA/Protein Mini Kit (Qiagen, Madrid, Spain), and from PCa cell lines using TRIzol Reagent (Thermo Fisher Scientific, Madrid, Spain), followed, in both cases, by DNase treatment using the RNase-Free DNase Kit (Qiagen). Total RNA concentration and purity was assessed using the Nanodrop One Spectrophotometer (Thermo Fisher Scientific). Total RNA was retrotranscribed using random hexamer primers and the cDNA First Strand Synthesis kit (Thermo Scientific). Details regarding the development, validation, and application of the qRT-PCR to measure expression levels of the transcripts of interest have been previously reported by our laboratory.[31-34] Specific and validated primers sets used to measure the expression levels (absolute mRNA copy number/50 ng of sample) of genes of interest in this study are described in Supplemental Table 1. To control for variations in the amount of RNA used and for the efficiency in the retrotranscription reaction, mRNA copy numbers of the different transcripts analyzed were adjusted by a normalization factor calculated by the expression levels of *ACTB* and *GAPDH* (used as housekeeping genes), using GeNorm 3.5,[35] wherein *ACTB* and *GAPDH* mRNA levels did not significantly vary among the different experimental conditions (data not shown).

SF3B1 IHC ANALYSIS

Inmunohistochemistry (IHC) analysis was performed in a representative set of FFPE pieces that had normal and tumoral regions from patients diagnosed with clinically localized PCa (n = 13). Briefly, deparaffinized sections were incubated overnight (4˚C) with a SF3B1 monoclonal antibody (ab172634, Abcam, Cambdridge, UK) at 1:250 dilution, followed by incubation with an antirabbit horseradish peroxidase-conjugated secondary antibody (#7074, Cell Signaling). Finally, sections were developed with 3,39-diaminobenzidine (Envision system 2-Kit Solution DAB) and contrasted with hematoxylin. Two independent pathologists performed histopathologic analysis of the tumors following a blinded protocol. In the analysis, +, ++, +++ indicate low, moderate, and high staining intensities.

qPCR DYNAMIC ARRAY BASED ON MICROFLUIDIC TECHNOLOGY

A qPCR dynamic array based on microfluidic technology (Fluidigm, San Francisco, CA) was implemented to determine the expression of 48 transcripts in 48 samples, simultaneously. Specific primers for human transcripts including components of the major spliceosome (n = 12), minor spliceosome (n = 4), associated SFs (n = 26), EJC (n = 6), SURF complex (n = 7), NMD factors (n = 11), and 3 housekeeping genes (*ACTB, GAPDH*, and *HPRT*) were specifically designed with the Primer3 software and StepOne Real-Time PCR System software v2.3 (Applied Biosystems, Foster City, CA) (Supplemental Table 2). Preamplification, exonuclease treatment, and qPCR dynamic array based on microfluidic technology were implemented as recently reported,[36] following manufacturer's instructions using the Biomark System and the Real-Time PCR Analysis Software (Fluidigm).

Western blotting. PCa cells were processed to analyze protein levels by western blot after 24 hours of pladienolide-B exposure, as previously described.[9] Briefly, 200,000 cells were seeded in 12-well plates and after 2 days, proteins were extracted using prewarmed (65˚C) SDS-DTT buffer (62.5 mM Tris-HCl, 2% SDS, 20% glycerol, 100 mM DTT, and 0.005% bromophenol

blue). Then, proteins were sonicated for 10 seconds and boiled for 5 minutes at 95°C. Proteins were separated by SDS-PAGE and transferred to nitrocellulose membranes (Millipore, Billerica, MA). Membranes were blocked with 5% nonfat dry milk in Tris-buffered saline/0.05% Tween 20 and incubated overnight with the specific antibodies for phospho-AKT (#4060S, Cell Signaling), phospho-ERK (#4370S, Cell Signaling), phospho-JNK (AF1205, R&D-Systems, Abingdon, UK), phospho-p53 (CS92845, Cell Signaling), AR (ab133273, Abcam), AR-v7 (ab198394, Abcam), TUBB (#2128S, Cell Signaling) as well as with the appropriate secondary antibodies: HRP-conjugated goat antirabbit IgG (#7074S, Cell Signaling) or HRP-conjugated rabbit antigoat IgG (#31753, ThermoFisher). Proteins were detected using an enhanced chemiluminescence detection system (GEHealthcare, Madrid, Spain) with dyed molecular weight markers (Bio-Rad, Madrid, Spain). A densitometry analysis of the bands obtained was carried out with ImageJ software, using TUBB protein levels as normalizing factor.

Statistical analysis. Statistical differences between 2 variables were calculated by unpaired parametric *t* test and nonparametric Mann-Whitney *U* test, according to normality, assessed by Kolmogorov-Smirnov test. For differences among 3 variables, one-way ANOVA analysis was performed. Spearman's or Pearson's bivariate correlations were performed for quantitative variables according to normality. Significant relation between categorized *SF3B1* mRNA expression and biochemical PCa recurrence was studied using the long-rank *P* value method with SPSS version 17.0. The rest of the statistical analyses were assessed using GraphPad Prism 7 (GraphPad Software, La Jolla, CA). Heatmaps were obtained from MetaboAnalyst 4.0.[37] All the experiments were performed in at least 3 experiments ($n \geq 3$), and with at least 2 technical replicates. Statistical significance was considered when $P < 0.05$. A trend for significance was indicated when *P* values ranged between >0.05 and <0.1.

RESULTS

SF3B1 is overexpressed in PCa and associated with aggressive features. *SF3B1* mRNA levels were significantly elevated in PCa compared to control (N-TAR) tissues (Fig 1a) from a cohort of patients with clinically localized PCa ($n = 84$; Table 1). Consistently, IHC analyses revealed that SF3B1 levels were higher in tumor glands compared to nontumor adjacent regions (Fig 1b and c). Notably, *SF3B1* expression was positively correlated with Gleason Score (Fig 1d) and directly associated with vascular and perineural invasion (Fig 1e and f). Furthermore, higher expression levels of *SF3B1* were associated with higher risk of developing PCa biochemical recurrence (Fig 1g).

In an independent cohort of highly aggressive PCa (Table 2), *SF3B1* expression was also positively correlated with Gleason score (Fig 1h) and tended to be higher in primary PCa samples from patients with metastasis compared to those without metastasis ($P = 0.067$; Fig 1i). Interestingly, *SF3B1* expression was directly correlated with *AR-v7* expression (Fig 1j), but not with *AR* expression (Supplemental Fig 1a), and tended to be positively correlated with the expression of the recently reported oncogenic splicing variant altered in PCa, *In1-ghrelin* ($P = 0.083$; Fig 1j), but not with ghrelin expression (Supplemental Fig 1b), as well as with *KLK3* expression ($P = 0.067$; Fig 1j). Consistently, a positive correlation between *SF3B1* mRNA levels and Gleason score as well as a clear association between higher expression levels of *SF3B1* and PCa with stage ≥T3b and biochemical recurrence was found in the TCGA dataset (Supplemental Fig 1c). Moreover, *SF3B1* expression was significantly higher in all PCa cell lines (androgen-dependent LNCaP and androgen-independent 22Rv1, DU145, and PC-3) compared to the normal-like RWPE-1 cell line (Fig 1k).

Pharmacological blockade of SF3B1 with pladienolide-B reduces malignant features of PCa cells. Initial screening using different concentrations of pladienolide-B (10^{-7} to10^{-11} M) and times of incubation (24−72 hours) indicated that a 10^{-7} M dose of pladienolide-B was more potent in reducing proliferation rate in 22Rv1 compared to RWPE-1 at any given time (Supplemental Fig 2); therefore, a 10^{-7} M dose was selected for further experiments. We found that proliferation rate was clearly decreased in all cell lines tested, and that the antiproliferative effect was consistently more pronounced in all PCa cell lines (LNCaP, 22Rv1, DU145, and PC-3) compared to RWPE-1 cell line (Fig 2a). In line with these results, the silencing of *SF3B1* expression also decreased the proliferation rate of LNCaP, 22Rv1, and DU145 cells at 24, 48, and 72 hours of incubation (Supplemental Fig 3).

Moreover, pladienolide-B markedly reduced the viability rate of primary cells derived from nontumor and tumor prostate tissues at 24, 48, and 72 hours of incubation, being this effect significantly more pronounced in PCa cells compared to nontumor control prostate cells (Fig 2b). Pladienolide-B also exerted a clear increase in the apoptotic rate in all PCa cell lines tested but not in RWPE-1 cell line after 24 hours of incubation (Fig 2c). In line with this latter result, we also had the opportunity to test whether the effect of pladienolide-B on apoptosis rate might be linked to alteration in p53 signaling in LNCaP cells. The results clearly indicated that pladienolide-B markedly increased the phosphorylation levels of p53 in LNCaP cells

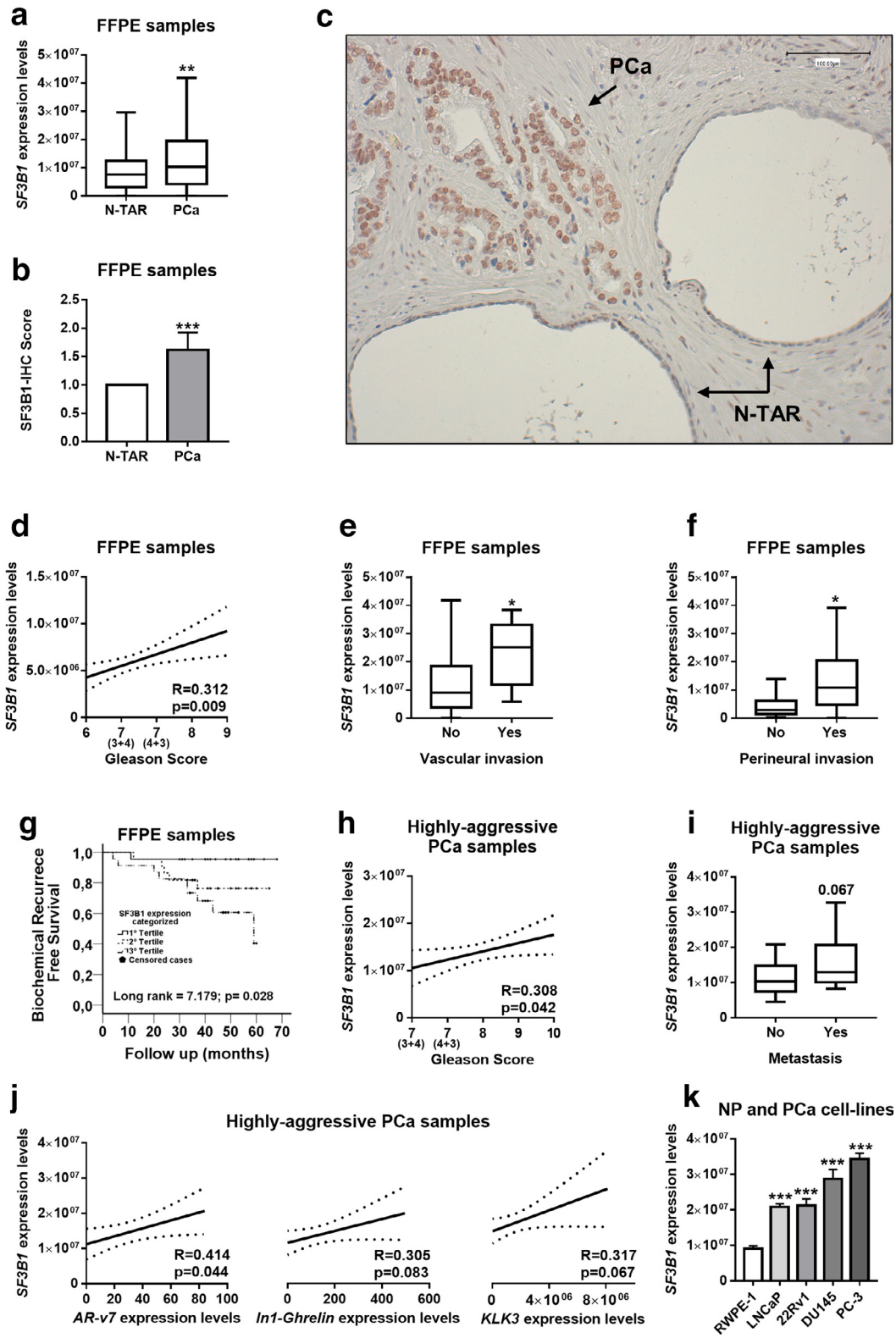

Fig 1. Expression of *SF3B1* in human samples and cell lines. (a) Comparison of *SF3B1* mRNA levels between formalin-fixed paraffin embedded (FFPE) samples from PCa tissues and nontumor adjacent regions (N-TAR) (n = 84). (b) Comparison of SF3B1 protein levels by immunohistochemistry (IHC) between PCa glands and N-TAR from a representative set of FFPE samples (n = 13). Data are represented as mean ± SEM. (c)

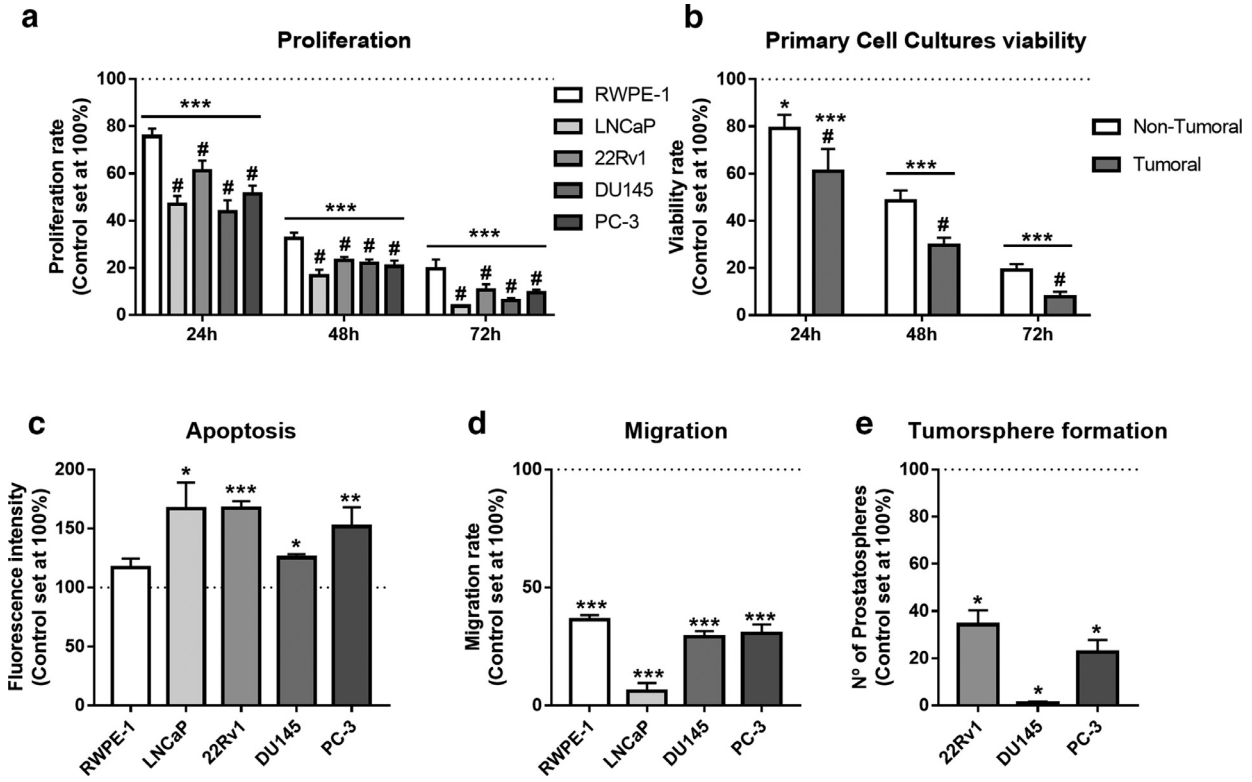

Fig 2. Functional consequences in response to pladienolide-B treatment in normal and tumor prostate cells. (a) Proliferation rate of normal prostate (RWPE-1) and PCa (LNCaP, 22Rv1, DU145, and PC-3) cell lines after 24, 48, and 72 hours of 10^{-7} M pladienolide-B treatment (n = 4). (b) Viability rate of primary normal prostate and PCa cells after 24, 48, and 72 hours of 10^{-7} M pladienolide-B treatment (n = 4). (c) Differences in apoptosis rate of normal prostate and PCa cell lines after 24 hours of 10^{-7} M pladienolide-B treatment (n = 3). (d) Differences in migration rate of normal prostate (RWPE-1) and PCa (LNCaP, DU145, and PC-3) cell lines after 12 hours of pladienolide-B 10^{-7} M treatment (n = 4). (e) Number of tumorspheres of high aggressive PCa (22Rv1, DU145, and PC-3) cell lines after 10 days of 10^{-7} M pladienolide-B incubation (n = 3). Data were represented as percent of vehicle-treated control cells (mean ± SEM). Asterisks (*$P < 0.05$; **$P < 0.01$, and ***$P < 0.001$) indicate statistically significant differences between pladienolide-B treatment and vehicle-treated control cells, while dash ($^{\#}P < 0.05$) indicates statistically significant differences of pladienolide-B effect between PCa cells and normal prostate cells.

(Supplemental Fig 4). Additionally, pladienolide-B treatment exerted an antimigratory effect on all the cell lines tested (RWPE-1, LNCaP, DU145, and PC-3) after 12 hours of incubation compared to vehicle-treated control cells (Fig 2d). Most importantly, pladienolide-B also decreased cell stemness-like capacity of 22Rv1, DU145, and PC-3 PCa cell lines since this treatment induced a significantly lower number of tumorspheres formation after 10 days of incubation compared to vehicle-treated cells (Fig 2e).

Pharmacologic blockade of SF3B1 with pladienolide-B modulates key signaling pathways and malignancy

Representative image of SF3B1 IHC at 200× magnification, showing PCa glands and N-TARs. Scale bar indicates 100 μm. (d) Correlation of *SF3B1* expression levels and Gleason score (GS) in FFPE samples (n = 84). (e and f) Association between *SF3B1* expression levels and vascular invasion (e), and perineural invasion (f) in the same cohort of FFPE samples (n = 84). (g) Association between *SF3B1* expression levels and biochemical PCa recurrence in 67 samples from FFPE cohort (samples from patients who underwent adjuvant radiotherapy were not included in the analysis). (h) Correlation of *SF3B1* expression levels and GS in a cohort of fresh samples from patients with highly aggressive PCa (n = 42). (i) Association between *SF3B1* expression levels and the presence of metastasis in the cohort of highly aggressive PCa patients (n = 42). (j) Correlation of *SF3B1* with *AR-v7, In1-ghrelin*, and *KLK3* expression levels in the highly aggressive PCa cohort (n = 42). (k) Comparison of *SF3B1* expression levels between a nontumor prostate cell line (RWPE-1) and PCa cell lines LNCaP, 22Rv1, DU145, and PC-3 (n = 5). Absolute mRNA levels were determined by qPCR and adjusted by normalization factor calculated from *ACTB* and *GAPDH* expression levels. Box plots represent the IQR ± the minimum and maximum values of the measure. Bar chart represent mean ± SEM. Asterisks (*$P < 0.05$; **$P < 0.01$; ***$P < 0.001$) indicate statistically significant differences between groups.

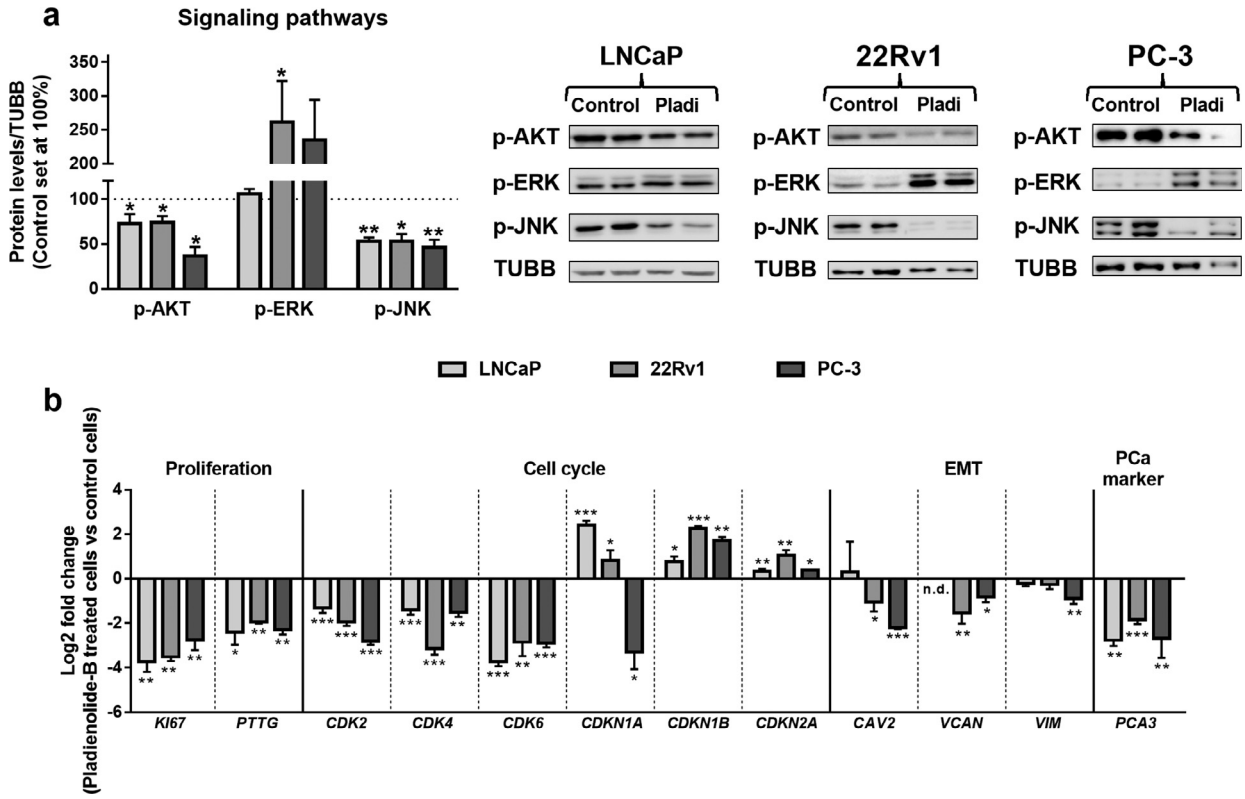

Fig 3. Molecular consequences of pladienolide-B treatment in PCa cells. (a) Protein levels of phospho-AKT, phospho-ERK1/2, and phospho-JNK in PCa cells (LNCaP, 22Rv1, and PC-3) after 24 hours of incubation with 10^{-7} M pladienolide-B compared to vehicle-treated cells (n = 4). Protein data were represented as percent of vehicle-treated control cells (mean ± SEM). Protein levels were normalized by TUBB protein levels. Representative images are shown in right panel. (b) Fold change of proliferation- (*KI67* and *PTTG*), cell cycle promoters and inhibitors (*CDK4, CDK6, CDKN1A, CDKN1B*, and *CDKN2A*), EMT- (*CAV2, VCAN*, and *VIM*) and aggressiveness (*PCA3)* markers in PCa cells (LNCaP, 22Rv1, and PC-3) treated with 10^{-7} M pladienolide-B for 24 hours (n = 5). mRNA levels were adjusted by normalization factor calculated from *ACTB* and *GAPDH* expression levels. mRNA data were represented as log2 of fold change of expression levels (treated/vehicle-treated cells; mean ± SEM). Asterisks (*$P < 0.05$; **$P < 0.01$, and ***$P < 0.001$) indicate statistically significant differences between pladienolide-B treatment and vehicle-treated control cells. Pladi: pladienolide-B. nd: non detected.

markers. Pladienolide-B treatment decreased AKT and JNK phosphorylation in LNCaP, 22Rv1, and PC-3 cell lines (Fig 3a). Particularly, 22Rv1 cells showed a statistically significant increase of ERK1/2 phosphorylation in response to pladienolide-B treatment as compared to vehicle-treated cells, whereas no statistically significant differences in ERK1/2 phosphorylation was found in LNCaP and PC-3 cell lines (Fig 3a). Moreover, pladienolide-B treatment significantly decreased the expression of proliferation markers (*KI67* and *PTTG*) and cell cycle promoters (*CDK2*, *CDK4*, and *CDK6*), whereas it clearly increased the expression of cell cycle suppressors (*CDKN1B* and *CDKN2A*) in LNCaP, 22Rv1, and PC-3 cells (Fig 3b). In the case of *CDKN1A*, pladienolide-B also exerted a profound upregulation in LNCaP and 22Rv1 cells, but a downregulation was observed in PC-3 cells (Fig 3b). Furthermore, pladienolide-B significantly downregulated the expression levels of genes involved in migration and/or epithelial-mesenchymal transition (EMT) such as *CAV2* and *VCAN* in the case of 22Rv1 and PC-3 cells and *VIM* in PC-3 cells as compared to vehicle-treated control cells (Fig 3b). Finally, a decrease in the expression levels of the PCa aggressiveness maker *PCA3* was also observed in response to pladienolide-B treatment in all PCa cell lines tested (LNCaP, 22Rv1, and PC-3; Fig 3b).

Pharmacologic blockade of SF3B1 with pladienolide-B modulates AR-v7 and In1-ghrelin expression. To test the possible effects of the pharmacologic blockade of SF3B1 with pladienolide-B over the expression of AR-v7, 2 *AR-v7*-expressing PCa cell lines (LNCaP and 22Rv1) were used (Supplemental Fig 5a). An initial assay in 22Rv1 cells revealed that pladienolide-B reduced *AR* and *AR-v7* expression dose dependently, being 10^{-7} M the most effective concentration (Supplemental Fig 5b). At this dose, pladienolide-B reduced both AR and AR-v7

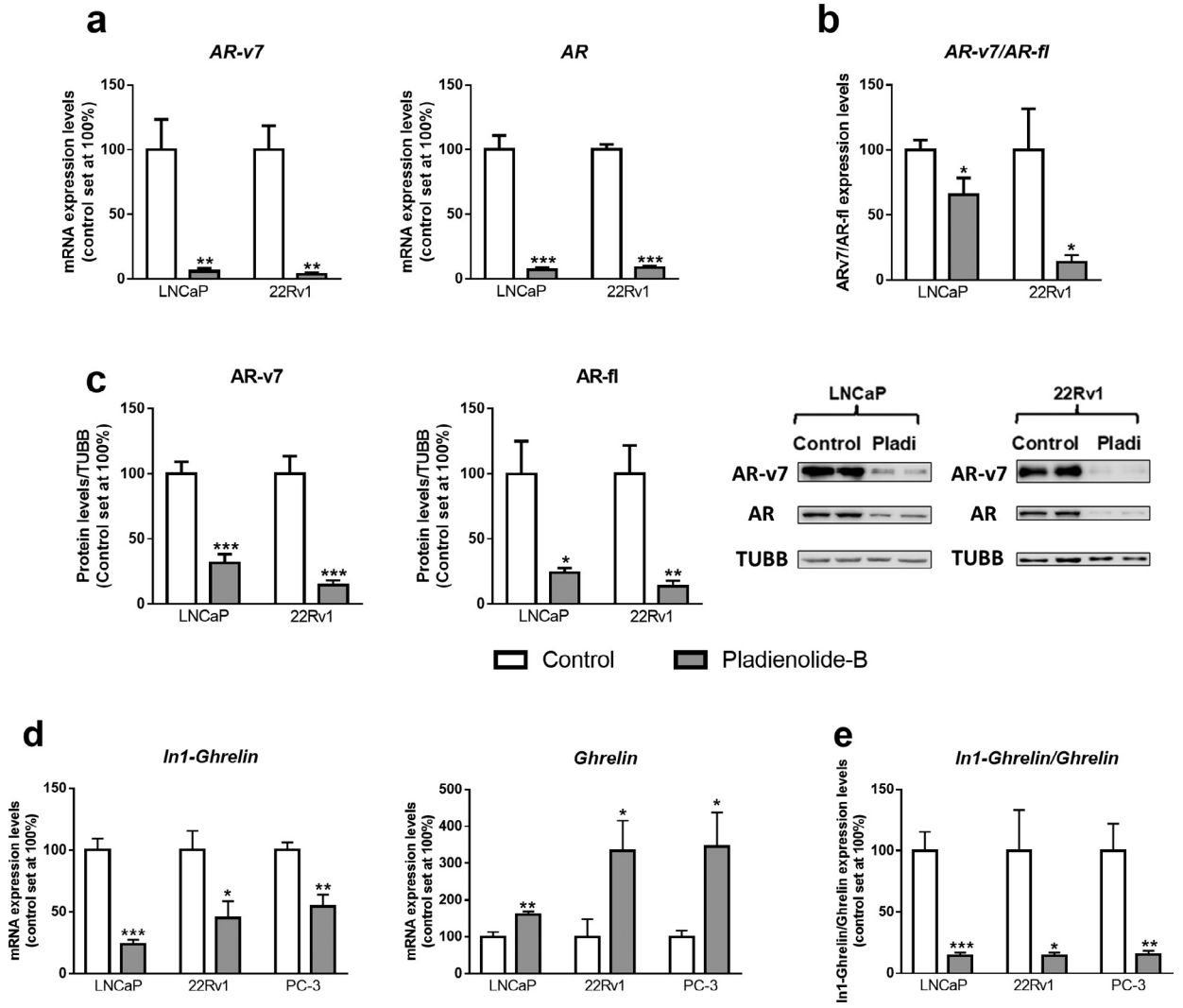

Fig 4. Dysregulation of mRNA expression and protein levels of oncogenic splicing variants in response to pladienolide-B. (a) mRNA expression levels of *AR-v7* (left panel) and *AR* (right panel) after pladienolide-B incubation in AR^{+}/AR-$v7^{+}$ PCa cells (LNCaP and 22Rv1). Absolute mRNA levels (n = 5) were determined by qPCR and adjusted by normalization factor calculated from *ACTB* and *GAPDH* expression levels. (b) Differences in the ratio of *AR-v7* and *AR* expression levels between PCa cells (LNCaP and 22Rv1) treated with pladienolide-B and vehicle-treated cells (n = 5). (c) Protein levels of AR-v7 (left panel) and AR (centered panel) after pladienolide-B incubation in LNCaP and 22Rv1 cells compared to vehicle-treated cells (n = 4). Data were normalized by TUBB protein levels. Representative images of western blot results were located at right panel. (d) mRNA expression levels of *In1-ghrelin* (left panel) and *ghrelin* (right panel) after pladienolide-B incubation in PCa cells LNCaP and 22Rv1. (e) Differences in the ratio of *In1-ghrelin/ghrelin* expression levels between PCa cells (LNCaP and 22Rv1) treated with pladienolide-B and vehicle-treated cells. The cells were incubated with 10^{-7} M pladienolide-B treatment for 24 hours in all cases. Data were represented as percent of control cells (mean ± SEM). Asterisks (*$P < 0.05$; **$P < 0.01$; ***$P < 0.001$) indicate statistically significant differences between groups.

expression in LNCaP and 22Rv1 cell lines (Fig 4a), which resulted in a decrease in the ratio between AR-v7 and AR (Fig 4b). In parallel, AR and AR-v7 protein levels were also reduced by pladienolide-B treatment in LNCaP and 22Rv1 cell lines (Fig 4c).

Interestingly, pladienolide-B treatment markedly reduced the expression of the oncogenic splice variant In1-ghrelin, while increasing that of native ghrelin in LNCaP, 22Rv1, and PC-3 cell lines (Fig 4d). Consequently, pladienolide-B treatment clearly decreased the ratio between In1-ghrelin/ghrelin expression in all PCa cell lines tested (Fig 4e).

Pharmacologic blockade of SF3B1 with pladienolide-B modulates the expression of spliceosome components and splicing factors. The expression pattern of several spliceosome components and associated SFs was

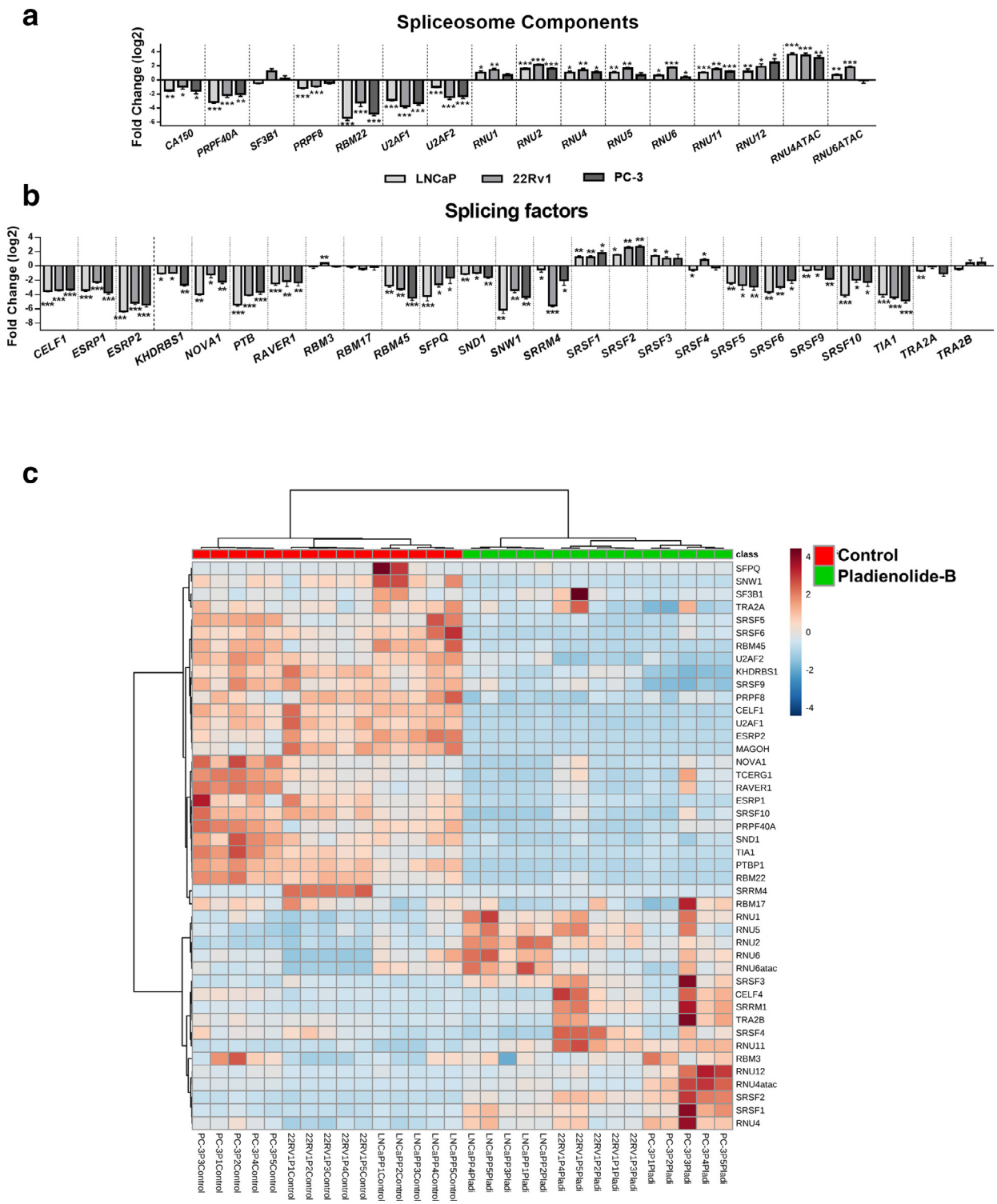

Fig 5. Dysregulation of spliceosome components and splicing factors expression by pladienolide-B treatment. mRNA expression levels of spliceosome components (a) and splicing factors (b) in PCa cells (LNCaP, 22Rv1, and PC-3) treated with 10^{-7} M pladienolide-B for 24 hours (n = 5). Data were represented as log2 of fold change of absolute mRNA levels (treated/vehicle-treated cells; mean ± SEM). (c) Heatmap showing nonsupervised hierarchical clustering of expression-pattern change of splicing machinery and splicing factors after 24 hours of pladienolide-B (10^{-7} M) treatment in LNCaP, 22Rv1, and PC-3 cell lines. Absolute mRNA levels have been scaled by autoscaling method to perform the heatmaps. Asterisks (*$P < 0.05$; **$P < 0.01$, and ***$P < 0.001$) indicate statistically significant differences between pladienolide-B treatment and vehicle-treated control cells.

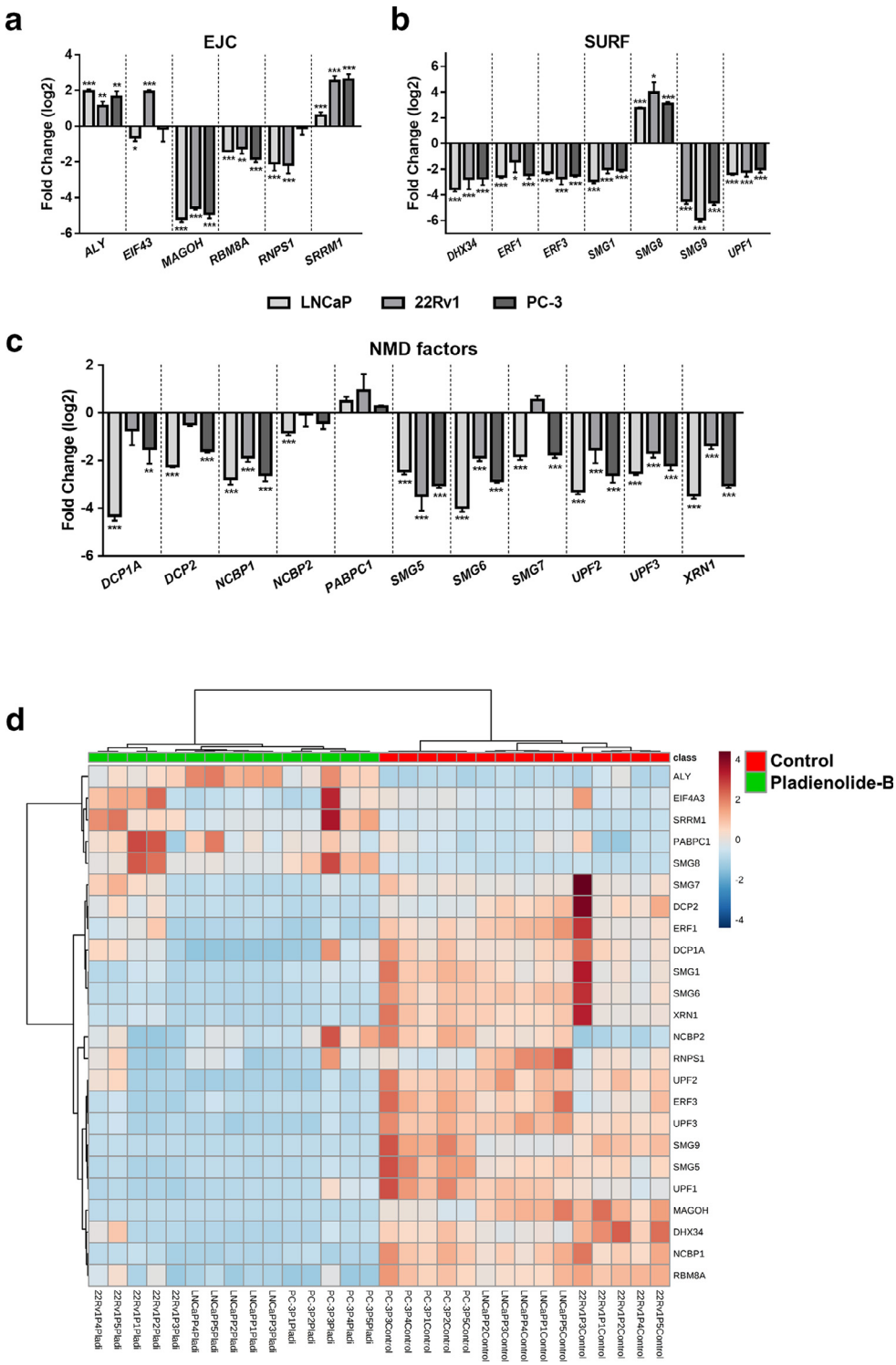

Fig 6. Pladienolide-B effects on the expression of EJC-, SURF-, and NMD-related genes in PCa cells. mRNA expression levels of EJC (a) and SURF (b) components, and associated NMD factors (c) expression after pladienolide-B treatment (10^{-7} M; 24 hours; n = 5) in PCa cells (LNCaP, 22Rv1, and PC-3). Data were represented as log2 of fold change of absolute mRNA levels (treated/vehicle-treated cells; mean ± SEM). (d) Heatmap showing nonsupervised hierarchical clustering of expression-pattern change of EJC-, SURF-, and NMD-related genes in LNCaP, 22Rv1, and PC-3 cell lines. Absolute mRNA levels have been scaled by autoscaling method to perform the heatmaps. Asterisks (*$P < 0.05$; **$P < 0.01$, and ***$P < 0.001$) indicate statistically significant differences between pladienolide-B treatment and vehicle-treated control cells.

consistently altered in response to pladienolide-B treatment in all PCa cell lines tested (Fig 5a and b). Furthermore, nonsupervised hierarchical clustering analyses showed that the expression pattern of these spliceosome components and SFs precisely discriminated between LNCaP, 22Rv1, and PC-3 cells treated or not with pladienolide-B (Fig 5c and Supplemental Fig 6). Specifically, the expression of the spliceosome components *CA150* (also known as *TCERG1*), *PRPF40A* (also known as *FBP11*), *PRPF8, RBM22, U2AF1*, and *U2AF2* were found to be consistently and significantly increased, while those of *RNU1, RNU2, RNU4, RNU5, RNU6, RNU11, RNU12*, and *RNU4ATAC* were decreased in response to pladienolide-B treatment in LNCaP, 22Rv1, and PC-3 cell lines (Fig 5a). Interestingly, significant changes were not found in *SF3B1* expression in any of the PCa cell lines tested in response to pladienolide-B exposure (Fig 5a). On the other hand, the treatment with pladienolide-B produced an upregulation of the SFs *SRSF1, SRSF2*, and *SRSF3*, whereas *CELF1, ESRP1, ESRP2,* and *KHDRBS1* (also known as SAM68), *NOVA1, PTB, RAVER1, RBM45, SFPQ, SND1, SNW1, SRRM4, SRSF5, SRSF6, SRSF9, SRSF10*, and *TIA1* were significantly downregulated in response to pladienolide-B in LNCaP, 22Rv1, and PC-3 cell lines (Fig 5b).

Pharmacologic blockade of SF3B1 with pladienolide-B modulates the expression of EJC and SURF components and NMD factors. The expression pattern of EJC and SURF components, as well as NMD-associated factors, was dramatically dysregulated in response to pladienolide-B treatment in LNCaP, 22Rv1, and PC-3 cells (Fig 6a–c, respectively). Moreover, expression pattern of EJC and SURF components as well as NMD-associated factors precisely discriminated between LNCaP, 22Rv1, and PC-3 cells treated or not with pladienolide-B (Fig 6d and Supplemental Fig 7). Specifically, EJC components *MAGOH* and *RBM8A* were significantly downregulated, whereas *ALY* and *SRRM1* were upregulated in LNCaP, 22Rv1, and PC-3 cell lines in response to pladienolide-B treatment (Fig 6a). On the other hand, pladienolide-B treatment evoked an upregulation of *SMG8* expression, while the genes coding for the rest of SURF components were found to be clearly downregulated (*DHX34, ERF1, ERF3, SMG1, SMG9*, and *UPF1*) in LNCaP, 22Rv1, and PC-3 cell lines (Fig 6b). Finally, NMD factors *NCBP1, SMG5, SMG6, UPF2, UPF3*, and *XRN1* were significantly and consistently downregulated in LNCaP, 22Rv1, and PC-3 cell lines in response to pladienolide-B treatment (Fig 6c). Interestingly, although *SMG7, DCP1A*, and *DCP2* were dramatically decreased in response to this drug in LNCaP and PC-3 cell lines, nonstatistically significant results were found in 22Rv1 cells (Fig 6c).

DISCUSSION

PCa is one of the most frequent cancer-related pathologies among male population in developed countries[1] and commonly progresses from indolent stages to the most aggressive phenotype of the disease, CRPC.[38] Although certain drugs (eg, antiandrogens/abiraterone/enzalutamide/chemotherapy, etc.) have been shown to improve the outcome of PCa patients and the overall survival in CRPC patients,[39,40] this latter pathology remains lethal nowadays. Consequently, new therapeutic targets are urgently required to tackle PCa and CRPC. In this context, dysregulation of alternative splicing and expression of aberrant splice variants are increasingly recognized as an important hallmark of cancer, including PCa.[41] Accordingly, we sought to evaluate the expression of a pivotal SF, *SF3B1,* in PCa samples and to explore the consequences of its blockade with the inhibitor pladienolide-B using *in vitro* models. Specifically, SF3B1 participates in the U2-snRNP complex and is involved in the assembly of the spliceosome,[42] the machinery that governs and catalyzes the splicing process.[12] Of note, although *SF3B1* mutations have been reported in PCa by some studies,[19,43] the pattern of *SF3B1* expression in PCa remained unreported, and its potential as an actionable functional target in PCa has not been addressed yet. Herein, we demonstrate for the first time that SF3B1 is overexpressed (at mRNA/protein levels) in PCa samples compared to nontumor adjacent regions. Furthermore, *SF3B1* expression levels were associated with important aggressiveness features (ie, Gleason score, presence of metastasis, biochemical recurrence, etc.) of PCa in 3 independent cohorts (clinically localized PCa, highly aggressive PCa, and TCGA database) suggesting that SF3B1 might represent a new prognostic biomarker in PCa.

SF3B1 activity can be pharmacologically blocked by available drugs, as is the case of pladienolide-B.[20] Indeed, pladienolide-B blockade of SF3B1 has been previously shown to exert antitumor effects in a reduced number of cancer cell types.[21,23,44] However, its putative action on PCa cells remained unknown hitherto. The present study demonstrates that pladienolide-B treatment is able to reduce functional aggressiveness features of PCa cell lines (eg, cell-proliferation, migration, and tumorsphere formation) as well as to decrease the viability rate of primary cells derived from PCa tissues. In addition, pladienolide-B treatment increased the apoptotic rate of PCa cell lines, wherein this effect (at least in LNCaP cells) might be associated with an increase in the p53 signaling pathway (ie, elevated phosphorylation levels of p53), an observation that is supported by a previous study by Huang et al, demonstrating that SF3B1 knockdown in human CD34+ cells lead to increased apoptosis and activation of p53 pathway.[45] Remarkably, the

antiproliferative and proapoptotic effects exerted by pladienolide-B were more pronounced in PCa cells compared to control nontumor prostate cells, as has been previously described for other SF3B1 inhibitors in different tumor-derived cells,[22,46] reinforcing the notion of a potential therapeutic role of pladienolide-B in PCa and CRPC. Indeed, these additional SF3B1 inhibitors have been reported to exert their main effects through the inhibition of the aberrant splicing variant AR-v7,[47] which has emerged as one of the main drivers of CRPC development,[48] as well as its distinctive resistance to Abiraterone and Enzalutamide.[7] Remarkably, we found that *SF3B1* and *AR-v7* (but not *AR*) expression levels were correlated in our cohort of highly aggressive PCa samples and that the blockade of SF3B1 activity by pladienolide-B resulted in a decrease of AR-v7/AR ratio at both, mRNA and protein levels. These results indicate that SF3B1 could participate in the control of *AR-v7* expression through the dysregulation of *AR* splicing process. The *AR-v7* expression modulation exhibited by pladienolide-B and other splicing inhibitors with antitumor effects on CRPC cells, as thailanstatins,[47] represents a critically relevant feature from a clinical perspective. However, splicing inhibitors other than pladienolide-B might present a limitation in their use, which could be restricted only to CRPCs patients with positive *AR-v7* expression. In striking contrast, we have observed that pladienolide-B consistently reduced the aggressiveness and altered the expression of numerous tumor markers in all the PCa cell lines tested herein, regardless of their *AR-v7* expression, providing suggestive evidence that pladienolide-B could represent a therapeutic option in all PCa subtypes (ie, those with or without *AR-v7* expression).

Mechanistically, this broad antitumor activity exhibited by pladienolide-B in all PCa cells tested may be explained by its capacity to modulate an ample repertoire of molecular events in the target cells. First, we have demonstrated herein that blockade of SF3B1 activity by the use of pladienolide-B markedly reduced AKT and JNK phosphorylation levels. It is widely known that PI3K/AKT and JNK pathways are associated with oncogenic processes, such as proliferation, migration, or invasion in several cancer types, including PCa.[49,50] Indeed, inhibition of PI3K/AKT signaling has been postulated as a potential therapeutic approach to combat PCa, especially CRPC.[51] Intriguingly, pladienolide-B treatment increased ERK phosphorylation only in 22Rv1-cells, presumably leading to a higher activation of MAPK/ERK pathway, which has been reported to be highly susceptible to be dysregulated in response to splicing changes.[52] Nevertheless, and despite the well-known oncogenic actions of MAPK-ERK pathway,[53] this pathway is also involved in selective protein degradation, increasing cell senescence and therefore, exerting antitumor effects under certain conditions.[54] In any case, the strong inactivation of these PI3K/AKT and JNK oncogenic pathways in response to pladienolide-B treatment, together with the fact that the expression of many aggressiveness markers such as *KI67, CAV2*, and *PCA3*, which are closely related to PCa aggressiveness,[55-57] was consistently reduced in all PCa cell lines tested in response to pladienolide-B treatment, may explain and reinforce the antitumor effect of targeting SF3B1 with pladienolide-B.

In addition, our results also demonstrated that, as expected, pladienolide-B treatment altered the splicing process of certain genes with oncogenic potential. Indeed, pladienolide-B treatment did not only alter the splicing of the widely known *AR* gene, leading to a pathologically relevant repression of the oncogenic AR-v7, but also decreased the expression of the less studied *In1-ghrelin* variant in PCa cells, an alternative splicing variant of the ghrelin gene with a strong oncogenic role in PCa.[8] This parallelism further underscores the capacity of pladienolide-B to inhibit aberrant splicing processes.

Finally, we have also shown that in addition to modulating signaling pathways, tumor molecular markers and oncogenic splicing variants, pladienolide-B was associated with the modulation of the expression of multiple genes involved in the main processes controlling the homeostasis of splicing variants (ie, splicing[12] and NMD[13]). Specifically, we found that the expression of a relevant proportion of the spliceosome components, SFs, EJC/SURF components, and NMD-associated factors analyzed herein was dramatically altered by pladienolide-B, suggesting that the "counter-dysregulation" of splicing variants that occurs in response to SF3B1 blockade could be due, at least in part, to the modulation of the expression of several factors involved in the control of mRNA processing. This hypothesis is reinforced by the fact that some of the SFs found to be altered by pladienolide-B treatment have been related to the generation of AR-v7 and therefore, associated with CRPC development, such as *SFPQ/PSF*,[58] *KHDRBS1/SAM68*,[59] and *U2AF2/U2AF65*,[60] but also by the fact that additional studies have demonstrated that the blockade of SF3B1 using other inhibitors resulted in a clear dysregulation of the expression of multiple genes, including SFs.[61] In contrast, the role of the NMD process in cancer, including PCa, is still controversial, since this process is able to eliminate tumor-suppressor transcripts but also alternative oncogenic splicing variants, which are commonly upregulated in cancer.[62] Inasmuch as SF3B1 blockade led to the suppression of several NMD-associated factors in our study, it is tempting to speculate that this inhibition, coupled to spliceosome alteration, could cause the decrease in aggressiveness features of PCa cells through both direct and indirect mechanisms,

possibly involving the modulation of different types of cellular stress processes (eg, ER stress, reactive oxygen species). Although elucidation of these possibilities would obviously require further experimental work, it is important to note that, to the best of our knowledge, the role of spliceosome and NMD components has not been extensively explored hitherto in PCa, and therefore, the present study opens a new possible avenue of research in PCa pathogenesis and aggressiveness.

Taken together, our results demonstrate that SF3B1 is overexpressed in PCa samples and associated with key aggressive features (ie, Gleasonscore, presence of metastasis and PCa recurrence, etc.), and its expression levels are directly correlated with the expression of several oncogenic splicing variants previously demonstrated to be associated with PCa aggressiveness (ie, *AR-v7*[63] and *In-ghrelin*[8]), thus suggesting that dysregulations in *SF3B1* expression could be involved in the development, progression, and aggressiveness of PCa and lending credence to the notion that SF3B1 could represent a new prognostic biomarker and a therapeutic target in this devastating pathology. Indeed, we show here that pladienolide-B, a selective inhibitor of SF3B1 activity, exerts potent antitumor actions in a battery of PCa cell lines, through the modulation of an ample repertoire of molecular events (signaling pathways, tumor markers, splicing variants, and mRNA homeostasis-associated machineries), providing convincing evidence for the putative utility of this drug as novel therapeutic tool for the treatment of PCa and CRPC.

ACKNOWLEDGMENTS

Conflicts of Interest: All authors have read the journal's authorship agreement and policy on conflicts of interest and have no conflicts of interest to declare.

This work was funded by Instituto de Salud Carlos III, co-funded by European Union (ERDF/ESF, "Investing in your future") [PI16/00264, PI17/02287, CP15/00156, CM16/00180, FI17/00282], FEDER (CCB.030PM), MINECO/MECD (BFU2016-80360-R, FPU16/06190, FPU17/00263, FPU16/05059), Junta de Andalucía (BIO-0139), and CIBERobn.

SUPPLEMENTARY MATERIALS

Supplementary material associated with this article can be found, in the online version, at doi:10.1016/j.trsl.2019.07.001.

REFERENCES

1. Bray F, Ferlay J, Soerjomataram I, Siegel RL, Torre LA, Jemal A. Global cancer statistics 2018: GLOBOCAN estimates of incidence and mortality worldwide for 36 cancers in 185 countries. CA Cancer J Clin 2018;68:394–424.
2. Bournakis E, Efstathiou E, Varkaris A, et al. Time to castration resistance is an independent predictor of castration-resistant prostate cancer survival. Anticancer Res 2011;31:1475–82.
3. Dhingra R, Sharma T, Singh S, et al. Enzalutamide: a novel anti-androgen with prolonged survival rate in CRPC patients. Mini Rev Med Chem 2013;13:1475–86.
4. Fizazi K, Scher HI, Molina A, et al. Abiraterone acetate for treatment of metastatic castration-resistant prostate cancer: final overall survival analysis of the COU-AA-301 randomised, double-blind, placebo-controlled phase 3 study. Lancet Oncol 2012;13:983–92.
5. Taylor BS, Schultz N, Hieronymus H, et al. Integrative genomic profiling of human prostate cancer. Cancer Cell 2010;18:11–22.
6. Ladomery M. Aberrant alternative splicing is another hallmark of cancer. Int J Cell Biol 2013;2013:463786.
7. Antonarakis ES, Lu C, Wang H, et al. AR-V7 and resistance to enzalutamide and abiraterone in prostate cancer. N Engl J Med 2014;371:1028–38.
8. Hormaechea-Agulla D, Gahete MD, Jimenez-Vacas JM, et al. The oncogenic role of the In1-ghrelin splicing variant in prostate cancer aggressiveness. Mol Cancer 2017;16:146.
9. Hormaechea-Agulla D, Jimenez-Vacas JM, Gomez-Gomez E, et al. The oncogenic role of the spliced somatostatin receptor sst5TMD4 variant in prostate cancer. FASEB J 2017;31:4682–96.
10. Narla G, DiFeo A, Yao S, et al. Targeted inhibition of the KLF6 splice variant, KLF6 SV1, suppresses prostate cancer cell growth and spread. Cancer Res 2005;65:5761–8.
11. Carstens RP, Eaton JV, Krigman HR, Walther PJ, Garcia-Blanco MA. Alternative splicing of fibroblast growth factor receptor 2 (FGF-R2) in human prostate cancer. Oncogene 1997;15:3059–65.
12. Matera AG, Wang Z. A day in the life of the spliceosome. Nat Rev Mol Cell Biol 2014;15:108–21.
13. Lykke-Andersen S, Jensen TH. Nonsense-mediated mRNA decay: an intricate machinery that shapes transcriptomes. Nat Rev Mol Cell Biol 2015;16:665–77.
14. Wahl MC, Will CL, Luhrmann R. The spliceosome: design principles of a dynamic RNP machine. Cell 2009;136:701–18.
15. Stephens PJ, Tarpey PS, Davies H, et al. The landscape of cancer genes and mutational processes in breast cancer. Nature 2012;486:400–4.
16. Harbour JW, Roberson ED, Anbunathan H, Onken MD, Worley LA, Bowcock AM. Recurrent mutations at codon 625 of the splicing factor SF3B1 in uveal melanoma. Nat Genet 2013;45:133–5.
17. Biankin AV, Waddell N, Kassahn KS, et al. Pancreatic cancer genomes reveal aberrations in axon guidance pathway genes. Nature 2012;491:399–405.
18. Yoshida K, Sanada M, Shiraishi Y, et al. Frequent pathway mutations of splicing machinery in myelodysplasia. Nature 2011;478:64–9.
19. Armenia J, Wankowicz SAM, Liu D, et al. The long tail of oncogenic drivers in prostate cancer. Nat Genet 2018;50:645–51.
20. Yokoi A, Kotake Y, Takahashi K, et al. Biological validation that SF3b is a target of the antitumor macrolide pladienolide. FASEB J 2011;278:4870–80.
21. Sato M, Muguruma N, Nakagawa T, et al. High antitumor activity of pladienolide B and its derivative in gastric cancer. Cancer Sci 2014;105:110–6.
22. Hepburn LA, McHugh A, Fernandes K, et al. Targeting the spliceosome for cutaneous squamous cell carcinoma therapy: a role for c-MYC and wild-type p53 in determining the degree of tumour selectivity. Oncotarget 2018;9:23029–46.
23. Kashyap MK, Kumar D, Villa R, et al. Targeting the spliceosome in chronic lymphocytic leukemia with the macrolides FD-895 and pladienolide-B. Haematologica 2015;100:945–54.

24. Gao J, Aksoy BA, Dogrusoz U, et al. Integrative analysis of complex cancer genomics and clinical profiles using the cBioPortal. Sci Signal 2013;6:pl1.
25. Cerami E, Gao J, Dogrusoz U, et al. The cBio cancer genomics portal: an open platform for exploring multidimensional cancer genomics data. Cancer Discov 2012;2:401–4.
26. Pedraza-Arevalo S, Hormaechea-Agulla D, Gomez-Gomez E, et al. Somatostatin receptor subtype 1 as a potential diagnostic marker and therapeutic target in prostate cancer. Prostate 2017;77:1499–511.
27. Goldstein AS, Drake JM, Burnes DL, et al. Purification and direct transformation of epithelial progenitor cells from primary human prostate. Nat Protoc 2011;6:656–67.
28. Hormaechea-Agulla D, Gomez-Gomez E, Ibanez-Costa A, et al. Ghrelin O-acyltransferase (GOAT) enzyme is overexpressed in prostate cancer, and its levels are associated with patient's metabolic status: potential value as a non-invasive biomarker. Cancer Lett 2016;383:125–34.
29. Ugalde-Olano A, Egia A, Fernandez-Ruiz S, et al. Methodological aspects of the molecular and histological study of prostate cancer: focus on PTEN. Methods (San Diego, Calif) 2015;77-78:25–30.
30. Barentsz JO, Weinreb JC, Verma S, et al. Synopsis of the PI-RADS v2 guidelines for multiparametric prostate magnetic resonance imaging and recommendations for use. Eur Urol 2016;69:41–9.
31. Luque RM, Ibanez-Costa A, Neto LV, et al. Truncated somatostatin receptor variant sst5TMD4 confers aggressive features (proliferation, invasion and reduced octreotide response) to somatotropinomas. Cancer Lett 2015;359:299–306.
32. Ibanez-Costa A, Gahete MD, Rivero-Cortes E, et al. In1-ghrelin splicing variant is overexpressed in pituitary adenomas and increases their aggressive features. Sci Rep 2015;5:8714.
33. Duran-Prado M, Gahete MD, Hergueta-Redondo M, et al. The new truncated somatostatin receptor variant sst5TMD4 is associated to poor prognosis in breast cancer and increases malignancy in MCF-7 cells. Oncogene 2012;31:2049–61.
34. Sampedro-Nunez M, Luque RM, Ramos-Levi AM, et al. Presence of sst5TMD4, a truncated splice variant of the somatostatin receptor subtype 5, is associated to features of increased aggressiveness in pancreatic neuroendocrine tumors. Oncotarget 2016;7:6593–608.
35. Vandesompele J, De Preter K, Pattyn F, et al. Accurate normalization of real-time quantitative RT-PCR data by geometric averaging of multiple internal control genes. Genome Biol 2002;3:research0034.1.
36. Gahete MD, Del Rio-Moreno M, Camargo A, et al. Changes in splicing machinery components influence, precede, and early predict the development of type 2 diabetes: from the CORDIOPREV study. EBioMedicine 2018;37:356–65.
37. Chong J, Soufan O, Li C, et al. MetaboAnalyst 4.0: towards more transparent and integrative metabolomics analysis. Nucleic Acids Res 2018;46(W1):W486–w94.
38. Litwin MS, Tan HJ. The diagnosis and treatment of prostate cancer: a review. JAMA 2017;317:2532–42.
39. de Bono JS, Logothetis CJ, Molina A, et al. Abiraterone and increased survival in metastatic prostate cancer. N Engl J Med 2011;364:1995–2005.
40. Scher HI, Fizazi K, Saad F, et al. Increased survival with enzalutamide in prostate cancer after chemotherapy. N Engl J Med 2012;367:1187–97.
41. Paschalis A, Sharp A, Welti JC, et al. Alternative splicing in prostate cancer. Nat Rev Clin Oncol 2018;15:663–75.
42. Kramer A, Gruter P, Groning K, Kastner B. Combined biochemical and electron microscopic analyses reveal the architecture of the mammalian U2 snRNP. J Cell Biol 1999;145:1355–68.
43. Je EM, Yoo NJ, Kim YJ, Kim MS, Lee SH. Mutational analysis of splicing machinery genes SF3B1, U2AF1 and SRSF2 in myelodysplasia and other common tumors. Int J Cancer 2013;133:260–5.
44. Suda K, Rozeboom L, Yu H, et al. Potential effect of spliceosome inhibition in small cell lung cancer irrespective of the MYC status. PloS One 2017;12:e0172209.
45. Huang Y, Hale J, Wang Y, et al. SF3B1 deficiency impairs human erythropoiesis via activation of p53 pathway: implications for understanding of ineffective erythropoiesis in MDS. J Hematol Oncol 2018;11:19.
46. Effenberger KA, Urabe VK, Jurica MS. Modulating splicing with small molecular inhibitors of the spliceosome. Wiley Interdiscip Rev RNA 2017;8.
47. Wang B, Lo UG, Wu K, et al. Developing new targeting strategy for androgen receptor variants in castration resistant prostate cancer. Int J Cancer 2017;141:2121–30.
48. Hu R, Dunn TA, Wei S, et al. Ligand-independent androgen receptor variants derived from splicing of cryptic exons signify hormone-refractory prostate cancer. Cancer Res 2009;69:16–22.
49. Hubner A, Mulholland DJ, Standen CL, et al. JNK and PTEN cooperatively control the development of invasive adenocarcinoma of the prostate. Proc Natl Acad Sci U S A 2012;109:12046–51.
50. Chen H, Zhou L, Wu X, et al. The PI3K/AKT pathway in the pathogenesis of prostate cancer. Front Biosci (Landmark Ed) 2016;21:1084–91.
51. Sarker D, Reid AH, Yap TA, de Bono JS. Targeting the PI3K/AKT pathway for the treatment of prostate cancer. Clin Cancer Res 2009;15:4799–805.
52. Siegfried Z, Bonomi S, Ghigna C, Karni R. Regulation of the Ras-MAPK and PI3K-mTOR signalling pathways by alternative splicing in cancer. Int J Cell Biol 2013;2013:568931.
53. Burotto M, Chiou VL, Lee JM, Kohn EC. The MAPK pathway across different malignancies: a new perspective. Cancer 2014;120:3446–56.
54. Deschenes-Simard X, Gaumont-Leclerc MF, Bourdeau V, et al. Tumor suppressor activity of the ERK/MAPK pathway by promoting selective protein degradation. Genes Dev 2013;27:900–15.
55. Richardsen E, Andersen S, Al-Saad S, et al. Evaluation of the proliferation marker Ki-67 in a large prostatectomy cohort. PloS One 2017;12:e0186852.
56. Sugie S, Mukai S, Yamasaki K, Kamibeppu T, Tsukino H, Kamoto T. Significant association of caveolin-1 and caveolin-2 with prostate cancer progression. Cancer Genomics Proteomics 2015;12:391–6.
57. Wang Y, Liu XJ, Yao XD. Function of PCA3 in prostate tissue and clinical research progress on developing a PCA3 score. Chin J Cancer Res 2014;26:493–500.
58. Takayama KI, Suzuki T, Fujimura T, et al. Dysregulation of spliceosome gene expression in advanced prostate cancer by RNA-binding protein PSF. Proc Natl Acad Sci U S A 2017;114:10461–6.
59. Stockley J, Markert E, Zhou Y, et al. The RNA-binding protein Sam68 regulates expression and transcription function of the androgen receptor splice variant AR-V7. Sci Rep 2015;5:13426.
60. Liu LL, Xie N, Sun S, Plymate S, Mostaghel E, Dong X. Mechanisms of the androgen receptor splicing in prostate cancer cells. Oncogene 2014;33:3140–50.
61. Wu G, Fan L, Edmonson MN, et al. Inhibition of SF3B1 by molecules targeting the spliceosome results in massive aberrant exon skipping. RNA (New York, NY) 2018;24:1056–66.
62. Ni JZ, Grate L, Donohue JP, et al. Ultraconserved elements are associated with homeostatic control of splicing regulators by alternative splicing and nonsense-mediated decay. Genes Dev 2007;21:708–18.
63. Guo Z, Yang X, Sun F, et al. A novel androgen receptor splice variant is up-regulated during prostate cancer progression and promotes androgen depletion-resistant growth. Cancer Res 2009;69:2305–13.

Supplemental Table 1

Gene	Accession Number	Primer Sequence (Sense)	Primer Sequence (Antisense)	Product Size (bp)
AR	NM_000044.4	GCAGGAAGCAGTATCCGAAG	GTTGTCAGAAATGGTCGAAGTG	112
AR-v7	NM_001348061.1	CAGGGATGACTCTGGGAAAA	TGAGGCAAGTCAGCCTTTCT	87
MKI67	NM_002417	GACATCCGTATCCAGCTTCCT	GCCGTACAGGCTCATCAATAAC	139
PTTG1	NM_004219.2	GGCTGTTAAGACCTGCAATAATC	TTCAGCCCATCCTTAGCAAC	101
CDK2	NM_001798.4	GCTCTCACTGGCATTCCTCTT	GAGGTTTAAGGTCTCGGTGG	109
CDK4	NM_000075.3	ACAGTTCGTGAGGTGGCTTT	TACCTTGATCTCCCGGTCAG	111
CDK6	NM_001259.7	TCGATGAACTAGGCAAAGACC	GTCCTGGAAGTATGGGTGAGA	101
CDKN1A	NM_001291549.1	TGCCCAAGCTCTACCTTCC	CACATGGTCTTCCTCTGCTGT	116
CDKN1B	NM_004064.4	ATAAGGAAGCGACCTGCAAC	TTGGGGAACCGTCTGAAA	88
CDKN2A	NM_000077	GACATCCCCGATTGAAAGAA	CAGTTGTGGCCCTGTAGGA	91
CAV2	NM_001233	ACGACTCCTACAGCCACCAC	CAGCTTGAGATGCGAGTTGA	107
VCAN	NM_004385.4	CAAGCATCCTGTCTCACGAA	CATCAGTCCAACGGAAGTCA	111
VIM	NM_003380.4	CCAGGCAAAGCAGGAGTC	TTCAACGGCAAAGTTCTCTTC	133
PCA3	NR_132312.1	CAGAGGGGAGATTTGTGTGG	TGTCATCTTGCTGTTTCTAGTGATG	172
In1-Ghrelin	GU942497.1	TCTGGGCTTCAGTCTTCTCC	GTTCATCCTCTGCCCCTTCT	215
SF3B1	NM_012433.3	CAGTTCCGTCTGTGTGTTCG	GCTGCCTTCTTGCCTTGA	101
ACTB	NM_001101	ACTCTTCCAGCCTTCCTTCCT	CAGTGATCTCCTTCTGCATCCT	176
GAPDH	NM_002046	AATCCCATCACCATCTTCCA	AAATGAGCCCCAGCCTTC	122

Supplemental Table 1. Specific primers for human transcripts used in this study. NCBI accession number, primers sequences and expected product sizes are included.

Supplemetal Table 2

	Gene	Accession Number	Primer Sequence (Sense. Se)	Primer Sequence (Antisense. As)	Product Size
Spliceosome components	*CA150*	NM_006706.3	GAGGAGCCCAAAGAAGAGGA	CACCAGTCCAAACGACACAC	112
	PRPF40A	NM_017892.3	GCTCGGAAGATGAAACGAAA	TGTCCTCAAATGCTGGCTCT	130
	SF3B1	NM_012433.3	CAGTTCCGTCTGTGTGTTCG	GCTGCCTTCTTGCCTTGA	101
	PRPF8	NM_006445.3	TGCCCACTACAACCGAGAA	AGGCCCGTCCTTCAGGTA	139
	RBM22	NM_018047.2	CTCTGGGTTCCAACACCTACA	GGCACAGATTTTGCATTCCT	137
	RNU11	NR_004407.1	AAGGGCTTCTGTCGTGAGTG	CCAGCTGCCCAAATACCA	108
	U2AF1	NM_006758.2	GAAGTATGGGGAAGTAGAGGAGATG	TTCAAGTCAATCACAGCCTTTTC	120
	U2AF2	NM_007279.2	CTTTGACCAGAGGCGCTAAA	TACTGCATTGGGGTGATGTG	130
	RNU12	NR_029422.1	ATAACGATTCGGGGTGACG	CAGGCATCCCGCAAAGTA	106
	RNU1	NR_004430.2	ATCACGAAGGTGGTTTTCC	GCAGTCGAGTTTCCCACA	94
	RNU2	NR_002716.3	CTCGGCCTTTTGGCTAAGAT	TATTCCATCTCCCTGCTCCA	116
	RNU4	NR_003925.1	TCGTAGCCAATGAGGTCTATCC	AAAATTGCCAGTGCCGACTA	103
	RNU5	NR_002756.2	TGGTTTCTCTTCAGATCGCA	GTTGTTCCTCTCCACGGAAA	65
	RNU6	NR_004394.1	CGCTTCGGCAGCACATATA	AAAATATGGAACGCTTCACGAA	101
	RNU11	NR_004407.1	AAGGGCTTCTGTCGTGAGTG	CCAGCTGCCCAAATACCA	108
	RNU12	NR_029422.1	ATAACGATTCGGGGTGACG	CAGGCATCCCGCAAAGTA	106
	RNU4ATAC	NR_023343.1	GTTGCGCTACTGTCCAATGA	CAAAAATTGCACCAAAATAA	85
	RNU6ATAC	NR_023344.1	TGAAAGGAGAGAAGGTTAGCACTC	CGATGGTTAGATGCCACGA	112
Splicing Factors	*CELF1*	NM_006560.3	AACAGAAGAGAATGGCCCAGC	TGCTGAAGGAGTGCTAAATACTG	121
	CELF4	NM_020180.3	CCCCAGCAGCAGAGAGAA	GAAGCCGAAAGGGAGGAA	108
	ESRP1	NM_020180.3	TTTTGGGATCACTGCTGGGG	TGTCCCACCTTCTTGTTGGC	108
	ESRP2	NM_024939.2	AGAGCCCAGCAGTCAATTGTT	GTCTCACTGTCCACCACATCAG	96
	KHDRBS1	NM_006559.2	GAGCGAGTGCTGATACCTGTC	CACCAGTCTCTTCCTGCAGTC	106
	NOVA1	NM_002515.2	TACCCAGGTACTACTGAGCGAG	CTGGTTCTGTCTTGGCCACAT	124
	PTBP1	NM_002819.4	TGGGTCGGTTCCTGCTATT	CAGATCCCCGCTTTGTAC	111
	RAVER1	NM_133452.2	GTAACCGCCGCAAGATACTG	CGAAGGCTGTCCCTTTGTATT	126
	RBM3	NM_006743.4	AAGCTCTTCGTGGGAGGG	TTGACAACGACCACCTCAGA	98
	RBM17	NM_032905.4	CAAAGAGCCAAAGGACGAAA	TACATGCGGTGGAGTGTCC	107
	RBM45	NM_152945.3	CCCATCAAGGTTTTCATTGC	TTCCCGCAGATCTTCTTCTG	123
	SFPQ	NM_005066.2	TGGTAGGGGGTGAAAGTG	TTAAAAACAAGAAATGGGGAAATG	125
	SND1	NM_014390.3	ACTACGGCAACAGAGAGGTCC	GAAGGCATACTCCGTGGCT	101
	SNW1	NM_001318844.1	ATGCGTGCCCAAGTAGAGAG	TCCCCATCCTCTTTTTCCA	134
	SRRM4	NM_194286.3	CCTTCACCACCTCCTCAC	TTCGGCACATTCCAGACA	113
	SRSF1	NM_006924.4	TGTCTCTGGACTGCCTCCA	TGCCATCTCGGTAAACATCA	98
	SRSF2	NM_003016.4	TGTCCAAGAGGGAATCCAAA	GTTTACACTGCTTGCCGATACA	113
	SRSF3	NM_003017.4	TAACCCTAGATCTCGAAATGCATC	CATAGTAGCCAAAAGCCCGTT	117
	SRSF4	NM_005626.4	GGAACTGAAGTCAATGGGAGAA	CTTCGAGAGCGAGACCTTGA	110
	SRSF5	NM_001039465.1	GCAAAAGGCACAGTAGGTCAA	TTTGCGACTACGGGAACG	92
	SRSF6	NM_006275.5	AGACCTCAAAAATGGGTACGG	CTTGCCGTTCAGCTCGTAA	82
	SRSF9	NM_003769.2	CCCTGCGTAAACTGGATGAC	AGCTGGTGCTTCTCTCAGGA	87
	SRSF10	NM_006625.5	CTACACTCGCCGTCCAAGAG	CCGTCCACAAATCCACTTTC	103
	TIA1	NM_022037.2	TAAATCCCGTGCAACAGCAGA	TATGCAGGAACTTGCCAACCA	124
	TRA2A	NM_013293.4	TCAAAGGAGGCTATGGAAAGG	TGTGTGCGCTCTCTTGGTTA	90
	TRA2B	NM_004593.2	GATGATGCCAAGGAAGCTAAAG	AGGTAGGTCTCCCCATGTAAATTC	130
EJC	*ALYREF*	NM_005782.3	CTACAGCAGGCCAAAACAACT	AGTTTCCCACCTGTCTCCAC	96
	EIF4A3	NM_014740.4	CAGCCACCTTCAGTATCTCAGT	TGCACAGCCAACTCTCTTGT	97
	MAGOH	NM_002370.3	GCCAACAACAGCAATTACAAGA	TTATTCTCTTCAGTTCCTCCATCAC	88
	RBM8A	NM_005105.4	GATTATGACAGCGTGGAGCA	GTCTTCTTCGGTGGCTTCCT	108
	RNPS1	NM_080594.3	TCTTCTGGCTCTCCAAGTCC	CGCCTTTTCCTCTCCTTTTC	104
	SRRM1	NM_001303448.1	GTAGCCCAAGAAGACGCAAA	TGGTTCTGTGACGGGGAG	108
SURF	*DHX34*	NM_014681.5	AAACCGCCATCCTCTACCTC	CAGCATCTTCCCAATCACAA	116
	ERF1	NM_004730.3	GCACACTCCAAGGAAACACA	AAAACGCAAGGCTGACTGAC	95
	ERF3	NM_002094.4	TGATGGAGGAGGAAGAGGAA	TTGACTTGCCAGCATCTACG	117
	SMG1	NM_015092.4	GAGCCAAAGAGCAAGTCAGG	AGTTCAAATAACGCCGCATC	111
	SMG8	NM_018149.6	ACCAACAGGGCTTTATTCCA	AGCAGGCCAAGAGTTTGTGT	107
	SMG9	NM_019108.3	ATTGCTGCCTTCCTTTTCAC	GGCTTCACCATCTCTGCTGT	107
	UPF1	NM_001297549.1	CTGCACACCAAGCTCTACCA	CACACAGGACAGGATGATGAA	90
NMD Factors	*DCP1A*	NM_018403.6	AGACAGCAGCAGCAAGAGTG	AGGCTGCACAAATACTTCAGG	107
	DCP2	NM_152624.5	TATGACCCCCAAATCCAAAC	AATCTTCGAGAAAGCCAGTCC	96
	NCBP1	NM_002486.4	TGAAAGTCCCAAACCGAAGT	GCAGGACACAGAGCTGAGAA	114
	NCBP2	NM_007362.3	CGTCTGGATGACCGAATCA	TCGTAGTCCTGCCGATACTCA	116
	PABPC1	NM_002568.3	AGTTCGCAATCCTCAGCAAC	CCAACATGGAAGCAGTCAAA	104
	SMG5	NM_015327.2	CCCCTCATAGGATGCAAGAA	GGACAAATCCCCCAGATACA	102
	SMG6	NM_017575.4	CTGACTGCAAAAGGGTCACA	GCCACTGACACATACTTTCCAC	103
	SMG7	NM_173156.2	ATGAAACCGAGCAGCACAC	GCACAGGATGCCAAGAAAA	92
	UPF2	NM_080599.2	CAATGAACGGCAAGAACAAG	CTCCCTTCGGATGTTGGTAG	116
	UPF3	NM_023011.3	ACAGTCCAGCACCCAGAAAA	CTGTTTCCGCCACACTCTC	106
	XRN1	NM_019001.4	AGATTTTGATCGGGAGCACTT	CTTCTTCTGCTGCGACACCT	110
Hk	*ACTB*	NM_001101	ACTCTTCCAGCCTTCCTTCCT	CAGTGATCTCCTTCTGCATCCT	176
	GAPDH	NM_002046	AATCCCATCACCATCTTCCA	AAATGAGCCCCAGCCTTC	122
	HPRT	NM_000194.2	CTGAGGATTTGGAAAGGGTGT	TAATCCAGCAGGTCAGCAAAG	157

Supplemetal Table 2. Specific primers for human transcripts used in this study, including spliceosome components, associated splicing factors, exon junction complex (EJC) components, SMG-1–Upf1–eRF1–eRF3 (SURF) components, associated non-sense mediated mRNA decay (NMD) factors and three housekeeping genes (Hk) that were specifically designed and used in qPCR-based microfluidic assays. NCBI accesion number, primers sequences and expected product sizes for the genes studied are included.

Supplemental Figure 1

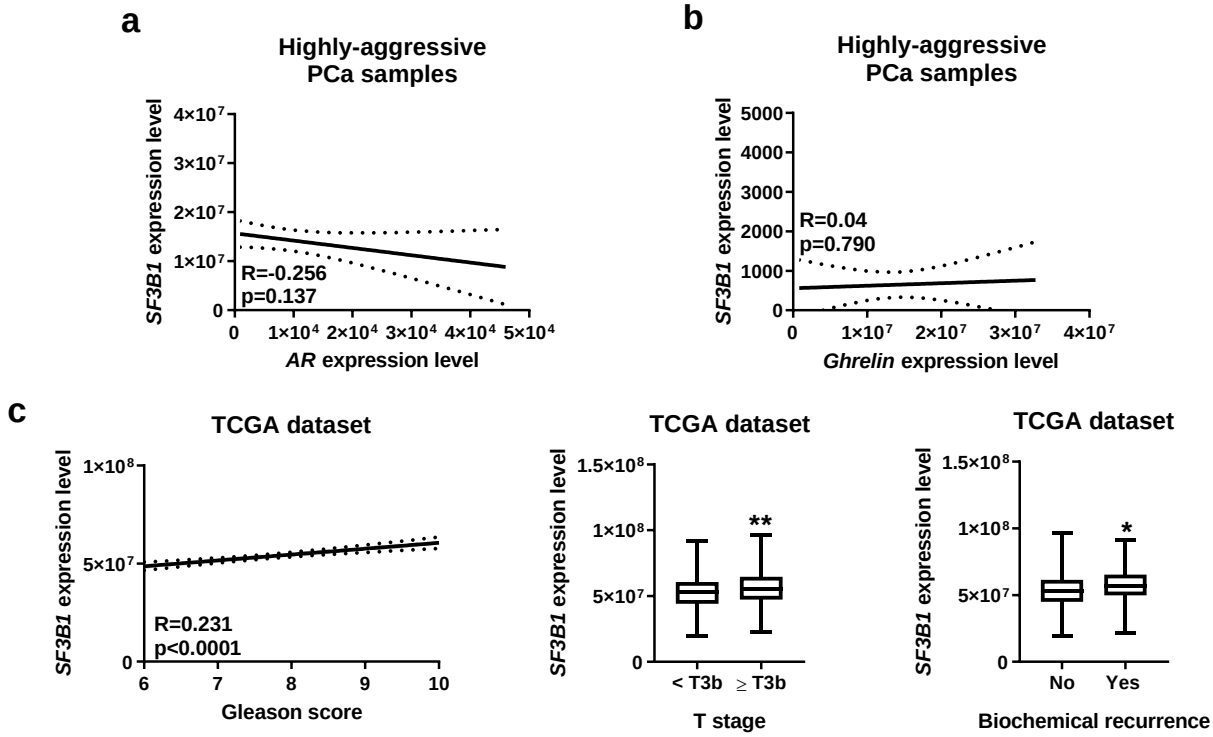

Supplemental Figure 1. Expression of SF3B1 in human samples. Correlation of SF3B1 expression levels with AR expression levels (**a**) and Ghrelin expression levels (**b**) in the highly-aggressive PCa cohort (n=42). mRNA levels were determined by qPCR and adjusted by normalization factor calculated from ACTB and GAPDH expression levels. **c**) Correlation between SF3B1 and Gleason score, primary tumor pathological staging (T stage) and biochemical recurrence in 497 PCa patients. Data were obtained from TCGA portal. Asterisks (* p <0.05; ** p <0.01) indicate statistically significant differences between groups. R: Pearson coefficient.

Supplemental Figure 2

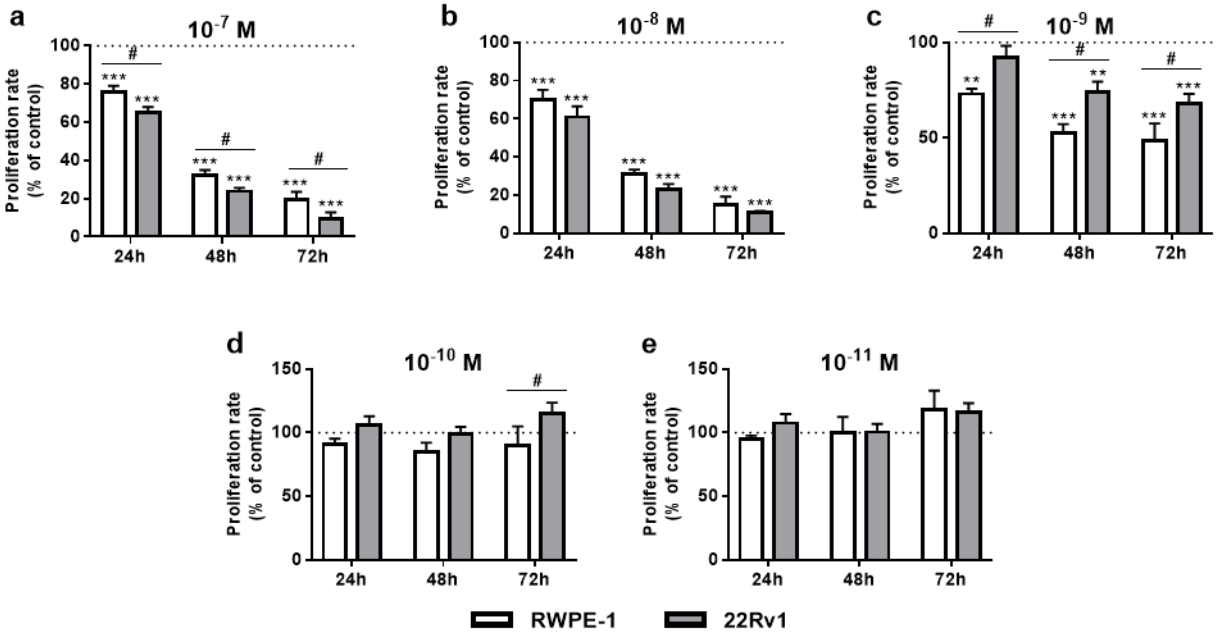

Supplemental Figure 2. Dose-response consequences of pladienolide-B treatment [10^{-7} (a), 10^{-8} (b), 10^{-9} (c), 10^{-10} (d) and 10^{-11} M (e)] on proliferation rate in RWPE-1 and 22Rv1 cells after 24-, 48- and 72 hours (n=4). Data were represented as percent of non-treated control cells. Asterisks (** $p < 0.01$ and *** $p < 0.001$) indicate statistically significant differences between pladienolide-B treatment and non-treated control cells while dash (# $p < 0.05$) indicates statistically significant differences of pladienolide-B effect between 22Rv1 cells and RWPE-1 cells.

Supplemental Figure 3

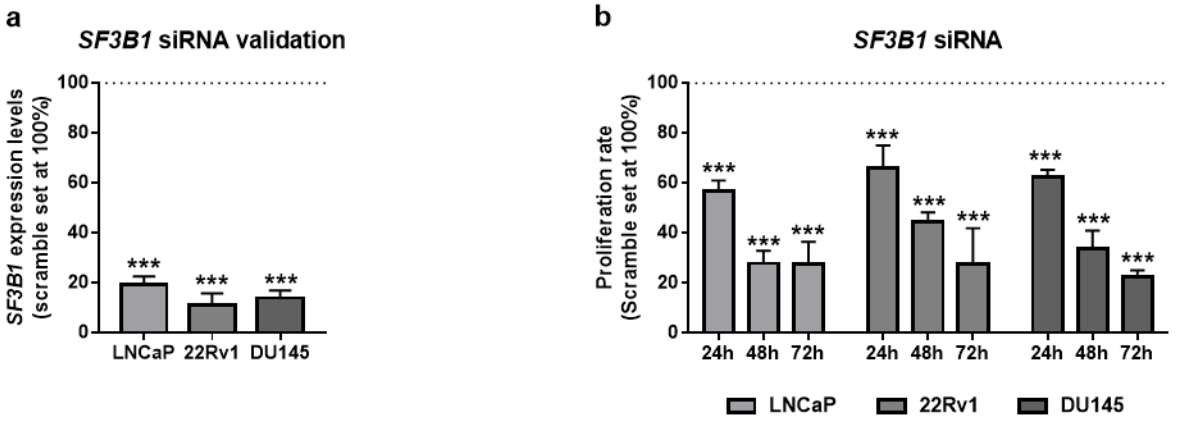

Supplemental Figure 3. Functional consequences of *SF3B1* silencing in prostate cancer-derived cell lines. **a)** Validation by qPCR of *SF3B1* silencing. mRNA levels were determined by qPCR and adjusted by normalization factor calculated from *ACTB* and *GAPDH* expression levels. **b)** Proliferation rate of LNCaP, 22Rv1 and DU145 cells after 24-, 48- and 72h of *SF3B1* silencing (n=3). Data were represented as percent of scramble cells (mean ± SEM). Asterisks (*** p <0.001) indicate statistically significant differences between groups.

Supplemental Figure 4

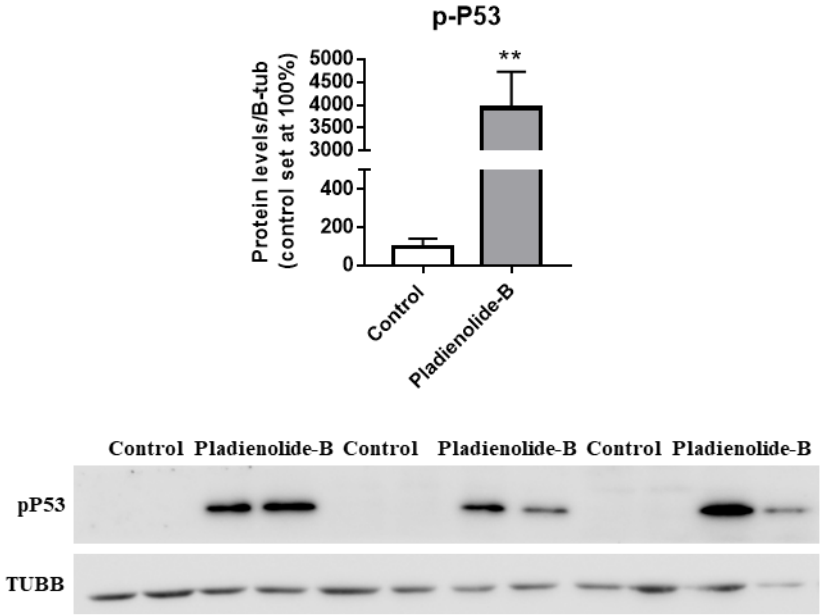

Supplemental Figure 4. Effects of pladienolide-b treatment on p53 phosphorylation levels. Basal phospho-p53 levels in LNCaP cells treated during 24h with pladienolide-b (n≥3). Protein levels were normalized by β-Tubulin protein levels. Protein data were represented as percent of scramble cells (mean ± SEM). Representative images are shown in bottom panel.

Supplemental Figure 5

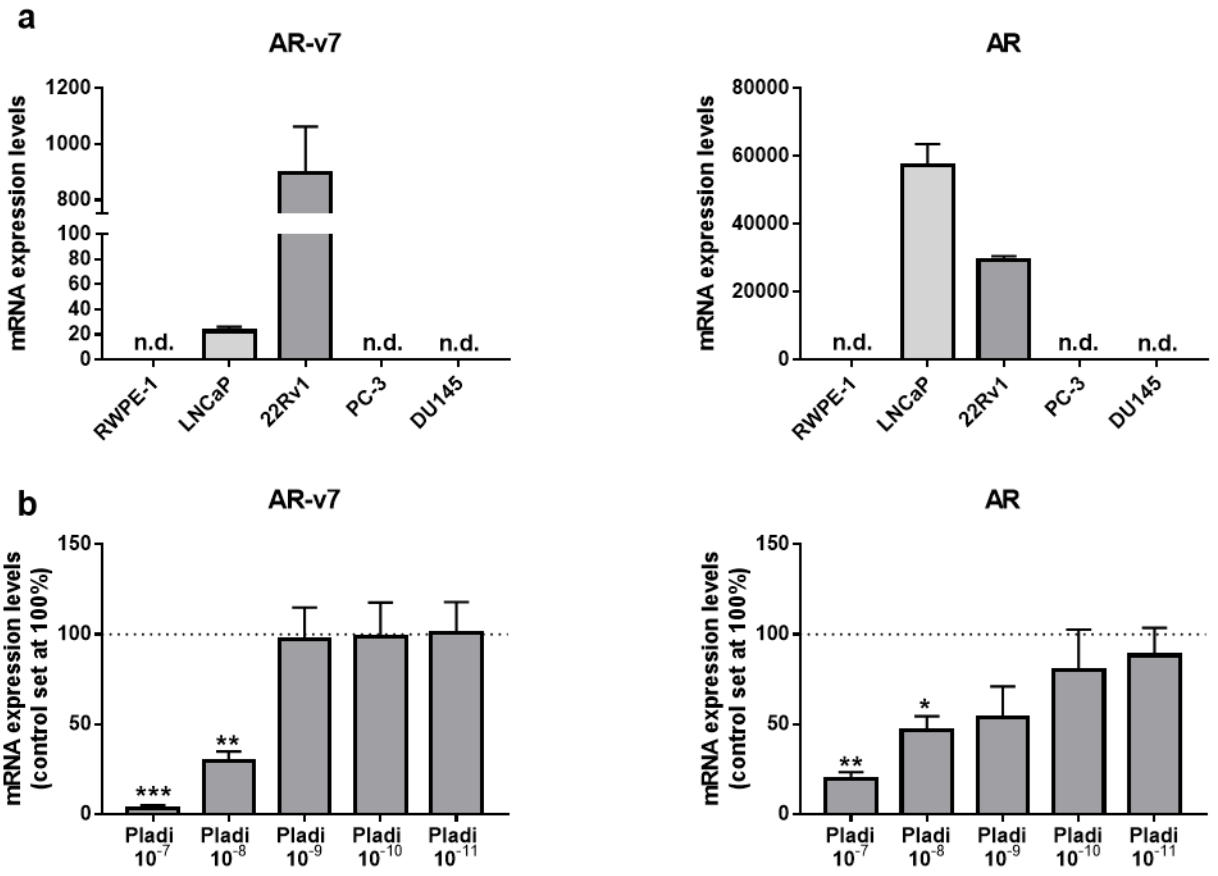

Supplemental Figure 5. **a**) AR-v7 (left panel) and AR expression (right panel) in RWPE-1, LNCaP, 22Rv1, PC-3 and DU145 cell lines (n=4). Absolute mRNA levels (n=4) were determined by qPCR and adjusted by normalization factor calculated from ACTB and GAPDH expression levels. Data were represented as absolute mRNA copies. n.d.: non detected. **b**) AR-v7 and AR expression in response to 10^{-7}, 10^{-8}, 10^{-9}, 10^{-10}, 10^{-11} M doses of pladienolide-B treatment (n=4). Data were represented as percent of non-treated control cells.

Supplemental Figure 6

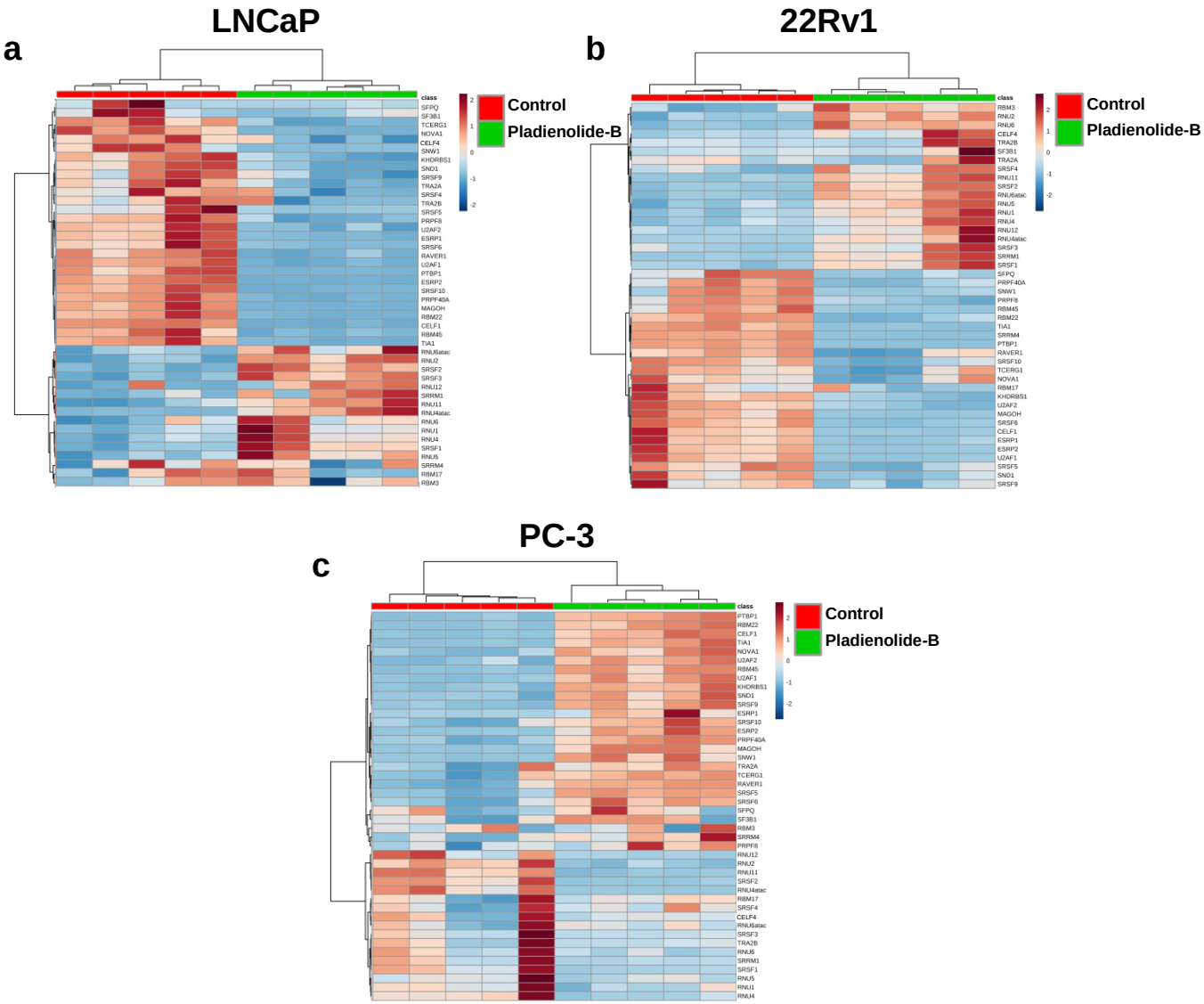

Supplemental Figure 6. Heatmaps showing non-supervised hierarchical clustering of changes in the expression-pattern of the splicing machinery and splicing factors after 24 hours of pladienolide-B treatment (10^{-7} M; n=5) in LNCaP (**a**), 22Rv1 (**b**) and PC-3 (**c**) cell lines.

Supplemental Figure 7

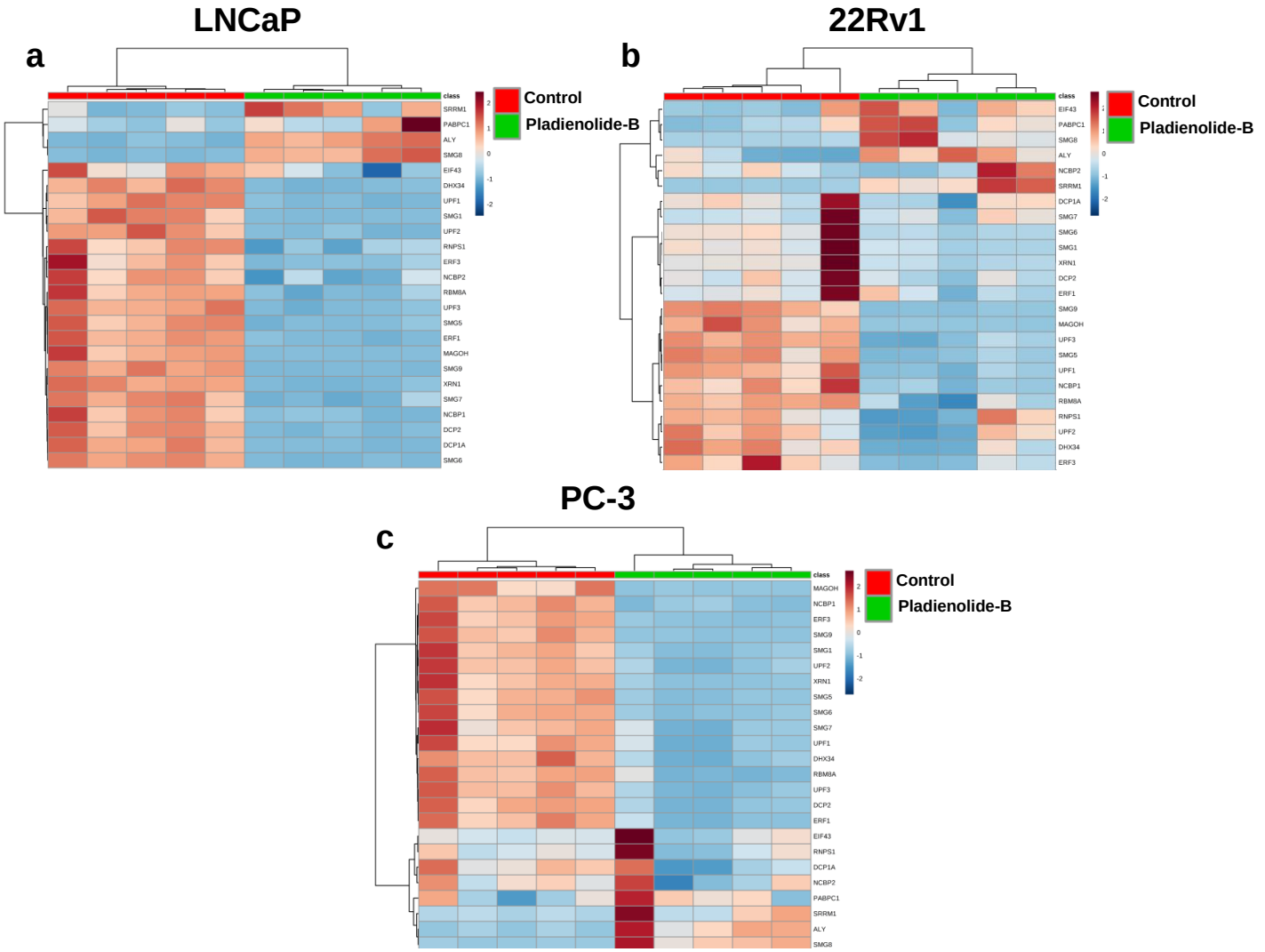

Supplemental Figure 7. Heatmaps showing non-supervised hierarchical clustering of changes in the expression-pattern of NMD related genes after 24 hours of pladienolide-B treatment (10^{-7} M; n=5) in LNCaP (**a**), 22Rv1 (**b**) and PC-3 (**c**) cell lines.

Article V

Title: Clinical, cellular and molecular evidence of the additive antitumor effects of biguanides and statins in prostate cancer

Authors: Juan M. Jiménez-Vacas[1,2,3,4], Vicente Herrero-Aguayo[1,2,3,4], Antonio J. Montero-Hidalgo[1,2,3,4], Prudencio Sáez-Martínez[1,2,3,4], Enrique Gómez-Gómez[1,3,5], Antonio J. León-González[1,2,3,4], Antonio C. Fuentes-Fayos[1,2,3,4], Elena M. Yubero-Serrano[1,3,4,6], María J. Requena-Tapia[1,3,5], Miguel Lopez[4,7], Justo P. Castaño[1,2,3,4], Manuel D. Gahete[1,2,3,4], Raúl M. Luque[1,2,3,4]

Affiliations: [1]Maimonides Institute for Biomedical Research of Córdoba (IMIBIC), Cordoba, Spain; [2]Department of Cell Biology, Physiology, and Immunology, University of Córdoba, Cordoba, Spain; [3]Hospital Universitario Reina Sofía (HURS), Cordoba, Spain; [4]Centro de Investigación Biomédica en Red de Fisiopatología de la Obesidad y Nutrición, (CIBERobn), Cordoba, Spain; [5]Urology Service, HURS/IMIBIC, Cordoba, Spain; [6]Unidad de Gestión Clinica Medicina Interna, Lipids and Atherosclerosis Unit, Reina Sofia University Hospital, Córdoba, Spain; [7]NeurObesity Group, Department of Physiology, CiMUS, University of Santiago de Compostela, Instituto de Investigación Sanitaria, Santiago de Compostela, Spain.

Short title: Biguanides and statins actions in prostate cancer

Keywords: metformin, simvastatin, prostate cancer, androgen receptor, mTOR, cell-cycle inhibitors.

Corresponding Author: Raúl M. Luque. Department of Cell Biology, Physiology and Immunology, University of Cordoba; Maimonides Institute of Biomedical Research of Cordoba (IMIBIC), Menéndez Pidal s/n, first floor; E-14004 Cordoba, Spain. Email: raul.luque@uco.es

Disclosure Statement: The authors have nothing to disclose.

Acknowledgements: This research was funded by Instituto de Salud Carlos III, co-funded by European Union (ERDF/ESF, "Investing in your future") [PI16/00264, PI17/02287, CD16/00092], MINECO/MECD (PID2019-105564RB-I00, FPU16/06190, FPU17/00263, FPU18/02485, BFU2016-80360-R), Junta de Andalucia (BIO-0139), and CIBERobn. Elena M Yubero-Serrano was the recipient of the Nicolas Monardes Programme from the "Servicio

Andaluz de Salud, Junta de Andalucia", Spain (C1-0005-2019). CIBER is an initiative of Instituto de Salud Carlos III, Ministerio de Sanidad, Servicios Sociales e Igualdad, Spain.

ABSTRACT

Prostate cancer (PCa) is one of the leading causes of cancer-related death among male population worldwide. Unfortunately, current medical treatments fail to prevent PCa progression in a high percentage of cases; therefore, new therapeutic tools to tackle PCa are urgently needed. Biguanides and statins have emerged as antitumor agents for several endocrine-related cancers. Therefore, we aimed to evaluate the direct effects of different biguanides (metformin/buformin/phenformin), statins (atorvastatin/simvastatin/lovastatin), and their combination, on key functional endpoints and the associated signalling mechanisms in normal and tumor prostate cells [normal (RWPE-cells/primary prostate cell-cultures); tumor (LNCaP/22RV1/PC3/DU145 cell-lines)]. We found that biguanides and statins exerted strong antitumor actions (i.e. inhibition of proliferation/migration/tumorspheres-formation) on PCa cells, and that their combination further decreased, additively, these functional parameters compared with the individual treatments. These actions were mediated through modulation of key oncogenic and metabolic signalling-pathways (i.e. AR/mTOR/AMPK/AKT/ERK) and molecular mediators (*MKI67*/*cMYC*/androgen-receptor/cell-cycle inhibitors). Interestingly, retrospective analysis of a cohort of patients with or without PCa, treated or not with metformin and/or statins, revealed that the combination of metformin+statins was associated to lower Gleason-score and longer biochemical recurrence-free survival. Altogether, our results reveal that biguanides and statins significantly reduced tumor aggressiveness in PCa, being this effect more potent (*in vitro* and *in vivo*) when both compounds are combined. Therefore, given the demonstrated clinical safety of biguanides and statins, our results suggest a potential therapeutic role of these compounds, especially their combination, for the treatment of PCa.

INTRODUCTION

Prostate cancer (PCa) is the most common endocrine-dependent tumor among men in developed countries and represents one of the leading causes of cancer-related death in this population (1). Although PCa treatment has been improved during the past decade, advanced stages of the disease are still difficult to manage. Indeed, the most aggressive phenotype of this pathology, named castration-resistant prostate cancer (CRPC) remains lethal nowadays (2). Therefore, the discovery and establishment of new therapeutic approaches to tackle PCa are urgently needed. An emerging approach against several tumor types is based in repositioning drugs already approved for other pathologies, since they are faster and easier to translate to clinical practise than are new drugs. In this scenario, treatment of patients with drugs such as biguanides (e.g. metformin) and statins (e.g. simvastatin), commonly used to treat metabolism-related pathologies [i.e. type 2 diabetes, obesity, hypercholesterolemia, all of which have been linked to PCa progression (3-5)] has been associated to a lower cancer-specific death and even lower risk to develop different cancer types, including PCa (6-8). However, some of these actions are still controversial (9-13), and, more importantly, as far as we know, the potential direct antitumor effects that different biguanides (i.e. metformin, buformin and phenformin), statins (i.e. atorvastatin, simvastatin and lovastatin), and the simultaneous combination of both types of drugs, may exert on PCa cells (androgen-dependent and –independent) and in normal prostate cells have not been yet compared side-by-side in previous reports.

The systemic mechanisms related to the actions exerted by biguanides (especially metformin) and statins are the modulation of the circulating levels of glucose and cholesterol, respectively (14, 15); however, the precise molecular mechanisms underlying the antitumor effects of metformin and statins are still controversial. For instance, both metformin and statins have been reported to exert antitumor effects on PCa cells *in vitro* (16, 17), through the modulation of different signalling pathways, which include the inhibition of mTOR pathway (both AMPK-dependent and -independent) (18), or the blockade of the mevalonate pathway (due to a specific blockade of HMG-CoA reductase) (19), respectively. But, these studies are somehow limited, fragmentary and unclear and, to the best of our knowledge, no studies have explored hitherto how metformin or statin alone, and especially in combination, can directly modulate the expression and/or activity of androgen receptor [a critical effector of PCa development and progression (20)] and other key signalling pathways and molecular mediators involved in tumor aggressiveness [e.g. cyclin-dependent kinase inhibitors (CKIs) (21), etc.].

Based on all the information mentioned above, this study was devised to explore and compare side-by-side the direct antitumor effects of different biguanides (i.e. metformin, buformin and phenformin) and statins (i.e. atorvastatin, simvastatin and lovastatin) alone, as

well as the combination of both types of drugs, on different PCa cells [androgen-dependent (LNCaP) and androgen–independent (22Rv1, PC-3 and DU145)] and in normal prostate cells (RWPE-1 and normal prostate primary cell cultures). In addition, we also analysed the ability of metformin and statin (i.e. simvastatin) to influence expression levels of critical effectors (i.e. androgen-receptor, c-MYC, CKIs) and the activity of different oncogenic signalling and metabolic pathways (i.e. AR, AMPK, AKT, ERK, mTOR) linked to PCa aggressiveness. Moreover, we aimed to assess the putative *in vivo* association between metformin and/or statins treatment and key tumor and clinical parameters (Gleason score and biochemical recurrence, respectively) using a well-characterized cohort of PCa patients.

MATERIALS AND METHODS

Human samples

This study was approved by the Reina Sofia University Hospital Ethics Committee and was conducted in accordance with the principles of the Declaration of Helsinki. The biobank of the public health system of Andalusia (Cordoba Node) coordinated the collection, processing, management and assignment of the biological samples used in this study, according to the standard procedures established for this purpose. Written informed consent was obtained from all patients. Formalin-fixed, paraffin-embedded (FFPE) PCa tissues (n=75) were obtained from radical prostatectomies from patients who were diagnosed with PCa (Table 1). Use of metformin and statins, as well as data of the time to biochemical recurrence [defined by two consecutive prostate-specific antigen (PSA) values > 0.2ng/mL and rising, after radical prostatectomy] and Gleason score [analysed by specialist uro-pathologists following the modified 2005, 2010 and 2014 ISUP criteria (22), based on the sample collection date] were collected from all patients included in this study. Significant PCa (SigPCa) was defined as Gleason score ≥7. Non-significant PCa (NonSigPCa) was defined as Gleason score = 6.

Cell culture and reagents

Normal prostate (RWPE-1) and PCa [androgen-dependent (LNCaP) and androgen–independent (22Rv1, PC-3 and DU145)] cell lines were obtained from the American Type Culture Collection (ATCC; Manassas, VA, USA) and cultured according to manufacturer instructions, as previously described (23-25). These cell lines were validated by analysis of short tandem repeats sequences (STRs) using GenePrint 10 System (Promega, Barcelona, Spain), and checked for mycoplasma contamination by PCR as previously reported (23-26). Biguanides [metformin (Merck KGaA, Darmstadt, Germany), buformin (Santa Cruz Biotechnology, Heidelberg, Germany) and phenformin (Merck KGaA)] and statins [atorvastatin (Merck KGaA), lovastatin (Merck KGaA) and simvastatin (Merck KGaA)] were used. The concentrations of the biguanides [metformin (5 mM), buformin (1 mM) and phenformin (1 mM)] and statins [atorvastatin (10 μM), lovastatin (10 μM) and simvastatin (10 μM)], were selected based in studies previously reported by our group and others (11, 27-30).

Primary cultures

Non-tumor prostate tissues from cystoprostatectomies were dispersed into single cells as previously reported (23). Briefly, tissue was mechanically and enzymatically digested using the protocol described by Goldstein and cols. (31), with modifications (32). One piece was included in paraffin to be analysed by expert anatomopathologists in order to ensure the absence of tumor tissue and the other piece was immediately placed in sterile cold (4 ^{o}C) DMEM High Glucose

with D-valine (Seralab, Oviedo, Spain) and transported to the laboratory for dispersion and primary culture experiments.

Cell proliferation and cell viability

Cell proliferation and cell viability were measured using Alamar Blue reagent (Bio-Source International, Camarillo, CA, USA) as previously reported (25). Briefly, cells were seeded in 96-well plates at a density of 3,000–5,000 cells/well and serum-starved for 24 h. Then, cell proliferation/viability was evaluated every 24 h using FlexStation III system (Molecular Devices, Sunnyvale, CA, USA) until 72 h. Results were expressed as percentage referred to control.

Cell migration

Cell migration was evaluated by wound-healing assay, as previously reported (23), in all cell lines except 22Rv1, due to its inability to migrate. Briefly, images of the scratch were taken at 0 and 12 h and wound healing was calculated as the area observed 12 h after the wound was made vs. the area observed just after wounding. Results were expressed as percentage referred to control.

Tumorspheres formation

Tumorspheres formation assay was carried out in representative cell-lines of androgen sensitive (LNCaP) and hormone refractory PCa (PC-3), as previously reported (23, 33). Briefly, 2,000 cells/well were seeded in Corning Costar 24-well ultra-low attachment plates (Merck KGaA) with DMEM F-12 medium supplemented with 20 ng/mL EGF (Merck KGaA). Treatments were added while plating the cells and refreshed every 3 days. The number of tumorspheres was determined after 14 days of incubation and analysed with ImageJ software. Results were expressed as percentage of tumorspheres number referred to control.

RNA extraction, retrotranscription and qPCR

Total RNA from FFPE samples was isolated and DNase-treated using the Maxwell 16 LEVRNA FFPE Kit (Promega, Madison, USA) according to manufacturer instructions in the Maxwell MDx 16 Instrument (Promega). Additionally, total RNA was extracted from fresh samples using the Qiagen AllPrep DNA/RNA/Protein Mini Kit (Thermo Fisher Scientific), and from PCa cell lines using TRIzol Reagent (Thermo Fisher Scientific, Waltham, MA, USA), followed, in both cases, by DNase treatment using the Qiagen RNase-Free DNase Kit (Thermo Fisher Scientific). RNA from PCa cells was isolated after 24 hours of incubation with metformin, simvastatin and combined treatment. Total RNA concentration and purity was assessed using the Nanodrop One Spectrophotometer (Thermo Fisher Scientific). Total RNA

was retrotranscribed using random hexamer primers and the cDNA First Strand Synthesis kit (Thermo Fisher Scientific). Details regarding the development, validation, and application of the qRT-PCR to measure expression levels of the transcripts of interest have been previously reported by our laboratory (23, 34, 35). Specific and validated primers sets used to measure the expression levels of genes of interest in this study are described in Jiménez-Vacas *et al.* (36). Expression levels were adjusted with a normalization factor calculated from the expression levels of *ACTB* and *GAPDH* housekeeping genes, using Genorm 3.3 (37), wherein the expression levels of the housekeeping genes did not differ among groups (data not shown).

Western blot analysis

Proteins from whole cell lysates were extracted after 12 h of incubation with metformin, simvastatin and combined treatment, separated on 10% SDS-polyacrylamide gels and transferred onto nitrocellulose membranes as previously described (23, 38). Membranes were incubated overnight at 4 ºC with specific primary antibodies against proteins of interest, and then for 1 h with the corresponding horseradish peroxidase-linked secondary antibody. Primary and secondary antibodies used in this study are summarized in Jiménez-Vacas *et al.* (36). Immunoreactive bands were detected using ECL chemiluminescence substrate solution (GE Healthcare, Madrid, Spain) in an enhanced chemiluminescence detection system (GE Healthcare). Observed bands were quantified using ImageJ software and results were expressed as percentage of control.

Statistical analyses

Statistical differences between two variables were calculated by unpaired parametric t-test and nonparametric Mann Whitney U test, according to normality, assessed by Kolmogorov-Smirnov test. For differences among more than two variables, One-Way ANOVA analysis was performed (followed by a Tukey post-hoc analysis). Chi-Square tests and Fisher's exact tests were performed to determine associations between treatment groups and Gleason score (NonSigPCa and SigPCa). Significant association between treatments and biochemical PCa recurrence was studied using the long-rank-p-value method. All the statistical analyses were assessed using GraphPad Prism 7 (GraphPad Software Inc, La Jolla, CA). All the experiments were performed in at least 3 experiments ($n \geq 3$). Statistical significance was considered when $p<0.05$.

RESULTS

The combination of metformin and simvastatin improves clinical parameters of PCa aggressiveness

To study the association between the treatments with metformin, any statin, or the combined treatment of both drugs with clinical parameters of PCa aggressiveness (i.e. time to biochemical recurrence and Gleason score), an available pilot cohort of 75 patients was analysed. Gleason score (not categorized) was not different among untreated patients, treated with metformin or statins alone and co-treated with both drugs (data not shown). However, when tumors were categorized in SigPCa and NonSigPCa, statistically significant differences were found among patients that were untreated, treated with metformin, treated with statins and co-treated with both drugs (p=0.028; Figure 1a). Specifically, co-treatment with metformin and any statin was associated to higher probability to develop NonSigPCa compared to: 1) untreated patients + patients treated with metformin or statins alone (p = 0.033; Figure 1b), or; 2) patients treated with metformin or statins alone (p = 0.011; Figure 1c). Moreover, treatment with metformin, any statin or the co-treatment of both drugs was not significantly associated with biochemical recurrence when comparing each group individually (36). However, patients co-treated with metformin and any statin tended to be associated (*p*= 0.13) with longer free biochemical recurrence survival compared to the group of patients without treatment, treated with metformin, and treated with any statin (Figure 1d). Additionally, patients co-treated with both drugs also tended to be associated to longer free biochemical recurrence survival (p = 0.08) as compared to those individually treated with metformin or with any statin (Figure 1e).

Biguanides exert antiproliferative effects on prostate cells

In *in vitro* assays, the three biguanides tested, metformin, buformin and phenformin reduced the proliferation rate of all the PCa cell lines assayed in a time-dependent manner (Figure 2a). Specifically, metformin effect was evidenced at 48- and 72-h of incubation, whereas buformin progressively decreased the proliferation rate of LNCaP cells at 24-, 48- and 72-h of incubation, and in 22Rv1, PC-3 and DU145 cells at 48- and 72-h of incubation (Figure 2a). Phenformin reduced cell proliferation in all tested PCa cell lines at 24-, 48- and 72-h of incubation (Figure 2a). The antiproliferative effect exerted by phenformin was significantly more pronounced than that exerted by metformin and buformin at 24-, 48- and 72-h of incubation in LNCaP cells, as well as at 48- and 72-h of incubation in 22Rv1 and PC-3 cells (Figure 2a).

In normal prostate RWPE-1 cells, phenformin increasingly reduced proliferation rate at 24-, 48- and 72-h, while metformin and buformin reduced this parameter at 48- and 72-h (Figure

2b). The antiproliferative effect of phenformin on RWPE-1 cells was significantly more pronounced than that exerted by metformin and buformin at 48- and 72-h of incubation (Figure 2b). Importantly, the use of primary non-tumor prostate cell cultures revealed that buformin and phenformin, but not metformin, were able to significantly reduce the viability rate in these primary cells, being the effect of phenformin significantly higher than that exerted by buformin at 24-, 48- and 72-h (Figure 2c).

Statins exert antiproliferative effects on prostate cells

In the case of statins, atorvastatin also reduced time-dependently the proliferation rate in LNCaP, 22Rv1 and PC-3 cells at 48- and 72-h (Figure 3a). Similarly, lovastatin decreased cell proliferation at 24-, 48- and 72-h in LNCaP, at 72-h in 22Rv1 and at 48- and 72-h in PC-3 cells (Figure 3a). Likewise, simvastatin reduced at 24-, 48- and 72-h, in a time-dependent manner, the proliferation rate of LNCaP, 22Rv1 and PC-3 cells (Figure 3a). In contrast, no changes were observed in response to any of the statins in DU145 cells. The antiproliferative effect of simvastatin was significantly higher than i) the effect exerted by atorvastatin and lovastatin at 24-, 48- and 72-h of incubation in LNCaP cells, at 72-h in 22Rv1 and PC-3 cells, and ii) the effect exerted by lovastatin at 48-h in 22Rv1 cells (Figure 3a).

In normal prostate RWPE-1 cells, atorvastatin, lovastatin and simvastatin decreased the proliferation rate at 48- and 72-h of incubation, being this effect less pronounced in the case of simvastatin as compared to that of atorvastatin at 72-h of incubation (Figure 3b). Subsequently, lovastatin and simvastatin reduced the viability rate of non-tumor primary prostate cultures at 48- and 72-h compared to vehicle-treated cells (Figure 3c), while atorvastatin only decreased this functional parameter significantly at 72-h (Figure 3c).

The combined treatment with biguanides and statins exerts additive antiproliferative effects in normal prostate and PCa cells

First, we evaluated the direct anti-proliferative effects of metformin and simvastatin alone or in combination in different PCa cell lines. We found that the reduction in the proliferation rate of LNCaP, 22Rv1, PC-3 and DU145 cells was more pronounced in response to the combination of metformin and simvastatin compared to each individual treatment after 48- and 72-h (Figure 4a). Similarly, the combination of metformin and atorvastatin also exerted an additive anti-proliferative effect in all the PCa cell lines tested at 48- and 72-h, and also at 24-h in the case of LNCaP and PC-3 cells (36). Likewise, the combination of metformin and lovastatin also evoked an additive effect at 48- and 72-h in 22Rv1, PC-3 and DU145 cells (36). It should be

mentioned that the effect of the combination of metformin and lovastatin was also seemingly more pronounced than the effect of metformin and lovastatin alone at 48- and 72-h in LNCaP cells, but this difference only reached statistical significance when comparing with the treatment of lovastatin, but not metformin alone (36).

Additionally, we also analysed the anti-proliferative effects of the combination of buformin or phenformin with all the statins (simvastatin, atorvastatin or lovastatin) and compared with the corresponding individual treatments (36). Similar to that found with the combination of metformin and simvastatin in PCa cells, our results revealed that the combination of buformin or phenformin with different statins resulted in apparently more pronounced/additive anti-proliferative effects compared with the individual treatments; however, it should be mentioned that the strongest additive effects were observed when combining metformin and simvastatin [results in Figure 4a and in Jiménez-Vacas *et al*. (36)].

In normal prostate RWPE-1 cells, incubation with metformin and simvastatin also decreased, in an additive manner, cell proliferation at 48- and 72-h (Figure 4b). In contrast, although the combination of metformin with atorvastatin or lovastatin also reduced cell proliferation in RWPE-1 (36), these effects did not differ from those exerted by atorvastatin (36) or lovastatin (36) alone. Similarly, the combination of buformin or phenformin with all the statins (simvastatin, atorvastatin or lovastatin) rendered comparable results (36).

Effects of metformin, simvastatin or their combination on additional functional parameters of aggressiveness in normal prostate and PCa cells

Based on the *in vitro* results obtained (Figures 2 and 3), we chose metformin (biguanide with the lowest effect on the viability of normal primary prostate cell cultures, but with strong effects of PCa cells, and the only FDA-approved biguanide) and simvastatin (the statin with the strongest antitumor effect on different PCa cells) to further evaluate the antitumor effects of the combination of both drug types and the underlying mechanisms of action in PCa cells.

Treatment with metformin and simvastatin significantly decreased the migration capacity of PCa cells (LNCaP, PC-3; Figure 4c) and normal prostate cells (RWPE-1; Figure 4d). Similar results were found in response to metformin, but not simvastatin, in DU145 cells (Figure 4c). The combined treatment of metformin and simvastatin reduced in an additive manner the migration rate in all these cell lines compared to the individual treatments (36). Moreover, metformin and simvastatin, alone and in combination, significantly decreased tumorspheres formation in LNCaP and PC-3 cells, being this effect significantly more pronounced (i.e. additive) in response to the combined treatment in PC-3 cells [Figure 4e; (36)]. In the case of

LNCaP cells, the combined treatment of metformin and simvastatin completely blocked the formation of tumorspheres in [Figure 4e; (36)].

Metformin and/or simvastatin treatment modulates androgen receptor (AR) expression/activity and other key oncogenic and metabolic pathways involved in PCa aggressiveness

Based on the overall results reported herein, we chose LNCaP cells to explore the effects of metformin and simvastatin, alone or in combination, on the expression and/or activity of well-known key effectors/elements associated to aggressiveness of PCa that might be linked to the antitumor effects observed in this study. Remarkably, our results revealed that the treatment with metformin, simvastatin, and their combination reduced the expression levels of AR in PCA cells, as well as its activity (measured by the ratio p-AR^{Ser213}/total AR ratio) (Figure 5a/b).

In addition, metformin, simvastatin and their combination also decreased the expression of *MKI67* (Figure 5c), while metformin, but not simvastatin, significantly reduced the expression levels of *c-MYC* compared to vehicle-treated cells (Figure 5d). As expected, metformin treatment, and also its combination with simvastatin, but not the latter alone, increased the phosphorylation levels of AMPKα (p-AMPKα^{Thr172}/total AMPKα ratio, which is a surrogate marker of AMPK activation; Figure 5e). In contrast, simvastatin treatment, alone or combined with metformin, but not metformin alone, decreased the activity of AKT and ERK signalling pathways (p-AKT^{Ser473}/total AKT ratio and p-ERK^{Thr202}/total ERK ratio, respectively) compared to vehicle-treated control cells (Figure 5f/g). Interestingly, while treatment with metformin or simvastatin alone did not significantly alter the activity of mTOR (p-mTOR^{Ser2448}/total mTOR ratio), the combined treatment of both drugs significantly reduced its activity (Figure 5h).

Metformin and/or simvastatin treatment modulates the expression of cell cycle inhibitors

Next, we interrogated the effect of metformin, simvastatin, and their combined treatment on the expression of critical cell cycle inhibitors. Remarkably, while metformin or simvastatin alone did not significantly alter the expression of *CDKN1A*, *CDKN1B*, *CDKN2A*, or *CDKN2D*, the combination of metformin and simvastatin drastically increased the expression of all these cell cycle inhibitors in PCa cells *in vitro* (Figure 6a). Notably, these *in vitro* data nicely resembled the results observed in samples derived from human samples subject *in vivo* to similar treatments, in which the expression of *CDKN1A*, *CDKN1B*, *CDKN2A* or *CDKN2D* was elevated in PCa samples from patients treated with both metformin and statins, but not with the

drugs alone, being these differences statistically significance for both, *CDKN1B* and *CDKN2A* (Figure 6b).

DISCUSSION

PCa remains an unmet clinical problem worldwide due to its high prevalence and mortality (1). Unfortunately, the therapeutic approaches currently available in clinical practice (i.e. surgery, hormone therapy, radiotherapy, chemotherapy) ultimately fail in a high proportion of patients. As a result, patient's quality of life is detrimentally affected in patients that are often diagnosed at advanced stages, and the associated health care costs are significantly elevated. Therefore, identification of alternative therapeutic options deems necessary to properly confront PCa. In this sense, earlier studies have suggested that drugs such as biguanides and statins exert antitumor actions in different endocrine-related cancers, including PCa (6-8, 11, 39-42). However, our current understanding of the direct effects that different types of biguanides and statins exert on normal prostate and PCa cells is quite scarce, partial and unclear. To the best of our knowledge, the present report provides the first comprehensive analysis of the direct side-by-side comparison of the antitumor effects that different biguanides (i.e. metformin, buformin and phenformin), statins (i.e. atorvastatin, simvastatin and lovastatin), and the combination of both classes of compounds, exert on PCa cells (androgen-dependent and –independent) and in normal prostate cells. In addition, we explored their possible underlying mechanisms, as well as the relation of these treatments to key clinical parameters of the patients *in vivo*.

First, we performed an observational retrospective study to assess the key clinical outcomes of patients with PCa treated (or not) with metformin or any type of statin, alone or in combination. Our results provide the first evidence indicating that patients treated with the combination of metformin and statins have less aggressive PCa disease (NonSigPCa) as compared to 1) those untreated or 2) treated only with metformin or any statin, and that this co-treatment was also associated with longer free biochemical recurrence survival as compared to those treated only with metformin or statins. To the best of our knowledge, only three studies have aimed to examine the effects that the combination of metformin and statins caused on PCa outcomes (43-45). Specifically, one study showed that this combination leads to synergistic effects to lower risk of biochemical recurrence in patients with PCa after radical prostatectomy (43), while another showed negative results (44). Most recently, in a large epidemiological study, Li and co-workers observed that the use of statins alone or in combination with metformin might be associated with lower PCa mortality among high-risk patients, particularly in post-diagnostic settings (45); however, the differences between the treatment of statin alone and the combination of both drugs were not statistically different, suggesting that these effects were mainly ascribed to the use of statins. Therefore, although a well-designed clinical trial is warranted to investigate the real effects of metformin or statins alone and the combination of metformin and statins to reduce key clinical aggressiveness features linked to PCa, our data strongly suggest that the combination of metformin and statins might be associated to more

beneficial effects in key clinical parameters of aggressiveness of patients with PCa (i.e. lower Gleason score, longer free biochemical recurrence survival) than the individual treatment of both drugs. While the interpretation of our data should be taken with caution since are derived from a cross-sectional study design analysing a limited cohort of patients (n=75), these results are supported by two previous reports using preclinical models indicating that the combination of metformin and atorvastatin caused stronger inhibition on tumor growth [immunodeficient mice bearing PC-3 xenograft tumors (46), and on tumor formation, bone metastasis and biochemical failure [C4-2B4 orthotopic NCr-nu/nu mice (47)] than either drug used individually.

The antitumor clinical associations previously observed *in vivo* were further supported by the *in vitro* data included herein since we provide solid evidence indicating that the treatment with different biguanides and statins significantly decrease the aggressiveness features of PCa cells (i.e. proliferation rate, migration capacity and tumorspheres formation), and that the combinations of different biguanides and statins strongly inhibit (i.e. in an additive manner) these antitumor effects compared to the individual treatment of both drug types. In line with a previous report (48), DU145 cells were found, as exception to be resistant to statins treatment. Specifically, and based on the results reported herein, co-treatment with metformin and simvastatin might represent the best combination, since metformin did not reduce the viability rate of non-tumor primary cultures and simvastatin exerted higher antiproliferative effects compared to atorvastatin and lovastatin in all PCa cells tested. In line with the present results observed in PCa cells, a similar pattern of response to biguanides, statins and the combination of both in terms of reduction of aggressiveness features has been found in other endocrine-related cancers (i.e. endometrial cancer, pituitary and neuroendocrine tumors) (11, 40-42, 49), suggesting that the utility of these drugs, and specially their combination, might be an effective therapeutic tool for the management of different human tumor pathologies, including PCa. Obviously, further work will be required to complete our understanding of this complex process and to fully elucidate the molecular mechanisms underlying these potential antitumor effects in PCa cells. However, consistently with the previous results, we found that metformin, simvastatin, and the combined treatment decreased the expression levels of the well-established PCa proliferation marker *MKI67* (50). Moreover, metformin, but not simvastatin treatment reduced the expression levels of *c-MYC* proto-oncogene, which is consistent with a previous report indicating that metformin can act as a chemopreventive agent to restrict prostatic neoplasia initiation and transformation by downregulating c-myc (51).

One of the most relevant observations in our study is the fact that metformin and simvastatin treatments decreased the expression of *AR*, which is in line with previous results in PCa cells *in vitro* (52, 53). However, to the best of our knowledge, this is the first study

reporting that the combination of both drugs further downregulates the expression of AR. Moreover, our results are also the first to document that metformin, simvastatin and especially their combined treatment not only reduce *AR* expression but also AR activity (i.e. phosphorylation-AR^{Ser213}), which is a more critical endpoint in PCa cells, thus leading to a lower transactivation of AR (54). Although the precise mechanistic underpinnings of this observation are still unknown, these results might be relevant from the (patho)physiological point of view in PCa, in that *AR* expression and activity play a pivotal role in prostate tumorigenesis and PCa aggressiveness (20). In this scenario, it is tempting to speculate that the striking change in the expression and activity of AR found in PCa cells in response to metformin, simvastatin and especially to the combined treatment may translate into a relevant clinical implication in this pathology [e.g. by decreasing the aggressiveness potential and sensitizing PCa cells to antihormonal agents (20, 55)]. Consequently, these findings suggest a putative utility of these drugs, specially their combination, as a potential new therapeutic tool for the management of human PCa, especially CRPC. Obviously, further work will be required to complete our understanding of this complex process and to fully elucidate the molecular mechanisms behind these interesting and potentially relevant observations.

To further interrogate the mechanisms underlying the antitumor actions of metformin, simvastatin and specially their combination, we analyzed additional signaling pathways important in the pathophysiology of PCa cells. Specifically, we initially selected AMPK, AKT and ERK based on previous reports from our group indicating that these signaling routes might be modulated by metformin and/or simvastatin in other endocrine-related cancer cellular systems (40-42). Our data revealed that metformin and simvastatin might modulate distinct intracellular signaling pathways to exert their antitumor actions in PCa cells. As expected, we found that AMPK signaling, considered the central mediator of metformin actions in different endocrine-related tumors (56), was significantly activated in response to metformin, but not simvastatin, in PCa cells. In contrast, simvastatin, but not metformin, decreased p-AKT^{Ser463}/AKT and p-ERK^{Thr202}/ERK ratio, presumably leading to an inactivation of PI3K/AKT and MAPK/ERK signalling pathways, which have been associated with the antitumor actions of different drugs in PCa cells (57, 58). Taken together, these observations could support the idea that metformin and simvastatin exert their antitumor actions in PCa cells through different signaling pathways (AMPK vs. AKT/ERK); however, they may not be sufficient to explain why the co-administration of both drugs exerts additive effects in PCa cells. To ascertain this question, we next studied mTOR signalling [a critical oncogenic route in PCa cells which represents a key downstream effector of PI3K/AKT pathway (59)] based on previous observations indicating: i) that the combined treatment of metformin and simvastatin strongly decreased AR expression/activity compared with the individual treatments (results from this

study), and ii) that the activation of AR enhances and reprograms mTOR chromatin-binding profiles and that nuclear mTOR activity is essential for androgen-mediated transcriptional reprogramming of metabolism in PCa cells (60). Interestingly, we found that the combination of metformin and simvastatin, but not any of the individual treatments, was able to significantly decrease the mTOR signaling pathway (i.e. by inhibiting Ser2448 phosphorylation). Moreover, since the expression levels of several cyclin-dependent kinase inhibitors (CKIs) are regulated by the pathways found to be altered in response to the combined treatment of metformin and simvastatin (i.e. AR, mTOR, AMPK, PI3K/AKT and MAPK/ERK) (61-67), we tested the expression of relevant CKIs in PCa [i.e. *CDKN1A*, *CDKN1B*, *CDKN2A* and *CDKN2D;* (68-71)]. Notably, we found that the expression levels of all these CKIs were upregulated in response to combined treatment *in vitro*. Consistently, in the samples from our PCa patient cohort, tumors from patients treated with metformin and statins in combination had higher CKIs expression levels (namely, *CDKN1B*, *CDKN2A*) than those who did not receive any of the treatments. Hence, based on all these results reported herein, it seems reasonable to suggest that the co-administration of metformin and simvastatin might exert additive antitumor actions through a hyper-inactivation of mTOR and AR, as well to an increase of the levels of CKIs.

Taken together, the present study provides the first detailed description of the direct effects that different biguanides and statins exert in PCa cells. Interestingly, our results clearly demonstrate that the combination of metformin and statins strongly reduces key parameters of aggressiveness *in vitro* (i.e. proliferation rate, migration capacity and formation of tumorspheres) and in patients (i.e. lower Gleason score, longer free biochemical recurrence survival), and that these effects are likely mediated through distinct signalling pathways (i.e. modulation of AMPK/mTOR, AR and CKIs levels) that may result in additive effects. Consequently, considering the clinical safety of metformin and statins, results from this study suggest that the combination of these compounds could represent an attractive and effective therapeutic approach to tackle PCa.

REFERENCES

1. Bray F, Ferlay J, Soerjomataram I, Siegel RL, Torre LA, Jemal A. Global cancer statistics 2018: GLOBOCAN estimates of incidence and mortality worldwide for 36 cancers in 185 countries. CA: a cancer journal for clinicians. 2018;68(6):394-424.
2. Sartor O, de Bono JS. Metastatic Prostate Cancer. The New England journal of medicine. 2018;378(7):645-57.
3. Polesel J, Gini A, Dal Maso L, Stocco C, Birri S, Taborelli M, et al. The impact of diabetes and other metabolic disorders on prostate cancer prognosis. Journal of diabetes and its complications. 2016;30(4):591-6.
4. Maj-Hes AB, Mathieu R, Ozsoy M, Soria F, Moschini M, Abufaraj M, et al. Obesity is associated with biochemical recurrence after radical prostatectomy: A multi-institutional extended validation study. Urologic oncology. 2017;35(7):460.e1-.e8.
5. Jamnagerwalla J, Howard LE, Allott EH, Vidal AC, Moreira DM, Castro-Santamaria R, et al. Serum cholesterol and risk of high-grade prostate cancer: results from the REDUCE study. Prostate cancer and prostatic diseases. 2018;21(2):252-9.
6. Spratt DE, Zhang C, Zumsteg ZS, Pei X, Zhang Z, Zelefsky MJ. Metformin and prostate cancer: reduced development of castration-resistant disease and prostate cancer mortality. European urology. 2013;63(4):709-16.
7. Yu O, Eberg M, Benayoun S, Aprikian A, Batist G, Suissa S, et al. Use of statins and the risk of death in patients with prostate cancer. Journal of clinical oncology : official journal of the American Society of Clinical Oncology. 2014;32(1):5-11.
8. Tan N, Klein EA, Li J, Moussa AS, Jones JS. Statin use and risk of prostate cancer in a population of men who underwent biopsy. The Journal of urology. 2011;186(1):86-90.
9. Dallaglio K, Bruno A, Cantelmo AR, Esposito AI, Ruggiero L, Orecchioni S, et al. Paradoxic effects of metformin on endothelial cells and angiogenesis. Carcinogenesis. 2014;35(5):1055-66.
10. Feng Z, Zhou X, Liu N, Wang J, Chen X, Xu X. Metformin use and prostate cancer risk: A meta-analysis of cohort studies. Medicine. 2019;98(12):e14955.
11. Sarmento-Cabral A, F LL, Gahete MD, Castano JP, Luque RM. Metformin Reduces Prostate Tumor Growth, in a Diet-Dependent Manner, by Modulating Multiple Signaling Pathways. Molecular cancer research : MCR. 2017;15(7):862-74.
12. Agalliu I, Salinas CA, Hansten PD, Ostrander EA, Stanford JL. Statin use and risk of prostate cancer: results from a population-based epidemiologic study. American journal of epidemiology. 2008;168(3):250-60.
13. Caro-Maldonado A, Camacho L, Zabala-Letona A, Torrano V, Fernandez-Ruiz S, Zamacola-Bascaran K, et al. Low-dose statin treatment increases prostate cancer aggressiveness. Oncotarget. 2018;9(2):1494-504.
14. Rena G, Hardie DG, Pearson ER. The mechanisms of action of metformin. Diabetologia. 2017;60(9):1577-85.
15. Alberts AW, Chen J, Kuron G, Hunt V, Huff J, Hoffman C, et al. Mevinolin: a highly potent competitive inhibitor of hydroxymethylglutaryl-coenzyme A reductase and a cholesterol-lowering agent. Proceedings of the National Academy of Sciences of the United States of America. 1980;77(7):3957-61.
16. Dowling RJO, Niraula S, Stambolic V, Goodwin PJ. Metformin in cancer: translational challenges. 2012;48(3):R31.
17. McFarland AJ, Anoopkumar-Dukie S, Arora DS, Grant GD, McDermott CM, Perkins AV, et al. Molecular mechanisms underlying the effects of statins in the central nervous system. International journal of molecular sciences. 2014;15(11):20607-37.
18. Clements A, Gao B, Yeap SH, Wong MK, Ali SS, Gurney H. Metformin in prostate cancer: two for the price of one. Annals of oncology : official journal of the European Society for Medical Oncology. 2011;22(12):2556-60.
19. Roy M, Kung HJ, Ghosh PM. Statins and prostate cancer: role of cholesterol inhibition vs. prevention of small GTP-binding proteins. American journal of cancer research. 2011;1(4):542-61.
20. Heinlein CA, Chang C. Androgen receptor in prostate cancer. Endocrine reviews. 2004;25(2):276-308.
21. Mossmann D, Park S, Hall MN. mTOR signalling and cellular metabolism are mutual determinants in cancer. Nat Rev Cancer. 2018;18(12):744-57.
22. Egevad L, Delahunt B, Srigley JR, Samaratunga H. International Society of Urological Pathology (ISUP) grading of prostate cancer - An ISUP consensus on contemporary grading. APMIS : acta pathologica, microbiologica, et immunologica Scandinavica. 2016;124(6):433-5.

23. Jimenez-Vacas JM, Herrero-Aguayo V, Gomez-Gomez E, Leon-Gonzalez AJ, Saez-Martinez P, Alors-Perez E, et al. Spliceosome Component SF3B1 as Novel Prognostic Biomarker and Therapeutic Target for Prostate Cancer. Translational research : the journal of laboratory and clinical medicine. 2019.
24. Hormaechea-Agulla D, Gahete MD, Jimenez-Vacas JM, Gomez-Gomez E, Ibanez-Costa A, F LL, et al. The oncogenic role of the In1-ghrelin splicing variant in prostate cancer aggressiveness. Mol Cancer. 2017;16(1):146.
25. Hormaechea-Agulla D, Jimenez-Vacas JM, Gomez-Gomez E, F LL, Carrasco-Valiente J, Valero-Rosa J, et al. The oncogenic role of the spliced somatostatin receptor sst5TMD4 variant in prostate cancer. Faseb j. 2017;31(11):4682-96.
26. Uphoff CC, Drexler HG. Detection of mycoplasma contaminations. Methods in molecular biology (Clifton, NJ). 2013;946:1-13.
27. Zhao Y, Zeng X, Tang H, Ye D, Liu J. Combination of metformin and paclitaxel suppresses proliferation and induces apoptosis of human prostate cancer cells via oxidative stress and targeting the mitochondria-dependent pathway. Oncology letters. 2019;17(5):4277-84.
28. Parris AB, Zhao Q, Howard EW, Zhao M, Ma Z, Yang X. Buformin inhibits the stemness of erbB-2-overexpressing breast cancer cells and premalignant mammary tissues of MMTV-erbB-2 transgenic mice. Journal of experimental & clinical cancer research : CR. 2017;36(1):28.
29. Jackson AL, Sun W, Kilgore J, Guo H, Fang Z, Yin Y, et al. Phenformin has anti-tumorigenic effects in human ovarian cancer cells and in an orthotopic mouse model of serous ovarian cancer. Oncotarget. 2017;8(59):100113-27.
30. Jiang P, Mukthavaram R, Chao Y, Nomura N, Bharati IS, Fogal V, et al. In vitro and in vivo anticancer effects of mevalonate pathway modulation on human cancer cells. British journal of cancer. 2014;111(8):1562-71.
31. Goldstein AS, Drake JM, Burnes DL, Finley DS, Zhang H, Reiter RE, et al. Purification and direct transformation of epithelial progenitor cells from primary human prostate. Nature protocols. 2011;6(5):656-67.
32. Hormaechea-Agulla D, Gomez-Gomez E, Ibanez-Costa A, Carrasco-Valiente J, Rivero-Cortes E, F LL, et al. Ghrelin O-acyltransferase (GOAT) enzyme is overexpressed in prostate cancer, and its levels are associated with patient's metabolic status: Potential value as a non-invasive biomarker. Cancer letters. 2016;383(1):125-34.
33. Del Rio-Moreno M, Alors-Perez E, Borges de Souza P, Prados-Gonzalez ME, CastaNo JP, Luque RM, et al. Peptides derived from the extracellular domain of the somatostatin receptor splicing variant SST5TMD4 increase malignancy in multiple cancer cell types. Translational research : the journal of laboratory and clinical medicine. 2019;211:147-60.
34. Jimenez-Vacas JM, Gomez-Gomez E, Montero-Hidalgo AJ, Herrero-Aguayo V, F LL, Sanchez-Sanchez R, et al. Clinical Utility of Ghrelin-O-Acyltransferase (GOAT) Enzyme as a Diagnostic Tool and Potential Therapeutic Target in Prostate Cancer. Journal of clinical medicine. 2019;8(12).
35. Taboada GF, Luque RM, Neto LV, Machado Ede O, Sbaffi BC, Domingues RC, et al. Quantitative analysis of somatostatin receptor subtypes (1-5) gene expression levels in somatotropinomas and correlation to in vivo hormonal and tumor volume responses to treatment with octreotide LAR. European journal of endocrinology. 2008;158(3):295-303.
36. Juan Manuel J-V, Vicente H-A, Antonio J. M-H, Prudencio S-M, Enrique G-G, Antonio J. L-G, et al. Supplementary Material. Clinical, cellular and molecular evidence of the additive antitumor effects of biguanides and statins in prostate cancer2020.
37. Vandesompele J, De Preter K, Pattyn F, Poppe B, Van Roy N, De Paepe A, et al. Accurate normalization of real-time quantitative RT-PCR data by geometric averaging of multiple internal control genes. Genome Biology. 2002;3(7):research0034.1.
38. Jimenez-Vacas JM, Herrero-Aguayo V, Montero-Hidalgo AJ, Gomez-Gomez E, Fuentes-Fayos AC, Leon-Gonzalez AJ, et al. Dysregulation of the splicing machinery is directly associated to aggressiveness of prostate cancer. EBioMedicine. 2020:102547.
39. Ben Sahra I, Laurent K, Loubat A, Giorgetti-Peraldi S, Colosetti P, Auberger P, et al. The antidiabetic drug metformin exerts an antitumoral effect in vitro and in vivo through a decrease of cyclin D1 level. Oncogene. 2008;27(25):3576-86.
40. Herrera-Martínez AD, Pedraza-Arevalo S, F LL, Gahete MD, Gálvez-Moreno MA, Castaño JP, et al. Type 2 Diabetes in Neuroendocrine Tumors: Are Biguanides and Statins Part of the Solution? The Journal of clinical endocrinology and metabolism. 2019;104(1):57-73.
41. Vázquez-Borrego MC, Fuentes-Fayos AC, Herrera-Martínez AD, Venegas-Moreno E, F LL, Fanciulli A, et al. Statins directly regulate pituitary cell function and exert antitumor effects in pituitary tumors. Neuroendocrinology. 2020.

42. Vázquez-Borrego MC, Fuentes-Fayos AC, Herrera-Martínez AD, F LL, Ibáñez-Costa A, Moreno-Moreno P, et al. Biguanides Exert Antitumoral Actions in Pituitary Tumor Cells Through AMPK-Dependent and -Independent Mechanisms. The Journal of clinical endocrinology and metabolism. 2019;104(8):3501-13.
43. Danzig MR, Kotamarti S, Ghandour RA, Rothberg MB, Dubow BP, Benson MC, et al. Synergism between metformin and statins in modifying the risk of biochemical recurrence following radical prostatectomy in men with diabetes. Prostate cancer and prostatic diseases. 2015;18(1):63-8.
44. Aminsharifi A, Howard LE, Amling CL, Aronson WJ, Cooperberg MR, Kane CJ, et al. Statins are Associated With Increased Biochemical Recurrence After Radical Prostatectomy in Diabetic Men but no Association was Seen in Men also Taking Metformin: Results From the SEARCH Database. Clinical genitourinary cancer. 2019;17(1):e140-e9.
45. Li K, Si-Tu J, Qiu J, Lu L, Mao Y, Zeng H, et al. Statin and metformin therapy in prostate cancer patients with hyperlipidemia who underwent radiotherapy: a population-based cohort study. Cancer management and research. 2019;11:1189-97.
46. Wang ZS, Huang HR, Zhang LY, Kim S, He Y, Li DL, et al. Mechanistic Study of Inhibitory Effects of Metformin and Atorvastatin in Combination on Prostate Cancer Cells in Vitro and in Vivo. Biological & pharmaceutical bulletin. 2017;40(8):1247-54.
47. Babcook MA, Shukla S, Fu P, Vazquez EJ, Puchowicz MA, Molter JP, et al. Synergistic simvastatin and metformin combination chemotherapy for osseous metastatic castration-resistant prostate cancer. Molecular cancer therapeutics. 2014;13(10):2288-302.
48. Raghu VK, Beckwitt CH, Warita K, Wells A, Benos PV, Oltvai ZN. Biomarker identification for statin sensitivity of cancer cell lines. Biochem Biophys Res Commun. 2018;495(1):659-65.
49. Kim JS, Turbov J, Rosales R, Thaete LG, Rodriguez GC. Combination simvastatin and metformin synergistically inhibits endometrial cancer cell growth. Gynecologic oncology. 2019;154(2):432-40.
50. Gerdes J, Lemke H, Baisch H, Wacker HH, Schwab U, Stein H. Cell cycle analysis of a cell proliferation-associated human nuclear antigen defined by the monoclonal antibody Ki-67. Journal of immunology (Baltimore, Md : 1950). 1984;133(4):1710-5.
51. Akinyeke T, Matsumura S, Wang X, Wu Y, Schalfer ED, Saxena A, et al. Metformin targets c-MYC oncogene to prevent prostate cancer. Carcinogenesis. 2013;34(12):2823-32.
52. Tyagi M, Cheema MS, Dryhurst D, Eskiw CH, Ausió J. Metformin alters H2A.Z dynamics and regulates androgen dependent prostate cancer progression. Oncotarget. 2018;9(97):37054-68.
53. Kong Y, Cheng L, Mao F, Zhang Z, Zhang Y, Farah E, et al. Inhibition of cholesterol biosynthesis overcomes enzalutamide resistance in castration-resistant prostate cancer (CRPC). The Journal of biological chemistry. 2018;293(37):14328-41.
54. Koryakina Y, Ta HQ, Gioeli D. Androgen receptor phosphorylation: biological context and functional consequences. Endocrine-related cancer. 2014;21(4):T131-45.
55. Coutinho I, Day TK, Tilley WD, Selth LA. Androgen receptor signaling in castration-resistant prostate cancer: a lesson in persistence. Endocrine-related cancer. 2016;23(12):T179-t97.
56. Zaidi S, Gandhi J, Joshi G, Smith NL, Khan SA. The anticancer potential of metformin on prostate cancer. Prostate cancer and prostatic diseases. 2019;22(3):351-61.
57. Nickols NG, Nazarian R, Zhao SG, Tan V, Uzunangelov V, Xia Z, et al. MEK-ERK signaling is a therapeutic target in metastatic castration resistant prostate cancer. Prostate cancer and prostatic diseases. 2019;22(4):531-8.
58. Bitting RL, Armstrong AJ. Targeting the PI3K/Akt/mTOR pathway in castration-resistant prostate cancer. Endocrine-related cancer. 2013;20(3):R83-99.
59. Edlind MP, Hsieh AC. PI3K-AKT-mTOR signaling in prostate cancer progression and androgen deprivation therapy resistance. Asian journal of andrology. 2014;16(3):378-86.
60. Audet-Walsh É, Dufour CR, Yee T, Zouanat FZ, Yan M, Kalloghlian G, et al. Nuclear mTOR acts as a transcriptional integrator of the androgen signaling pathway in prostate cancer. Genes & development. 2017;31(12):1228-42.
61. Katayama K, Nakamura A, Sugimoto Y, Tsuruo T, Fujita N. FOXO transcription factor-dependent p15(INK4b) and p19(INK4d) expression. Oncogene. 2008;27(12):1677-86.
62. Qi H, Liu Y, Li S, Chen Y, Li L, Cao Y, et al. Activation of AMPK Attenuated Cardiac Fibrosis by Inhibiting CDK2 via p21/p27 and miR-29 Family Pathways in Rats. Molecular therapy Nucleic acids. 2017;8:277-90.
63. Ciccarelli C, Marampon F, Scoglio A, Mauro A, Giacinti C, De Cesaris P, et al. p21WAF1 expression induced by MEK/ERK pathway activation or inhibition correlates with growth arrest, myogenic differentiation and onco-phenotype reversal in rhabdomyosarcoma cells. Mol Cancer. 2005;4:41.

64. Moss SC, Lightell DJ, Jr., Marx SO, Marks AR, Woods TC. Rapamycin regulates endothelial cell migration through regulation of the cyclin-dependent kinase inhibitor p27Kip1. The Journal of biological chemistry. 2010;285(16):11991-7.
65. Chen B, Xu X, Luo J, Wang H, Zhou S. Rapamycin Enhances the Anti-Cancer Effect of Dasatinib by Suppressing Src/PI3K/mTOR Pathway in NSCLC Cells. PloS one. 2015;10(6):e0129663.
66. Ye D, Mendelsohn J, Fan Z. Androgen and epidermal growth factor down-regulate cyclin-dependent kinase inhibitor p27Kip1 and costimulate proliferation of MDA PCa 2a and MDA PCa 2b prostate cancer cells. Clinical cancer research : an official journal of the American Association for Cancer Research. 1999;5(8):2171-7.
67. Hessenkemper W, Roediger J, Bartsch S, Houtsmuller AB, van Royen ME, Petersen I, et al. A natural androgen receptor antagonist induces cellular senescence in prostate cancer cells. Molecular endocrinology (Baltimore, Md). 2014;28(11):1831-40.
68. Bott SR, Arya M, Kirby RS, Williamson M. p21WAF1/CIP1 gene is inactivated in metastatic prostatic cancer cell lines by promoter methylation. Prostate cancer and prostatic diseases. 2005;8(4):321-6.
69. Sirma H, Broemel M, Stumm L, Tsourlakis T, Steurer S, Tennstedt P, et al. Loss of CDKN1B/p27Kip1 expression is associated with ERG fusion-negative prostate cancer, but is unrelated to patient prognosis. Oncology letters. 2013;6(5):1245-52.
70. Steiner MS, Wang Y, Zhang Y, Zhang X, Lu Y. p16/MTS1/INK4A suppresses prostate cancer by both pRb dependent and independent pathways. Oncogene. 2000;19(10):1297-306.
71. Pencik J, Schlederer M, Gruber W, Unger C, Walker SM, Chalaris A, et al. STAT3 regulated ARF expression suppresses prostate cancer metastasis. Nat Commun. 2015;6:7736.

Table 1. Clinical parameters of patients with prostate cancer. BMI: Body mass index; PSA: Prostate specific antigen; IQR: Interquartile range

Figure 1. Effects of metformin, statins and combined treatment in patients with PCa. A) . Percentage of patients untreated (n=38), treated with metformin (n=7), statins (n=21) and both drugs (n=9) with NonSigPCa and SigPCa. **B)** Percentage of NonSigPCa and SigPCa in untreated patients & treated with metformin or statins alone (n=66) and patients co-treated with metformin and statins (n=9). **C)** Percentage of NonSigPCa and SigPCa in patients treated with metformin or statins alone (n=28) and patients co-treated with metformin and statins (n=9). C) Kaplan-Meier survival curve of biochemical recurrence-free survival of PCa patients untreated (n=11) vs. treated with metformin (n=5), vs. treated with simvastatin (n=22) vs. treated with both treatments (n=9). **D)** Kaplan-Meier survival curve of biochemical recurrence-free survival of PCa untreated patients & treated with metformin or statins alone (n=62) and patients co-treated with metformin and statins (n=9). **E)** Kaplan-Meier survival curve of biochemical recurrence-free survival of PCa patients treated with metformin or statins alone (n=24) and patients co-treated with metformin and statins (n=9). Patients with coadjuvant treatment were excluded from the Kaplan-Meier analysis (n=4). Asterisks indicate values that significantly differ from untreated patients (*$p < 0.05$). NonSigPCa: Non-significant PCa (defined as Gleason score = 6). SigPCa: Significant PCa (defined as Gleason score ≥ 7).

Figure 2. Effect of biguanides (metformin, buformin and phenformin) on cell proliferation/viability of prostate derived cells. Cell proliferation was assessed by Alamar Blue after 24-, 48- and 72 hours of treatment in **a)** PCa cell lines (LNCaP, 22Rv1, PC-3 and DU145) and **b)** normal-prostate like cell line RWPE-1. **c)** Cell-viability was assessed by Alamar Blue after 24-, 48- and 72 hours of treatment in primary normal prostate cells. The data are expressed as percentage of proliferation rate compared to vehicle-treated control cells (set at 100%). Values represent the mean ± SEM. Asterisks (comparison to control), "a" (comparison to metformin) and "b" (comparison to buformin) (* $p < 0.05$; ** $p < 0.01$; *** $p < 0.001$) indicate statistically significant differences.

Figure 3. Effect of statins (atorvastatin, lovastatin and simvastatin) on cell proliferation/viability of prostate derived cells. Cell proliferation was assessed by Alamar Blue after 24-, 48- and 72 hours of treatment in **a)** PCa cell lines (LNCaP, 22Rv1, PC-3 and DU145) and (**b)** normal-prostate like cell line RWPE-1. **c)** Cell-viability was assessed by Alamar Blue after 24-, 48- and 72 hours of treatment in primary normal prostate cells. The data are expressed as percentage of proliferation rate compared to untreated control cells (set at 100%). Values represent the mean ± SEM. Asterisks (comparison to control), "a" (comparison to atorvastatin) and "b" (comparison to simvastatin) (* $p < 0.05$; ** $p < 0.01$; *** $p < 0.001$) indicate statistically significant differences.

Figure 4. Effects of metformin, simvastatin and its combination on functional parameters of PCa cells. a) Proliferation rate of PCa cell lines (LNCaP, 22Rv1, PC-3 and DU145) and (**b)** normal-prostate like cell line RWPE-1 after 24, 48, and 72 hours of metformin (5mM), simvastatin (10µM) and combined treatment. The data are expressed as percentage of proliferation rate compared to untreated control cells (set at 100%). **c)** Migration rate of PCa cell lines (LNCaP, PC-3 and DU145) and (**d)** normal-prostate like cell line RWPE-1 after 12 hours of metformin (5mM), simvastatin (10µM) and combined treatment. The data are expressed as percentage of migration rate compared to untreated control cells (set at 100%). Representative images of migration assay in PC-3 are shown [similar representative images for LNCaP, DU145 and RWPE-1 cells are represented in Jiménez *et al.* (36)]. **e)** Number of tumorspheres produced by PCa cell lines (LNCaP and PC-3) in response to metformin (5mM), simvastatin (1mM) and combined treatment after 14 days of incubation (treatment refreshed each 3 days). The data are expressed as percentage of number of tumorspheres compared to untreated control cells (set at

100%). Representative images of tumorspheres assay in PC-3 cells are shown (similar representative images for LNCaP cells are represented in Jiménez-Vacas *et al.* (36)]. Values represent the mean ± SEM. Asterisks (comparison to control), "a" (comparison to metformin) and "b" (comparison to simvastatin) (* p <0.05; ** p <0.01; *** p <0.001) indicate statistically significant differences. MF: Metformin; SMV: Simvastatin; CMB: Combined treatment.

Figure 5. Molecular consequences of treatment with metformin, simvastatin and its combination in LNCaP cells. a) Expression levels of *AR*, **(b)** Protein levels of p-AR^{Ser213}, **(c)** expression levels of *MKI67*, **(d)** expression levels of *c-MYC*, **(e)** protein levels of p-AMPK^{Thr172}, **(f)** protein levels of p-AKT^{Ser473}, **(g)** protein levels of p-ERK^{Thr202} and **(h)** protein levels of p-mTOR^{Ser448} after treatment with metformin (5mM), simvastatin (10μM) and combined treatment. Cells were treated for 24 hours and 12 hours for protein and RNA isolation, respectively. mRNA expression levels were adjusted by NF (calculated by *ACTB* and *GAPDH* expression). Phospho-protein levels were adjusted by protein levels of total target protein (AR, AMPK, AKT, ERK1/2 and mTOR, respectively). **i)** Representative images of western blot results are shown. Data are expressed as percentage of untreated cells (set at 100%). Values represent the mean ± SEM. Asterisks (comparison to control), "a" (comparison to metformin) and "b" (comparison to simvastatin) (* p <0.05; ** p <0.01; *** p <0.001) indicate statistically significant differences. MF: Metformin; SMV: Simvastatin; CMB: Combined treatment.

Figure 6. Effects of metformin, simvastatin and combined treatment on expression levels of cyclin-dependent kinase inhibitors. a-d) Expression levels of *CDKN1A* **(a)**, *CDKN1B* **(b)**, *CDKN2A* **(c)** and *CDKN2D* **(d)** after 24 hours of incubation with metformin (5mM), simvastatin (10μM) and combined treatment in LNCaP cells. Expression levels of *CDKN1A* **(e)**, *CDKN1B* **(f)**, *CDKN2A* **(g)** and *CDKN2D* **(h)** in PCa samples taken from patients treated with metformin, simvastatin or both treatments. **mRNA** expression levels were adjusted by NF (calculated by *ACTB* and *GAPDH* expression). Data are expressed as percentage of untreated cells or untreated patients (set at 100%). Values represent the mean ± SEM. Asterisks (comparison to control), "a" (comparison to metformin) and "b" (comparison to simvastatin) (* p <0.05; ** p <0.01; *** p <0.001) indicate statistically significant differences. MF: Metformin; SMV: Simvastatin; CMB: Combined treatment.

Table 1.

Patients [*n*]		75
Age, years [median (IQR)]		61 (56-66)
BMI [median (IQR)]		28.2 (26.8-31.5)
PSA, ng/mL [median (IQR)]		5.1 (4.2-8.0)
Recurrence [*n* (%)]		12 (16.0%)
Time to recurrence, months [median (IQR)]		23.5 (14.0-33.0)
Gleason score [*n* (%)]	**6**	7 (9.33%)
	7 (3+4)	42 (56%)
	7 (4+3)	21 (28%)
	8	3 (4%)
	9	2 (2.67%)
Stage [n (%)]	**T2**	24 (32.0%)
	T3A	49 (65.3%)
	T3B	2 (2.7%)
Treatment [*n* (%)]	**Untreated**	38 (50.7%)
	Metformin	7 (9.3%)
	Statins	21 (28.0%)
	Both	9 (12.0%)

Figure 1

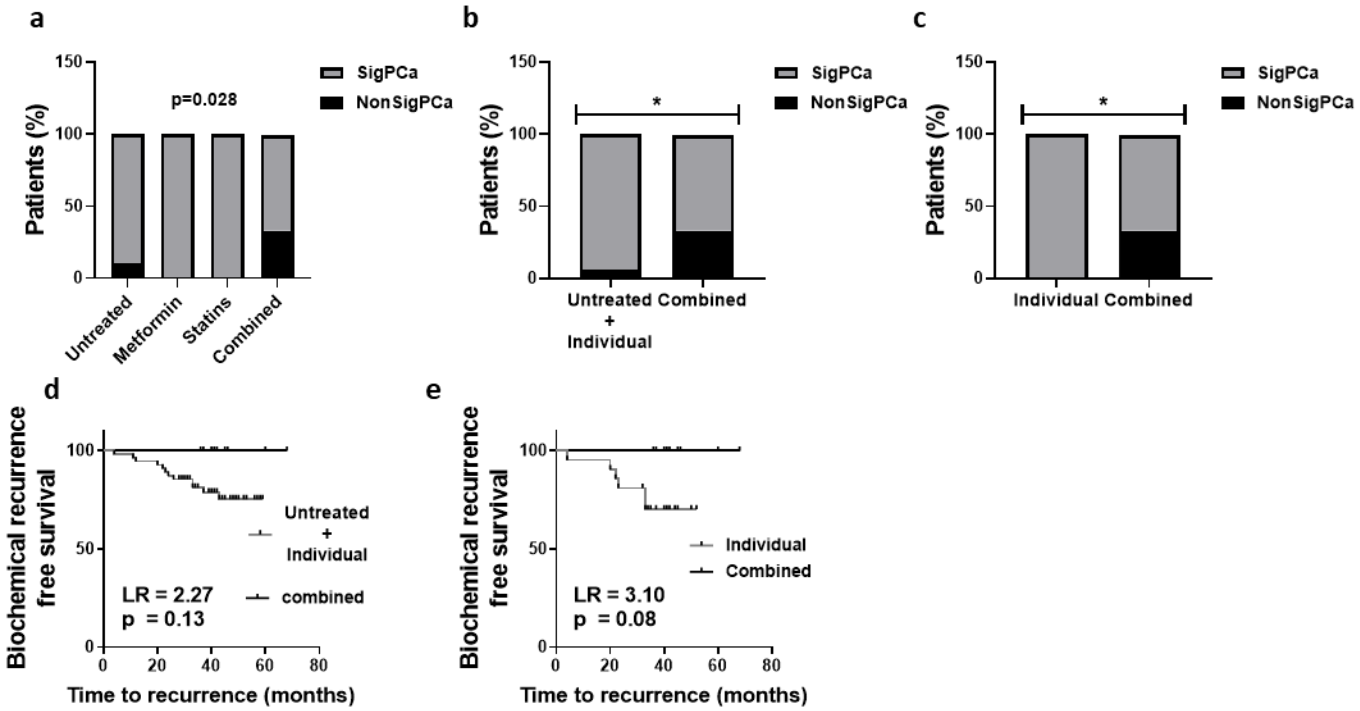
a
b
c
Patients (%)
SigPCa
NonSigPCa
p=0.028
Untreated
Metformin
Statins
Combined
*
Untreated + Individual
Combined
Individual
d
e
Biochemical recurrence free survival
Time to recurrence (months)
Untreated + Individual
combined
LR = 2.27
p = 0.13
Individual
Combined
LR = 3.10
p = 0.08

Figure 2

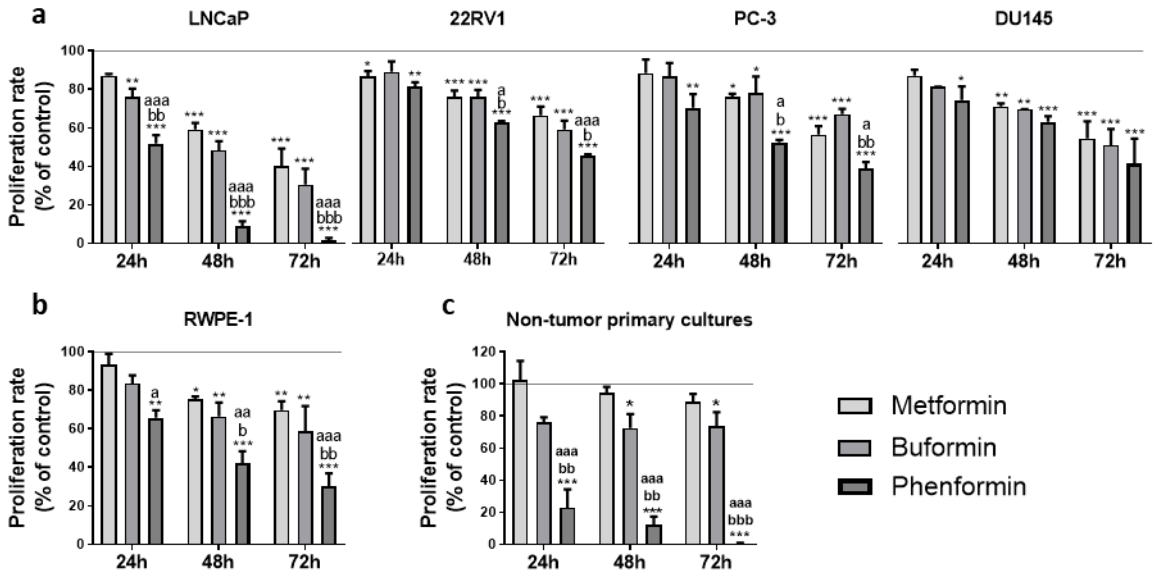
a
LNCaP
22RV1
PC-3
DU145
Proliferation rate (% of control)
24h
48h
72h
b
RWPE-1
c
Non-tumor primary cultures
Metformin
Buformin
Phenformin

Figure 3

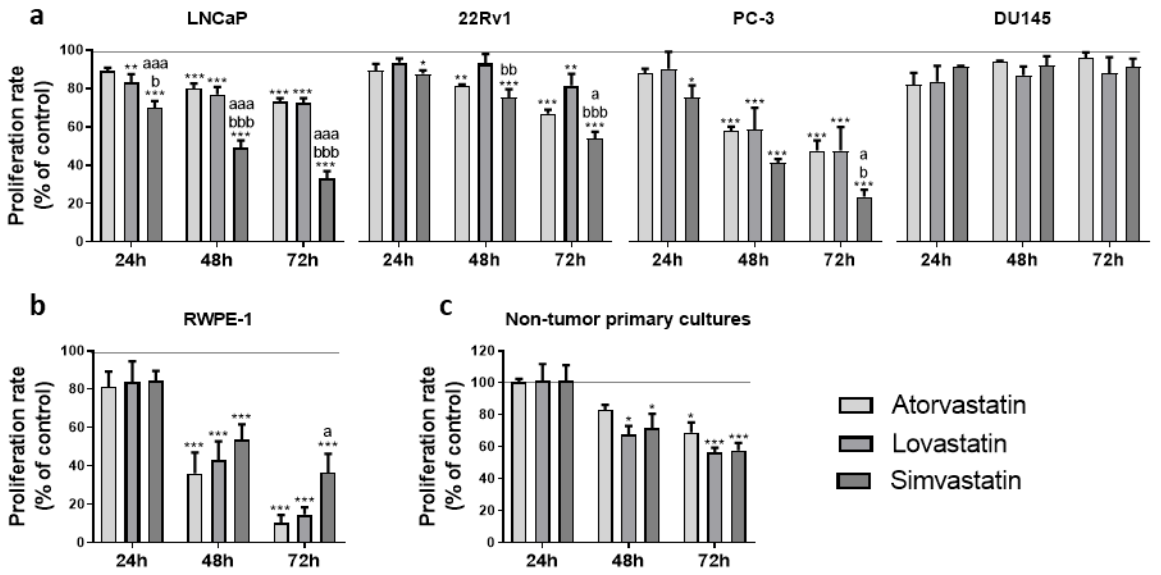
a
LNCaP
22Rv1
PC-3
DU145
Proliferation rate (% of control)
24h
48h
72h
b
RWPE-1
c
Non-tumor primary cultures
Atorvastatin
Lovastatin
Simvastatin

Figure 4

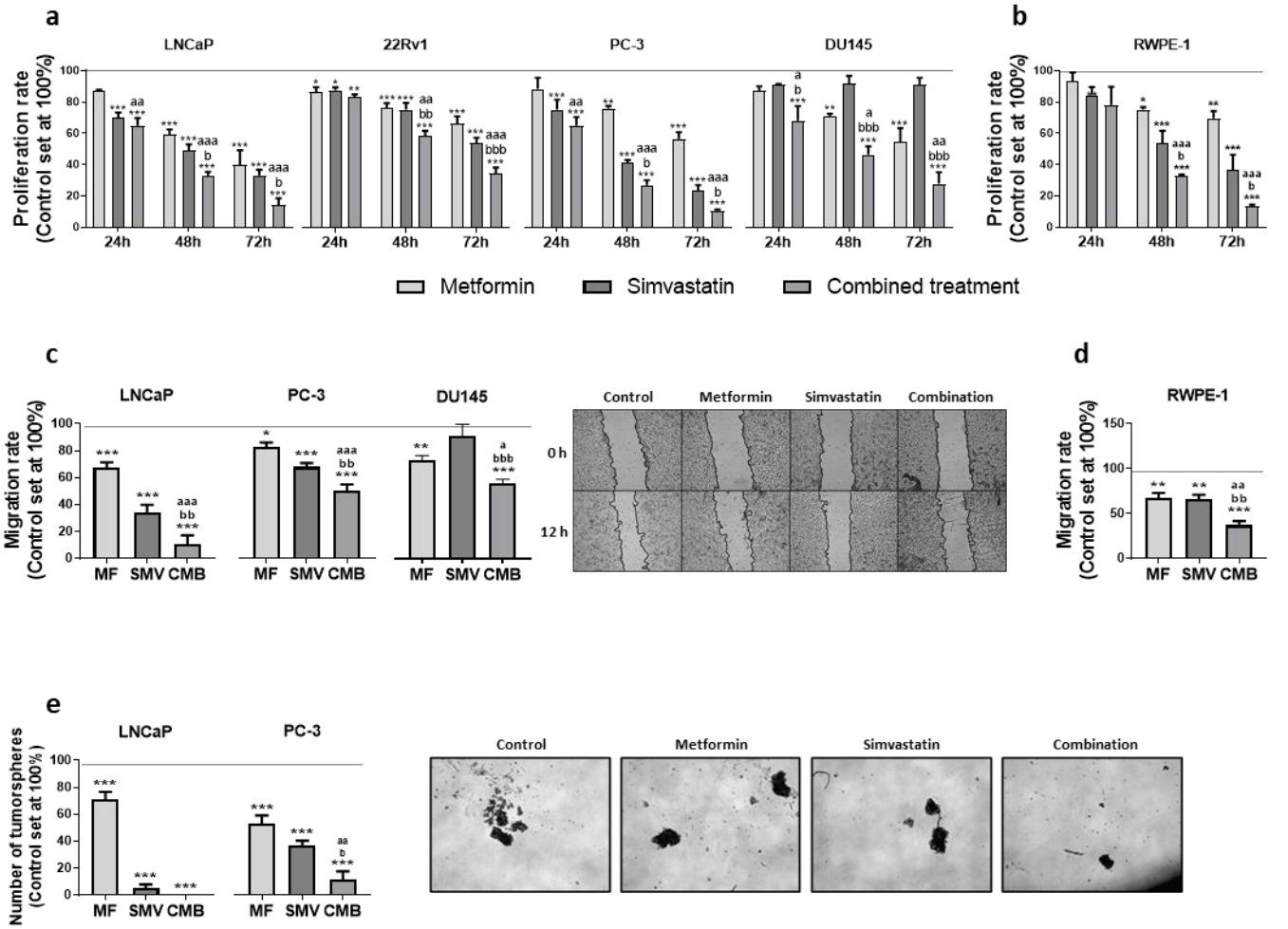
a
LNCaP
22Rv1
PC-3
DU145
Proliferation rate (Control set at 100%)
24h
48h
72h
b
RWPE-1
Metformin
Simvastatin
Combined treatment
c
LNCaP
PC-3
DU145
Migration rate (Control set at 100%)
MF SMV CMB
Control
Metformin
Simvastatin
Combination
0 h
12 h
d
RWPE-1
e
Number of tumorspheres (Control set at 100%)

Figure 5

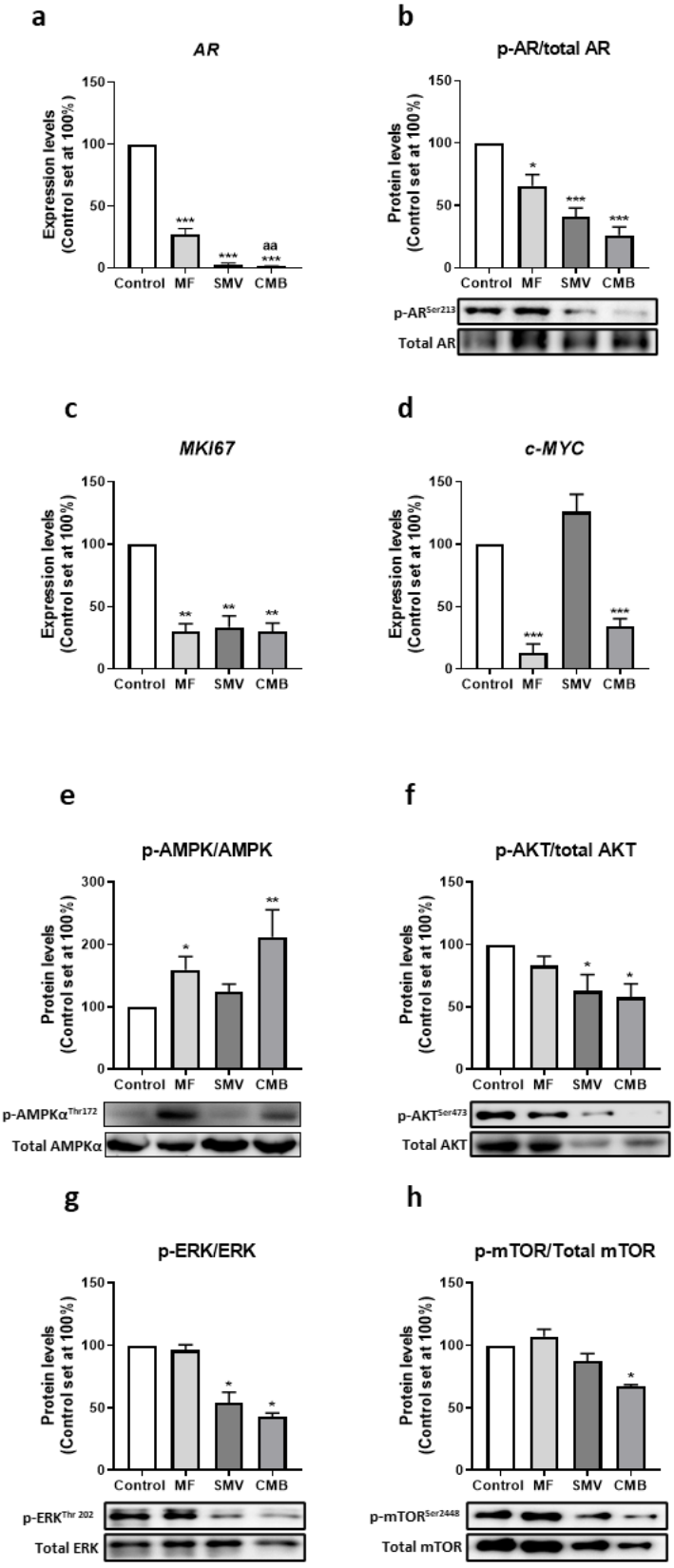
a
AR
Expression levels (Control set at 100%)
Control MF SMV CMB
b
p-AR/total AR
Protein levels (Control set at 100%)
p-AR Ser213
Total AR
c
MKI67
d
c-MYC
e
p-AMPK/AMPK
p-AMPKα Thr172
Total AMPKα
f
p-AKT/total AKT
p-AKT Ser473
Total AKT
g
p-ERK/ERK
p-ERK Thr 202
Total ERK
h
p-mTOR/Total mTOR
p-mTOR Ser2448
Total mTOR

Figure 6

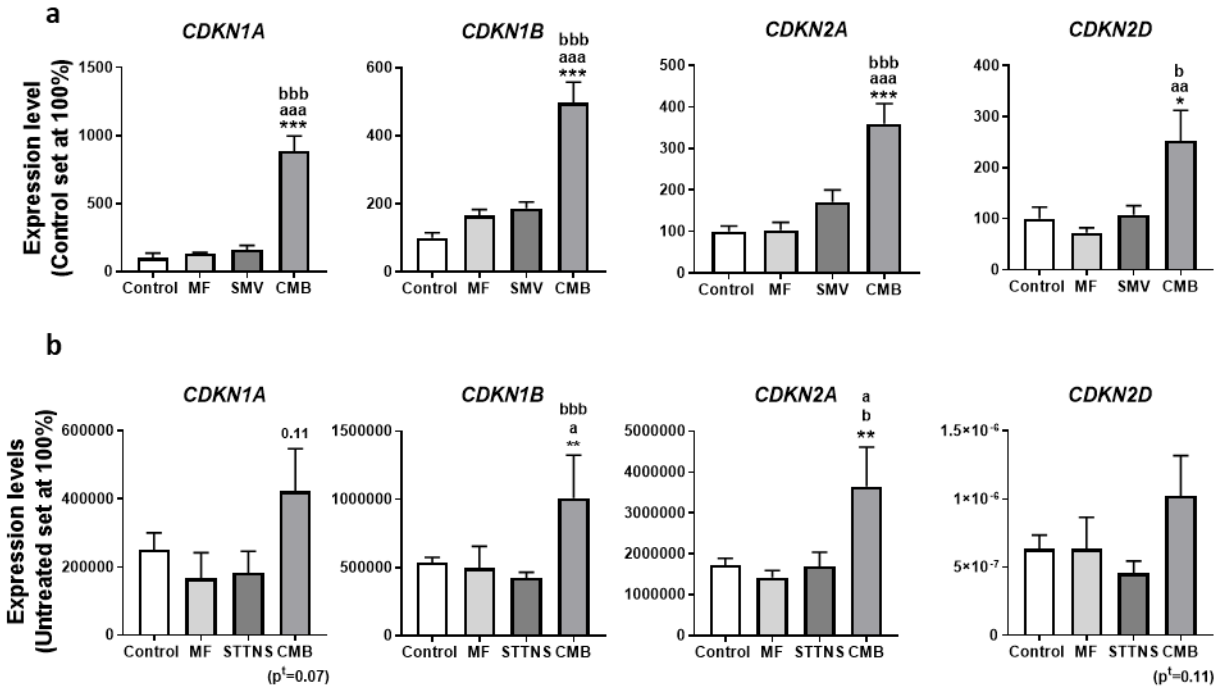
a
CDKN1A
CDKN1B
CDKN2A
CDKN2D
Expression level (Control set at 100%)
Control MF SMV CMB
bbb aaa ***
b aa *
b
STTNS
0.11
a b **
(p^t=0.07)
(p^t=0.11)

Supplementary information

Supplemental Table 1

Gene	Accession Number	Primer Sequence (Sense)	Primer Sequence (Antisense)	Product Size (bp)
AR	NM_000044.4	GCAGGAAGCAGTATCCGAAG	GTTGTCAGAAATGGTCGAAGTG	112
c-MYC	NM_001348061.1	CAGGGATGACTCTGGGAAAA	TGAGGCAAGTCAGCCTTTCT	87
MKI67	NM_002417	GACATCCGTATCCAGCTTCCT	GCCGTACAGGCTCATCAATAAC	139
CDKN1A	NM_001291549.1	TGCCCAAGCTCTACCTTCC	CACATGGTCTTCCTCTGCTGT	116
CDKN1B	NM_004064.4	ATAAGGAAGCGACCTGCAAC	TTGGGGAACCGTCTGAAA	88
CDKN2A	NM_000077	GACATCCCCGATTGAAAGAA	CAGTTGTGGCCCTGTAGGA	91
CDKN2D	NM_001800.4	AACCGCTTCGGCAAGAC	GCTGGCACCTTGCTTCA	84
ACTB	NM_001101	ACTCTTCCAGCCTTCCTTCCT	CAGTGATCTCCTTCTGCATCCT	176
GAPDH	NM_002046	AATCCCATCACCATCTTCCA	AAATGAGCCCCAGCCTTC	122

Supplemental Table 1. Specific primers for human transcripts used in this study. NCBI accession number, primers sequences and expected product sizes are included.

Supplemental Table 2

Protein	Reference	Company
p-AR^{Ser213}	ab133273	Abcam
Total AR	ab71948	Abcam
p-AMPKα^{Thr172}	2535	Cell Signalling
Total AMPKα	2532	Cell Signalling
p-AKT^{Ser473}	9271	Cell Signalling
Total AKT	9272	Cell Signalling
p-ERK^{Thr202}	4370	Cell Signalling
Total ERK	sc-154	Santa Cruz Biotechnology
p-mTOR^{Ser2448}	2971	Cell Signalling
Total mTOR	2972	Cell Signalling

Supplemental Table 2. Specific antibodies used for western blot in this study. Reference and company names are included.

Supplemental Figure 1

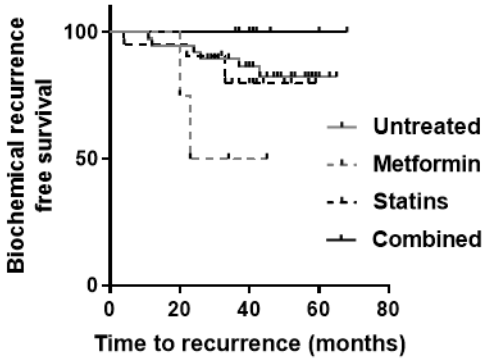

Supplemental Figure 1. Effects of metformin, statins and combined treatment in patients with PCa. Kaplan-Meier survival curve of biochemical recurrence-free survival of PCa patients untreated (n=38) vs. treated with metformin (n=4), vs. treated with simvastatin (n=20) vs. treated with both treatments (n=9). Patients with coadjuvant treatment were excluded from the Kaplan-Meier analysis (n=4).

Supplemental Figure 2

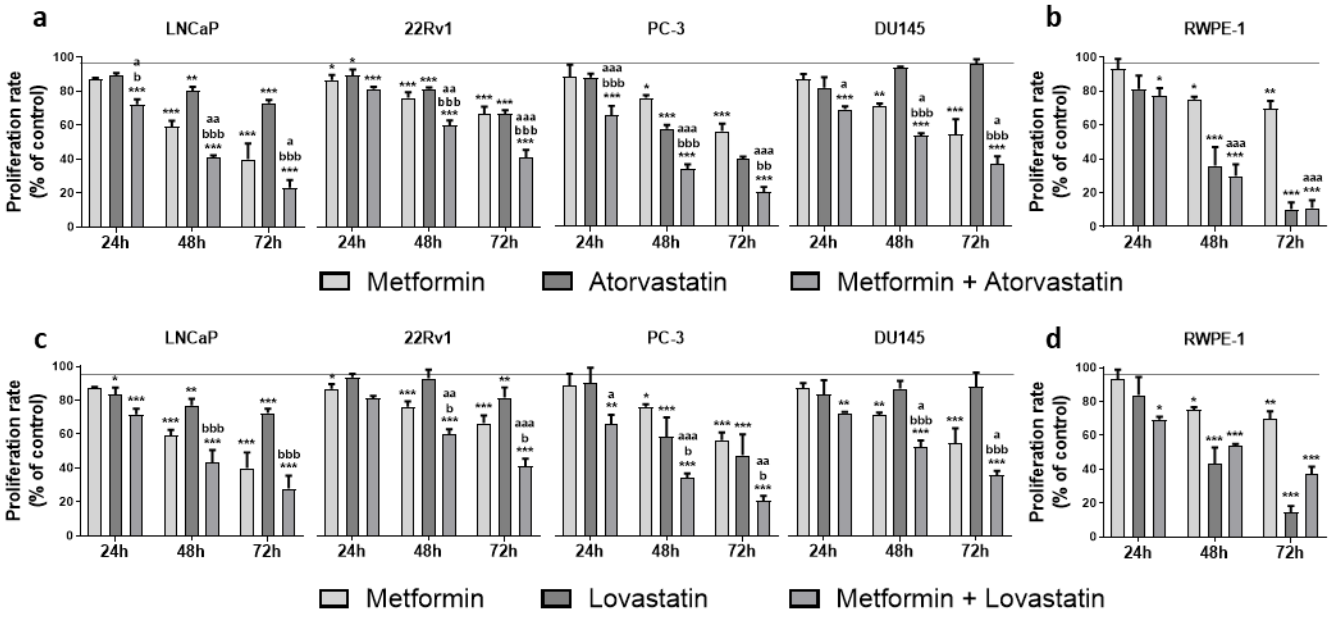

Supplemental Figure 2. Effects of metformin and statins (atorvastatin and lovastatin) and its combination on cell-proliferation of prostate derived cells. a-b) Proliferation rate of PCa cell lines (LNCaP, 22Rv1, PC-3 and DU145) **(a)** and normal-prostate like cell line RWPE-1 **(b)** after 24, 48, and 72 hours of metformin (5mM), atorvastatin (10µM) and combined treatment. **c-d)** Proliferation rate of PCa cell lines (LNCaP, 22Rv1, PC-3 and DU145) **(c)** and normal-prostate like cell line RWPE-1 **(d)** after 24, 48, and 72 hours of metformin (5mM), lovastatin (10µM) and combined treatment. The data are expressed as percentage of proliferation rate compared to untreated control cells (set at 100%). Values represent the mean ± SEM. Asterisks (comparison to control), "a" (comparison to metformin) and "b" (comparison to atorvastatin/lovastatin) (* $p < 0.05$; ** $p < 0.01$; *** $p < 0.001$) indicate statistically significant differences.

Supplemental Figure 3

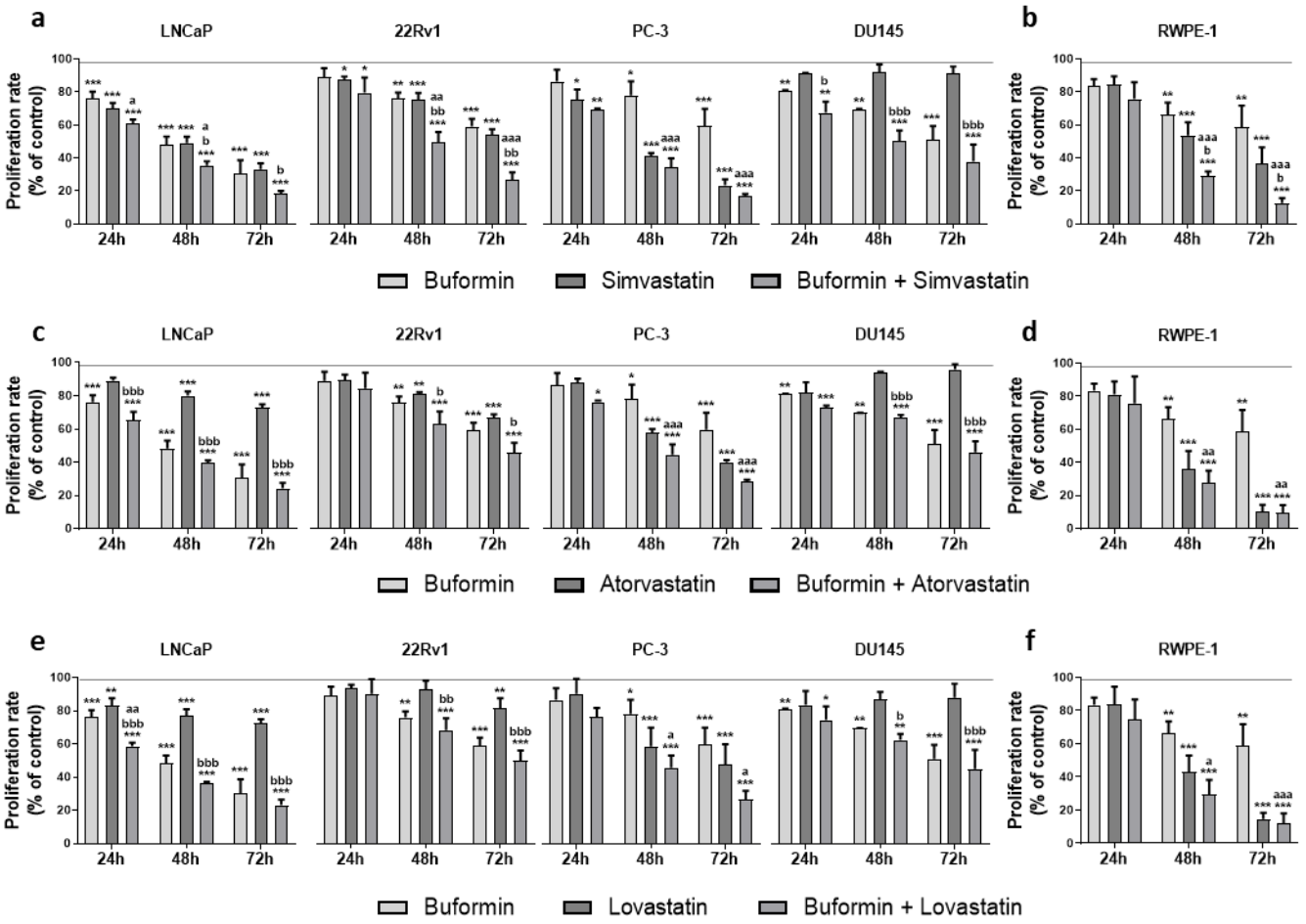

Supplemental Figure 3. Effects of buformin and statins (simvastatin, atorvastatin and lovastatin) and its combination on cell-proliferation of prostate derived cells. a-b) Proliferation rate of PCa cell lines (LNCaP, 22Rv1, PC-3 and DU145) **(a)** and normal-prostate like cell line RWPE-1 **(b)** after 24, 48, and 72 hours of buformin (1mM), simvastatin (10μM) and combined treatment. **c-d)** Proliferation rate of PCa cell lines (LNCaP, 22Rv1, PC-3 and DU145) **(c)** and normal-prostate like cell line RWPE-1 **(d)** after 24, 48, and 72 hours of buformin (5mM), atorvastatin (10μM) and combined treatment. **e-f)** Proliferation rate of PCa cell lines (LNCaP, 22Rv1, PC-3 and DU145) **(e)** and normal-prostate like cell line RWPE-1 **(f)** after 24, 48, and 72 hours of buformin (1mM), lovastatin (10μM) and combined treatment. The data are expressed as percentage of proliferation rate compared to untreated control cells (set at 100%). Values represent the mean ± SEM. Asterisks (comparison to control), "a" (comparison to buformin) and "b" (comparison to statins) (* $p < 0.05$; ** $p < 0.01$; *** $p < 0.001$) indicate statistically significant differences.

Supplemental Figure 4

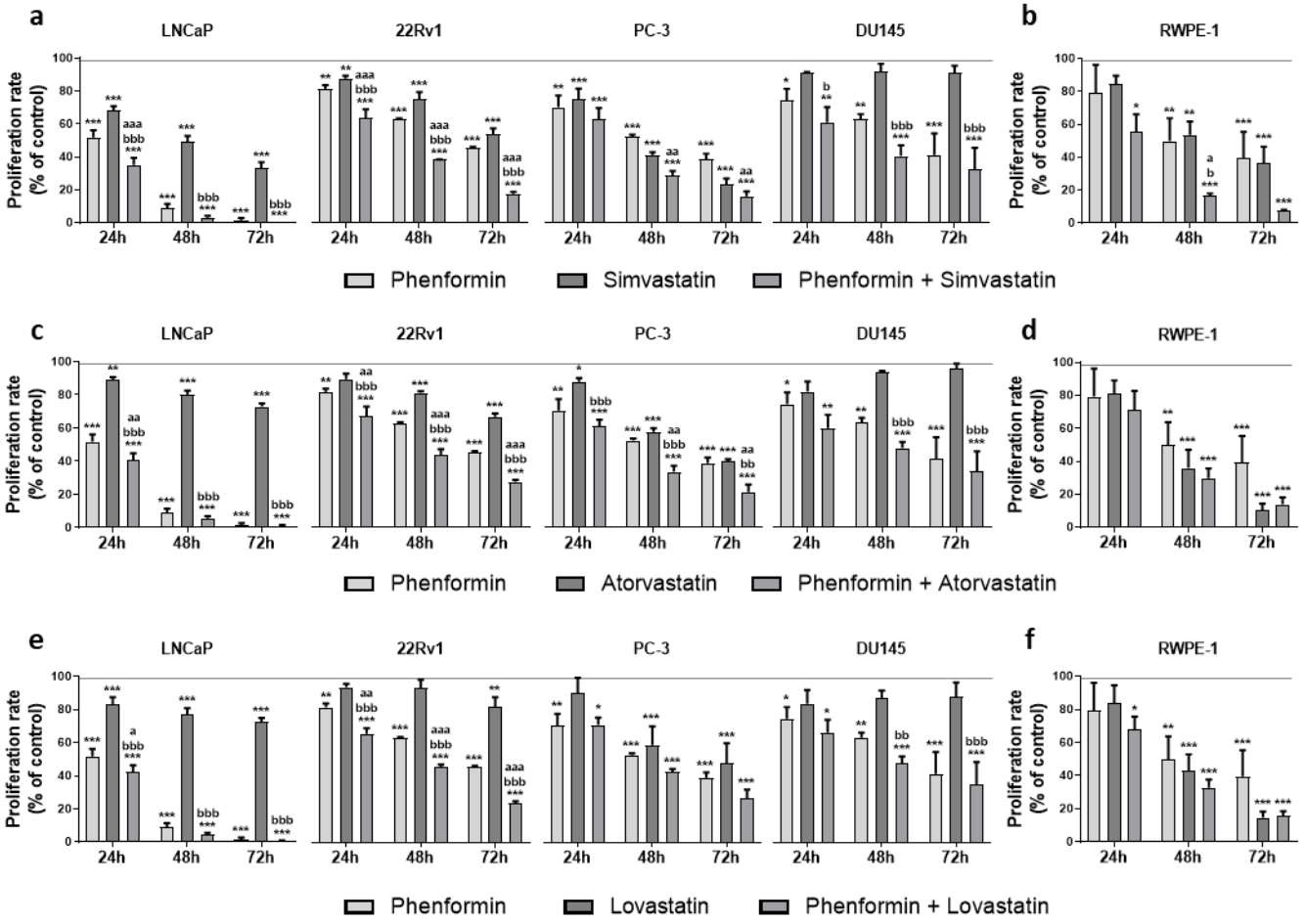

Supplemental Figure 5. Representative images of functional assays in response to metformin, simvastatin and combined treatment in LNCaP, DU145 and RWPE-1 cells. a) Images of migration assay in LNCaP (upper panel), DU145 (middle panel) and RWPE-1 (lower panel) after 12 hours of incubation with metformin (5mM), simvastatin (10μM) and combined treatment. **(b)** Images of LNCaP tumorspheres after 14 days of incubation (treatment refreshed every 3 days) with metformin (5mM), simvastatin (10μM) and combined treatment.

Supplemental Figure 5

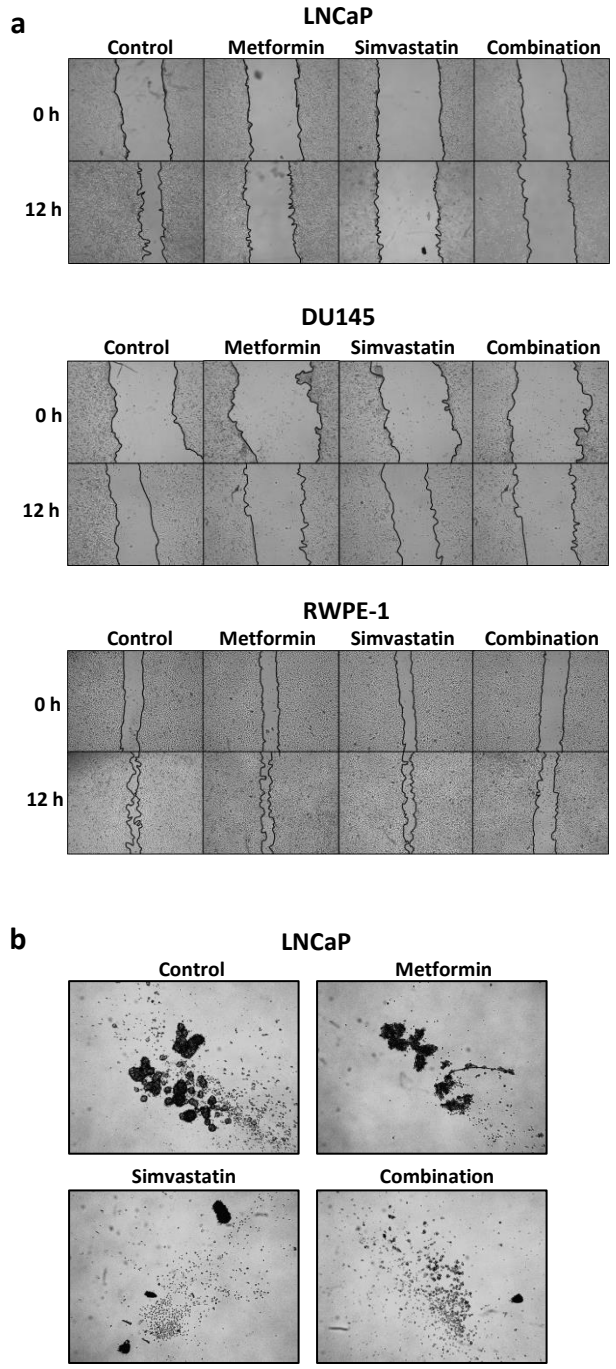

Supplemental Figure 4. Effects of phenformin and statins (simvastatin, atorvastatin and lovastatin) and its combination on cell-proliferation of prostate derived cells. a-b) Proliferation rate of PCa cell lines (LNCaP, 22Rv1, PC-3 and DU145) **(a)** and normal-prostate like cell line RWPE-1 **(b)** after 24, 48, and 72 hours of phenformin (1mM), simvastatin (10µM) and combined treatment. **c-d)** Proliferation rate of PCa cell lines (LNCaP, 22Rv1, PC-3 and DU145) **(c)** and normal-prostate like cell line RWPE-1 **(d)** after 24, 48, and 72 hours of phenformin (1mM), atorvastatin (10µM) and combined treatment. **e-f)** Proliferation rate of PCa cell lines (LNCaP, 22Rv1, PC-3 and DU145) **(e)** and normal-prostate like cell line RWPE-1 **(f)** after 24, 48, and 72 hours of phenformin (1mM), lovastatin (10µM) and combined treatment. The data are expressed as percentage of proliferation rate compared to untreated control cells (set at 100%). Values represent the mean ± SEM. Asterisks (comparison to control), "a" (comparison to buformin) and "b" (comparison to statins) (* $p < 0.05$; ** $p < 0.01$; *** $p < 0.001$) indicate statistically significant differences.

Article VI

Journal of
Clinical Medicine

MDPI

Article

Clinical Utility of Ghrelin-O-Acyltransferase (GOAT) Enzyme as a Diagnostic Tool and Potential Therapeutic Target in Prostate Cancer

Juan M. Jiménez-Vacas [1,2,3,4], Enrique Gómez-Gómez [1,2,3,5], Antonio J. Montero-Hidalgo [1,2,3,4], Vicente Herrero-Aguayo [1,2,3,4], Fernando L-López [1,2,3,4], Rafael Sánchez-Sánchez [1,3,6], Ipek Guler [1,3,7], Ana Blanca [1,3,5], María José Méndez-Vidal [1,3,8], Julia Carrasco [1,3,5], José Lopez-Miranda [1,3,9], María J. Requena-Tapia [1,3,5], Justo P. Castaño [1,2,3,4], Manuel D. Gahete [1,2,3,4] and Raúl M. Luque [1,2,3,4,*]

1 Maimonides Institute for Biomedical Research of Córdoba (IMIBIC), 14004 Córdoba, Spain; b12jivaj@uco.es (J.M.J.-V.); enriquegomezgomez@yahoo.es (E.G.-G.); antonio.montero.96@gmail.com (A.J.M.-H.); b22heagv@uco.es (V.H.-A.); ferll_@hotmail.com (F.L.-L.); patologiahrs@gmail.com (R.S.-S.); ipek.guler@imibic.org (I.G.); anblape78@hotmail.com (A.B.); mjosemv@yahoo.es (M.J.M.-V.); julia.carrasco.sspa@juntadeandalucia.es (J.C.); md1lomij@uco.es (J.L.-M.); josefa.requena.sspa@juntadeandalucia.es (M.J.R.-T.); justo@uco.es (J.P.C.); bc2gaorm@uco.es (M.D.G.)
2 Department of Cell Biology, Physiology, and Immunology, University of Córdoba, 14071 Córdoba, Spain
3 Hospital Universitario Reina Sofía (HURS), 14004 Córdoba, Spain
4 Centro de Investigación Biomédica en Red de Fisiopatología de la Obesidad y Nutrición, (CIBERobn), 14004 Córdoba, Spain
5 Urology Service, HURS/IMIBIC, 14004 Córdoba, Spain
6 Anatomical Pathology Service, HURS, 14004 Córdoba, Spain
7 Department of Innovation and Methodology, IMIBIC, 14004 Córdoba, Spain
8 Oncology Department, IMIBIC, 14004 Córdoba, Spain
9 Lipids and Atherosclerosis Unit, Reina Sofia University Hospital, 14004 Córdoba, Spain
* Correspondence: raul.luque@uco.es

Received: 15 October 2019; Accepted: 19 November 2019; Published: 22 November 2019

Abstract: Recent data suggested that plasma Ghrelin O-Acyl Transferase enzyme (GOAT) levels could represent a new diagnostic biomarker for prostate cancer (PCa). In this study, we aimed to explore the diagnostic and prognostic/aggressiveness capacity of GOAT in urine, as well as to interrogate its putative pathophysiological role in PCa. We analysed urine/plasma levels of GOAT in a cohort of 993 patients. In vitro (i.e., cell-proliferation) and in vivo (tumor-growth in a xenograft-model) approaches were performed in response to the modulation of GOAT expression/activity in PCa cells. Our results demonstrate that plasma and urine GOAT levels were significantly elevated in PCa patients compared to controls. Remarkably, GOAT significantly outperformed PSA in the diagnosis of PCa and significant PCa in patients with PSA levels ranging from 3 to 10 ng/mL (the so-called PSA grey-zone). Additionally, urine GOAT levels were associated to clinical (e.g., Gleason-score, PSA levels) and molecular (e.g., *CDK2*/*CDK6*/*CDKN2A* expression) aggressiveness parameters. Indeed, *GOAT* overexpression increased, while its silencing/blockade decreased cell-proliferation in PCa cells. Moreover, xenograft tumors derived from GOAT-overexpressing PCa (DU145) cells were significantly higher than those derived from the mock-overexpressing cells. Altogether, our results demonstrate that GOAT could be used as a diagnostic and aggressiveness marker in urine and a therapeutic target in PCa.

Keywords: GOAT-enzyme; prostate cancer; diagnosis; therapy; PSA

1. Introduction

Prostate cancer (PCa) is one of the tumor pathologies with the highest incidence among the male population and represents a severe health problem worldwide [1]. Early detection of PCa is a crucial step for the successful management of patients with this pathology. The detection of PCa cases has been refined with the establishment of the prostatic specific antigen (PSA) as the gold standard tool for PCa diagnosis. However, although PSA levels are used in clinical practice, this diagnostic tool poses important limitations, especially in the so-called "grey zone" (defined as a PSA range of 3–10 ng/mL). The most important drawback is the compromised specificity, which is due to the fact that there are several non-tumor factors (i.e., benign prostatic hyperplasia, prostatitis) associated to an increase of PSA levels [2]. For these reasons, the anatomo-pathological analysis of prostate biopsies, which represent a highly invasive technique, is still essential to appropriately diagnose PCa. Therefore, the use of PSA levels as diagnostic tool for PCa is linked to many unnecessary biopsies, which are potentially associated to clinical side effects (e.g., infections, bleeding), overdiagnosis and overtreatment, thus leading to an increase in economic burden [3]. In this sense, many efforts have been made in order to identify novel and more accurate PCa biomarkers, which has led to the identification of certain promising candidates [4]. However, these candidates have not been globally introduced in the clinical practice, likely due to the lack of validation in sufficiently ample cohorts and/or the high cost associated to their determination. For these reasons, new biomarkers for PCa diagnosis are necessary, ideally non-invasive biomarkers with also prognostic/aggressiveness and/or therapeutic potential.

In this regard, a ghrelin system has emerged as a pivotal regulatory axis in PCa pathophysiology [5,6], as well as a source of potential PCa biomarkers, since certain peptides derived from this pleiotropic system (i.e., native ghrelin, In1-ghrelin splice variant) are secreted by PCa cells and associated to PCa aggressiveness [7,8]. Ghrelin axis is controlled, at least in part, by the Ghrelin O-Acyl Transferase (GOAT or MBOAT4), an enzyme involved in the acylation and, thus, activation of ghrelin. This acylation is necessary for the binding of ghrelin to GHSR1a [9]. The GOAT enzyme is mainly produced in stomach and pancreas [10] and regulated by energy status and relevant metabolic cues [11]. Interestingly, our laboratory has previously reported that GOAT is overexpressed in PCa tissues and released by PCa cells [12]. Moreover, we have recently demonstrated in a cohort of 312 patients that plasma GOAT levels are higher in patients with PCa and particularly, in patients with clinically significant PCa (SigPCa, defined as PCa with Gleason score ≥ 7) as compared to controls, which included patients with suspected PCa but negative biopsy results and those with indolent PCa (defined as PCa with Gleason 6) [13]. Indeed, this study also showed that plasma GOAT levels were able to outperform the diagnostic capability of PSA, especially in the grey zone [13]. However, to date, the clinical utility of GOAT as a diagnostic (or prognostic/aggressiveness) tool in urine samples (a body sample less invasive and with a more prostate-specific content) from PCa patients has not been explored. Furthermore, although the actions of other elements of the ghrelin system (ghrelin, In1-ghrelin) in PCa have been well defined [7,8], the putative pathophysiological role of GOAT in this cancer type remains unknown. For these reasons, in this study, we aimed to explore, for the first time, the clinical utility of urine GOAT levels (and compared with plasma levels) to diagnose PCa, using an ample cohort of patients (almost 1000 patients) and to determine the role of GOAT in the pathophysiology of PCa.

2. Experimental Section

2.1. Patients and Samples

This study was approved by the Hospital Ethic Committee and written informed consent from all patients was obtained. All samples were obtained through the Andalusian Biobank (Nodo Córdoba, Servicio Andaluz de Salud, Spain). The patients included in this study were divided in 3 different cohorts.

Cohort 1: healthy volunteers ($n = 97$) that donated urine and blood samples.

Cohort 2: Patients with suspect of PCa but negative results in the biopsy (n = 549).

Cohort 3: Patients diagnosed with PCa (biopsy-proven, n = 347). Specifically, this cohort was divided in patients with non-significant PCa (NonSigPCa; defined as Gleason score of 6 in the biopsy; n = 143; cohort 3a), and in patients with significant PCa (SigPCa; defined as Gleason score ≥ 7 on the biopsy; n = 204; cohort 3b).

This is a retrospective study wherein patients (both from cohorts 2 and 3) were collected between 2013 and 2015 by consecutive recruitment of individuals with suspicion of PCa that underwent a transrectal ultrasound (TRUS) guided prostate biopsy according to clinical practice in the Urology Department of Reina Sofia Hospital (Córdoba, Spain). Blood and plasma samples were collected early in the morning after an overnight fast and just before the prostate biopsy. Recommendations for biopsy indication were suspicious findings on digital rectal examination (DRE), PSA > 10 ng/mL, or PSA 3–10 ng/mL if free PSA ratio was low (usually, <25–30%), and in patients with previous biopsies, a persistent suspicion of PCa (i.e., persistently elevated PSA, suspicious DRE, etc.). For transrectal prostate biopsy, 12 biopsy cores were obtained from patients undergoing the first biopsy procedure and a minimum of 16 biopsy cores for those who had a previous biopsy. All biopsy specimens were analyzed by experienced urologic pathologists according to the International Society of Urological Pathology 2005 modified criteria [14]. Tumor regions (n = 84) were identified from the Formalin-Fixed Paraffin-Embedded (FFPE) samples by expert urologic pathologists as previously reported [15,16] and used to isolate RNA and perform gene expression analyses. The FFPE pieces were taken from radical prostatectomies (patients belonging to cohort 3).

2.2. GOAT and PSA Determinations

A commercial ELISA (MBS2019923; MyBioSource, San Diego, CA, USA) was used to determine urine and plasma GOAT levels following the instructions of the manufacturer. The ELISA kit shows a detection limit lower than 0.31 ng/mL and a detection range of 0.78–50 ng/mL, as well as an intra- and inter-assay accuracy with a coefficient of variation lower than 10% and 12%, respectively. The donated urine samples were stored in 1.5 mL aliquots at −80 °C. Urine samples were diluted 1:100 before performing the assay. Measurement of PSA levels was performed in the laboratory service of the Reina Sofia University Hospital of Córdoba using the Chemiluminescent Microparticle Immunoassays technology (7k70; Abbott, Madrid, Spain) following the manufacturer's instructions.

2.3. Cell Culture and Reagents

DU145 and LNCaP cell lines were obtained from American Type Culture Collection (ATCC; Manassas, VA, USA), cultured according to the manufacturer's instructions, validated by analysis of short tandem repeats sequences using GenePrint 10 System (Promega, Barcelona, Spain) and checked for mycoplasma contamination by PCR as previously reported [8,16]. DU145 cells were selected for functional in vitro and in vivo analyses based on its high expression levels of In1-ghrelin, the main oncogenic element of the ghrelin axis in prostate cancer, which is also a putative target of GOAT [8]. The GOAT inhibitor "GO-CoA-Tat" (032-37; Phoenix Biotech, Burlingame, CA, USA) was resuspended in water and used at 10 μM since this dose has been previously reported to be effective reducing GOAT activity [17].

2.4. Transient Transfection with siRNAs

For silencing assays, 200,000 cells (DU145) were seeded in 6-well culture plates and grown until 70% confluence was achieved. Then, cells were transfected with a specific siRNA against GOAT (s54791; Thermo Fisher Scientific, Madrid, Spain) or with the control siRNA ("scramble"; 4390844; Thermo Fisher Scientific) at 100 nM using Lipofectamine-RNAiMAX (Thermo Fisher Scientific) according to the manufacturer's instructions. The efficiency of *GOAT* silencing was confirmed by qPCR and subsequently, proliferation assay was performed in siRNA-transfected or scramble-transfected cells.

2.5. Stable Transfection with Plasmids

A DU145 cell line was stably transfected with pCDNA3.1 vector containing *GOAT* transcript (OHu31938; GenScript, Leiden, Netherlands) and with a "mock" or empty-control pCDNA3.1 vector (GenScript, Leiden, Netherlands) following the manufacturer's instructions. The transfected cells were selected adding Geneticine (Thermo Fisher Scientific) at 1% to the culture media. The efficiency of *GOAT* overexpression was confirmed by qPCR and subsequently, proliferation assay was performed in response to transfected (GOAT-overexpression vs. mock) cells. Moreover, in vivo xenograft analyses were performed using these transfected (GOAT-overexpression vs. mock) cells (see below).

2.6. Cell Proliferation

Cell proliferation was evaluated using Alamar-Blue assay (Bio-Source International, Camarillo, CA, USA) in DU145 cells, as previously reported [16]. Briefly, cells were seeded in 96-well culture plates at a density of 3000–5000 cells/well and serum-starved for 24 h. Then, fluorescence (560 nm) was evaluated using the FlexStation III system (Molecular Devices, Sunnyvale, CA, USA) after 3 h of incubation with Alamar-Blue compound at 10%. This assay was performed during 3 days in response to different experimental conditions (silencing, overexpression, or treatment).

2.7. RNA Extraction and Retrotranscription

Total RNA from FFPE samples was isolated and DNase-treated using the Maxwell 16 LEVRNA FFPE Kit (Promega, Madison, WI, USA) in the Maxwell MDx 16 Instrument (Promega, Madrid, Spain) according to the manufacturer's instructions. Additionally, total RNA from PCa cell lines was extracted using TRIzol Reagent (Thermo Fisher Scientific), followed by DNase treatment using RNase-Free DNase Kit (Qiagen, Hilden, Germany). Total RNA concentration and purity were assessed using Nanodrop One Spectrophotometer (Thermo Fisher Scientific). Total RNA was retrotranscribed using random hexamer primers and the cDNA First Strand Synthesis kit (Thermo Fisher Scientific).

2.8. Real-Time qPCR

The expression levels of selected transcripts were evaluated by real-time qPCR (RT-qPCR) using a Mx3000P thermocycler (Agilent, Madrid, Spain). Development and validation of the primers used in the RT-qPCR have been previously reported by our laboratory [18–20]. Specific primers used in this study were previously validated [12]: *GOAT* (sense: TTGCTCTTTTTCCCTGCTCTC; antisense: ACTGCCACGTTTAGGCATTCT; 161 bp); *ACTB* (sense: ACTCTTCCAGCCTTCCTTCCT antisense: CAGTGATCTCCTTCTGCATCCT; 176 bp); *GAPDH* (sense: AATCCCATCACCATCTTCCA; antisense: AAATGAGCCCCAGCCTTC; 122 bp). To control for variations in the efficiency of the retro-transcription reaction, mRNA copy numbers of the different transcripts analyzed were adjusted by a normalization factor, which was calculated with the expression levels of *ACTB* and *GAPDH* using GeNorm 3.3 (CMMG, Ghent, Belgium) [21].

2.9. Xenograft Assay

Experiments with mice were carried out according to the European Regulations for Animal Care under the approval of the university/regional government research ethics committees. Ten-week-old male athymic BALB/cAnNRj-Foxn1nu mice (n = 5; Janvier Labs, Le Genest-Saint-Isle, France) were subcutaneously grafted in one of the flanks with 106 mock-transfected (n = 5 tumors) and in the other flank with 106 stably GOAT-transfected DU145 cells (n = 5 tumors), which were resuspended in 100 mL basement membrane extract (Trevigen, Gaithersburg, MD, USA). Tumor growth was monitored once per week for one month using a digital caliper. After euthanasia of mice, each tumor was dissected, fixed, and sectioned for RNA isolation (snap-frozen) and histopathological-examination after hematoxylin-eosin staining. The examination of the number of mitosis and positive KI67 cells in the

immunohistochemistry sections of xenograft tumors were performed by expert anatomo-pathologists as previously reported [16].

2.10. Statistical Analyses

Statistical differences between two groups (cell lines and patients' data) were calculated by unpaired parametric t-test or a nonparametric Mann–Whitney *U* test, according to normality, assessed by the Kolmogorov–Smirnov test. For differences among the three groups, a one-way ANOVA analysis was performed. For cohorts' clinical descriptive characteristics comparison, a chi-square test and ANOVA test with Bonferroni post hoc analysis were performed. Spearman's or Pearson's bivariate correlations were performed for quantitative variables according to normality. Statistical analyses were assessed using GraphPad Prism 7 (GraphPad Software, La Jolla, CA, USA) or SPSS version 17.0. (IBM, Armonk, NY, USA). All the in vitro experiments were performed at least 3 independent times ($n \geq 3$) and with at least 2 technical replicates. Univariate logistic regressions were performed for the estimation of the effect of urine GOAT and PSA levels on the risk of SigPCa and NonSigPCa to further assess the predictive capacity of each biomarker separately by using receiver operating characteristics (ROC) analysis with area under the curve (AUC). A multivariate logistic regression was performed to detect risk factors for SigPCa and NonSigPCa, and the confidence intervals (CIs) of odds ratios (ORs) were calculated by ordinary bootstrapping techniques with 2000 boostrap replicates. Logistic regression models and ROC curve analysis were assessed using R software (version 3.5.0.; The R Foundation, Vienna, Austria). Statistical significance was considered when $p < 0.05$. A trend for significance was indicated when p values ranged between >0.05 and <0.1.

3. Results

3.1. Description of the Cohort

The clinical characteristics of the three different cohorts evaluated ($n = 993$ patients) are depicted in Table 1. Patients with PCa (cohort 3) were older compared to patients with negative biopsy (cohort 2) and healthy patients (cohort 1) (67 years (62–72) vs. 63 years (57–69) vs. 62 years (57–67), respectively; $p < 0.01$). Patients with PCa had significantly higher plasma PSA levels compared to healthy patients (cohort 3 vs. cohort 1: 6.64 (4.49–11.32) vs 0.82 (0.57–1.33) ng/mL; $p < 0.05$), while a similar, albeit non-significant trend was found compared to patients with negative biopsy (cohort 3 vs. cohort 2: 6.64 (4.49–11.32) vs. 5.27 (3.84–7.39) ng/mL; $p = 0.11$). No differences in BMI between groups were found. The proportion of patients with previous biopsy and normal DRE was significantly higher in patients with negative biopsy compared to the patients with PCa (cohort 2 vs. cohort 3; $p < 0.01$). The percentage of patients with family history of PCa did not differ between patients with PCa and with negative biopsy. Finally, 59% of the patients with PCa (cohort 3) had a Gleason score (GS) of 7 or higher on the biopsy (those classified as SigPCa; cohort 3b; $n = 204$ and 8.8% ($n = 18$) presented metastasis at the diagnosis (Table 1). Patients with SigPCa (cohort 3b) had significantly higher plasma PSA levels compared to healthy patients and negative biopsy patients ($p < 0.001$), while a similar, albeit non-significant difference was found compared to patients with NonSigPCa (cohort 3a).

Table 1. Clinical and anatomopathological data of the three cohorts of patients included in this study.

Variable	Healthy $n = 97$ Cohort 1	NegBiopsy $n = 549$ Cohort 2	PCa $n = 347$		
			All $n = 347$ Cohort 3	NonSigPCa $n = 143$ Cohort 3a	SigPCa $n = 204$ Cohort 3b
Age Median (IQR)	62 (57–67)	63 (57–69)	67 (61–72)	65 (59–69)	69 (63–75)
PSA level (ng/mL) Median (IQR)	0.82 (0.57–1.33)	5.27 (3.84–7.39)	6.64 (4.49–11.32)	5.62 (3.79–9.09)	7.44 (4.83–16.09)

Table 1. *Cont.*

Variable	Healthy $n = 97$ Cohort 1	NegBiopsy $n = 549$ Cohort 2	PCa $n = 347$		
			All $n = 347$ Cohort 3	NonSigPCa $n = 143$ Cohort 3a	SigPCa $n = 204$ Cohort 3b
BMI	28.41 (25.54–32.09)	28.31 (25.96–30.86)	28.62 (26.30–31.63)	28.41 (26.44–31.15)	28.72 (26.15–32.05)
Patients with previous negative biopsy	-	174 (31.7)	66 (19.0)	35(24.5)	31 (15.2)
DRE (Abnormal)	-	59 (10.7)	125 (36.0)	34 (23.8)	91 (44.6)
5 alpha reductase inhibitors		20 (3.6)	5 (1.4)	1(0.7)	4 (0.2)
Family History		106 (19.3)	55 (15.9)	25 (17.5)	30 (14.7)
GS < 7	-	0	143 (41.2)		
GS ≥ 7	-	0	204 (58.8)		
Metastasis (%)	-	0	18 (5.2)	0	18 (8.8)

BMI: Body mass index; DRE: Digital rectal examination; PCa: Prostate cancer; SigPCa: Significant prostate cancer; IQR: Interquartile range; GS: Gleason score. Information about five alpha reductase inhibitors and family history of PCa was only collected for NegBiopsy and PCa patients.

3.2. Levels of GOAT in Non-Invasive Samples from Patients with and without PCa

Consistently with a previous study [13], the plasma levels of GOAT were significantly higher in SigPCa patients compared to healthy individuals, NegBiopsy- and NonSigPCa-patients (Supplementary Figure S1a). Similarly, urine levels of GOAT were found to be higher in SigPCa patients as compared to healthy individuals and NegBiopsy patients (Supplementary Figure S1b). Moreover, urine GOAT levels from NonSigPCa patients were higher compared to healthy individuals and NegBiopsy patients (Supplementary Figure S1b). Remarkably, although the ROC curve analysis revealed that the levels of both plasma and urine GOAT were able to significantly discriminate healthy individuals vs. PC patients, healthy individuals vs. SigPCa patients, NegBiopsy vs. PCa patients and NegBiopsy vs. SigPCa patients, urine GOAT significantly outperformed the capability of plasma GOAT to distinguish among these groups of patients (Supplementary Figure S1c–f). Therefore, based on these results, we decided to continue the present study by focusing on the analysis of GOAT urine levels.

3.3. Comparison of Diagnostic Capacity of Urine GOAT and Plasma PSA

In order to investigate the diagnostic capacity of urine GOAT levels and compare it with that of plasma PSA levels, we evaluated these levels in patients with initial suspect of PCa (cohorts 2 and 3). In particular, urine GOAT levels and plasma PSA levels were significantly higher in PCa patients compared to NegBiopsy patients (Figure 1a,b). No differences were found when comparing the AUCs of GOAT and PSA to detect PCa (Figure 1c). Similarly, urine GOAT levels and plasma PSA levels were significantly higher in SigPCa patients compared to NegBiopsy + NonSigPCa patients (Figure 1d,e), while no differences were found when comparing the AUCs of GOAT and PSA to detect SigPCa (Figure 1f). However, when patients in the grey zone were analyzed, although both urine GOAT and plasma PSA levels were significantly higher in patients with PCa compared to those with NegBiopsy (Figure 1g,h), only urine GOAT levels were able to significantly discriminate between PCa vs. NegBiopsy patients (Figure 1i). In addition, urine GOAT levels (but not PSA levels) were higher in SigPCa compared to NegBiopsy +NonSigPCa patients (Figure 1j,k) and were able to distinguish between SigPCa patients and NegBiopsy +NonSigPCa patients (Figure 1l).

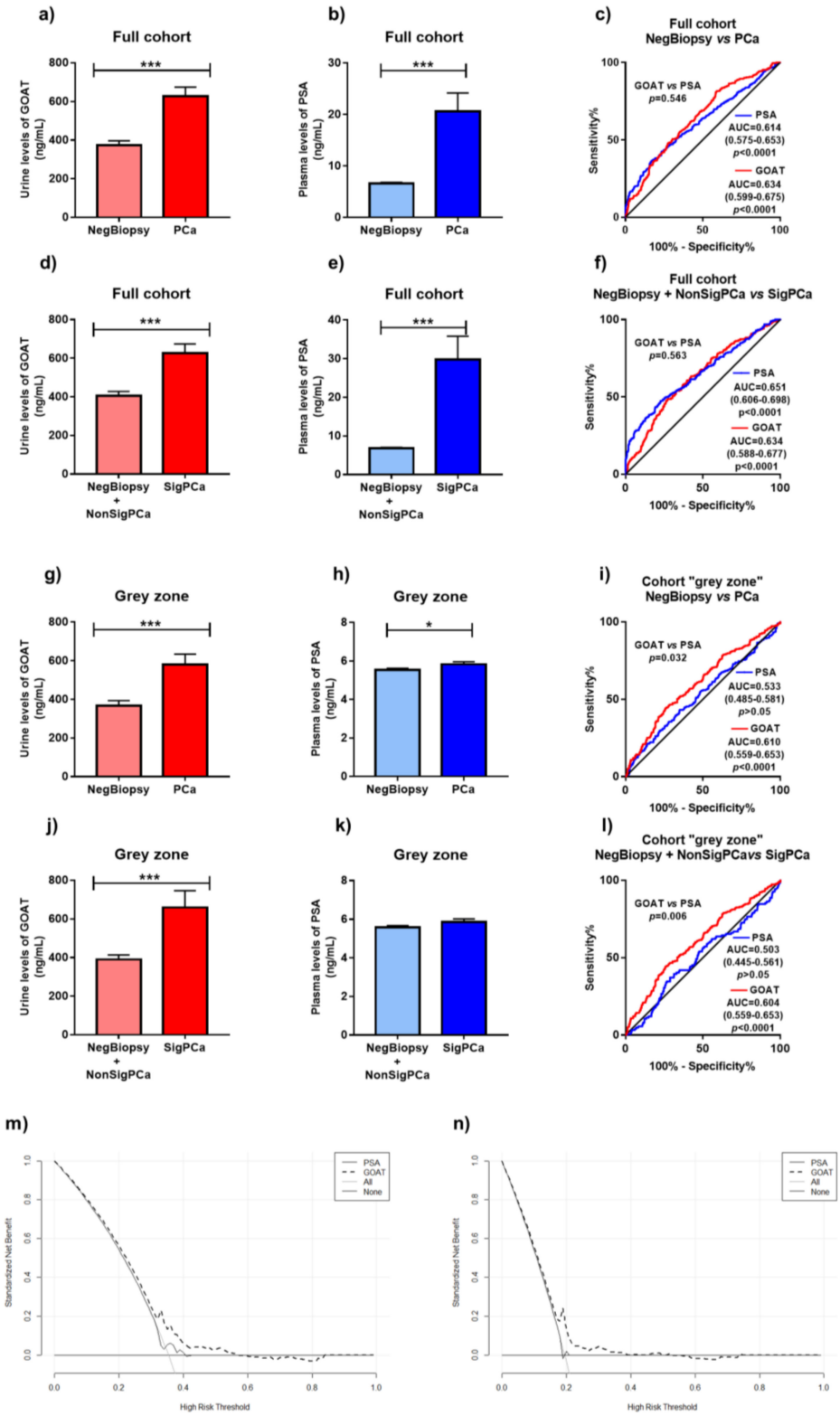
a)
Full cohort
***
Urine levels of GOAT (ng/mL)
NegBiopsy
PCa
b)
Full cohort
***
Plasma levels of PSA (ng/mL)
NegBiopsy
PCa
c)
Full cohort
NegBiopsy vs PCa
GOAT vs PSA p=0.546
PSA AUC=0.614 (0.575-0.653) p<0.0001
GOAT AUC=0.634 (0.599-0.675) p<0.0001
Sensitivity%
100% - Specificity%
d)
Full cohort
***
Urine levels of GOAT (ng/mL)
NegBiopsy + NonSigPCa
SigPCa
e)
Full cohort
***
Plasma levels of PSA (ng/mL)
NegBiopsy + NonSigPCa
SigPCa
f)
Full cohort
NegBiopsy + NonSigPCa vs SigPCa
GOAT vs PSA p=0.563
PSA AUC=0.651 (0.606-0.698) p<0.0001
GOAT AUC=0.634 (0.588-0.677) p<0.0001
Sensitivity%
100% - Specificity%
g)
Grey zone
***
Urine levels of GOAT (ng/mL)
NegBiopsy
PCa
h)
Grey zone
*
Plasma levels of PSA (ng/mL)
NegBiopsy
PCa
i)
Cohort "grey zone"
NegBiopsy vs PCa
GOAT vs PSA p=0.032
PSA AUC=0.533 (0.485-0.581) p>0.05
GOAT AUC=0.610 (0.559-0.653) p<0.0001
Sensitivity%
100% - Specificity%
j)
Grey zone
***
Urine levels of GOAT (ng/mL)
NegBiopsy + NonSigPCa
SigPCa
k)
Grey zone
Plasma levels of PSA (ng/mL)
NegBiopsy + NonSigPCa
SigPCa
l)
Cohort "grey zone"
NegBiopsy + NonSigPCavs SigPCa
GOAT vs PSA p=0.006
PSA AUC=0.503 (0.445-0.561) p>0.05
GOAT AUC=0.604 (0.559-0.653) p<0.0001
Sensitivity%
100% - Specificity%
m)
PSA
GOAT
All
None
Standardized Net Benefit
High Risk Threshold
n)
PSA
GOAT
All
None
Standardized Net Benefit
High Risk Threshold

Figure 1. Urine Ghrelin O-Acyl Transferase enzyme (GOAT) and plasma PSA levels according to patient categorization. (**a**,**b**) Comparison between urine GOAT (**a**) and plasma PSA (**b**) levels in patients with suspect of PCa but with negative results in the biopsy (NegBiopsy; n = 549) and patients diagnosed with PCa (PCa; n = 347). (**c**) Comparison between the receiver operating characteristic (ROC) curves analyses of the capacity of GOAT (**red line**) and PSA (**blue line**) to discriminate among NegBiopsy and PCa patients. (**d**,**e**) Comparison of urine GOAT (**d**) and plasma PSA (**e**) levels in NegBiopsy patients (n = 549) and patients diagnosed with non-significant PCa (NonSigPCa; n = 143) vs. patients diagnosed with significant PCa (SigPCa; n = 204). (**f**) Comparison between the ROC curves analyses of the capacity of GOAT (**red line**) and PSA (**blue line**) to discriminate among NegBiopsy and NonSigPCa patients vs. PCa patients. (**g**,**h**) Comparison between urine GOAT (**g**) and plasma PSA (**h**) levels in patients in the grey zone of PSA (range 3–10 ng/mL) with suspect of PCa but with negative result in the biopsy (NegBiopsy; n = 411) and patients in the grey zone of PSA diagnosed with PCa (PCa; n = 225). (**i**) Comparison between the ROC curves analyses of the capacity of GOAT (**red line**) and PSA (**blue line**) to discriminate among NegBiopsy and PCa patients in the grey zone of PSA. (**j**,**k**) Comparison of urine GOAT (**j**) and plasma PSA (**k**) levels of patients in the grey zone of PSA with NegBiopsy and patients in the PSA grey zone diagnosed with NonSigPCa vs. PCa patients in the PSA grey zone diagnosed with SigPCa (n = 124). (**l**) Comparison between the ROC curves analyses of the capacity of GOAT (**red line**) and PSA (**blue line**) to discriminate among patients in the grey zone of PSA with NegBiopsy and those diagnosed with NonSigPCa vs. patients in the PSA grey zone diagnosed with SigPCa. (**m**,**n**) Results of the decision curve analysis. The net benefit for the prediction of PCa (**m**) and SigPCa (**n**) on biopsy is shown, by using the different models (GOAT and PSA) as a function of the risk threshold, compared to the benefits of strategies for treating all patients (**grey thin line**) and treating none (**grey thick line**). In all cases, data represent mean ± SEM. Asterisks (*, $p < 0.05$; ***, $p < 0.001$) indicate values that significantly differ between groups.

In addition, to address the potential clinical utility of the measurement of both proteins (GOAT and PSA), we performed a decision curve analysis on our data, as proposed by Vickers and Elkin [20]. Based on the net plotting against the threshold probabilities for the comparisons between GOAT and PSA estimates, a clear benefit of GOAT against PSA was found, particularly in the mid-(0.2–0.5) range of the risk thresholds for PCa (Figure 1m) and SigPCa (Figure 1n).

Relevantly, although other PCa diagnostic markers can be altered in response to inflammatory conditions of the prostate, our results show a mild but non-statistically significant increase of urine GOAT levels in patients with prostatic inflammation as compared to healthy individuals (Supplementary Figure S2).

We next applied a multivariate analysis adjusted with variables usually considered in clinical practice for the diagnose of PCa (PSA, age, DRE, etc.; Tables 2–5) to evaluate the association of urine GOAT levels with the presence of PCa and SigPCa. This analysis revealed that urine GOAT levels were independently associated with an increased risk of PCa and SigPCa in the full cohort and in the cohort of patients in the grey zone of PSA. Additionally, urine GOAT levels were also found to be independently associated with an increased risk of PCa and SigPCa, even when PSA levels were excluded from the analyses.

Table 2. Multivariate analysis of the association of plasma GOAT levels with the diagnosis of prostate cancer in the full cohort of patients adjusting with common clinical variables.

Variable	OR	Bootstrap CI 95%	p Value
Age	1.036	1.014, 1.058	<0.001
PSA	1.047	1.019, 1.073	<0.001
Prior biopsy	0.522	0.3137, 0.7134	<0.001
GOAT	1.514	1.253, 1.755	<0.001
DRE	3.139	1.804, 4.307	<0.001

OR: Odds ratio; CI: Confidence interval; PSA: Prostatic specific antigen; DRE: Digital rectal examination.

Table 3. Multivariate analysis of the association of plasma GOAT levels with the diagnosis of Significant PCa (SigPCa) in the full cohort of patients adjusting with common clinical variables.

Variable	OR	Bootstrap CI 95%	*p* Value
Age	1.052	1.025, 1.079	<0.001
PSA	1.051	1.023, 1.075	<0.001
Prior biopsy	0.452	0.233, 0.662	<0.001
GOAT	1.477	1.171, 1.753	<0.001
DRE	2.878	1.639, 3.996	<0.001

OR: Odds ratio; CI: Confidence interval; PSA: Prostatic specific antigen; DRE: Digital rectal examination.

Table 4. Multivariate analysis of the association of plasma GOAT levels with the diagnosis of prostate cancer (PCa) in the patients with a PSA range of 3–10 ng/mL adjusting with common clinical variables.

Variable	OR	Bootstrap CI 95%	*p* Value
Age	1.039	1.013, 1.064	<0.001
PSA	1.144	1.014, 1.271	0.011
Prior biopsy	0.431	0.217, 0.633	<0.001
GOAT	1.553	1.226, 1.838	<0.001
DRE	1.553	1.212, 4.080	<0.001

OR: Odds ratio; CI: Confidence interval; PSA: Prostatic specific antigen; DRE: Digital rectal examination.

Table 5. Multivariate analysis of the association of plasma GOAT levels with the diagnosis of Significant PCa (SigPCa) in the patients with PSA a range of 3–10 ng/mL, adjusting with common clinical variables.

Variable	OR	Bootstrap CI 95%	*p* Value
Age	1.0532	1.020, 1.085	<0.001
PSA	1.119	0.958, 1.275	0.07
Prior biopsy	0.366	0.121, 0.596	0.001
GOAT	1.526	1.144, 1.859	<0.001
DRE	2.497	1.017, 3.762	<0.001

OR: Odds ratio; CI: Confidence interval; PSA: Prostatic specific antigen; DRE: Digital rectal examination.

3.4. Correlation of Urine GOAT Levels with Clinical and Molecular Parameters of Tumor Aggressiveness

The urine levels of GOAT were positively correlated with age (Figure 2a), PSA levels (Figure 2b), Gleason score (Figure 2c), plasma C-reactive protein (CRP) levels (Figure 2d) and negatively correlated with plasma Apolipoprotein A1 (APOA) levels (Figure 2e) in PCa patients. In addition, GOAT urine levels were also associated to clinical parameters of aggressiveness. Specifically, a positive correlation between urine GOAT levels and the expression levels (in the tumor pieces) of *CDK6*, *EGF*, *EZH2* and *NF-KB* was found in patients with PCa (Figure 2f–h). Moreover, *CDK2* and *SIRT1* expression in the tumor pieces of these patients tended to directly, while *CDKN2A* inversely, be correlated with GOAT urine levels (Figure 2i–l).

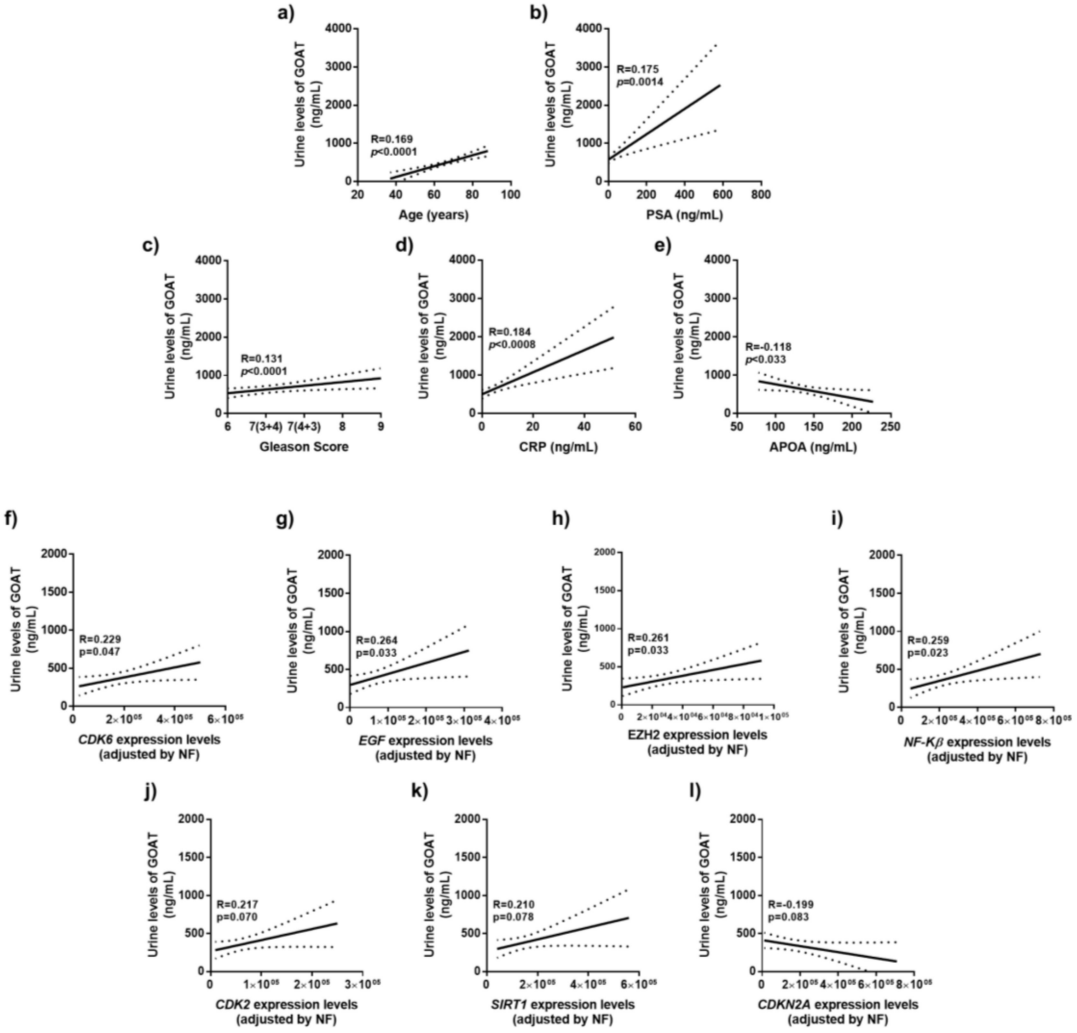

Figure 2. Correlations of urine GOAT levels and molecular parameters. Correlations of urine GOAT levels in PCa patients with the tissue expression levels of *CDK6*, *EGF*, *EZH2*, *NF-KB*, *CDK2*, *SIRT1* and *CDKN2A*. mRNA levels were determined by qPCR and adjusted by a normalization factor (calculated with the expression levels of *ACTB* and *GAPDH* using GeNorm). Coefficients of correlation (R) were evaluated by Pearson's test. The graphics show the lineal adjusted method and mean confidence interval.

3.5. In Vitro and In Vivo Effects of the Modulation of GOAT Expression and/or Activity

The overexpression of *GOAT* (Supplementary Figure S3a) increased the proliferation rate of DU145 cells at 48 and 72 h (Figure 3a). Similar results were observed in one experiment using LNCaP cells (Supplementary Figure S4). On the other hand, *GOAT* silencing (Supplementary Figure S3b) decreased the proliferation rate of DU145 cells at 24, 48, and 72 h (Figure 3b). Moreover, the inhibition of GOAT activity (using the specific GOAT inhibitor GO-CoA-Tat) evoked a significant decrease in the proliferation rate of DU145 cells after 24 h of incubation (Figure 3c). Moreover, xenograft tumors derived from DU145 cells overexpressing *GOAT* (Supplementary Figure S3c) were significantly higher (Figure 3d), showed a greater number of mitosis per mm2 (Figure 3e) and a higher KI67 staining (Figure 3f) than the tumors derived from control cells (transfected with the mock plasmid).

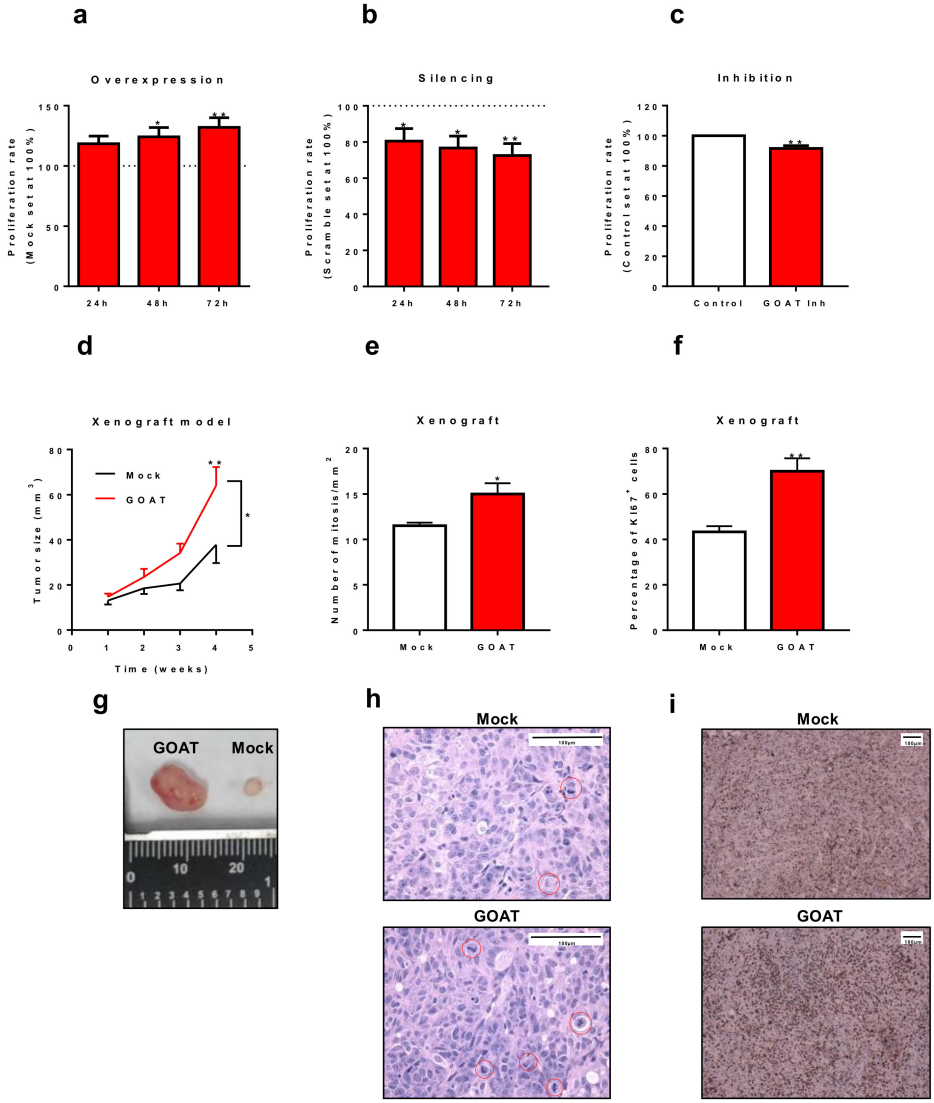

Figure 3. Effects of GOAT in vitro and in vivo. Cell proliferation rate (determined by Alamar-Blue assay) at 24, 48 and/or 72 h in response to *GOAT* overexpression (**a**), silencing (**b**) and pharmacological blockade with the specific GOAT inhibitor GO-CoA-Tat (**c**). Results are referred as a percentage of the control condition (mock, scramble and vehicle-treated cells, respectively). (**d**) Comparison between the growth of xenograft tumors derived from mock-transfected cells (black line) and GOAT-overexpressing cells (**red line**) over time. (**e**) Number of mitosis per mm^2 in the xenograft tumors derived from mock-transfected DU145 cells and GOAT-overexpressing DU145 cells. (**f**) Percentage of positive KI67 cells in mock and GOAT xenograft tumors. (**g**) Representative image of tumor size of mock and GOAT xenograft tumors. (**h**) Representative image of xenograft tumors derived from mock-transfected DU145 cells and GOAT-overexpressing DU145 cells with hematoxylin-eosin staining. (**i**) Representative images of KI67 staining of xenograft tumors derived from mock-transfected DU145 cells and GOAT-overexpressing DU145 cells. The asterisks (*, $p < 0.05$; **, $p < 0.01$) indicate values that significantly differ between groups.

4. Discussion

The measurement of plasma PSA levels remains the current gold standard to diagnose PCa, which represents one of the tumors types with the highest incidence worldwide [1]. Unfortunately, PSA continues to show important limitations (especially in the range of 3–10 ng/mL, also named the "grey zone"), including compromised specificity, inasmuch as non-tumoral conditions (e.g., infections, inflammation) can also increase PSA levels [2]. Consequently, numerous unnecessary

biopsies are carried out in the current clinical practice, generating preventable adverse effects to patients and increasing public costs [3]. Therefore, considerable research efforts have been focused on the identification of novel biomarkers that could complement or even replace plasma PSA in order to improve the capacity of the clinicians to diagnose PCa. In this sense, our group has recently demonstrated that GOAT, an enzyme involved in the acylation and activation of ghrelin and, likely, other components of this hormonal axis (e.g., In1-ghrelin, In2c-ghrelin) [9], are overexpressed in PCa tissues, but most importantly, secreted by PCa cells [12]. Interestingly, results previously reported by our group suggested that plasma GOAT levels might be used as a putative complement for plasma PSA (especially in the grey zone of PSA) for the diagnosis of PCa [13]. In the present study, we further corroborated in an ampler cohort of patients (almost 1000 patients) that GOAT plasma levels are higher in patients with PCa (especially those diagnosed with clinically significant PCa) as compared to those with negative biopsy, which is consistent with previous results reported by our group analyzing a more limited cohort of patients (n = 312) [13]. Moreover, we demonstrated herein that GOAT levels can also be detected in urine, being also significantly increased in PCa patients compared to control individuals. Remarkably, the differences found in urine GOAT levels were significantly more pronounced among control and cancer groups than those obtained when analyzing plasma GOAT levels from the same patients. This observation could be due to the fact that urine is enriched in prostate-derived proteins compared to the plasma and therefore, urine can act as a more reliable and specific non-invasive fluid for the diagnosis of PCa patients [22].

In line with this idea, the results obtained herein demonstrate that high urine GOAT levels were associated to a higher risk of developing PCa as well as clinically significant PCa, independently of other parameters clinically relevant for PCa diagnosis and PCa patient's management, including Gleason score, PSA, age and DRE [14,23,24]. Indeed, the diagnostic capacity of urine GOAT levels to identify patients with PCa is comparable to that of the current gold standard plasma PSA levels. However, it should be noted that the diagnostic capacity of urine GOAT levels significantly outperforms the capacity of plasma PSA to detect PCa patients in the PSA grey zone (wherein the capacity of PSA is significantly worse). In fact, when analyzing patients in the grey zone of PSA, urine GOAT levels (but not PSA levels) are able to discriminate between SigPCa patients and patients with negative result in the biopsy or with NonSigPCa. Therefore, although no direct comparison between GOAT and other emerging and well-studied biomarkers [25,26] have been performed (inasmuch as different cohorts and approximations have been used), these results suggest that GOAT could represent a novel and valuable complement for the PSA as non-invasive diagnostic biomarker to diagnose PCa (and/or SigPCa), especially in patients with PSA ranging from 3 to 10 ng/mL. Indeed, the results presented herein are merely based on the determination of urine GOAT, and it can be therefore anticipated that the development of novel diagnostic tools that integrate urine GOAT levels with other laboratory and/or clinical parameters could result in enhanced diagnostic potential. In line with this, additional prospective validations to assess the potential of diagnostic models that include GOAT in combination with other available parameters are warranted.

Remarkably, we also found that urine GOAT levels were directly correlated to key clinical parameters associated to PCa aggressiveness, such as Gleason score [14], age [27] and PCR [28]. Henceforth, GOAT urine levels could be also used as non-invasive biomarker for the PCa aggressiveness status. This idea was reinforced by the fact that the urine levels of GOAT were also associated to the expression levels of *CDK6*, *CDKN2A*, *EZH2*, *SIRT1* in PCa tissues, all of them being closely associated to PCa aggressiveness [29–32].

This study is also the first to provide novel evidence supporting the pathological role of GOAT in PCa development and progression. Specifically, we observed that overexpression of *GOAT* evoked an increase of tumor aggressiveness features (i.e., cell proliferation) in vitro and in vivo. Specifically, GOAT-overexpressing DU145 cells induced bigger tumors compared to mock-overexpressing DU145 cells. Consistently with this, GOAT-overexpressing tumors showed a higher number of mitotic cells and a higher percentage of KI67-positive cells than the mock-control tumors. Therefore, this report

demonstrates that GOAT plays an pathophysiological role in PCa, which, together with other elements of the ghrelin system that we have recently demonstrated that also have oncogenic potential and are activated by the GOAT enzyme (i.e., ghrelin and In1-ghrelin splicing variant) [8], might integrate a regulatory circuit that is altered in patients with PCa to promote the oncogenic capacity of PCa cells. Notably, the silencing of *GOAT* expression resulted in a decrease of PCa cells proliferation, reinforcing the oncogenic role of GOAT in PCa. In line with this, we tested, for the first time in tumor cells, the GO-CoA-Tat compound, which has been previously reported to specifically inhibit GOAT activity [17]. Consistently with the silencing results, the blockade of GOAT activity reduced the aggressiveness of PCa cells in vitro, further supporting the oncogenic role of GOAT and suggesting the potential novel therapeutic role of GOAT in PCa.

The present study has some limitations. First, despite the prospectively collected information, it followed a retrospective design. Secondly, the use of TRUS biopsy for PCa diagnosis, although it remains as the standard in most populations, suffers from random error compared with template biopsy [33] and therefore, could affect the prediction results. Furthermore, at the time of patients' recruitment, mpMRI was not established in the clinical practice of our institution and therefore, a further prospective validation study in an additional cohort collected following current recommendation of performing mpMRI previous to the biopsy (GUIAS 2019) will be designed. This study was carried out with plasma and urine samples, while the ELISA kit manufacturer recommends using serum instead of plasma (although the recovery using EDTA-plasma samples is higher compared to that obtained when using serum samples; 96% vs. 89%, respectively)".

Taken together, our results demonstrate that (1) GOAT plays an oncogenic role in PCa, (2) urine GOAT levels are directly associated to key clinical parameters of aggressiveness, and (3) urine GOAT levels outperform, at least in the grey zone, the capacity of plasma PSA to distinguish between SigPCa/PCa patients and non-PCa patients. Therefore, this report demonstrates that the GOAT enzyme could represent a novel diagnostic and aggressiveness biomarker and a potential and effective therapeutic target in PCa.

Supplementary Materials: The following are available online at http://www.mdpi.com/2077-0383/8/12/2056/s1.

Author Contributions: Conceptualization: J.M.J.-V., E.G.-G., M.D.G. and R.M.L.; Methodology: J.M.J.-V., A.J.M.-H.; F.L.-L., R.S.-S., I.G. and A.B.; Software: I.G. and A.B.; Validation: J.M.J.-V., E.G.-G., A.J.M.-H., V.H.-A., M.D.G. and R.M.L.; Formal analysis: J.M.J.-V., E.G.-G., A.J.M.-H., V.H.-A., F.L.-L., and R.M.L.; Investigation: J.M.J.-V., E.G.-G., A.J.M.-H., V.H.-A., F.L.-L. and R.S.-S.; Resources: E.G.-G., I.G., A.B., M.J.M.-V., J.C., J.L.-M., M.J.R.-T., J.P.C., M.D.G. and R.M.L.; Data curation: J.M.J.-V., I.G., M.D.G. and R.M.L.; Writing—Original draft preparation: J.M.J.-V., and R.M.L.; Writing—Review and editing: J.M.J.-V., E.G.-G., M.D.G and R.M.L.; Visualization: J.M.J.-V., E.G.-G., A.J.M.-H. and R.M.L.; Supervision: J.P.C., M.D.G. and R.M.L.; Project administration: M.D.G and R.M.L.; Funding acquisition: J.P.C., M.D.G. and R.M.L.

Funding: This research was funded Instituto de Salud Carlos III, co-funded by European Union (ERDF/ESF, "Investing in your future") (PI16/00264, PI17-02287, CM16/00180), FEDER (CCB.030PM), MINECO/MECD (BFU2016-80360-R; FPU18/02485, FPU16/06190), Junta de Andalucía (BIO-0139), and CIBERobn.

Acknowledgments: The biological samples repository node (Córdoba, Spain) is gratefully acknowledged for coordination tasks in the selection of samples.

Conflicts of Interest: The authors declare no conflict of interest. The funders had no role in the design of the study; in the collection, analyses, or interpretation of data; in the writing of the manuscript, or in the decision to publish the results.

References

1. Bray, F.; Ferlay, J.; Soerjomataram, I.; Siegel, R.L.; Torre, L.A.; Jemal, A. Global cancer statistics 2018: GLOBOCAN estimates of incidence and mortality worldwide for 36 cancers in 185 countries. *CA A Cancer J. Clin.* **2018**, *68*, 394–424. [CrossRef] [PubMed]
2. Nadler, R.B.; Humphrey, P.A.; Smith, D.S.; Catalona, W.J.; Ratliff, T.L. Effect of inflammation and benign prostatic hyperplasia on elevated serum prostate specific antigen levels. *J. Urol.* **1995**, *154*, 407–413. [CrossRef]
3. Loeb, S.; Bjurlin, M.A.; Nicholson, J.; Tammela, T.L.; Penson, D.F.; Carter, H.B.; Carroll, P.; Etzioni, R. Overdiagnosis and overtreatment of prostate cancer. *Eur. Urol.* **2014**, *65*, 1046–1055. [CrossRef] [PubMed]

4. Hendriks, R.J.; van Oort, I.M.; Schalken, J.A. Blood-based and urinary prostate cancer biomarkers: A review and comparison of novel biomarkers for detection and treatment decisions. *Prost. Cancer Prost. Dis.* **2017**, *20*, 12–19. [CrossRef]
5. Chopin, L.K.; Seim, I.; Walpole, C.M.; Herington, A.C. The ghrelin axis—Does it have an appetite for cancer progression? *Endocr. Rev.* **2012**, *33*, 849–891. [CrossRef]
6. Gahete, M.D.; Rincon-Fernandez, D.; Villa-Osaba, A.; Hormaechea-Agulla, D.; Ibanez-Costa, A.; Martinez-Fuentes, A.J.; Gracia-Navarro, F.; Castano, J.P.; Luque, R.M. Ghrelin gene products, receptors, and GOAT enzyme: Biological and pathophysiological insight. *J. Endocrinol.* **2014**, *220*, R1–R24. [CrossRef]
7. Yeh, A.H.; Jeffery, P.L.; Duncan, R.P.; Herington, A.C.; Chopin, L.K. Ghrelin and a novel preproghrelin isoform are highly expressed in prostate cancer and ghrelin activates mitogen-activated protein kinase in prostate cancer. *Clin. Cancer Res. Off. J. Am. Assoc. Cancer Res.* **2005**, *11*, 8295–8303. [CrossRef]
8. Hormaechea-Agulla, D.; Gahete, M.D.; Jimenez-Vacas, J.M.; Gomez-Gomez, E.; Ibanez-Costa, A.; Fernando, L.-L.; Rivero-Cortes, E.; Sarmento-Cabral, A.; Valero-Rosa, J.; Carrasco-Valiente, J.; et al. The oncogenic role of the In1-ghrelin splicing variant in prostate cancer aggressiveness. *Mol. Cancer* **2017**, *16*, 146. [CrossRef]
9. Yang, J.; Brown, M.S.; Liang, G.; Grishin, N.V.; Goldstein, J.L. Identification of the acyltransferase that octanoylates ghrelin, an appetite-stimulating peptide hormone. *Cell* **2008**, *132*, 387–396. [CrossRef]
10. Gutierrez, J.A.; Solenberg, P.J.; Perkins, D.R.; Willency, J.A.; Knierman, M.D.; Jin, Z.; Witcher, D.R.; Luo, S.; Onyia, J.E.; Hale, J.E. Ghrelin octanoylation mediated by an orphan lipid transferase. *Proc. Natl. Acad. Sci. USA* **2008**, *105*, 6320–6325. [CrossRef]
11. Gahete, M.D.; Cordoba-Chacon, J.; Salvatori, R.; Castano, J.P.; Kineman, R.D.; Luque, R.M. Metabolic regulation of ghrelin O-acyl transferase (GOAT) expression in the mouse hypothalamus, pituitary, and stomach. *Mol. Cell. Endocrinol.* **2010**, *317*, 154–160. [CrossRef] [PubMed]
12. Hormaechea-Agulla, D.; Gomez-Gomez, E.; Ibanez-Costa, A.; Carrasco-Valiente, J.; Rivero-Cortes, E.; Fernando, L.-L.; Pedraza-Arevalo, S.; Valero-Rosa, J.; Sanchez-Sanchez, R.; Ortega-Salas, R.; et al. Ghrelin O-acyltransferase (GOAT) enzyme is overexpressed in prostate cancer, and its levels are associated with patient's metabolic status: Potential value as a non-invasive biomarker. *Cancer Lett.* **2016**, *383*, 125–134. [CrossRef] [PubMed]
13. Gomez-Gomez, E.; Jimenez-Vacas, J.M.; Carrasco-Valiente, J.; Herrero-Aguayo, V.; Blanca-Pedregosa, A.M.; Leon-Gonzalez, A.J.; Valero-Rosa, J.; Fernandez-Rueda, J.L.; Gonzalez-Serrano, T.; Lopez-Miranda, J.; et al. Plasma ghrelin O-acyltransferase (GOAT) enzyme levels: A novel non-invasive diagnosis tool for patients with significant prostate cancer. *J. Cell. Mol. Med.* **2018**, *22*, 5688–5697. [CrossRef] [PubMed]
14. Epstein, J.I.; Allsbrook, W.C., Jr.; Amin, M.B.; Egevad, L.L. The 2005 International Society of Urological Pathology (ISUP) Consensus Conference on Gleason Grading of Prostatic Carcinoma. *Am. J. Surg. Pathol.* **2005**, *29*, 1228–1242. [CrossRef] [PubMed]
15. Jimenez-Vacas, J.M.; Herrero-Aguayo, V.; Gomez-Gomez, E.; Leon-Gonzalez, A.J.; Saez-Martinez, P.; Alors-Perez, E.; Fuentes-Fayos, A.C.; Martinez-Lopez, A.; Sanchez-Sanchez, R.; Gonzalez-Serrano, T.; et al. Spliceosome Component SF3B1 as Novel Prognostic Biomarker and Therapeutic Target for Prostate Cancer. *Transl. Res. J. Lab. Clin. Med.* **2019**, *212*, 89–103. [CrossRef]
16. Hormaechea-Agulla, D.; Jimenez-Vacas, J.M.; Gomez-Gomez, E.; Fernando, L.-L.; Carrasco-Valiente, J.; Valero-Rosa, J.; Moreno, M.M.; Sanchez-Sanchez, R.; Ortega-Salas, R.; Gracia-Navarro, F.; et al. The oncogenic role of the spliced somatostatin receptor sst5TMD4 variant in prostate cancer. *FASEB. J.* **2017**, *31*, 4682–4696. [CrossRef] [PubMed]
17. Barnett, B.P.; Hwang, Y.; Taylor, M.S.; Kirchner, H.; Pfluger, P.T.; Bernard, V.; Lin, Y.Y.; Bowers, E.M.; Mukherjee, C.; Song, W.J.; et al. Glucose and weight control in mice with a designed ghrelin O-acyltransferase inhibitor. *Science* **2010**, *330*, 1689–1692. [CrossRef]
18. Duran-Prado, M.; Gahete, M.D.; Hergueta-Redondo, M.; Martinez-Fuentes, A.J.; Cordoba-Chacon, J.; Palacios, J.; Gracia-Navarro, F.; Moreno-Bueno, G.; Malagon, M.M.; Luque, R.M.; et al. The new truncated somatostatin receptor variant sst5TMD4 is associated to poor prognosis in breast cancer and increases malignancy in MCF-7 cells. *Oncogene* **2012**, *31*, 2049–2061. [CrossRef]
19. Ibanez-Costa, A.; Gahete, M.D.; Rivero-Cortes, E.; Rincon-Fernandez, D.; Nelson, R.; Beltran, M.; de la Riva, A.; Japon, M.A.; Venegas-Moreno, E.; Galvez, M.A.; et al. In1-ghrelin splicing variant is overexpressed in pituitary adenomas and increases their aggressive features. *Sci. Rep.* **2015**, *5*, 8714. [CrossRef]

20. Luque, R.M.; Ibanez-Costa, A.; Neto, L.V.; Taboada, G.F.; Hormaechea-Agulla, D.; Kasuki, L.; Venegas-Moreno, E.; Moreno-Carazo, A.; Galvez, M.A.; Soto-Moreno, A.; et al. Truncated somatostatin receptor variant sst5TMD4 confers aggressive features (proliferation, invasion and reduced octreotide response) to somatotropinomas. *Cancer Lett.* **2015**, *359*, 299–306. [CrossRef]
21. Vandesompele, J.; De Preter, K.; Pattyn, F.; Poppe, B.; Van Roy, N.; De Paepe, A.; Speleman, F. Accurate normalization of real-time quantitative RT-PCR data by geometric averaging of multiple internal control genes. *Genome Biol.* **2002**, *3*, research0034.1. [CrossRef] [PubMed]
22. Principe, S.; Kim, Y.; Fontana, S.; Ignatchenko, V.; Nyalwidhe, J.O.; Lance, R.S.; Troyer, D.A.; Alessandro, R.; Semmes, O.J.; Kislinger, T.; et al. Identification of prostate-enriched proteins by in-depth proteomic analyses of expressed prostatic secretions in urine. *J. Proteome Res.* **2012**, *11*, 2386–2396. [CrossRef] [PubMed]
23. Duffy, M.J. PSA as a marker for prostate cancer: A critical review. *Ann. Clin. Biochem.* **1996**, *33*, 511–519. [CrossRef] [PubMed]
24. Jones, D.; Friend, C.; Dreher, A.; Allgar, V.; Macleod, U. The diagnostic test accuracy of rectal examination for prostate cancer diagnosis in symptomatic patients: A systematic review. *BMC Fam. Pract.* **2018**, *19*, 79. [CrossRef]
25. Van Neste, L.; Hendriks, R.J.; Dijkstra, S.; Trooskens, G.; Cornel, E.B.; Jannink, S.A.; de Jong, H.; Hessels, D.; Smit, F.P.; Melchers, W.J.; et al. Detection of High-grade Prostate Cancer Using a Urinary Molecular Biomarker-Based Risk Score. *Eur. Urol.* **2016**, *70*, 740–748. [CrossRef]
26. Gronberg, H.; Adolfsson, J.; Aly, M.; Nordstrom, T.; Wiklund, P.; Brandberg, Y.; Thompson, J.; Wiklund, F.; Lindberg, J.; Clements, M.; et al. Prostate cancer screening in men aged 50-69 years (STHLM3): A prospective population-based diagnostic study. *Lancet Oncol.* **2015**, *16*, 1667–1676. [CrossRef]
27. Calvocoressi, L.; Uchio, E.; Ko, J.; Radhakrishnan, K.; Aslan, M.; Concato, J. Prostate cancer aggressiveness and age: Impact of p53, BCL-2 and microvessel density. *J. Investig. Med. Off. Publ. Am. Fed. Clin. Res.* **2018**, *66*, 1142–1146. [CrossRef]
28. Thurner, E.M.; Krenn-Pilko, S.; Langsenlehner, U.; Stojakovic, T.; Pichler, M.; Gerger, A.; Kapp, K.S.; Langsenlehner, T. The elevated C-reactive protein level is associated with poor prognosis in prostate cancer patients treated with radiotherapy. *Eur. J. Cancer* **2015**, *51*, 610–619. [CrossRef]
29. Deshpande, A.; Sicinski, P.; Hinds, P.W. Cyclins and cdks in development and cancer: A perspective. *Oncogene* **2005**, *24*, 2909–2915. [CrossRef]
30. Cao, Z.; Wei, L.; Zhu, W.; Yao, X. Meta-analysis of CDKN2A methylation to find its role in prostate cancer development and progression, and also to find the effect of CDKN2A expression on disease-free survival (PRISMA). *Medicine* **2018**, *97*, e0182. [CrossRef]
31. Liu, X.; Wu, Q.; Li, L. Functional and therapeutic significance of EZH2 in urological cancers. *Oncotarget* **2017**, *8*, 38044–38055. [CrossRef] [PubMed]
32. Jung-Hynes, B.; Nihal, M.; Zhong, W.; Ahmad, N. Role of sirtuin histone deacetylase SIRT1 in prostate cancer. A target for prostate cancer management via its inhibition? *J. Biol. Chem.* **2009**, *284*, 3823–3832. [CrossRef] [PubMed]
33. Ahmed, H.U.; Hu, Y.; Carter, T.; Arumainayagam, N.; Lecornet, E.; Freeman, A.; Hawkes, D.; Barratt, D.C.; Emberton, M. Characterizing clinically significant prostate cancer using template prostate mapping biopsy. *J. Urol.* **2011**, *186*, 458–464. [CrossRef] [PubMed]

Supplementary Figures:

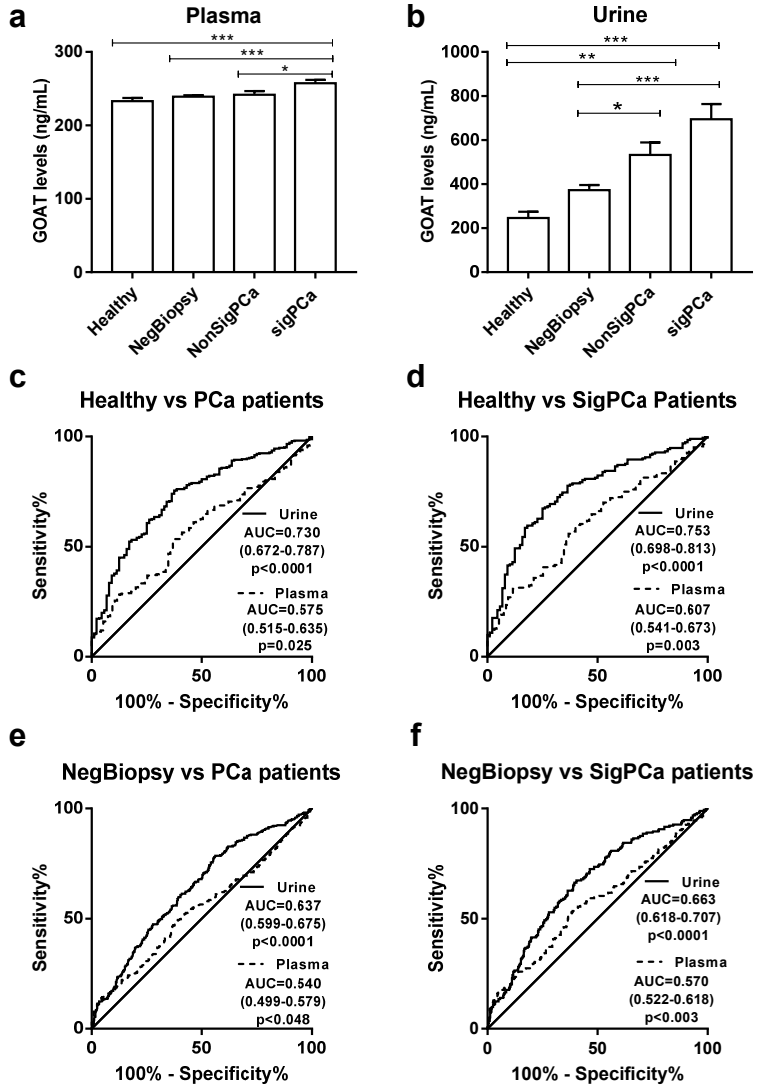

Supplemental Figure S1. GOAT levels in urine and plasma from patients with and without PCa. Levels of GOAT in plasma (**a**) and urine (**b**) of healthy individuals (n = 97), patients with suspect of PCa but negative result in the biopsy (NegBiopsy; n = 549), patients diagnosed with non-significant PCa (NonSigPCa; n = 143) and patients diagnosed with significant PCa (SigPCa; n = 204). Data represent mean ± SEM. c-f) Comparison of the receiver operating characteristic (ROC) curves analyses of urine (solid line) and plasma GOAT (dashed line) capacity to discriminate between healthy individual and PCa patients (**c**), healthy individuals and SigPCa patients (**d**), NegBiopsy and PCa patients (**e**), or NegBiopsy and SigPCa patients (**f**). Asterisks (*, $p < 0.05$; **, $p < 0.01$, ***, $p < 0.001$) indicate values that significantly differ between groups.

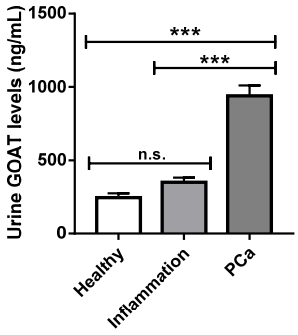

Supplemental Figure S2. Comparison of urine GOAT levels among healthy individuals (n = 97), patients with prostatic inflammatory diseases (n = 211) and PCa patients (n = 347). Data represent mean ± SEM. Asterisks (***, $p < 0.001$) indicate values that significantly differ between groups. n.s.: non statistically significant differences.

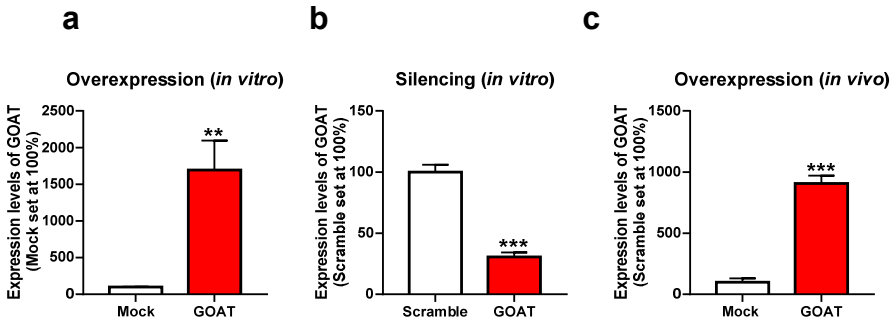

Supplemental Figure S3. Validation of *GOAT* overexpression (**a**) and silencing (**b**) in DU145 cells. (**c**) Validation of *GOAT* overexpression in the xenograft tumors. mRNA levels were determined by qPCR and adjusted by a normalization factor (calculated with the expression levels of *ACTB* and *GAPDH* using GeNorm). Data represent percentage of control cells (mock or scramble; mean ± SEM). Asterisks (**, $p < 0.01$, ***, $p < 0.001$) indicate values that significantly differ between groups.

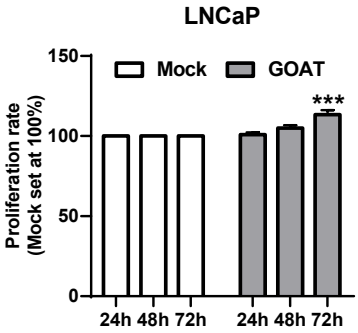

Supplemental Figure S4. Cell proliferation rate (determined by Alamar-Blue assay) at 24, 48 and 72 h in response to *GOAT* overexpression in LNCaP cells. One experiment was carried out (n = 1) with four technical replicates. Results are referred as percentage of mock. Statistically differences were calculated using the technical replicates. Asterisks (***, $p < 0.001$) indicate values that significantly differ between groups.